

CRADA Final Report ANL/CSE/C0001401-01

“Bipolar Plate Materials in Molten Carbonate Fuel Cells”

This CRADA involved Argonne National Laboratory as the Contractor and overall Project Manager. The CRADA Industrial Participant was Fuel Cell Energy Corporation of Danbury CN. The project subcontractors, who did the majority of the work, included the Russian Federal Nuclear Center-All Russia Institute of Experimental Physics (RFNC-VNIEF) and the Institute of High Temperature Electrochemistry of Ural Department of Sciences (IHTE).

To improve logistics in contracting in the Russian Federation, an international not-for-profit organization, the International Science and Technology Center (ISTC), put in place the subcontract. The project number is 2281p. Argonne National Laboratory served as the technical manager of this contract under the NIS-IPP program.

The attached ISTC/RFNC-VNIEF final report serves as the CRADA Final Report.

FINAL TECHNICAL REPORT

*For the 1-8 quarters
(June 1, 2002 – May 31, 2004z)*

ISTC Project #2281p
Date of commencement of the Project: June 01, 2002,
Duration of the Project: 24 months.

Development of New Materials for Fuel Cells

Agreement between International Science and Technology Center (ISTC)
and
Russian Federal Nuclear Center –
All-Russia Research Institute of Experimental Physics
(RFNC-VNIIEF)

Project Manager: Alexander Mikhailovich Gorelov,
Representative of the Leading Institution RFNC-VNIIEF
37 Mira Avenue, Sarov, Nizhny Novgorod Region, Russia
Telephone: 7+83130+ 42724
Fax: 7+83130+ 45798
E-mail: gorelov@astra.vniief.ru

Participating Institute 1: IHTE (Institute of High Temperature Electrochemistry of the Ural Department of the Russian Academy of Sciences, Yekaterinburg, Sverdlovsk Region, Russia)

Participating Institute 2: RFNC-VNIITF (Russian Federal Nuclear Center – All-Russia Research Institute of Theoretical Physics, Snezhinsk, Cheliabinsk Region).

Sarov
2004

Table of Contents

	page
Introduction	5
1. Cost-effective nickel coating (Task 1)	8
1.1. Galvanic nickel plating of 20X23H18 steel	8
1.1.1. Preparation of steel surface and selection of an electrolyte	8
1.1.2. Scheme of the technological process	13
1.1.3. Metallographic research on the coatings after 1500-hour corrosion tests	14
1.1.4. Inter-diffusion of nickel and iron in the process of 1500-hour tests	16
1.1.5. A technology to weld plates of 400-mm wide tapes	17
1.1.6. Site of galvanic nickel-plating	18
1.1.7. A combined Ni-Cu coating	21
1.1.8. Technical and economical analysis	23
1.1.9. Delivery of plates to FCE (Tasks 1 and 2)	24
1.1.10. Conclusions	24
1.2. Explosion cladding of 20X23H18 steel	25
1.2.1. Peculiarities of explosion cladding. Choice of a cladding scheme	25
1.2.2. Experimental polishing of explosion cladding	28
1.2.3. Metallographic research on coatings after 1500-hour corrosion tests	32
1.2.4. Inter-diffusion of iron and nickel in the process of 1500-hour tests	37
1.2.5. Conclusions	38
List references	38
2. Development of a new material with higher corrosion resistance for MCFC bipolar plate (Task 2)	40
2.1. Fabrication of monolithic specimens from the Y or Ti - doped alloys 30Cr-45Ni-1Al. Carrying out of the research.	40
2.2. Fabrication of thin sheet cold-rolled specimens on lab equipment. Determination of deformation-plastic characteristics.	43
2.3. Research on conductivity of oxide films, phase composition and structure of the Russian steel analogous to 310S and of a new alloy produced using industrial equipment	44
2.3.1. Perfection of the method	44
2.3.2. Research on conductivity of contacts of metallic materials using thin sheet samples with porous electrodes in the cathode gas environment	47
2.3.3. Research on conductivity of contacts of metallic materials using thin sheet samples with porous electrodes in the anode gas environment	51
2.3.4. Research on corrosion stability of thin sheet samples in the melt of lithium and potassium carbonates at 650°C during 500 h.	53
2.4. Test smelting in industrial furnaces. Fabrication of forgings for rolled sheet stock.	58
2.5. Delivery of a batch of sheets to the Partner for the research	62
2.6. Cost evaluation for manufacturing of a batch of sheets	63
2.7. Conclusions	65
3. New ceramic materials for an MCFC bipolar plate and an anode (Task 3)	67
3.1. Development of pore-free cermet compositions on the basis of LiAlO ₂ and Ni	67
3.1.1. Research on microstructure and electric conductivity of cermets	67

3.1.2. Research on corrosion stability of cermets in the melt of electrolyte during 100 hours	67
3.2. Development of pore-free cermets on the basis of conductive ceramics BaCeO ₃ with metal binders of Ni, Ni-Mo	68
3.2.1. Properties of the powder and sintered BaCeO ₃ ceramics	68
3.2.2. Electric conductivity of BaCeO ₃ at a high temperature	69
3.2.3. Manufacturing and microstructure of cermets on the basis of BaCeO ₃ with metal binders of Ni, Ni-Mo	71
3.2.4. Electric conductivity of cermets on the basis of BaCeO ₃ with metal binders of Ni, Ni-Mo.	72
3.2.5. Corrosion stability tests of cermets on the basis of BaCeO ₃ with metal binders of Ni, Ni-Mo	73
3.3. Development of pore-free cermets on the basis of ceramics reinforced with metal fiber	73
3.3.1. Manufacturing of cermets on the basis of ceramics reinforced with metal fiber	73
3.3.2. Micro structural research on cermets on the basis of ceramics reinforced with metal fiber	74
3.3.3. Electric conductivity of cermets on the basis of ceramics reinforced with metal fiber	79
3.3.4. Research on corrosion stability of cermets on the basis of ceramics reinforced with metal fiber	81
3.4. Tests of bipolar plates within a MCFC cell	81
3.5. Manufacturing and research on porous metal-ceramic plates that are MCFC anodes	82
3.5.1. Formulation of the task	82
3.5.2. Free sintering in vacuum	82
3.5.3. Making samples of porous metal-ceramic plates using pore-forming agent	83
3.5.4. Hot-pressing in a mold	83
3.5.5. Results of the tests on creep stability	85
3.6. Research on intermetallide compounds	88
3.7. Delivery of porous metal ceramic plates to FCE	88
3.8. Conclusions	89
List of references	89
4. Development of a new alloy and alloys with a ceramic coating for SOFC	90
4.1. Development of alloys Ti – V, Ti – Nb	90
4.1.1. Development of the technology to make Ti – V, Ti – Nb alloys	90
4.1.2. Research on the properties of Ti – V, Ti – Nb alloys	90
4.1.3. Research on TEC of the 8% YSZ electrolyte.	91
4.1.4. Research on alloys of the Ti-Nb system	92
4.1.5. Conclusions	94
4.2. Development of alloys with small content of Cr	94
4.2.1. Smelting of specimens and selection of deoxidizers.	94
4.2.2 Adjustment of the ingots deformation technology	94
4.2.3. Adjustment of the technique to measure linear expansion temperature coefficient (LETC) and dilatometer tests	95
4.2.4. Evaluation of mechanical stress in metal-ceramic compounds	97
4.2.5. Residual postrelaxation stresses (rough estimation)	98
4.2.6. Research on corrosion stability of alloys of Ni-Co-Cr-Fe system and ferrite steel	102

4.2.7. Research on corrosion stability of alloys of Ni-Co-Cr-Fe system and of 15X25T ferrite steel in the anode and cathode conditions	103
4.2.7.1 Research methods on corrosion stability	103
4.2.7.2. Tests results for samples at 800°C	104
4.2.7.3 Methods and results of micro X-ray spectrum analysis (MXSA) and X-ray phase analysis (XPhA) of he samples	105
4.2.8. Conclusions	107
4.3. Development of ferrite stainless steel (brand 400) with an oxide coating	109
4.3.1. Materials for coatings	109
4.3.2 Polishing of the coating application process	109
4.3.3 Results of research on the properties of the coatings	111
4.3.4. Results of tests in contact assemblies	112
4.3.5 Conclusions	113
4.4. Delivery of batch of sheets to the Partner for the research	113
4.5. Evaluation of the manufacturing cost of alloys on the basis of Fe-Ni-Co-Cr and Ti – Nb systems	114
List of references	114
5. Status of Work	115
6. A list of published articles and reports	115
7. A list of reports at the conferences and meetings	115
8. Information on Patents and Rights	124
Appendix 1. Content of Section 4 of the Work Plan after the first correction	126
Appendix 2. The second correction of the Work Plan	130
Appendix 3. Testing methods for corrosion stability	133
Appendix 4. Technical and economical analysis of establishment of an enterprise to make bipolar separator plates	135

INTRODUCTION

Advantages of implementation of power plants based on electrochemical reactions are successfully demonstrated in the USA and Japan. One of the most promising types of fuel cells (FC) is a type of high temperature fuel cells. At present, thanks to the efforts of the leading countries that develop fuel cell technologies power plants on the basis of molten carbonate fuel cells (MCFC) and solid oxide fuel cells (SOFC) are really close to commercialization. One of the problems that are to be solved for practical implementation of MCFC and SOFC is a problem of corrosion of metal components of stacks that are assembled of a number of fuel cells. One of the major components of MCFC and SOFC stacks is a bipolar separator plate (BSP) that performs several functions – it is separation of reactant gas flows, sealing of the joints between fuel cells, and current collection from the surface of electrodes.

ISTC Partner Project #2281p "Development of New Materials for Fuel Cells" was done in accordance with a three party agreement (DOE –ISTC-VNIIEF) and with an executive Agreement between ANL and RFNC-VNIIEF. An official partner on Project #2281p is the Department of Energy of the USA. Foreign collaborators on the Project are FCE, MSRI and ANL.

ISTC Project #2281 was sequential to works under agreement between RFNC-VNIIEF and ANL №981562402 «Materials for Bipolar Plates for Molten Carbonate Fuel Cells » (1998-1999).

4 Tasks were to be solved within the Project using efforts of three institutions: RFNC-VNIIEF, RFNC-VNIITF and IHTE with involvement of more than 200 specialists.

The goal of the 1st Task of the Project is to develop new *cost-effective* nickel coatings for the Russian 20X23H18 steel for an MCFC bipolar separator plate using technological processes usually implemented to apply corrosion stable coatings onto the metal parts for products in the defense. There was planned the research on production of nickel coatings using different methods, first of all the galvanic one and the explosion cladding one. **As a result of the works**, 0.4 x 712x 1296 mm plates coated with nickel on one side were to be made and passed to ANL (USA). A line of 4 galvanic baths 600 liters was to be built for the galvanic coating application.

The goal of Task 2 of the Project is the development of a new material of an MCFC bipolar separator plate with an upgraded corrosion stability, and development of a technology to produce cold roll sheets of this material the sizes of which will be 0.8 x 712x 1296 mm. **As a result of these works**, a pilot batch of the rolled material in sheets 0.8 x 712x 1296 mm in size is to be made (in accordance with the norms and standards of the Russian metallurgical industry) and supplied to the partner for tests in a stack of fuel cells.

A feasibility study on the cost of the Russian material for a BSP is to be done on Tasks 1, 2 in case the annual order makes up 400 000 sheets.

The goal of Task 3 of the Project is to research on possible implementation of cermet compositions on the basis of LiAlO_2 , TiN , B_4C , ceramics with Ni and Ni-Mo binders. BaCeO_3 conductive ceramics with metal binders of Ni, Ni-Cr etc. were also planned to be studied. **As a result of these works**, a pilot batch of samples is to be made and passed to FCE for tests.

The goal of Task 4 of the Project is development of a new alloy or alloys with a ceramic coating that will have upgraded corrosion stability in operation within a SOFC. A new alloy was to be worked out by the way of modification of compositions of industrial alloys. Ceramic coatings are to be applied onto ferrite steel produced serially by iron and steel industry of Russia as sheet iron.

As a result of these works, technical requirements for the technology of sheet iron production process are to be worked out, a pilot batch of samples is to be made and passed to ANL.

Goals, tasks and expected results of the works on the Project as they were initially formulated are shown in the diagram of Fig. 1. The changes in the course of the Project initiated by the Customer are shown in respective changes in the Work Plan (see Appendices 1 and 2) and are de-

scribed in «ADDENDUM #2» and «ADDENDUM #3», signed by three parties (DOE-ISTC-RFNC-VNIIEF).

Technical approach and methodology of the works on the Project were based on the experience gained by specialists of RFNC-VNIIEF, RFNC-VNIITF and IHTE of the Ural Department of the Russian Academy of Sciences in the area of protective coating application techniques, creation of new alloys and cermet compositions. Project participants have large experience in corrosion tests, in technological and design work, calculations on electrochemical processes, metallographic and mass-spectrum research.

Main sections of the report below describe the most important results of the work for the whole Project.

All tasks of 1-8 quarters of the Work Plan are completed.

Goals: making use of defense technologies,

To DEVELOP A BIPOLAR PLATE FOR A FUEL CELL

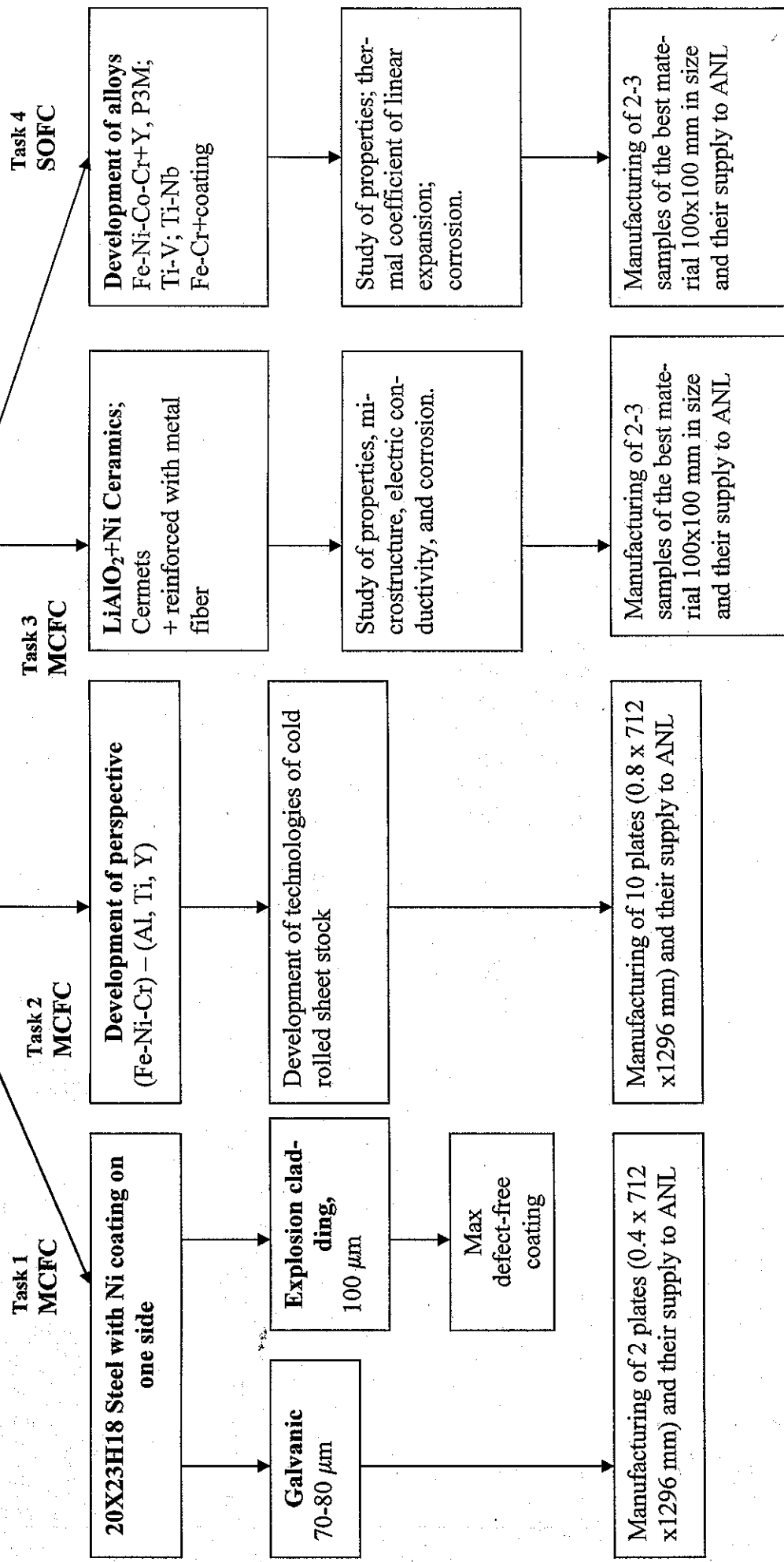


Fig. I-1.

1. COST-EFFECTIVE NICKEL COATING (TASK 1)

1.1. Galvanic nickel-plating of 20X23H18 steel.

1.1.1. Preparation of steel surface and selection of an electrolyte.

1.1.1.1. A galvanic nickel coating should meet both technical and economical requirements. It should have a good adhesion with the substrate and protect it from the influence of the aggressive environment; the technology of coating application should be cost-effective and environmentally friendly.

Issues related to the surface treatment of 20X23H18 steel to be nickel-plated and to the modes of nickel plating were to be solved to produce a good quality nickel coating for an MCFC bipolar separator plate.

The necessity of preparation of the steel surface comes from a high tendency of a stainless steel to passivation [1-4].

According to the environmental considerations the choice was made in favor of an electrochemical way of surface treatment in a solution of sulphuric acid. The best results were obtained in case of the anode-cathode treatment of the surface as one of the electrochemical ways of surface treatment. The criterion of the preparation was the condition of the etched surface and the adhesion of the coating.

Anode-cathode treatment of the surface was done in the following way. Anode etching was done with variation of concentration of the sulphuric acid, current density and time of treatment. After water flushing the sample was subjected to the cathode treatment in the diluted sulphuric acid (20% wgt) at the current density of 10-20 A/dm² during 1-2 minutes to remove products of etching produced during the anode treatment. Table 1.1 shows the experimental results of the selection of the most optimum mode of the surface treatment.

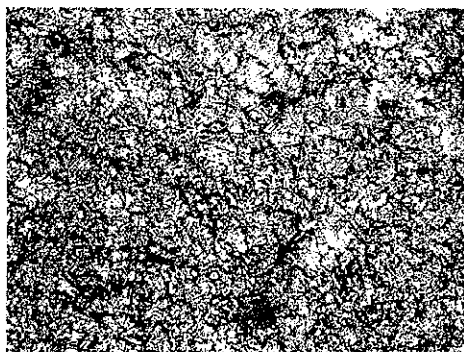
Table 1.1.

Anode-cathode treatment of the steel surface.

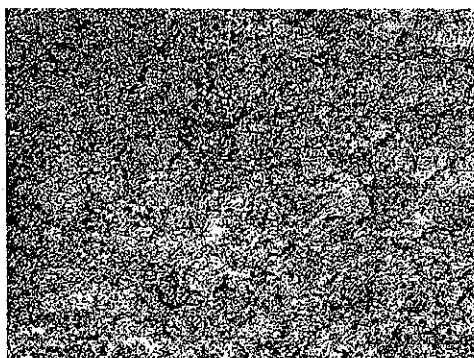
No	H ₂ SO ₄ , % wgt.	Current density, A/dm ²	Time of treatment, min	Removal of metal, μm	Nature of the surface
1	20	3	10	3	Is not etched
2			15	5	Uniform etching
3		10	1	2	Is not etched
4			2	4	Uniform etching
5			5	7	Uniform etching
6			10	14	Over etched
7		20	1	4	Is not etched
8			2	7	Uniform etching
9			5	14	Uniform etching
10			10	24	Over etched
11	40	10	1	1,5	Is not etched
12			2	3	Uniform etching
13			5	5	Uniform etching
14			10	10	Over etched
15		20	1	3	Is not etched
16			2	7	Partly polished surface
17			5	13	Partly polished surface
18			10	27	Polished surface

As it comes from the data obtained, a uniform etching of steel can be done at different modes of etching. When H_2SO_4 concentration is 40% and $D= 20 A/dm^2$ a polishing effect of the surface is observed.

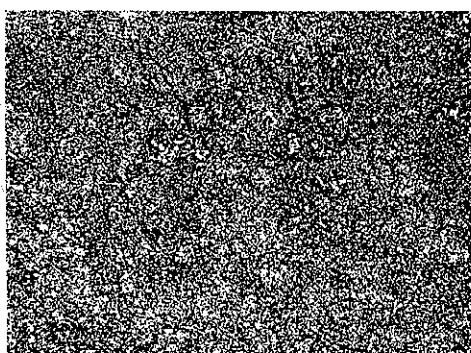
Fig.1.1 shows the microstructure of the samples after the anode-cathode treatment of the surface of steel samples.



a)



b)



c)

- a) a uniform etched surface,
- b) a polished surface,
- c) an under-etched surface

Fig.1.1. Microstructure of steel samples after the anode-cathode treatment of the surface.

The following etching mode was chosen for further research and etching of large scale plates for BSP: 20% sulphuric acid, current density of $3 A/dm^2$, the time of etching of 15-20 minutes. The specified mode requires a relatively low electric power supply and does not impose a limit on the time of etching.

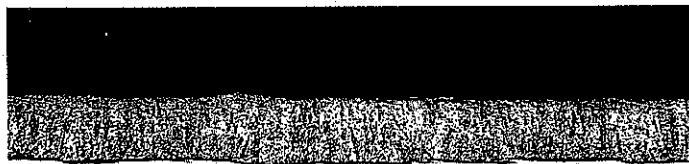
1.1.1.2. Two electrolytes were selected for nickel plating; their composition and operating modes are given in Table 1.2.

Table 1.2.

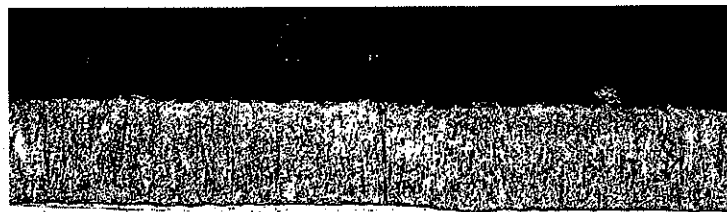
Composition of electrolytes and modes of nickel plating.

Sulfuric electrolyte		Sulfaminic electrolyte	
$\text{NiSO}_4 \times 7\text{H}_2\text{O}$	140-200 g/l	$\text{Ni}(\text{NH}_2\text{SO}_3)_2 \times 4\text{H}_2\text{O}$	300-400 g/l
$\text{NiCl}_2 \times 6\text{H}_2\text{O}$	30-40 g/l	$\text{NiCl}_2 \times 6\text{H}_2\text{O}$	12-15 g/l
H_3BO_3	25-40 g/l	H_3BO_3	25-40 g/l
Na_2SO_4	60-80 g/l	D_k	2-3 A/dm ²
D_k	0,5-2,0 A/dm ²	pH	3,6-4,2
pH	5,0-5,5	t	40-50 °C
t	40-50 °C		

Fig.1.2 shows the microstructure of galvanic nickel on the steel when deposition was done from the sulfuric and sulfaminic electrolytes.



a)



b)

- a) structure of a nickel coating from a sulfuric electrolyte (x250),
 b) structure of a nickel coating from a sulfaminic electrolyte (x250)

Fig. 1.2. Microstructure of the nickel coating from different electrolytes.

Metallographic research has shown that a nickel coating from the Watts sulfuric electrolyte has a columnar structure, and a nickel coating from a sulfaminic electrolyte has a layered structure.

The quality of the produced coatings was evaluated by the following parameters: adhesion, porosity, the structure of the coating, and the chemical composition. Adhesion tests were done using bending-unbending tests to $\pm 90^\circ$. Good adhesion is the one when the internal and external surfaces of the bend do not reveal any delaminating or cracking. Besides, adhesion was evaluated by a thermal shock when the sample was heated to 650°C in the air and then it was cooled down at the room temperature in the water.

The porosity was identified by application of filter paper preliminary wetted in the solution of the following composition:

- $\text{K}_3\text{Fe}(\text{CN})_6$ - 3 g/l
- NaCl - 10 g/l

A number of blue points showed the porosity of the coating. Results of the porosity analysis are given in Table 1.3.

Table 1.3.

Thickness of nickel, μm	Number of pores/ cm^2	
	Sulfuric electrolyte	Sulfaminic electrolyte
< 10	20-35	2-5
10-20	9-15	No pores
20-30	No pores	No pores

As it is shown by chemical analysis, the content of sulfur in the coating is 0.01% for the sulfuric electrolyte and 0.02% for the sulfaminic electrolyte.

In the result of the research the choice was made in favor of the sulfuric electrolyte (Watts) as it is the most inexpensive and environmentally friendly as compared to the sulfaminic one. Besides, the allowed time of exposure of the sample in the air after the anode-cathode treatment before nickel-plating in the sulfuric electrolyte is more than the one in case of the sulfaminic electrolyte. It is an important criterion for nickel-plating of large-scale parts in industrial production.

1.1.1.3. A break between the operations of the anode-cathode treatment and nickel-plating is inevitable in the nickel-plating technology, i.e. the sample will be in the air for some time. Polarization curves of potential variation on the steel surface as a function of time of the exposure of the samples in the air before nickel-plating were taken to evaluate the permissible time of breaks between the operations. Then the influence of the potential of the steel surface on the adhesion of the coating with the substrate was studied

The surface of a steel sample was cleaned, degreased; it underwent the anode-cathode treatment and was installed in an electrochemical cell. The results of measurement are given in Fig. 1.3.

The potential of the steel is shifted to the positive under the influence of steel passivation with the growth of time of exposure of the sample in the air. In the initial section, when thickness of the oxide film is small and does not influence the diffusion rate of oxygen in the zone of growth of the passivation film the oxidization follows the law of a direct a line. With the growth of film thickness the dependency becomes more complex, and the growth of the film follows the law of parabola as the diffusion processes slow down with the growth of thickness and density of the oxide film.

Adhesion of the coating and the substrate as a function of the potential and of the time of exposure in the air was determined in the following way. Potential of the steel surface was meas-

ured after the anode-cathode preparation. Then the samples were nickel-plated. Adhesion of the nickel coating was evaluated by bending the samples to 90° until their fracture.

The results of tests are given in Table 1.4.

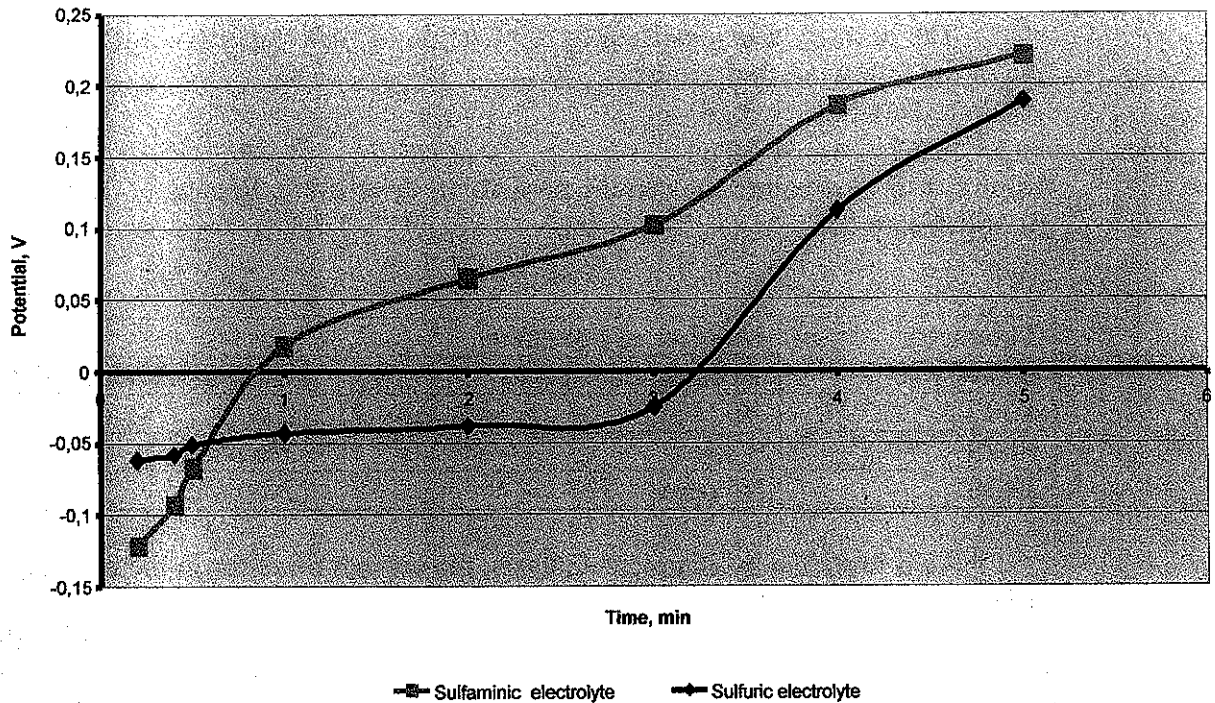


Fig. 1.3. Potential of the surface of 20X23H18 steel as a function of the time of exposure in the air.

Table 1.4.

Adhesion of the nickel coating and the substrate as a function of potential of the surface of the treated steel and the time of its exposure in the air.

Nº	Potential of the steel surface, B	Time of exposure in the air, min.	Adhesion of the coating and the substrate.
Sulfuric electrolyte			
1	-0,062	0,2	Good
2	-0,058	0,4	
3	-0,051	0,5	
4	-0,043	1	
5	-0,038	2	
6	-0,025	3	
7	0,112	4	No adhesion
8	0,189	5	
Sulfaminic electrolyte			
1	-0,121	0,2	Good

2	-0,093	0.4	No adhesion
3	-0,067	0,5	
4	0,018	1	
5	0,065	2	
6	0,102	3	
7	0,186	4	
8	0,221	5	

As it comes from Table 1.4, with the growth of time of the exposure in the air the potential is shifted to the positive and the adhesion of nickel with the substrate worsens. So, it was found out that a maximum break between the operations of the anode-cathode treatment and nickel-plating in the sulfuric electrolyte is 3 minutes and in the sulfaminic electrolyte it is 30 seconds.

1.1.2. Scheme of the technological process

In the second quarter /5/ samples with $\sim 75 \mu\text{m}$ nickel coating after thermal treatment in vacuum at 800°C during an hour were tested. The structure of the coating at the not annealed samples is columnar with an evident stripy nature. After annealing there were changes in the structure of the coating. After 100-hour corrosion tests the microstructure of both samples became identical, i.e. thermal treatment does not influence the properties of the coating in the long run.

Basing on the results of the research performed, there was taken the following scheme of the technological nickel application process onto 20X23H18 steel using a galvanic method, which is given in Fig. 1.4.

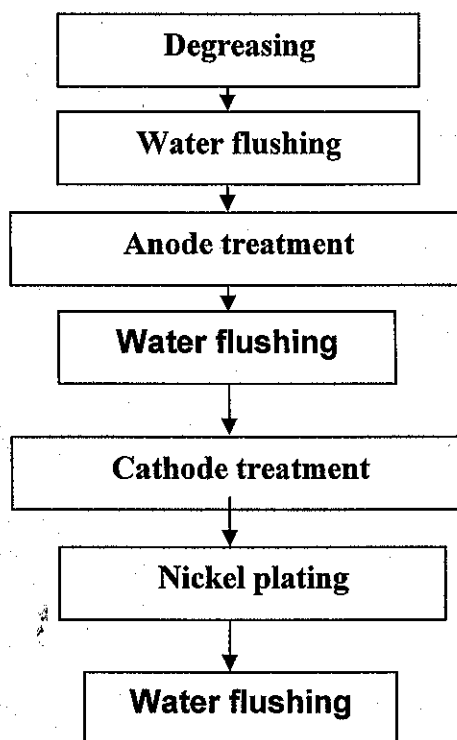


Fig.1.4. Scheme of the technological process.

1.1.3. Metallographic research on the coatings after 1500-hour corrosion tests.

Samples of 20X23H18 steel nickel-coated on one side using a galvanic method underwent metallographic research before corrosion tests and after them (following the technique described in Appendix 3); the tests were held during 250, 500, 750, 1000 and 1500 hours.

Micro specimens were made in a cross-section of the samples using common methods. Microstructure of coated steel samples before the tests in molten carbonates is shown in Fig. 1.5. Thickness of the coating is 50-60 microns.

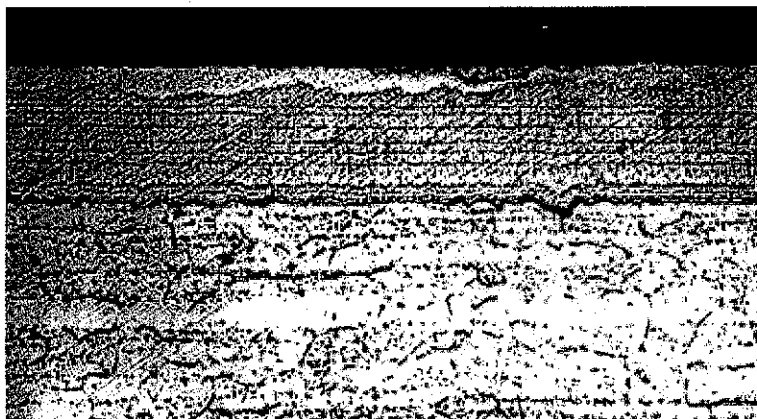
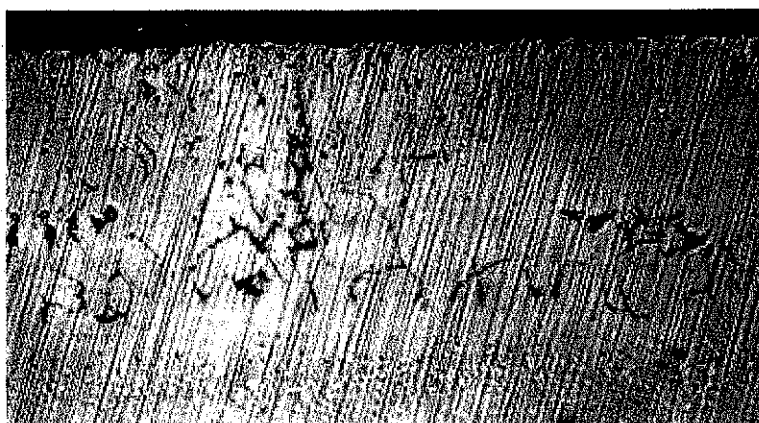


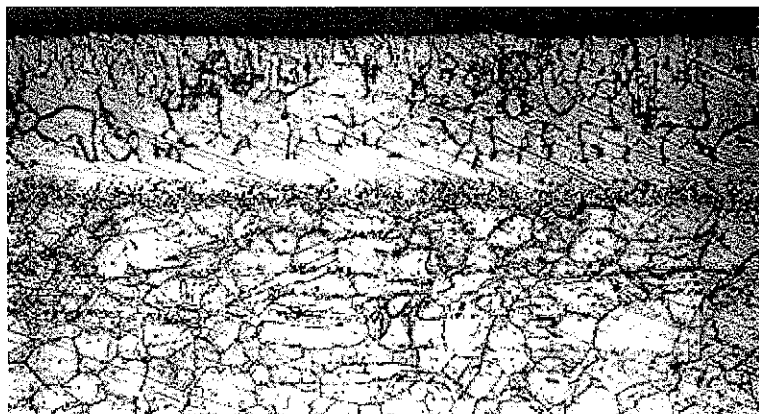
Fig.1.5. Microstructure of a sample coated with galvanic nickel (before corrosion tests), x 400

Microstructure of the coating before corrosion tests comprises columnar crystals with evident stripy character. Microstructure of steel represents austenite grains of polyhedral shape with doubles.

All samples after corrosion tests show inter-crystalline corrosion of nickel coating observed without chemical etching of micro specimens (Fig.1.6a, 1.7a, 1.8a). The depth of inter-crystalline corrosion after 250 and 500-hour exposure of the samples is 30-50 microns, after the tests during 750 hours it is ~ 70 microns and after exposure during 1000 and 1500 hours it is ~75 microns.

Microstructure of the samples after corrosion tests is shown in Fig. 1.6-1.8. Microstructures of the samples after corrosion tests during 250 and 500 hours are identical and are shown in Fig.1.6. Microstructure of the samples after corrosion tests during 750 hours is shown in Fig.1.7. Fig.1.8 shows microstructure of the sample after the tests during 1000 and 1500 hours.





a – without etching, x 800; b – after etching, x 400

Fig.1.6. Microstructure of a sample coated with galvanic nickel after the tests during 250 and 500 hours.

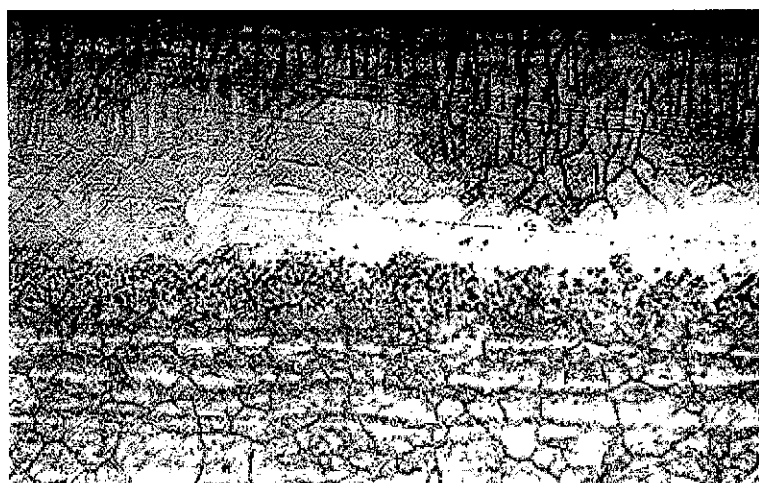


Fig.1.7. Microstructure of a sample coated on one side with galvanic nickel after the tests during 750 hours, x400.

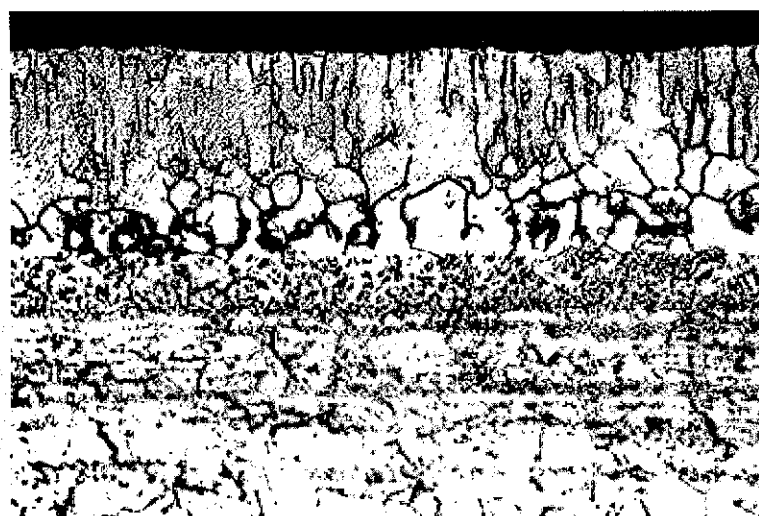


Fig.1.8. Microstructure of a sample coated on one side with galvanic nickel after the tests during 1000 and 1500 hours, x400.

Microstructure of the galvanic nickel coating after corrosion tests has changed considerably as compared to the initial sample. All the samples are characterized by the presence of the zone of columnar crystals going from the surface of the coating 12-30 microns deep and a diffusion layer comprising two structural zones: a zone of a light color 12-21 microns thick adjacent to the coating and a zone of a gray color with a fine-dispersed structure 12-21 microns thick adjacent to the substrate.

Microstructure of 20X23H18 steel comprises two austenite grains without traces of inter-crystalline corrosion.

The results of microhardness measurements on the nickel coating and on the steel in the middle zone of thickness of the plate are given in Table 1.5.

Table 1.5.

Microhardness of a one-side nickel coating and steel before and after corrosion tests

The place where microhardness is measured	Microhardness, kgs/mm ²					
	Before corrosion tests	Time of testing, hour				
		250	500	750	1000	1500
Nickel coating	254	218	178	164	206	181
Steel	258	223	247	258	254	223

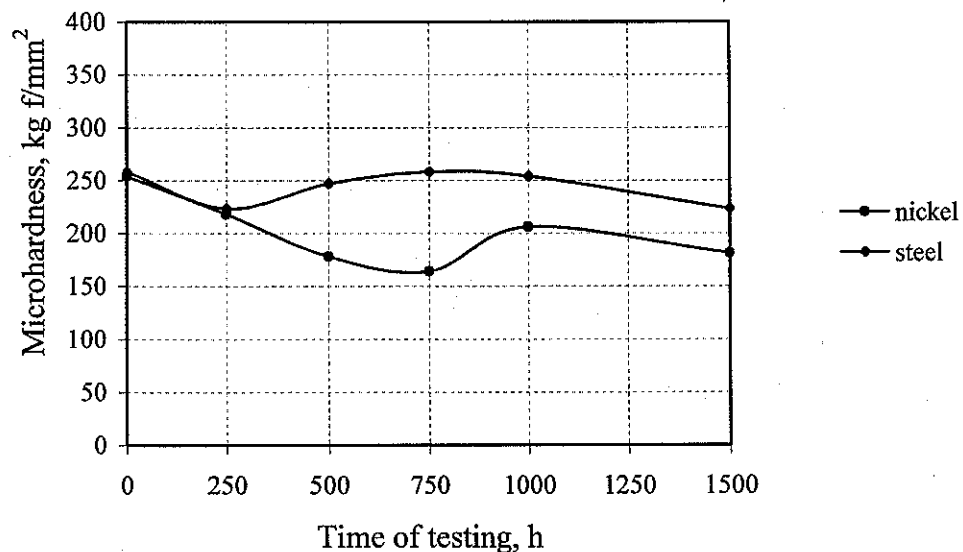


Fig.1.9. Microhardness of the coating and of the steel as a function of time of corrosion tests.

Microhardness of the samples was measured using the IIMT-3 device with loading at the indenter of 20 g.

1.1.4. Inter-diffusion of nickel and iron in the process of 1500-hour tests.

Study of the samples before and after corrosion tests was done using electron probe microanalysis device. Quantitative measurements of the chemical composition of the coating were registered in the modes of linear semi-quantitative and quantitative microrentgeno-spectrum analyses. The samples were studied after 250, 500, 750, 1000 and 1500-hour corrosion tests.

Thickness of the nickel coating with consideration of nickel diffusion into the substrate measured by images in the modes of BEI makes up from 55 up to 82 microns.

The depth and the profile of inter-diffusion of iron and nickel were measured using program of linear X-ray spectrum analysis under the following scanning conditions: a step of scanning is 2 microns, the controlled parameters are Ni, Fe, Cr, K, O.

The sample after 1500-hour tests revealed that Fe diffusion into the nickel layer measured by level 0.1 from the average concentration of Fe goes through all the layer of the nickel coating. In the samples that underwent 1000 hour and longer testing, concentration profiles go through the pores – incorporations of a dark color with average atomic mass less than that of the substrate. Besides the basic elements in pores (Ni, Fe, Cr, Mn, Si) K and O are also registered there, i.e. presence of the electrolyte is noticed there.

1.1.5. A technology to weld the plates from 400 mm wide tapes.

1.1.5.1. Full-size sheets for bipolar plates are made by welding of steel tapes, the width of which is about 420 mm.

A set of research work was done in order to choose the best kind of welding and the best way to treat the edges to be welded /5,6/.

As a result of this research, it was found out that the best quality of the welded seams is provided by the argon-arc welding (AAW) with $0.5 \div 0.8$ mm overcloaks of the welded edges (cm. Fig.1.10):

- The welded seams have austenite structure;
- there is a stable formation of the welded joint with melting-through the whole thickness (0.4 mm) of metal samples;
- burn-through of the metal is surely eliminated;
- selected geometry of the seams is produced with the width of $1.5 \div 2.3$ mm with a local height of strengthening of seams up to 0.05mm, there is no thinning of seams;
- the samples have minimum hogging up to 4.8mm when the sample is 500mm long. Deformation of the samples is "soft" and is easily removed with a slight pressing to provide flatness of the samples.

Microstructure of a pilot welded seam is given in Fig.1.10 /6/.

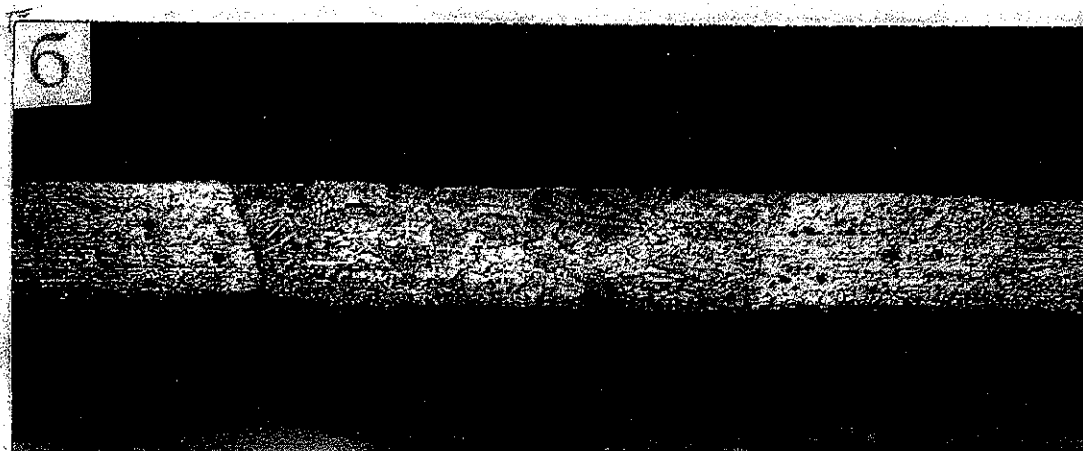


Fig. 1.10. Structure of the welded seam made by auto argon-arc welding in the longitudinal axial section of the sample made of 20X23H18 steel (x30).

КД А0712/3 – P313 design documentation was worked out for welding of full-scale sheets for А0711-Р871.01.050 bipolar plates; the assembling and welding riggings were made with a steel cooling lining and steel clamping bars as long as the joint (1600 mm). А0712/3-Р307 device [7] was designed and made to check the impermeability of the weld of the full-scale sheets.

1.1.5.2. Technological process of manufacturing a full-size plate comprises the following basic operations.

A0711-P871.01.050 sheet is made by welding of stripes from the tape 0.4x420-IIT-HO-20X23H18 (state standard GOST 4986-79).

Stripe billets were cut out from the tape with allowance for finishing. The stripes were given the final sizes using cushion plates made of steel of a regular quality (st.3, steel 10, steel 20). Parallelism of sides was ensured during the processing, it was controlled by diagonals of the stripes. After finishing, there was done milling of the edges for welding according to Fig.1.11. At the place of welding rough edges were not removed, feathered edges were not blunted.

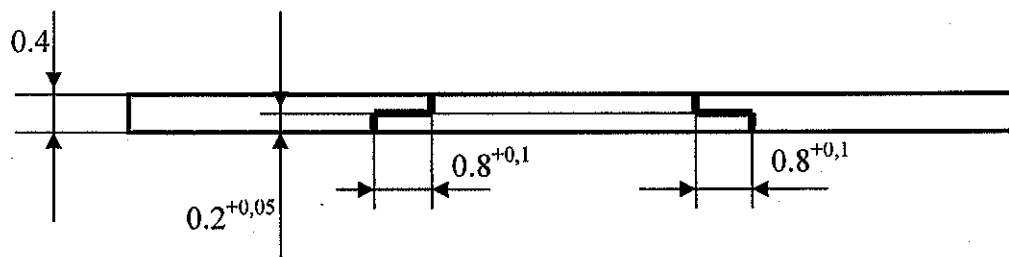


Figure 1.11

Before welding, the edges of the stripes were degreased in alcohol. The joints of two stripes were tied up preliminary. The assembled in couples stripes pressed to the linings were joint together by mechanized AAW at a high speed of welding (about 10 mm/s) in sections of 10-15 mm with a step of joining of 50÷60mm. The joining was done from the middle to the edge along all the length of the stripe joint (to reduce deformation of the stripes). High welding rate let us have the surface joining with a small depth of fusing and fix the edges being welded preventing shifting and overlapping and pressing to each other /7/.

Welding is done in accordance with state standard GOST 14771-76. The assembled and tied up stripes were installed in the appliance on the welding table. A steel cooling-down lining (support) is put and fixed to the joint of stripes; its forming groove is strictly combined with the axis of the joint to be welded. ЭЗП-5-2 burner is fixed at the tripod of the manipulator; the movements of the burner is adjusted to the axis of the joint in a no-operation mode. Stick-out distance of the electrode makes up 7÷8mm; the arc space is 0.5÷1mm. The electrode is made of tungsten of BJI-1 type, $\varnothing_{el}=1\text{mm}$, an electrode tip is «needle-like».

The welding is done in a pulse mode of the current.

The welding mode:

Current of a pilot arc	5A
Current of welding	10÷12A
Welding rate	4÷6mm/sec
Pulse time	0.22 sec
Pause time	0.02 sec

Requirements for the welded seams are of the II group of the standard OCT B95 1487-86.

The welding of the stripe joints to reduce the stress and deformation is done using the techniques called a "reverse- step" technique and "from the middle to the edge" technique.

1.1.6. Site of galvanic nickel plating

1.6.1. Design documentation for a line of galvanic baths and auxiliary equipment (ventilation, electric wiring etc.) was worked out. Its volume is about 300 pages (A4 format). Assembly units and parts of the line are shown in the assembly drawing and in the structure chart /5/.

The materials and equipment were acquired; special riggings for nickel plating were made.

A room was prepared for location of galvanic baths. Equipment earlier located there was removed; the ventilation system, electric supply, water supply and industrial sewerage systems were reconstructed; redecoration of the room was done.

After the baths were made in the workshop, assembling of the line was done to reveal and remove the defects. In the process of installation the galvanic baths were put at the places of their permanent operation in a sequence according to the technological process of nickel plating: a bath of the anode etching – a rinse tank – a bath of the cathode etching – a bath of nickel plating. On-board ventilation exhausts were connected. Water-jacket of the nickel-plating bath was connected to the hot water supply system and industrial sewerage system, and a rinse tank was connected to the cold water supply system and to the industrial sewerage system. An electric supply unit and a switchgear board were installed; electric wiring work was completed.

The internal surface of the baths made of ferrous metal is protected from the contact with the rinsing water and electrolyte with special welding bags of plastic 4 mm thick.

Lead and nickel electrodes were put and fixed in the etching and nickel-plating baths, respectively. Cathode section of nickel plating was assembled. There was mounted a monorail with a carriage and a lifting mechanism to move the cathode assembly with the part being coated along the line of baths and putting it into the bath and lifting it.

In the course of installation and after it had been completed, there were performed some tests and adjustment and alignment:

- Impermeability of the water-jacket of the nickel plating bath was checked;
- Reliability of the sealing of the internal surface of the sheet covered on one side was checked;
- A mode of heating for the electrolyte to reach the operating temperature was determined;
- Operability of a power supply for its equivalent load was checked, tests of current supply under the load of 500A were done using a cathode etching bath;
- Operability of a mechanism to move and to lift the cathode assembly was checked.

It was found out that it takes a trained operator not more than 1.5 minutes to take the cathode assembly out the etching bath, to move it to the nickel-plating bath and put it into the bath. It takes not more than 0.5 minute to switch on the nickel-plating bath loaded with the cathode assembly. The resulted time behavior meets the requirements of the technological process (3 minutes).

1.1.6.2. During improvement of the nickel coating technology on sheets of stainless steel 0.4 x 712x 1296 mm in size the following research was conducted at the site of galvanic nickel plating /7/:

1. Adjustment of the process of reactivation of the anode-etching electrolyte.
2. Adjustment of the operation of slime removal from the steel surface.

In long exploitation of the anode-etching electrolyte (20 % of sulfuric acid) it gets contaminated with sulfates of iron and chromium, which are accumulated in the solution and change elemental composition of the electrolyte. Solution of a sulfuric acid turns yellow and requires periodic clearing. When a large amount of sulphates salts are present in the solution, they cake at the bottom of baths. They drain clean solution, and the sink is cleaned from the deposit. However, this method is inconvenient when we work with baths of large volumes. There was done some research on electrolytic removal of metallic impurities. It was found out that the periodic work through of the electrolyte at a current density of 0.1-0.5 A/dm² provides clearing of solution from ions of iron and chromium.

After the anode etching the steel surface keeps some traces of slime, which consists of iron oxides Fe₃O₄ and iron carbides Fe₃C indissoluble in a sulfuric acid and poorly removed during washdown in water. The slime traditionally is removed by mechanical wiping with a cotton pad; then the surface is pickled at the cathode in 20% solution of sulfuric acid within 1 minute. The

research on the electrolytic deleting of slime at the cathode in the 20 % solution of sulfuric acid was conducted. The outcomes of the experiments are shown in Table 1.6.

Table 1.6

Mode of Slime Removal		
Cathode density of current, A/dm ²	Time, min	Condition of the Surface
3	1	Presence of slime
	10	Presence of slime
	15	Presence of slime
6	1	Presence of slime
	3	Presence of slime
	5	No slime
10	0,5	Presence of slime
	1	No slime

As an outcome of the research the modes of slum removal using an electrolytic method were identified:

- Current density is 6 A/dm², the time of etching is 5 min,
- or
- Current density is 10 A/dm², the time of etching is 1 min.

The solutions for chemical desmutting were tested. The characteristics of solutions, the structure and treatment schedules are shown in Table 1.7.

Table 1.7

Characteristic of dips				
№	Structure of solutions	Concentration, g/l	Mode of treatment	
			Temperature, °C	Time, min
1	Sulfuric acid	25	Room	5
	Chromium anhydride	100		
	Sodium salt	4		
2	Caustic soda	80	70	3
3	Nitrogen acid	80	Room	5 sec.
	Sulfuric acid	100		

All chemical reactants, acids, laboratory equipment, utensils and devices to prepare the electrolyte (dissolution, filtering etc.) were purchased. A special vessel (about 1000 liters) was bought for the distilled water.

A site of galvanic nickel-plating was prepared for application of the nickel coatings onto the full-size sheets for BSP (see. Fig. 1.12).



Fig. 1.12.

1.1.7. A combined Ni – Cu coating.

Implementation of **barrier-free layers** on 20X23H18 steel to prevent diffusion of elements of steel into the nickel coating was studied in experiments with two types of the coating – a TiN protective coating and a copper galvanic one.

Implementation of a TiN protective coating is well known. Tests under MCFC operation conditions during 1000 hours also gave a good result.

Titanium nitride was sprayed on using a vacuum method – a method of **condensation with ionic bombardment** (CIB). Metallurgical analyses showed that microstructure of TiN-coated steel was practically identical after corrosion tests during 250, 500, 750 and 1000 hours. Thickness of the coating on samples was from 6 up to 8 microns. Not coated areas, separations, cracks and other defects of the coatings were not revealed. There was observed minor closed porosity characteristic for such kind of coatings.

Fig.1.13 shows microscopical maps of structures of the titanium nitride coatings on steel samples after corrosion test during 250 and 1000 hours, respectively.

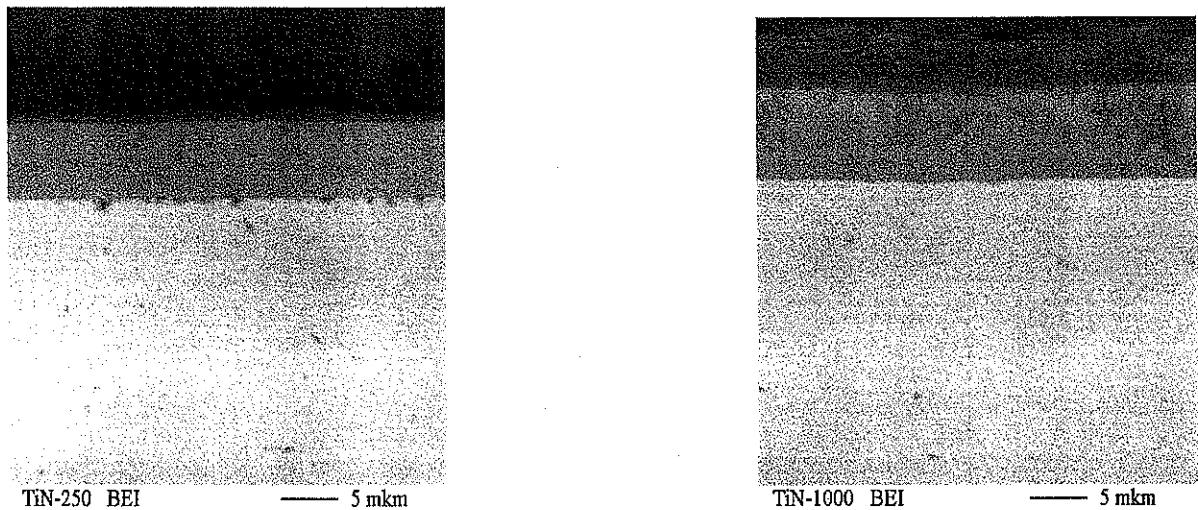


Fig.1.13. Electron microscopical maps of the structures of the titanium nitride coatings on steel samples after corrosion test during 250 and 1000 hours.

Titanium nitride coatings protect well under operation conditions of an MCFC.

The attempts to coat titanium nitride with galvanic nickel, as it was required by the task of the Project, failed. However, a protective coating of titanium nitride has the right to exist by itself. Earlier in Russia there were known facilities of "Bulat" type to coat not large areas only, but now industrial facilities make it possible to coat large surfaces keeping the cost of the coating low.

Special interest was drawn to the results of the tests of nickel coating with the copper sub-layer on 20X23H18 steel. Results of metallographic analyses of these samples are given below. Samples of 20X23H18 steel coated on two sides (the coating consisted of several layers – a thin layer of galvanic nickel applied immediately onto the steel, followed by a layer of copper and the main layer of galvanic nickel) were studied before and after corrosion tests in the melt of carbonates at 650⁰ C during 1500 hours. Microstructure of the coated steel was studied in cross sections of the samples on micro-slices made by the generally accepted technique using "NEOPHOT - 32" light microscope.

Microstructure of the sample before corrosion tests is shown in Fig.1.14.

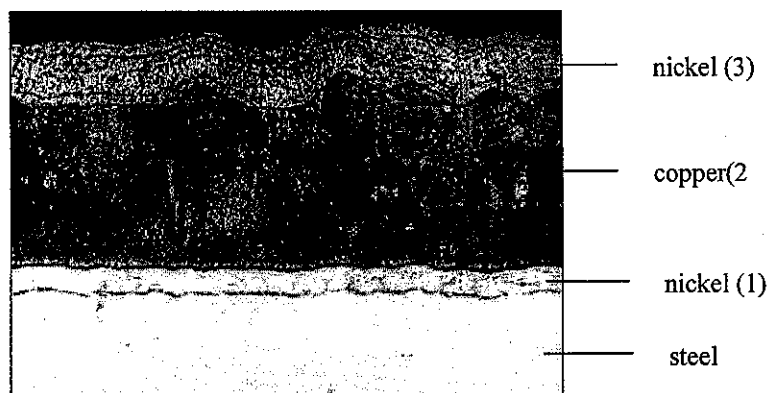


Fig. 1.14. Microstructure of the coating on the steel before corrosion tests, x320

According to Fig. 1.14, the coating consists of several layers: a layer of nickel (1) ~ 9 – 13 microns thick, which is applied immediately onto the steel; there is a layer of copper above it (2) ~ 70 – 80 microns thick and a layer of nickel (3) ~ from 40 up to 60 microns thick. All the layers in this coating have a columnar structure characteristic for galvanic coatings. The layer of nickel (3) reveals some stripes besides the columnar structure.

Microstructure of the sample after corrosion tests is shown in Fig. 1.15.



Fig. 1.15. Microstructure of the coating after corrosion tests, x320

Microstructure of the coating after corrosion tests underwent considerable changes. The grain structure is observed in the nickel layer, the same as in the layer of copper. There are friable areas in the layer of copper. Two diffusion zones are observed between the layer of copper and a layer of steel. The diffusion zone of light color adjacent to the steel has the thickness of ~ 10 microns, and above it there is a zone of dark color ~ 8 microns thick. The light and dark diffusion zones were apparently formed as a result of inter-diffusion of members of steel, of the nickel layer (1) and the copper layer (2), and as a result of infiltration of a carbonate electrolyte from an opened circumferential shear deep into of the sample. Results of chemical analysis testify to this, too. Traces of K and O are detected in the diffusion zones. Opened circumferential shear of the sample is the only path of infiltration of the electrolyte, as the basic coating is pore-free and represents a Ni-Cu solution.

Traces of corrosion after corrosion tests during 1500 hours were not revealed in the outside nickel layer or in the steel under the coating.

So, Ni-Cu coating can appear a promising one, as operations of nickel plating and copper-plating can be easily parts of a unified manufacturing process //.

1.1.8. Technical and economical analysis.

Technical and economical evaluation of the cost parameters of bipolar plates of 20X23H18 stainless steel coated with galvanic nickel was done. According to the initial information from Fuel Cell Energy (FCE), the final goal of production is to be the level of 400 thousand full-scale plates a year. In order to get a saleable price of a nickel-plated bipolar plate on the basis of FOB conditions, Saint-Petersburg, Russia (in accordance with rules of INKOTERMS) three variants to establish production of the above-mentioned plates are considered in this project and they are characterized by the following:

- Computerized manufacturing of plates, where a portion of manual work is big, within a specially established entity – a juridical person (entity). Equipment necessary for galvanic coating is made in RFNC-VNIIEF;

- Large-scale manufacture on the basis of automated galvanic lines within a separate juridical entity. Equipment necessary for automated production is purchased at the most acceptable commercial price;
- Large-scale automated manufacture of plates, when a leasing mechanism is implemented in purchasing necessary equipment.

According to the calculations performed, the cost of one 0.4 x 712x 1296mm bipolar plate coated with galvanic nickel under conditions of large-scale manufacture (400,000 plates a year) is 44 dollars US. The initial data, approaches and results of calculations are given in Appendix 4.

1.1.9. Delivery of the plates to FCE (Tasks 1 and 2)

A meeting of the Russian delegation of Project participants with collaborators from ANL (M. Krumpelt, D. Ehst et al) and a representative of the industrial partner on the Project, Chao-Yi Yuh from FCE (USA), took place in the Argonne National Laboratory (USA, November 18 – 23, 2003) to discuss main outcomes of the work in the II – V quarters of this Partner's Project. After the discussion the parties came to the agreement that the Tasks of the Project were completed at full scale and in time. Representatives of ANL and FCE suggested our doing additional research on Tasks 3 and 4 in the rest of the time on the Project without changing the total funding. Additional work was to be done at the expense of re-distribution of the funds for Tasks 1 and 2, having refused from the delivery of both nickel-plated stainless steel sheets (20X23H18) 0.4 x 712x 1296 mm in size (Task 1) and sheets 0.8 x 712x 1296 mm in size made of a new alloy (Task 2). The outcomes of the discussions held and the decisions made at the meeting are reflected in the joint Records of the Meeting; on the basis of them there were made changes in the Work Plan (“ADDENDUM #3 TO PARTNER PROJECT AGREEMENT #2281p”).

According to «ADDENDUM #3», 4 samples of 20X23H18 steel 180x180x0.4 mm in size and 4 samples of a new alloy X30H45IOT (a new alloy on Task 2) 180x180x0.8 mm in size were sent to FCE (USA) instead of nickel-plated sheets of 20X23H18 steel 0.4 x 712x 1296 mm in size (Task 1) and sheets of a new alloy 0.8 x 712x 1296 mm in size (Task 2). The specified samples and a set of documentation including the decision of a Commission of Experts #002/161/IICIP dated April 6, 2004 that approves the delivery to the USA without licensing were passed to ISTC for further sending them to the FCE (USA) according to the “Acceptance Report and Deed of Conveyance dated April 22, 2004” (see i.2.5).

The reasons for the refusal from the coated plates and from the new alloy from BSP are evidently as follows. In autumn 2003 a problem of reduction of the State subsidies for expensive PP on FC was critical. There was formulated a condition to reduce considerably the prime cost of FC manufacturing. The manufacturers found themselves in the search for urgent reduction of the cost. At the «First International Conference on Fuel Cell Development and Deployment» (07 March 2004 - 10 March 2004, Storrs, CT, USA) Hans Maru (the President of Fuel Cell Energy, Inc., USA) answering the questions after his presentation said that FCE refused from implementation of coatings. Judging by what was said by some other specialists improvement of the lifetime at the expense of coatings and more stable but more expensive alloys was put off till some other time in future, though maybe not so far future.

1.1.10. Conclusions

1.1.10.1. An environmentally friendly nickel-plating process was worked out to coat 20X23H18 steel. It makes it possible to produce coatings with good adhesion. The process is simple in realization and cost-effective.

1.1.10.2. The research revealed that there was no need of thermal treatment of samples with nickel coatings in vacuum at 800°C during an hour. Thermal treatment does not influence the properties of the coating, as after testing under implementation conditions the microstructure in

the annealed samples became identical to the microstructure of the samples that had not been annealed.

1.1.10.3. Results of 1500-hour corrosion tests show that a galvanic nickel coating is characterized by the following:

- inter-crystalline corrosion with formation of pores filled with the electrolyte develops;
- as the metallographic analysis shows, small pores locally pass to the full depth of the coating;
- a method of micro X-ray spectrum analysis reveals that Fe diffusion into the nickel layer goes through all the layer of the nickel coating.

However, the microstructure of the substrate (20X23H18 steel) kept fine austenite grains without any traces of inter-crystalline corrosion. So, a galvanic nickel coating completed its protective function under conditions of 1500-hour implementation.

1.1.10.4. A combined Ni – Cu coating can appear rather promising as no traces of corrosion after the tests during 1500 hours were observed in the external protective layer, there is no iron diffusion. Besides, the procedures of galvanic nickel plating and copper plating suit one engineering process.

1.1.10.5. A technology to weld full-scale plates of 20X23H18 steel tapes 400mm wide was worked out. The technology provides the impermeability of the welded seams, as well as flaring and wallows of the seams for not more than 0.05 mm.

1.1.10.6 Design documentation was worked out; the materials and equipment were purchased; special riggings were made for the nickel-plating area. A line of galvanic baths was made and mounted. There was worked out a technology to apply nickel coating onto the sheets of stainless steel 0.4 x 712x 1296 mm in size. The site of galvanic nickel plating was prepared for application of nickel coatings onto full-scale sheets of BSP.

1.1.10.7. According to the calculations, the cost of one 0.4x712x1296 mm bipolar plate coated with galvanic nickel under conditions of large-scale production (400 000 plates a year) makes 44 dollars US.

1.2. Explosion cladding of 20X23H18 steel

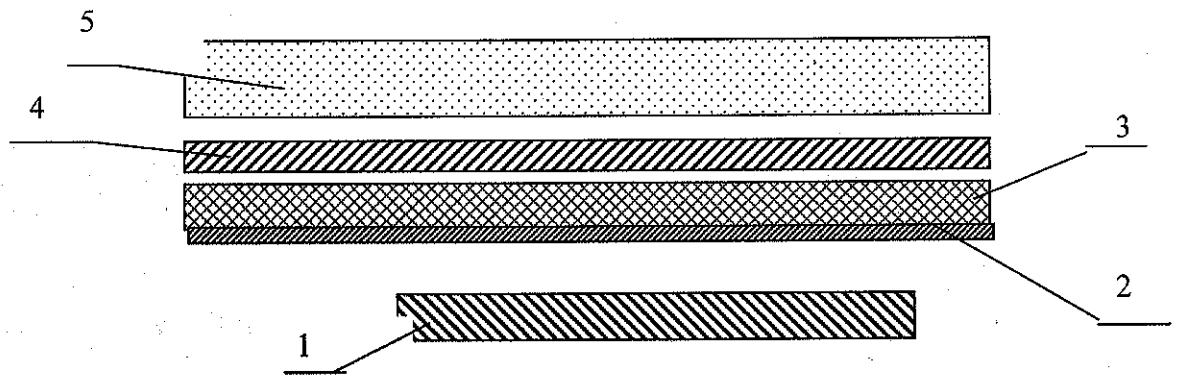
1.2.1. Peculiarities of explosion cladding. Choice of a cladding scheme.

For the tasks of the Project the difficulty in explosion cladding lies in the fact, that coating application is done by throwing of the nickel foil 0.1 mm thick on a fixed substrate (20X23H18 steel) 0.4mm thick. And a common explosion cladding is considered to be the one when the plate to be thrown (applied) is several millimeters thick. Implementation of a foil not thicker than 0.1 mm stipulates additional precautions to prevent destruction or damage of the foil by the explosive. General peculiarity of the explosion cladding lies in the difficulty of its theoretical simulation and necessity of a lot of experimental work.

With consideration of specific features of the given task, development of the cladding technique comprised the following stages: a choice of a scheme of explosion cladding and of an explosive, identification of the criteria to evaluate the quality of the explosion cladding, experimental determination of the parameters of the process to produce a necessary plate. It was considered expedient to start experiments with plates with a small area of cladding ($S \approx 100\text{cm}^2$) gradually followed up by experiments with larger sizes. Cladding of plates with a small area is a less difficult task, and the experimental results can be used when making the plates of necessary sizes.

The choice of explosion cladding schemes was also based on the specific character of the given task (small thickness of the layer being thrown and a danger of its destruction). The layout given in Fig. 1.16 /8 / was chosen having analyzed the information accumulated by the Project participants and after the study of patents. The specified scheme differs inconsiderably from the scheme of explosion cladding with a foil described in /9/. According to the mentioned scheme

/9/, for welding with a gap or not, the cladding material (e.g. foil) is fixed to a thicker false plate. A thin layer of lubricant is put onto the false plate to prevent welding of the foil to the false plate. Availability of the false plate prevents destruction of the foil with the explosive and formation of sagging; it allows us to have a uniform gap and to produce a high-quality joining. It is known /8-10/ that analogous functions are performed by a metal plate and a not metal plate, which are called a hard plate and a soft plate, respectively.

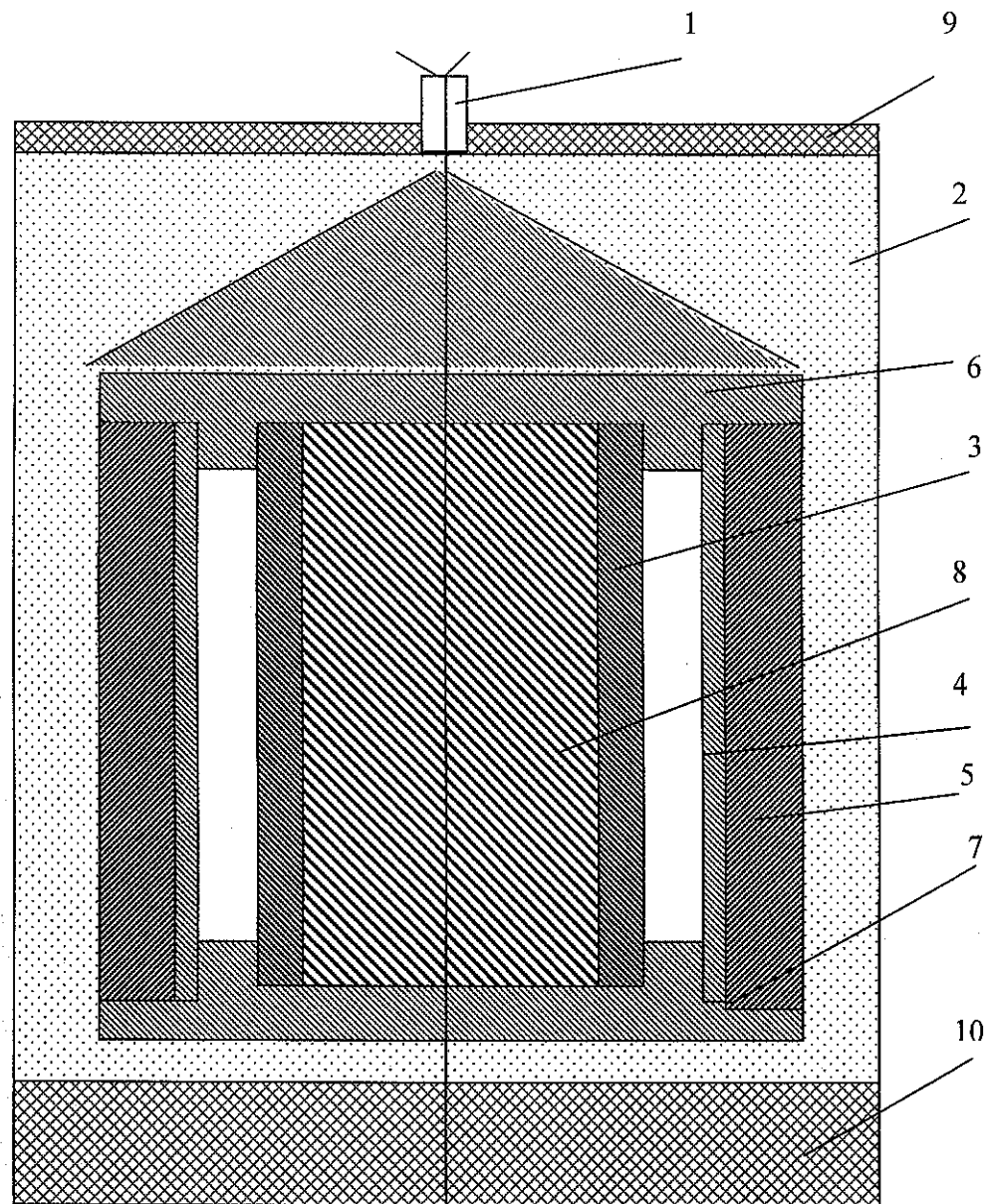


- 1- a substrate (a fixed component being coated);
- 2- a foil (a cladding component being thrown (applied));
- 3- a soft plate;
- 4- a hard plate;
- 5- an explosive.

Fig.1.16. A scheme of direct cladding.

Besides the scheme of Fig.1.16, it is also possible to use a cladding scheme with a cylindrical surface (see Fig.1.17).

To do the cladding following the mentioned scheme, the substrate (the part to be coated) and the nickel foil are folded to make a tube, and then they are unfolded after cladding to make a plate (a sheet) of the coated plate. In this scheme an intermediate component 5 is designed for the same purpose as a hard plate in the scheme of Fig.1.16



1-an electric detonator, 2-an explosive, 3-a part being coated, 4- a cladding component,

5-an intermediate component, 6-a centering cone,

7- a centering basis, 8- a mandrel, 9,10- end plates.

Fig. 1.17.

At the same time with the choice of schemes, the most preferable for the task explosive was selected. In accordance with recommendations /9,10/, the rate of detonation D of the explosive used for the explosion welding must be more than 1500 m/s and less than the value of acoustic speed in the metals being welded. As an acoustic speed in nickel is $C = 4780$ m/s, and in steel it is 5000 - 6000 m/s, a recommended range of detonation values for the implemented explosive is: $1500 < D < 4780$ m/s. Mix explosives (ammonite № 6ЖБ ($D = 3600-4800$ m/s) and ammonite AT ($D = 2000-3600$ m/s)) meet this requirement.

Two basic criteria were selected to evaluate the quality of cladding. The first one is the condition of the coating (any cracks, swellings or dents etc.), the second criteria is the strength of

adhesion between the coating and the substrate. Comparative evaluation of the coating condition was done by the ratio of the total area of defects of the coating S_d revealed visually to the cladding area S_c . The strength of adhesion between the substrate and the coating was evaluated using bending-unbending test to $\pm 90^\circ$. During this test these samples of bimetal plates must not reveal any delaminating (exfoliation) in the zone of contact of nickel and 20X23H18 steel.

Additionally the quality of the explosion cladding was evaluated by condition of the zone of contact between the foil and the steel. It was considered satisfactory if the metallographic analysis of the bipolar plates in the contact zone did not reveal pores, voids etc. Besides, by the character of the contact zone you can judge about necessity to change or not to change the parameters of the process (thickness of the explosive ($H_{expl.}$) and welding clearance (Δ)).

1.2.2. Experimental polishing of explosion cladding.

The necessity of experimental work arose primarily from the lack of information on the basic parameters of the process, such as the weight of the explosive charge, the size of the gap between the plates to be welded etc.

At the initial stage of experimental work explosion cladding was done using plates with the area of cladding of $S \approx 100\text{cm}^2$ (the scheme in Fig. 1.16) and explosion cladding was done following a cylindrical scheme (Fig. 1.17) with the area of cladding of $S \approx 220\text{cm}^2$.

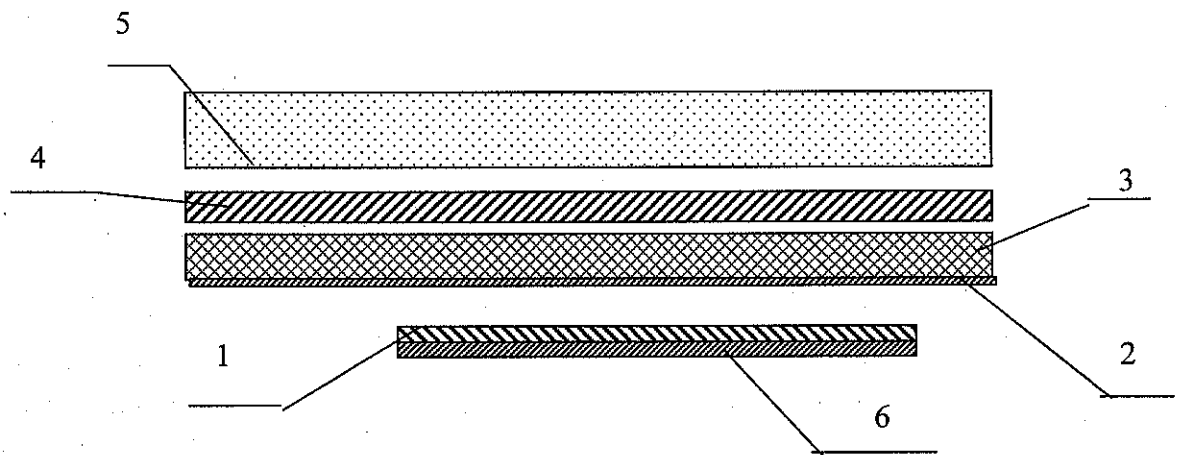
The goal of the experiments was to determine in a preliminary way parameters of the explosion cladding and to evaluate the effect of different components of the scheme on the quality of cladding. Ammonite 6ЖБ and ammonite АТ were used as explosives for the explosion cladding in the flat and cylindrical schemes, respectively. Thickness of the explosive was minimum possible (close to the critical one).

As a result of preliminary experiments, there were produced bimetal plates with satisfactory strength of adhesion between the substrate and the coating; S_d as related to the total area of cladding S_c was 20% and 30 % for the flat and cylindrical schemes, respectively. Besides, when evaluating results of experiments performed by the scheme of Fig.1.16, significant deformation of bimetal plates was noted. A steel substrate was introduced into the assembly to eliminate deformation. Further experiments were done according to the scheme of Fig.1.18.

Basing on the results of the preliminary experiments there was made a conclusion that when studying the parameters of the process as they influence the quality of the explosion cladding the main attention should be focused on the thickness of the soft and hard plates (T_T , T_M) and the welding clearance (Δ). The specified parameters were evaluated using the areas of cladding of $S_{cl} = 400\text{cm}^2$. The parameters varied in the following way: Δ from 0.5 to 4.0 mm with a step of 1.0mm; T_T from 1.0 to 2.5 mm with a step of 0.5mm; T_M from 1.0 to 4.0 mm with a step of 1.0 mm. Having analyzed the experimental data the preferences were given to: $T_T=2.0$ mm, $T_M=2.0$ mm and $\Delta=2.0$ mm. However, even in case of the optimum parameters there were defects of the coating on the plates.

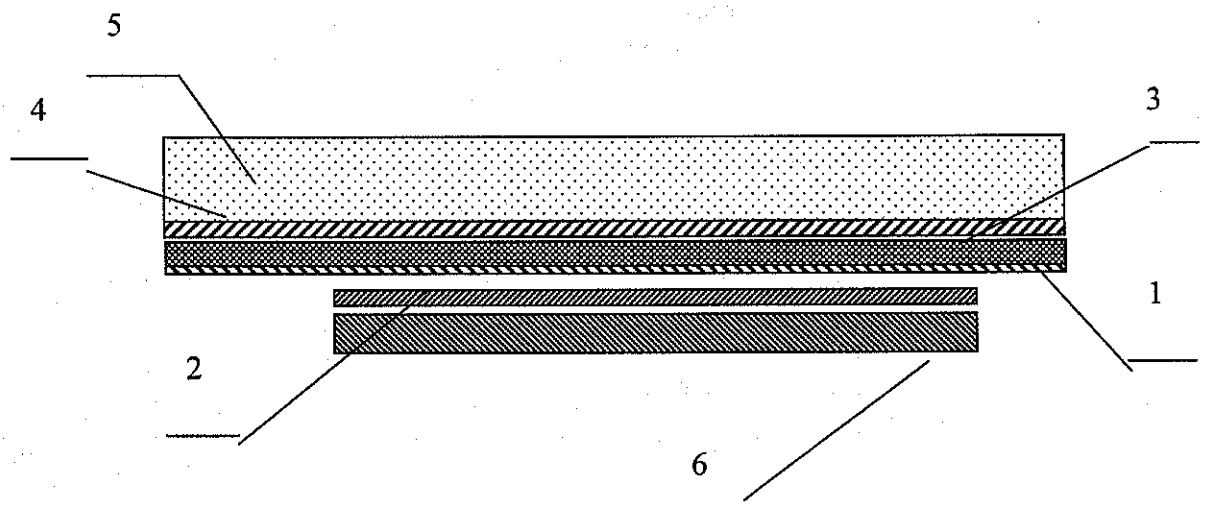
A scheme of inverted cladding recommended in/11/ and presented in Fig. 1.19 was tried out with the purpose of reduction of defects. In this scheme, a substrate of 20X23H18 steel is a plate being thrown and a nickel foil is a fixed plate. However, implementation of a new scheme did not result into improvement of the quality.

When inverted cladding was done following the cylindrical scheme, where a drum made of 20X23H18 steel was a cladding component being thrown and a drum made of nickel foil was a fixed component to be coated, the results were also unstable. There were blanks with S_d / S_c ratio of $\sim 40\%$ and with S_d / S_c ratio of $\sim 20\%$. So, we decided to be back to the previous scheme of direct cladding (where the foil was thrown onto the fixed substrate).



- 1- a substrate (a fixed component being coated);
- 2- a foil (a cladding component to be thrown);
- 3- a soft plate;
- 4- a hard plate;
- 5- an explosive;
- 6 - a substrate.

Fig.1.18.



- 1 - 20X23H18 steel (a plate to be applied/thrown);
- 2 - a foil (a fixed plate);
- 3 - a soft plate;
- 4 - a hard plate;
- 5 - an explosive;
- 6 - a substrate (steel).

Fig.1.19. A scheme of inverted cladding.

When matching the outcomes of experiments on EC of plates with different areas it was found out that the plates with a smaller area have defects of smaller sizes in comparison with the plates of greater area. This happens despite the fact that the experiments are conducted following the same schemes and keeping the same parameters of the process of the explosion cladding. So, we may expect that when the area of cladding (and the area of plates) is increased further, the sizes of the defects in the coatings and their quantity will grow. Defects in the form of a through destruction of the coating are not acceptable for bipolar plates. That is why proceeding with the works aimed at the increase of the area of cladding not having eliminated the reasons of defect formation was considered illogical.

It was supposed to eliminate defects of the coatings by a more thorough assembling of the unit and a more successful selection of the material for the "soft" plate. This supposition was made on the basis of the following possible reasons of damage of the cladding layer:

- Presence of the air between the "soft" plate and the foil,
- Non-uniformity of rubber – the material used for "soft" plate (porosity, density etc.).

In order to eliminate the mentioned reasons special attention in experiments on explosion cladding (plates with the area of cladding $S_{cl} \approx 400\text{cm}^2$) was paid to the quality of gluing of the "soft" plate and the foil to prevent presence of the air between them. Besides, there were made experiments with implementation of the "soft" plate made of different materials, for example, several layers of cardboard pasted together, or liquid glass (between the solid plate and the foil).

The results of the research on different parameters as they influence the quality of the explosion cladding are given in Table 1.8.

Table 1.8.

Thickness of the coating, microns	Parameter being measured	Range of values, mm	Area of cladding, S_{cl} , cm^2	Ratio of S_d/S_{cl} , %	Notes
1	2	3	4	5	6
100	Thickness of the explosive, mm	10-12	100, 220, 400	30 -15	Strength of the adhesion between the coating and the substrate is satisfactory
	Welding clearance, Δ , mm	0.5 - 4.0			
	Thickness of the solid plate, T_T , mm	1.0 -2.5			
	Thickness of the soft plate, T_M , mm	1.0 - 4.0			
	Material of the soft plate: TMKIII rubber (c), TMKIII rubber (r)				
Lubricant: Liquid glass, "Moment -1" glue					

So, when 100-micron foil was used as a cladding layer there were produced bi-meal plates with satisfactory strength of adhesion between the cladding layer and the substrate (see Fig 1.20). However, we could not get rid of the defects in the coating completely when working with the plates with $S_{cl} \approx 400\text{cm}^2$ following the **flat scheme of cladding**. Less quantity of the defects is produced if a **cylindrical scheme of cladding** is followed. The defects are local and are arranged in the place of the joint of the nickel manacle ring.

The difficulty of the task is the fact that there is no clear explanation of the real reasons of the defects appearing in the coating. A deeper study of the explosion cladding process is necessary, as well-known solutions do not allow us reach the desirable result.

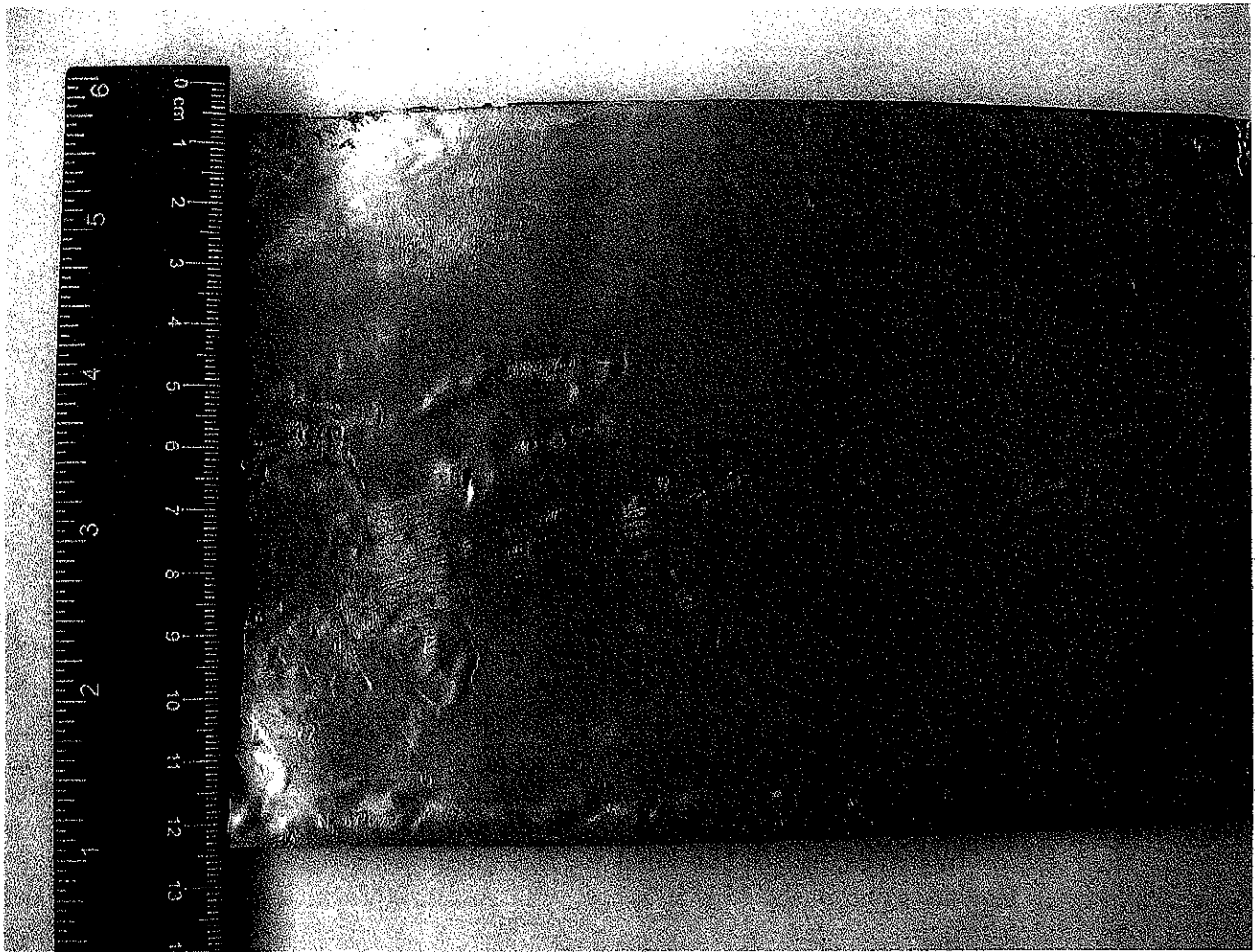


Fig. 1.20

A number of experiments with 300-micron foil was held to get additional information on the explosion cladding processes; they were aimed at evaluation of the thickness of the foil as it influences the number of defects in the coating. Parameters of EC and the experimental results for 300-micron foil are given in Table 1.9.

Table 1.9.

Thickness of the coating, microns	Parameter being measured	Range of values, mm	Area of cladding, S_{cl} , cm^2	Ratio of S_d/S_{cl} , %	Notes
1	2	3	4	5	6
300	Thickness of the explosive, mm	10 -15	320*, 600, 900	10 - 0	320 – flat scheme
	Welding clearance, Δ , mm	2,0			
	Thickness of the solid plate T_T	2,0			
	Thickness of the soft plate T_M	2,0			

Much less defects in the coating were produced when 300-micron foil was used. When the flat scheme of cladding was followed, there were produced plates with $S_{cl} \approx 320cm^2$ that did not have defects of the coating.

Difficulties in production of defect-free coatings come from not high level of scrutiny of the processes of cladding when thickness of the cladding layer is small, and that was already mentioned at a formulation of the tasks. Rather complex engineering tasks are solved successfully in the Institute with implementation of the EC technique when thicknesses of the cladding layer are large. There were produced cylindrical parts, plates and tables with different combinations of metals: aluminum - copper, steel - titanium, brass - titanium etc., and the area of cladding was up to $5m^2$ at thickness of a cladding layer from 2 up to 50mm.

1.2.3. Metallographic research on the coatings after 1500-hour corrosion tests.

Metallographic research was done on the samples of 20X23H18 steel coated from nickel foil by explosion cladding following the cylindrical layout. It was done before and after corrosion tests run during 250, 500, 750, 1000 and 1500 hours using the technique described in Appendix 3.

Microstructure of the samples was studied in the direction perpendicular to the direction of detonation. Micro specimens were made following the common technique. Microstructure of the samples of the coated steel before the tests is given in Fig.1.21.

The zone where 20X23H18 steel joins nickel is undulating. Minimum thickness of the coating is 30-55 microns; maximum thickness is 145-165 microns. The length of the wave (roll) is ~ 265-450 microns.

Structure of the nickel coating represents polyhedral grains; the steel reveals deformation stripes.

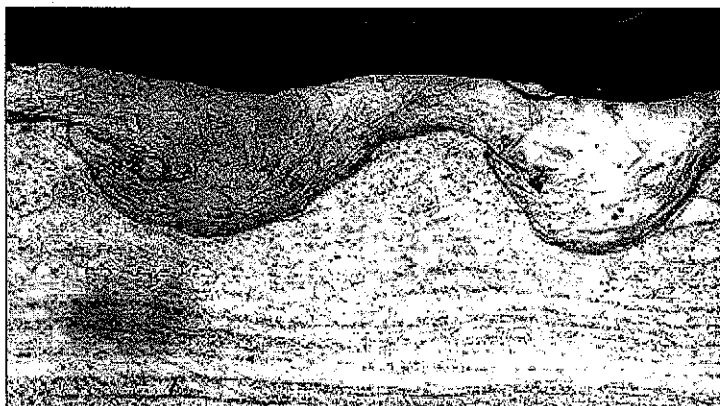


Fig.1.21. Microstructure of the nickel foil coating at 20X23H18 steel produced by explosion welding following the cylindrical layout (before corrosion tests), x250

Intercrystalline corrosion of the nickel coating along all its minimum thickness (up to 55 microns) is observed in all the samples after corrosion tests, it is evident without chemical etching of micro specimens (Fig.1.23a, 1.24a, 1.25a). Intercrystalline corrosion in the nickel coating in samples after the tests during 750 and 1000 hours in some places (in cavities) goes as deep as 135 microns, and when the exposure was 1500 hours it went to 165 microns deep. The plotted dependency of the depth of the intercrystalline corrosion on the time of the tests is given in Fig.1.22.

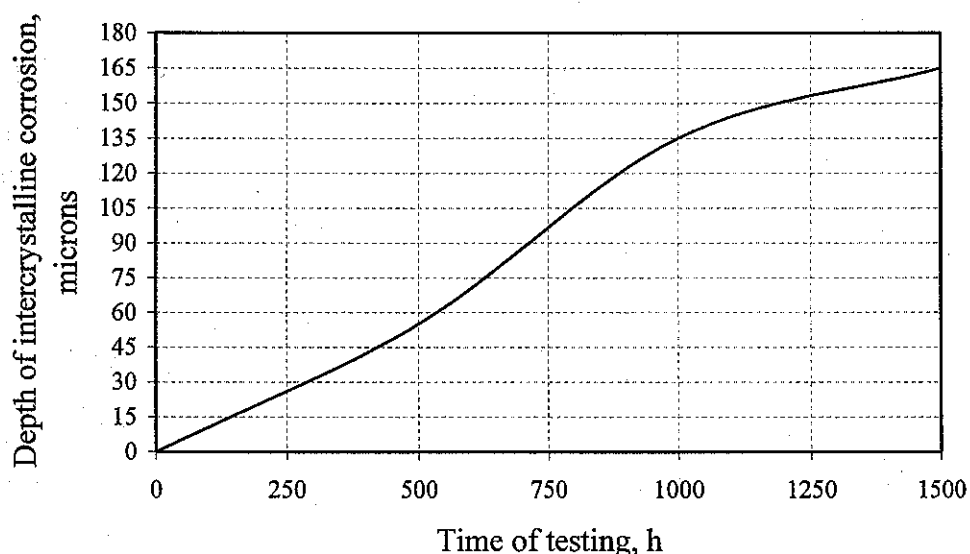
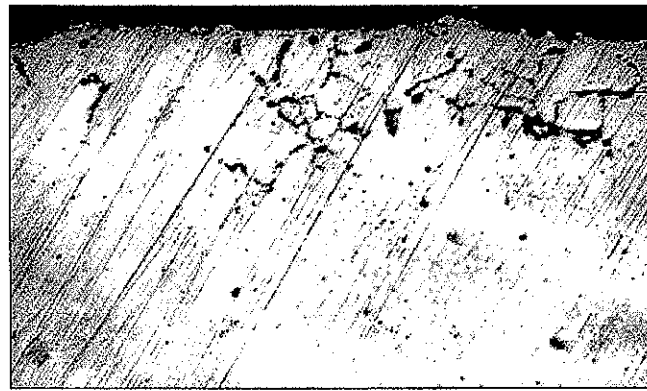
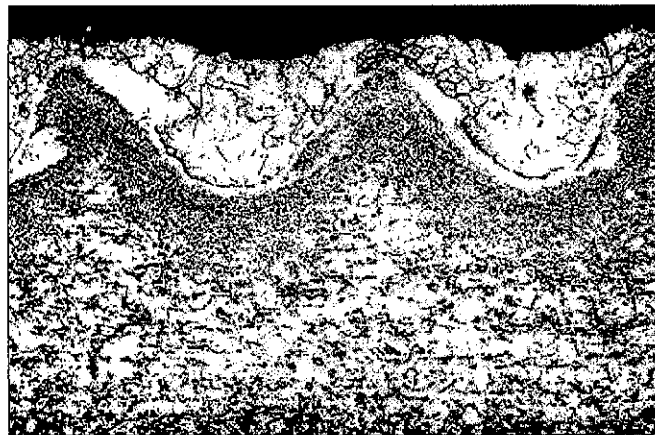


Fig.1.22. Dependency of inter-crystalline corrosion depth on the time of testing for the coated samples produced by explosion welding following the cylindrical layout.

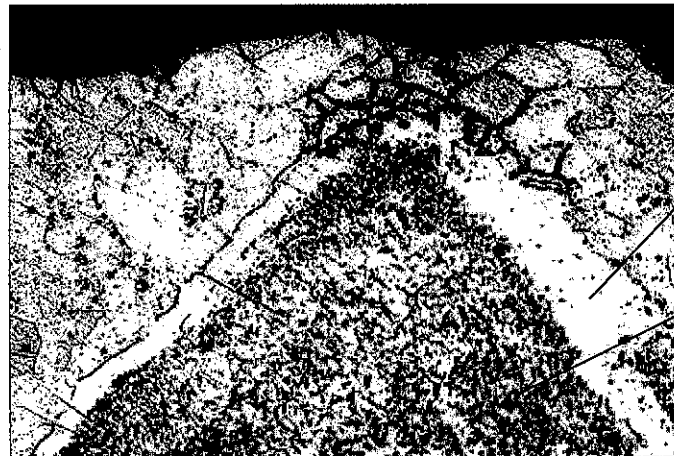
Microstructure of the samples after corrosion tests is shown in Fig. 1.23. – 1.25. Microstructures of the samples after 250h and 500h tests are identical and are shown in Fig.1.23. Microstructures of the samples after 750h and 1000h tests are also identical and are shown in Fig.1.24. Fig.1.25 shows microstructure of samples after the tests during 1500 hours.



a



b



c

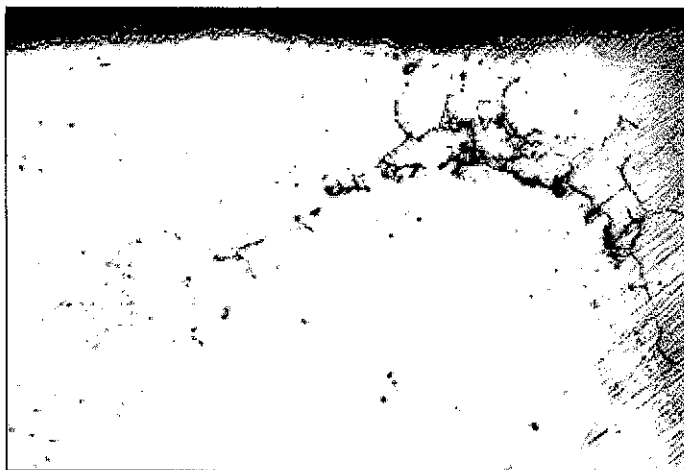
Inter-crystalline corrosion

Light diffusion zone

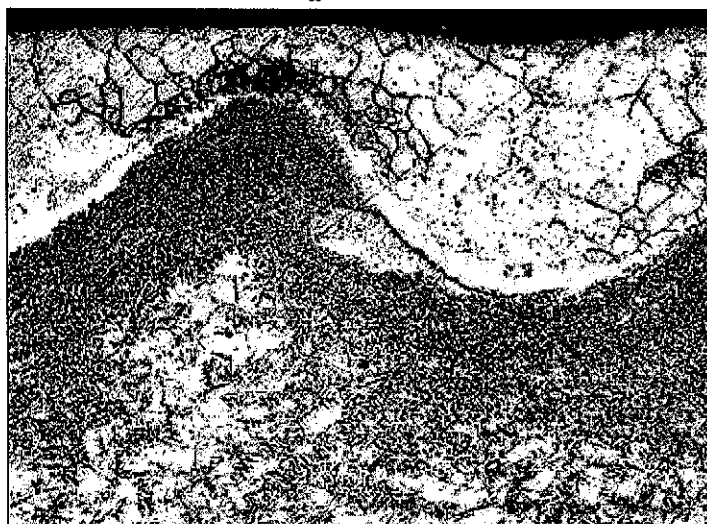
Grey diffusion zone

- a – without etching, x400;
- b – zones of the welded joint after etching, x125;
- c – corrosion in the minimum thickness of the coating after etching, x400.

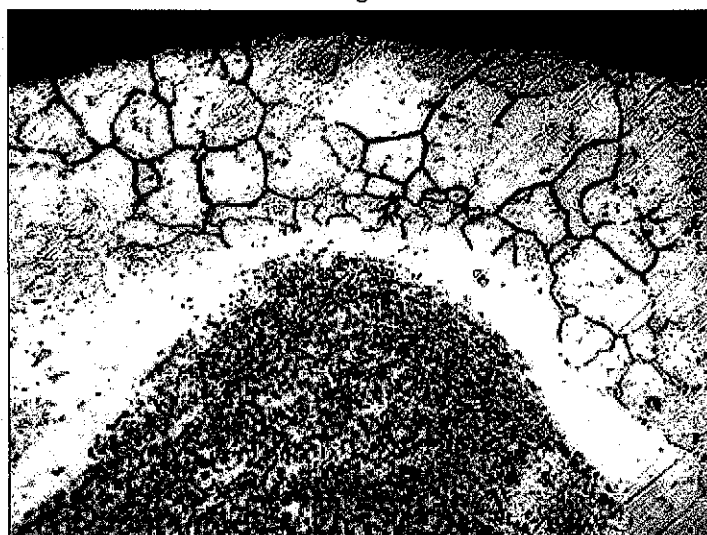
Fig.1.23. Microstructure of the nickel foil coating produced by explosion welding following cylindrical layout after tests during 250 and 500 hours.



a



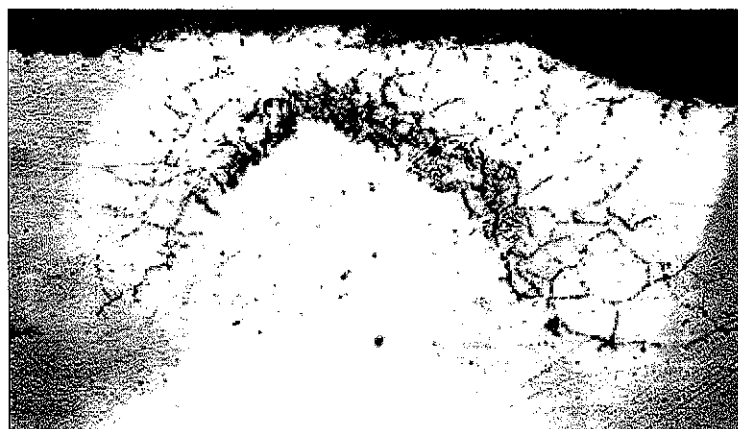
b



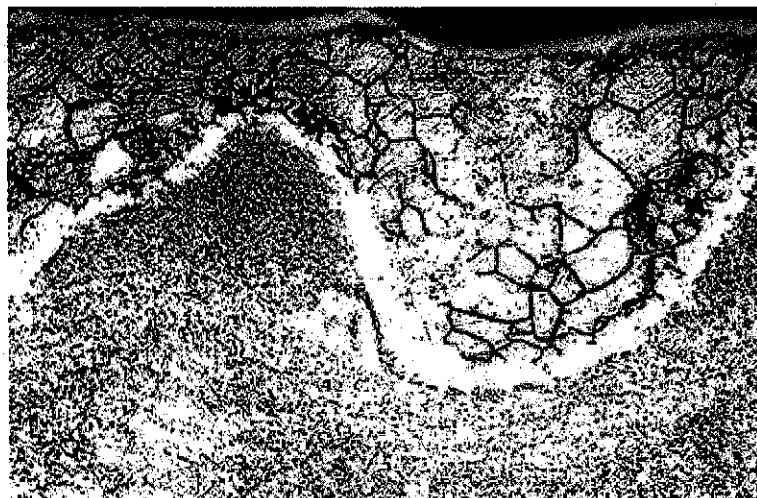
c

a – without etching, x400;
 b – zones of the welded joint after etching, x125;
 c – corrosion in the coating after etching, x400.

Fig. 1.24. Microstructure of the nickel foil coating produced by explosion welding following cylindrical layout after tests during 750 and 1000hours.



a



b

a – without etching, x250

b – after etching, x400

Fig.1.25. Microstructure of the nickel-foil coating produced by explosion welding following cylindrical layout after 1500-hour tests.

Microstructure of the welded joints after corrosion tests changed considerably as compared to the initial sample. The presence of two diffusion zones characterize all the samples: -a light zone 20-30 microns thick (up to 40 microns thick in some places) is on the side of the steel, which repeats configuration of the wave; under the light zone in the steel there is a diffusion zone of gray color up to 100 microns thick, which also repeats configuration of the wave (grain structure in the steel is not observed in this zone).

The structure of steel looks like re-crystallized grains of austenite of 8 points (average symbolic grain size is ~ 22 microns). Steel under the coating does not reveal corrosion of inter-crystalline type.

Measurements of microhardness of the nickel coating and of the steel in the middle zone of thickness of the sheet are represented in Table 1.10, and a plotted dependency of microhardness on the time of testing is given in Fig.1.26.

Table 1.10.

Microhardness of the nickel coating and of the steel before and after corrosion tests.

Place microhardness was measured	Microhardness, kgf/mm ²					
	Before corrosion tests	Time of testing, hours				
		250	500	750	1 000	1 500
Nickel coating	332	96	108	115	112	111
Steel	386	211	270	274	271	272

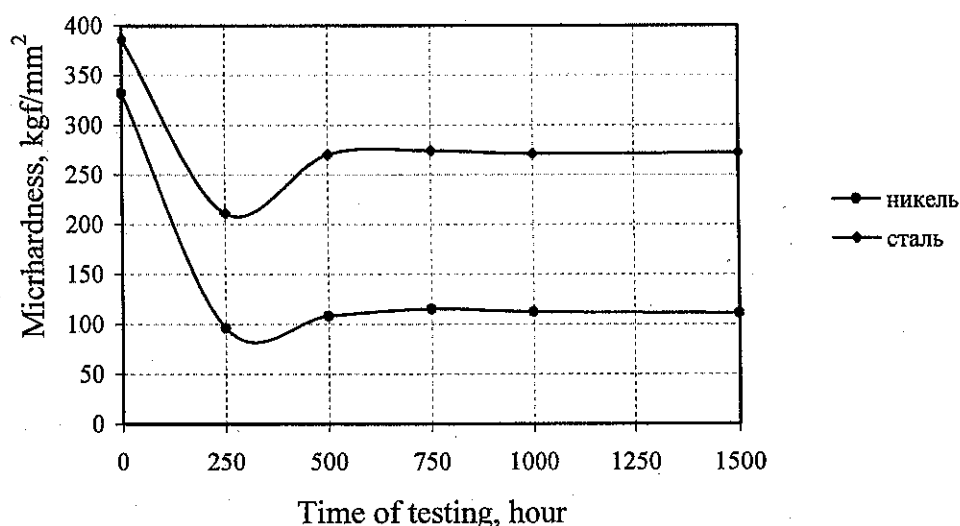


Fig. 1.26. Microhardness of the coating and of the steel as a function of time of corrosion tests.

1.2.4. Inter diffusion of iron and nickel in the process of 1500-hour test.

Analysis of the samples before and after corrosion tests was done with an electron probe microanalysis device. Quantitative changes in chemical composition of the coating were registered in the modes of semi-quantitative and quantitative microrentgenospectrum analyses. Samples were studied after corrosion tests 250, 500, 750, 1000 and 1500 hours long.

Thickness of the nickel layer on the samples, which was measured in the modes of BEI, is characterized by high heterogeneity. Maximum thickness is 145-165 microns, minimum 50-75 microns (see Fig., metallographic research). In the samples after the tests 500-1500 hours long intercrystalline corrosion is registered at some sections, where thickness of the coating is the minimum one.

The depth and the profile of iron/nickel inter-diffusion are measured using the program of linear X-ray spectrum analysis under the following conditions: scanning step was 2 microns, controlled parameters were Ni, Fe, Cr, K, O. Fe diffusion at the level of 0.1 from the average concentration of Fe goes to 2/3 of thickness of the coating; after 750 hours Fe traces are also noticed at the edge of the coating.

In the samples that underwent 750 and 1500 hour testing concentration profiles go through the pores – they are incorporations of a dark color with an average atomic mass less than

that of the substrate. Besides the basic elements (Ni, Fe, Cr, Mn, Si) in the pores of the coating K and O are registered there, i.e. presence of the electrolyte is observed in the pores of the coating.

1.2.5. Conclusions.

1.2.5.1. A significant volume of experimental research was performed and there was gained new experience in explosion cladding of 0.4 mm 20X23H18 steel with 0.1 mm foil. There were produced bimetal plates with satisfactory adhesion of the cladding layer and the substrate. However, we failed to eliminate all the defects of the coating on plates with $S_{cl} \leq 400\text{cm}^2$ when following the **flat scheme of cladding**. The ratio of S_d/S_{cl} is not stable and is about 15-30%. Fewer defects were produced when following the **cylindrical scheme of cladding**. The defects are local and are arranged in the place of the joint of the nickel manacle ring. When following the cylindrical scheme of cladding there were produced bimetal plates with the area of cladding of $S=320\text{cm}^2$ with the defect-free zone of 220cm^2

When using 300-micron foil, considerably less quantity of defects was produced in the coating. So, when following the **flat scheme of cladding** there were produced plates with $S_{cl} \approx 320\text{cm}^2$ that did not have defects of the coating.

The difficulty of the task is the fact that there is no clear explanation of the real reasons of the defects appearing in the coating. A deeper study of the explosion cladding process is necessary, as well-known solutions do not allow us to reach the desirable result.

1.2.5.2. As a result of 1500-hour tests it was found out that nickel-foil coatings produced by explosion welding following cylindrical layout:

- have inter-crystalline corrosion to the full minimum depth of the of the coating (up to 55microns), and when the exposure was 1500 hours it was up to 165 microns; formation of pores filled with electrolyte was noted;
- microrentgenospectrum analysis revealed Fe diffusion into the nickel layer to the 2/3 of the thickness of the coating, after 750 hours Fe traces were also noticed at the edge of the coating.

However, microstructure of the substrate (20X23H18 steel) did not reveal any inter-crystalline corrosion under the coating. So, nickel foil coatings produced by explosion cladding following the cylindrical scheme performed their function of protection when used in the conditions of 1500 hours of testing.

List of References:

1. A.S. USSR №505750 cl. MIIK C23F1/00, publ.05.03.76 BHN№9, Institute of general and non-organic chemistry of Academy of Science of the Ukrainian SR.
2. Patent of Great Britain №1387458, class C23, 1975.
3. A.S. USSR №1382876 cl. MIIK C23 F1/28, publ.02.03.88 Khar'kov University in the name of M. Gorky.
4. S.Y. Grilikhes. «Degreasing, etching, passivation of metals». Supplement to the journal «Galvanotekhnika and obrabotka poverkhnosti» - Moscow, 1994, p.112.
5. ISTC Project #2281p. Development of new materials for fuel cells. Technical Report for the 2nd quarter (September 01, 2002 – November 30, 2002).
6. ISTC Project #2281p. Development of new materials for fuel cells. Technical Report for the 3rd quarter (December 01, 2002 – February 28, 2003).
7. ISTC Project #2281p. Development of New Materials for Fuel Cells. Technical Report for the 5th quarter (June 01, 2003 – August 31, 2003).
8. Application 458908, Sweden, MKI B23K 20/08.
9. A. V. Krupin et al. Processes of metal treatment with an explosion, Moscow; "Metallurgy", 1996

10. V.M. Kudinov, A.Y. Korotev. Explosion Welding in Metallurgy, Moscow, "Metallurgy", 1978
11. A. V. Krupin et al. Deformation of metals with an explosion, Moscow, "Metallurgy", 1975

2. DEVELOPMENT OF A NEW MATERIAL WITH THE HIGHER CORROSION RESISTANCE FOR THE MCFC BIPOLAR SEPARATOR PLATES (TASK 2)

2.1. Fabrication of monolithic specimens from the Y or Ti - doped alloys 30Cr-45Ni-1Al. Carrying out research.

The Y, Ti and Cu-doped group of 30Cr-45Ni-1Al alloys have been smelted in a lab furnace; the monolithic specimens have been fabricated. The alloys were tested in carbonate in the atmosphere of the gas mixture *air-carbon dioxide* (20%) and the gas mixture *-hydrogen-carbon dioxide* (20%) saturated by water at 55°C.

The chemical composition of the alloys is presented in Table 2.1.

Table 2.1

Main elements content in the alloys, % mass.

Alloy	Cr	Ni	Fe	Ti	Al	Y	Cu
1	25,7	47,3	25,6	0,01	1,05	0,002	-
2	29,5	45,2	23,7	0,01	1,06	0,035	-
3	30,5	45,7	22,4	0,05	0,95	-	-
4	30,2	46,1	19,2	0,01	1,05	0,005	3,0

Note: C content – within the limits of 0,007-0,016; Si - 0,10-0,18; S - 0,001-0,003; Mn - 0,16-0,26 %.

Table 2.2. presents the average values of the rate of corrosion based on the results of examination of 21 specimens (ratio error not more than 10 %).

Table 2.2

Change of the mass of the specimens after the 200 hour detention in the melt

Alloy	Rate of corrosion, g/m ² h	Alloy	Rate of corrosion, g/m ² h
1	0,09	1H	0,09
2	0,06	2H	0,04
3	0,04	3H	0,03
4	0,03	4H	0,03

After testing, the salt fusion was dissolved in the diluted (1:4) hydrochloric acid. The solutions were analyzed for the main components content. The results of the chemical analysis of the solution are presented in Table 2.3.

Table 2.3

Content of the main elements in the melt, mg

Alloy	Cr	Ni	Fe	Mn	Other	Amount
1	1,43	0,28	2,26	0,37	-	4,34
2	9,64	0,46	2,14	0,58	-	12,82
3	2,21	0,21	1,43	0,26	Ti 0,004	4,11
4	3,73	0,30	1,97	0,26	Cu 0,086	6,35
1H	0,15	0,15	1,33	0,46	Si 0,08	2,17
2H	0,18	0,07	0,34	0,74	Si 0,04	1,37
3H	0,33	0,32	1,28	0,74	Ti 0,008	2,68
4H	1,56	0,15	0,58	0,54	Cu 0,06	2,89

The X-ray phase analysis of the corrosion products was carried out. The radiographs were taken from the face surface of cylindrical specimens and the following phases were detected:

- 1 - (Ni, Fe), LiFeO_2 , LiNiO_2 , LiCrO_2 ,
- 2 - (Cr-Ni-Fe), LiFeO_2 , LiCrO_2 , LiNiO_2 ;
- 3 - LiFeO_2 , NiCr_2O_4 , LiCrO_2 , LiFeO_2 , NiO;
- 4 - (Ni, Fe), LiFeO_2 , LiCrO_2 , NiCrMnO_4 , NiO;
- 1H - (Ni, Fe), LiCrO_2 , LiNiO_2 , NiCrMnO_4 ;
- 2H - (Cr-Ni-Fe), LiCrO_2 , LiFeO_2 , NiCr_2O_4 ;
- 3H - (Cr-Ni-Fe), LiCrO_2 , $\text{Fe}(\text{Cr, Al})_2\text{O}_4$, LiFeO_2 ;
- 4H - (Ni, Fe), LiCrO_2 , LiFeO_2 , NiCr_2O_4 .

Micro X-ray analysis of the changed zone on the surface of the specimens demonstrated:

- 1 - The oxide layer thickness (by the oxygen line) - 20 μm , nickel content in the oxide layer is higher, the changed zone thickness - 10 μm (by Fe);
- 2 - The oxide layer thickness (by the oxygen line) - 25 μm , iron and nickel are contained in the middle part, chrome being in the internal part, the changed zone thickness - 15 μm ;
- 3 - The oxide layer thickness (by the oxygen line) - 25 μm , there are titanium and aluminum in the external part, iron and nickel are contained in the inner part of the oxide layer, the layer on the bound Me-oxide is enriched with chrome, the changed zone thickness - 20 μm ;
- 4 - The oxide layer thickness about 12 μm ; aluminum is contained in the external part, the changed zone thickness - 23 μm ;
- 1H - The oxide layer thickness (by the oxygen line) - 25 μm , the external layer is enriched with aluminum, the middle layer is doped with nickel and iron, the internal layer is enriched with chromium and aluminum, the changed zone thickness - 17 μm ;

2H - The oxide layer thickness (by the oxygen line) - 20 μm , the external layer is enriched with chromium and aluminum, the changed zone thickness - 15 μm ;

3H - The oxide layer thickness (by the oxygen line) - 20 μm , the external layer is enriched with titanium and aluminum, the internal part is enriched with iron and nickel, the layer on the bound Me-oxide is enriched with chromium, the changed zone thickness - 20 μm ;

4H - The oxide layer thickness (by the oxygen line) \sim 25 μm , the external layer is enriched with chromium, the internal part is enriched with iron, the Me-oxide bound contains more aluminum, the changed zone thickness - 15 μm .

Alloy 30Cr-45Ni-1Al is the most promising one. Doping of the alloy by Y normalizes the alloy structure. Besides, Y forms well-conductive complex oxides on the bounds of the grains. Ti-doping stabilizes the structure, its grain effect. Cu-doping is inefficient, since it results in local defects of the structure.

The research results of the group, which are the best ones from the viewpoint of corrosion resistance of commercial steels and alloys (see Table.2.4.), obtained earlier in Task 2 of the contract 981562402 with ANL, are presented in Table 2.5.

Table 2.4

Content of the main elements in alloys, % mass.

#	Alloy	C	Si	Mn	Cr	Ni	Ti	Fe	Al	Other
1	16Cr-45Ni-3Al	0,1	1,0	1,0	15,0-17,0	44,0-46,0	-	the rest	2,9-3,9	-
2	20Cr-32Ni-0,5Ti-0,5Al	0,05	0,7	0,7	19,0-22,0	30,0-34,0	0,25-0,6	the rest	0,5 max	-
3	17Cr-57Ni-3Al	0,10	0,9	0,3	15,0-18,0	55,0-58,0	-	the rest	2,6-3,5	(Ba-0,1; Ce-0,03) max
4	23Cr-28Ni-1Ti-2,5Mo-3Cu	0,03	0,8	0,8	22,0-25,0	26,0-29,0	0,5-0,9	the rest	-	Mo-2,5-3,0; Cu-2,5-3,5
5	23Cr-18Ni(0,2C)	0,20	1,0	2,0	22,0-25,0	17,0-20,0	-	the rest	-	-

Table 2.5.

Mass change of the specimens after aggregate exposure in the melt during 200 hours.

Alloy	Rate of corrosion, $\text{g/m}^2\text{ч}$
16Cr-45Ni-3Al	0,028
20Cr-32Ni-0,5Ti-0,5Al	0,12
17Cr-57Ni-3Al	0,085
23Cr-28Ni-1Ti-2,5Mo-3Cu	0,19
23Cr-18Ni(0,2C)	0,342

Comparison of the new alloy with the group of commercial alloys and steel X23H18 (310SS) (see Tables. 2.4 and 2.5) demonstrates that the alloy has the corrosion resistance under the anode and cathode conditions higher than with any other alloy. Exclusive are the alloys doped with Al more than 3%, but their oxide film has high specific electric resistance, which limits

their application in FC. Corrosion resistance of the new alloy is about an order higher than that of the X23H18 (310SS) steel.

2.2. Fabrication of thin sheet cold-rolled specimens on lab equipment. Determination of deformation-plastic characteristics.

Smelting of the commercial melts of both the basic alloy 30Cr-45Ni-1Al, and a Y, Ti – doped one (see Table. 2.6) was done.

Table 2.6

Laboratory melts composition (mass portion, %)

№	Car- bon	Silicon	Manga- nese	Chro- mium	Nickel	Tita- nium	Alumi- num	Other ele- ments
1	0,033	0,5	0,5	28,8	46,0	0,01	0,8	Ce-0,028 La-0,011
2	0,034	0,65	0,4	29,7	45,2	0,29	0,72	Ce-0,018 La-0,005
3	0,04	0,48	0,38	30,2	46,1	0,01	0,92	Y-0,025
4	0,039	0,48	0,37	30,0	45,8	0,35	0,78	Y-0,027

Smelting was done in an induction industrial furnace applying commercial charge materials: nickel N1Y, electrotechnical steel 10895, ferrochromium FH 006, aluminum A-97, titanium BT-1-0, metal manganese MM-95, ferrosilicium FS-65.

The quantity of the charge material was estimated for the melt of 30 kg. Each melt was poured into two ingots with subcharging for the specified composition. The first melt was smelted on the basis of composition with 0.05% of misch metal. One ingot was poured without additives; the rest material was doped with titanium (compositions 1 and 2). The second melt was smelted in the same way on the basis of the yttrium base metal and also with the titanium subcharging (compositions 3 and 4). Pouring was effected into the moulds of the round cross-section for the ingots with the mass of 15 kg.

After smelting, a thin sheet rolled metal technology was adjusted, which included:

- heating before rolling up to the temperature of 1130÷1150°C;
- hot rolling up to the thickness of 1,5 mm with the deformation of 20÷25% per each passage with the intermediate heating of the sheet;
- thermal treatment at 1000÷1050°C in the air during 30 minutes;
- etching using acid-base method;
- cold rolling up to the thickness 0,8 mm;
- thermal treatment at 1000÷1050°C during 30 minutes with cooling in the air;
- etching using acid-base method.

Thin sheet specimens to study thermomechanical and corrosion properties have been fabricated.

Comprehensive study of mechanical characteristics of the base alloy (30Cr-45Ni-1Al) and the Y, Ti – doped alloys in the temperature range of 20-700°C were carried out. The sheets with the thickness of 0.8 mm were thermally treated at the mode: the temperature is 1050 °C, the aggregate exposure is 20 min, cooling down in the air. The research results are presented in Tables 2.7, 2.8.

Table 2.7

Alloy	Temperature, °C	σ_B , N/mm ²	$\sigma_{0,2}$, N/mm ²	δ_5 , %
30Cr-45Ni-1Al - (Ti, Y)	20	740	390	50
30Cr-45Ni-1Al	20	670	300	46
30Cr-45Ni-1Al - (Ti)	20	700	380	44
30Cr-45Ni-1Al - (Y)	20	730	385	47

Table 2.8

Alloy	Temperature, °C	σ_B , N/mm ²	$\sigma_{0,2}$, N/mm ²
30Cr-45Ni-1Al - (Ti, Y)	20	740	390
	500	590	250
	600	510	225
	700	375	205

2.3. Research on conductivity of oxide films, phase composition and structure of the Russian steel analogous to 310S and of a new alloy produced using industrial equipment

2.3.1. Perfection of the method

The technique to study the conduction of metal materials contact with the porous electrodes under FC conditions was polished. A diagram of a single measured cell is shown in Fig.2.1.

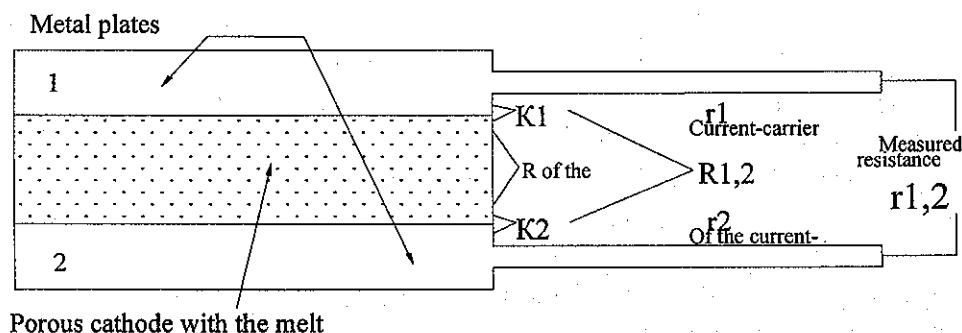


Fig.2.1.

In Fig.2.1., figures 1, 2 designate the studied metal separation plates connected with the current-carriers. The current-carriers were connected to the AC bridge (operating frequency 1 kHz). The plates were pressed to and got in contact with the porous electrodes that were beforehand saturated with the carbonate melt (fusion). Resistance $r_{1,2}$ is the sum of resistances of the wires of the measuring instrument and the current-carriers r_1 and r_2 , of two resistances of transient layer K_1 and K_2 (contact ones between the tested plates and the electrode) and the resistance of the R -cathode electrode itself. The electrode is a porous, filled with lithium-potassium-carbonate eutectic plate made from nickel oxide for the cathode or from metal nickel for the anode. I.e. $r_{1,2} = r_1 + K_1 + R \text{ cathode} + K_2 + r_2$. In the cell structure, it seems impossible that the

contact resistances K_1 and K_2 may be separately measured (in case when the plates are made from one material, they will be equal). R of the cathode катод to a first approximation may be considered as a negligibly small one, though it may be estimated by a separate measurement using golden contacts and current-carriers (or calculated by the specific conduction of the Li-doped nickel oxide or the other electrode material, by the porosity and the thickness of the plate). In such a way, at determining contact resistances (in total for the contact between two plates), a task arose to isolate the resistance of the wires of the measuring instrument and the current carriers from the resistance value measured in practice. The resistance of the wires of the measuring instrument and the current carriers makes a considerable part of the total resistance since the specific resistance of stainless steel is high enough. For this, a multilayer cell was used, in which three single cells were consecutively connected. That permitted to exclude in turn the separate current-carriers from the circuit and also to include into it the contact resistances of not only two contacts, but of four or six ones.

The scheme of three-layer cell is shown in Fig. 2.2.

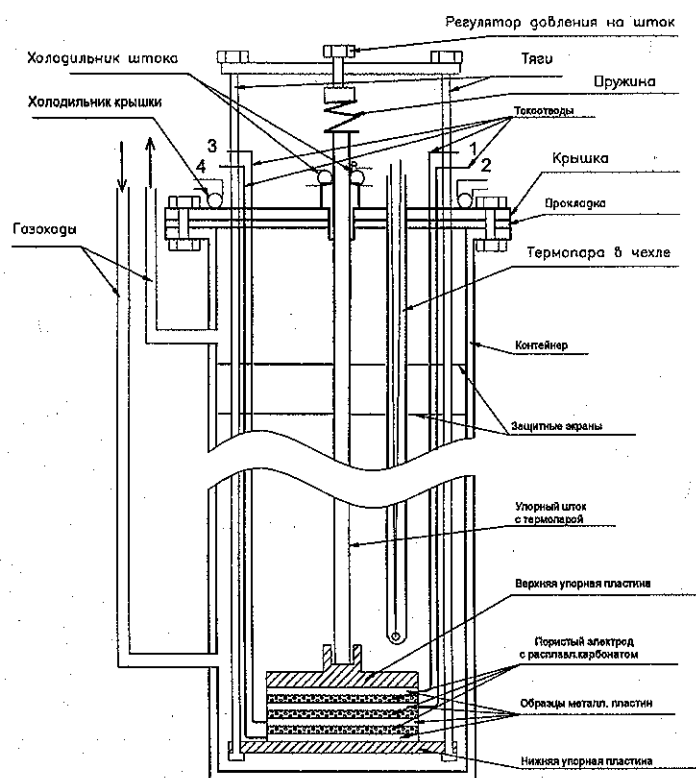


Fig. 2.2.

Fig. 2.2 on the right presents numeration of the studied plates with the connected current-carriers. By analogy with a single cell, the practically measured resistances between different electrodes may be divided into the constituents:

$$r_{1,2} = r_1 + r_2 + R_{1,2}$$

$$r_{2,3} = r_2 + r_3 + R_{2,3}$$

$$r_{3,4} = r_3 + r_4 + R_{3,4}$$

$$r_{1,4} = r_1 + r_4 + R_{1,2} + R_{2,3} + R_{3,4}$$

$$r_{1,3} = r_1 + r_3 + R_{1,2} + R_{2,3}$$

$$r_{2,4} = r_2 + r_4 + R_{2,3} + R_{3,4}$$

Deducting the values of measured resistances between different pairs of electrodes one may pick out their constituents and directly find the resistances of both the contacts and the current-carriers. One should note that at reduction of the members of integral expressions, the additional errors caused by the difference in these constituents measurements with different extent of accuracy and authenticity are not included. These constituents are just excluded from the circuits at measuring different pairs of electrodes. Calculations may be made, for example, by the following scheme:

$$r_{1,4} - r_{3,4} - r_{1,2} + r_{2,3} = r_1 - r_3 + R_{1,2} + R_{2,3} - r_1 + r_3 - R_{1,2} + R_{2,3} = 2R_{2,3}$$

$$2r_{2,3} - r_{1,3} + r_{1,2} + r_{2,4} - r_{3,4} - 2R_{2,3} = 4r_2$$

$$r_{2,3} - r_3 - R_{2,3} = r_3$$

The left part of these expressions contains the values that are directly measured or calculated before that, the right part contains the found values of the resistances of the middle cell 2 and the resistances 2, 3 of the current-carrier. Then, due to the impossibility of separation of the resistances of the current-carriers and of the contact resistances at the last electrodes of the set, one has to make the only assumption that the r_1 and r_4 values at these electrodes do not essentially differ from the middle ones r_2 and r_3 . This is justified at least by the fact that r_2 and r_3 calculated separately (without any assumptions) are close to each other within the limits of 1-2 Ohm. In such a way, having admitted the average: $(r_2 + r_3)/2 = r_1 = r_4$, we may find the other contact resistances.

$$r_{1,2} - r_1 - r_2 = R_{1,2}$$

$$r_{3,4} - r_3 - r_4 = R_{3,4}$$

These are the binary resistances, i.e. $R_{1,2} = K_1 + K_2$, $R_{2,3} = K_2 + K_3$, $R_{3,4} = K_3 + K_4$. In such a way, in a single experiment the measurements are duplicated three times. In case the middle plates 2 and 3 are made from the same material, while the last ones 1 and 4—from the other one, one may also evaluate their contact resistances in one cell (being sure that both surfaces of the middle plates and the porous electrodes are identical). The conducted tests of standard specimens (steel 20X23H18- the 310SS analog) on determination of binary contact resistances in the anode atmosphere (the electrode plates' area - 8.12 cm² at the thickness of 0.95 mm, porosity - 60%, $m_{plates}=2.9g$, $m_{electrolyte}=0.8g$) have demonstrated the adaptability of the given technique (See Fig.2.3). The resistance of the connecting wires in this case amounted to 450 mΩ (each).

During the second quarter, the standard specimens made from steel grade 20X23H18B have been tested with an eye to determine contact resistances in the cathode atmosphere (the mixture - 30% CO₂ + 70% air). On the expiry of 200 hours testing, the resistance of the current conductors from the stainless steel spot-welded to the studied plates was estimated as 550mΩ. The transition to platinum conductors will permit to decrease this resistance. To increase the accuracy of relative measurements of contact resistances, the contact area was decreased as compared with the previous tests up to 1.00 cm². In this case, to avoid the difference in the area at insignificant displacement of the specimens, the sizes were specified to the porous electrode preliminary saturated with carbonate, as a square 10x10 mm with the thickness of 0.95 mm, cathode porosity - 60%.

The measurements were made using an AC bridge with the frequency of 1 kHz. The measured and calculated by the above method values are shown in Fig.2.4. Here $R_{1,2}$ - binary contact resistances between the studied plates and the first porous electrode, etc. Since all the specimens have the same composition, the lower curve K_m is presented as the averaged single contact resistance.

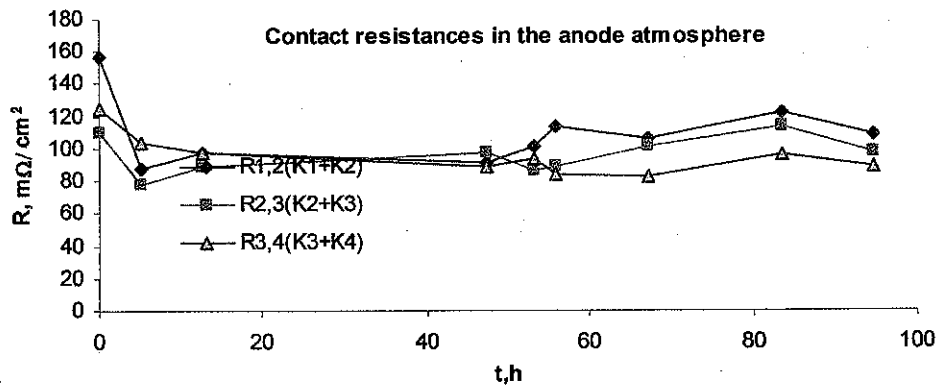


Fig. 2.3

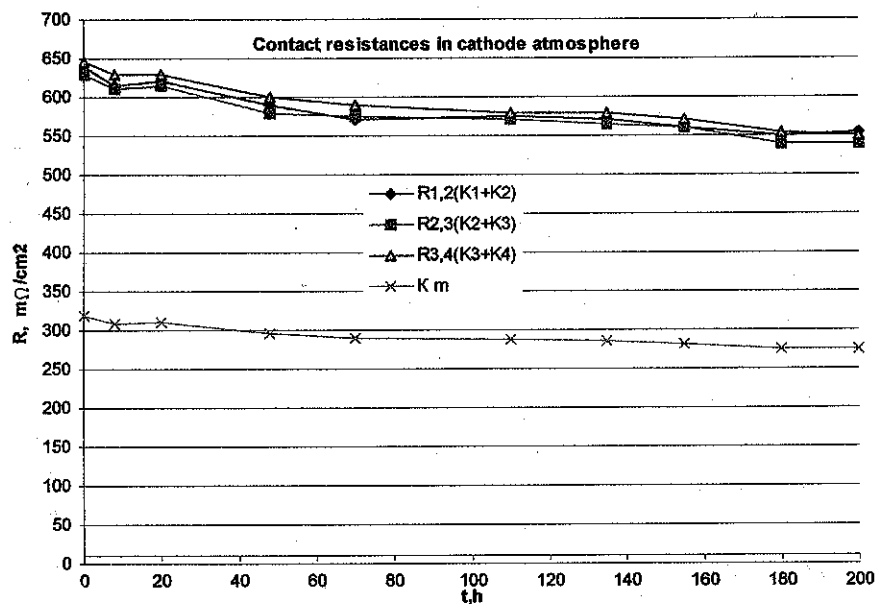


Fig. 2.4

2.3.2. Research on conductivity of contacts of metallic materials using thin sheet samples with porous electrodes in the cathode gas environment

We have carried out comparative studies of the specimens of the steel of 20X23H18 grade and of the new alloy X30H45IOT in order to determine contact resistances in the cathode atmosphere ($0.05 O_2 + 0.05 CO_2 + 0.20 H_2O + N_2$ (balance)) during 500 h (the area of the electrode plates - $1.0 cm^2$ - a square of 10×10 mm with the thickness of 0.95 mm). The porosity of nickel electrodes filled with Li-Ka eutectics amounted to $\sim 60\%$). The obtained data are shown in Tables 2.9, 2.10,

Table 2.9

Contact resistances, $m\Omega/cm^2$
of the alloy X30H45IOT in atmosphere medium
 $0.05 O_2 + 0.05 CO_2 + 0.20 H_2O + N_2$ (balance)

No i/i	t, h	R _{1,2}	R _{2,3}	R _{3,4}	K m
1	1	590	573	587	292
2	7	572	555	573	283
3	19	558	541	543	274
4	27	533	528	529	265
5	43	525	523	537	264
6	65	517	519	528	261
7	92	510	514	528	259
8	110	504	510	519	255
9	141	506	491	505	250
10	164	502	491	501	249
11	166	512	514	528	259
12	180	507	510	519	256
13	203	496	491	505	249
14	228	498	491	501	248
15	263	500	514	508	254
16	283	493	510	504	251
17	302	486	491	505	247
18	324	490	491	501	247
19	348	497	514	528	256
20	351	518	510	519	258
21	356	500	491	505	249
22	363	501	491	501	249
23	371	498	493	505	249
24	396	500	504	518	254
25	423	502	503	512	253
26	451	493	501	507	250
27	474	495	491	505	249
28	492	490	491	501	247

Table 2.10

Contact resistances, $m\Omega/cm^2$
Contact resistances of the steel 20X23H18 (type
310s) in atmosphere medium $0.05 O_2 + 0.05 CO_2 +$
 $0.20 H_2O + N_2$ (balance)

No i/i	t, h	R _{1,2}	R _{2,3}	R _{3,4}	K m
1	0	448	441	452	223
2	6	431	427	441	216
3	18	421	416	418	209
4	26	413	406	407	204
5	42	399	403	413	202
6	64	403	399	406	201
7	91	399	396	406	200
8	109	392	392	399	197
9	140	385	378	389	192
10	163	389	378	385	192
11	165	399	396	406	200
12	179	392	392	399	197
13	202	385	378	389	192
14	227	389	378	385	192
15	262	399	396	406	200
16	282	392	392	399	197
17	301	385	378	389	192
18	323	389	378	385	192
19	347	399	396	406	200
20	350	392	392	399	197
21	355	385	378	389	192
22	362	389	378	385	192
23	370	385	378	389	192
24	395	399	396	406	200
25	422	399	396	406	200
26	450	392	392	399	197
27	473	385	378	389	192
28	491	389	378	385	192

Here:

t, h – Time from the start of settling into the mode – temperature of 650°C (after the emergency shut-downs, the total time at this temperature is taken into account),

$R_{1,2}$ ($K1+K2$) or $R1$, $R_{2,3}$ ($K2+K3$) or $R2$, $R_{3,4}$ ($K3+K4$) or $R3$, $m\Omega$ – resistances of 2 contacts + resistance of the porous electrode, resistance of a single cell being measured excluding the resistances of current-leading wires;

$r1, r2, r3, r4, m\Omega$ - resistances of current leaders;

$r12, r23, r34, r14, r13, r24, m\Omega$ – resistances between the cell contacts measured directly with the help of an AC bridge:

Computation of contact resistances is shown in different examples (data 1,28 from Table 2.9 and 1,2,27 from Table.2.10) in Table.2.11. We have also represented the auxiliary computation values, varying which one may trace the correctness of measurements, course of computations and fluctuations of the values.

Basic values are shown in the picture for a single cell.

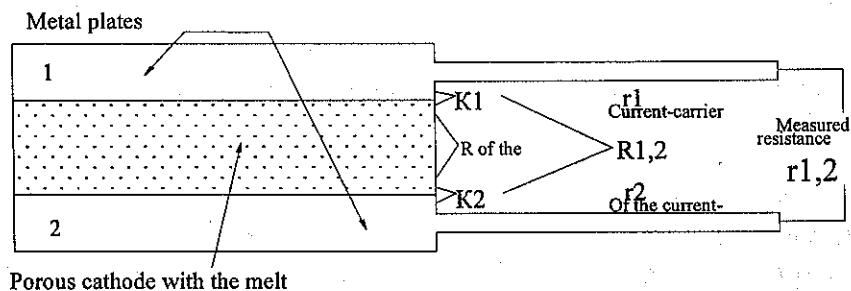


Table 2.11

Directly measured (in italics) and calculated resistance values

Value and its relation with the others	for	№ of i/i 20X23H18		№ of i/i for alloy X30H45IOT	
		1	2	1	2
$r12=r1+r2+R1$	598	603,5	580	817	735
$r23=r2+r3+R2$	591	598	570	803	737
$r34=r3+r4+R3$	602	610,5	578	820	748
$r14=r1+r4+R1+R2+R3$	1491	1470	1344	1980	1728
$r13=r1+r3+R1+R2$	1039	1027,5	952	1396	1228
$r24=r2+r4+R2+R3$	1043	1040,5	962	1387	1237
$a1=r13-r12=r3-r2+R2$	441	424	372	579	493
$a2=r13-r23=r1-r2+R1$	448	429,5	382	593	491
$a3=r24-r23=r4-r3+R3$	452	442,5	392	584	500
$a4=r24-r34=r2-r3+R2$	441	430	384	567	489
$a5=r14-r13=r4-r3+R3$	452	442,5	392	584	500
$a6=r14-r24=r1-r2+R1$	448	429,5	382	593	491
$a7=r14-r12=r4-r2+R2+R3$	893	866,5	764	1163	993
$a8=r14-r23=r1+r4-r2-r3+R1+R3$	900	872	774	1177	991
$a9=r14-r34=r1-r3+R1+R2$	889	859,5	766	1160	980
$a10=r12-r23=r1-r3+R1-R2$	7	5,5	10	14	-2
$a11=r23-r34=r2-r4+R2-R3$	-11	-12,5	-8	-17	-11
$a9-a10=2R2$	882	854	756	1146	982
$a1-a4=2r3-2r2$	0	-6	-12	12	4
$a12=2r23+(a1-a4)=4r3+2R2$	1182	1190	1128	1618	1478
$4r3=a12-(a9-a10)$	300	336	372	472	496

r1=	75	86	96	115	123
r2	75	87	99	112	122
r3=	75	84	93	118	124
r4=	75	86	96	115	123
R1= r12-r1-r2	<u>448</u>	<u>431</u>	<u>385</u>	<u>590</u>	<u>490</u>
R2=r23-r2-r3	<u>441</u>	<u>427</u>	<u>378</u>	<u>573</u>	<u>491</u>
R3=r34-r3-r4	<u>452</u>	<u>441</u>	<u>389</u>	<u>587</u>	<u>501</u>
K=(R1+R2+R3)/6	<u>224</u>	<u>217</u>	<u>192</u>	<u>292</u>	<u>247</u>

The above measured values are the averaged ones, since the data vary at the substitution of current leads from an electrode to another one. It is important that one could simultaneously obtain correct data for all six pairs in a single measurement, so that the results of differential computations do not shift. However, as it is shown for example in Table 2.12, at artificial change of different pairs' values for 10 mΩ, which is possible in a process of measurements (the changed values are section-lined), the final contact resistance's value changes less than 2 mΩ. At the second start, we achieved the coincidence of the measured and initial values. At sharp cooling of a cell, one could not achieve the initial results; therefore the experiment was conducted once again.

Table 2.12

Shift of contact resistance value at changing the data being measured for the point 28 in Table 2.9

Value and its relation with the others	Measurement 28 in Table 2.9	Variants of values' fluctuations by the 28 th measurement (by 10 mOhm)				
		735	737	748	1728	1228
r12	735	735	735	735	735	735
r23	737	737	737	737	737	747
r34	748	748	748	748	748	758
r14	1728	1728	1728	1728	1728	1728
r13	1228	1228	1228	1228	1228	1228
r24	1237	1237	1237	1237	1237	1237
a1	493	503	493	503	503	493
a12	491	501	481	491	491	481
a3	500	500	490	500	500	490
a4	489	489	489	489	479	479
a5	500	490	500	500	500	500
a6	491	491	491	491	491	491
a7	993	993	993	1003	1003	993
a8	991	991	981	991	991	981
a9	980	980	980	980	970	970
a10	-2	-2	-12	-12	-12	-12
a11	-11	-11	-1	-11	-21	-11
a9-a10	982	982	992	992	982	982
a1-a4	4	14	4	14	24	14
a12	1478	1488	1498	1488	1498	1508
4r3=a12-(a9-a10)	496	506	506	496	516	526
r1=	123	123	126	121	123	128
r2=	122	120	125	117	117	125
r3=	124	127	127	124	129	132
r4=	123	123	126	121	123	128
R1= r12-r1-r2	490	493	485	488	485	483
R2=r23-r2-r3	491	491	496	496	491	491
R3=r34-r3-r4	501	499	496	504	506	499
K=(R1+R2+R3)/6	247	247	246	248	247	245

2.3.3. Research on conductivity of contacts of metallic materials using thin sheet samples with porous electrodes in the anode gas environment.

We have tested the steel(X30H45IOT and 20X23H18) specimens with the purpose of determining contact resistances in anode atmosphere ($0.20 \text{ H}_2 + 0.80 \text{ CO}_2$) + $0.20 \text{ H}_2\text{O}$ (60°C in equilibrium, with water) during 500 h (the area of the electrode plates - 1.0 cm^2 - square 10×10 mm with the thickness of 0.95 mm. The porosity of nickel electrodes filled with Li-Ka eutectics amounted to $\sim 60\%$). The obtained data are shown in Tables 2.13, 2.14.

Table 2.13

Contact resistances $\text{m}\Omega/\text{cm}^2$
Of alloy X30H45IOT in the atmosphere
($0.20 \text{ H}_2 + 0.80 \text{ CO}_2$) + $0.20 \text{ H}_2\text{O}$ (60°C in equilibrium, with water)

No i/i	t, h	R _{1,2}	R _{2,3}	R _{3,4}	K m
1	2	490	461	487	240
2	6	500	470	471	240
3	17	495	465	443	234
4	27	433	407	401	207
5	38	425	400	387	202
6	48	417	392	377	198
7	63	410	385	373	195
8	90	404	380	371	192
9	102	372	350	350	179
10	116	361	339	341	174
11	132	347	333	328	168
12	151	351	339	319	168
13	176	350	338	330	170
14	192	348	331	325	167
15	204	340	320	308	161
16	227	336	318	304	160
17	240	342	321	305	161
18	254	340	320	301	160
19	279	333	313	318	161
20	301	328	308	309	158
21	317	332	312	305	158
22	342	341	321	301	160
23	354	331	311	305	158
24	370	336	316	318	162
25	381	308	304	294	151
26	396	325	306	307	156
27	404	319	300	305	154
28	424	315	296	301	152
29	441	321	302	298	153
30	452	326	306	289	154
31	478	322	303	295	153
32	491	318	299	299	153
33	502	330	310	307	158

Table 2.14

Contact resistances $\text{m}\Omega/\text{cm}^2$
of steel 20X23H18 (type 310s) in the atmosphere
($0.20 \text{ H}_2 + 0.80 \text{ CO}_2$) + $0.20 \text{ H}_2\text{O}$ (60°C in equilibrium, with water)

No i/i	t, h	R _{1,2}	R _{2,3}	R _{3,4}	K m
1	0	375	376	364	186
2	4	412	400	396	201
3	15	423	430	410	211
4	25	395	411	383	198
5	36	371	382	360	185
6	46	351	350	340	174
7	61	334	317	332	164
8	88	322	306	312	157
9	100	315	309	306	155
10	114	294	293	294	147
11	130	300	302	291	149
12	149	292	279	283	142
13	174	288	274	279	140
14	190	291	265	278	139
15	202	275	261	269	134
16	225	279	255	271	134
17	238	265	252	267	131
18	252	272	258	264	132
19	277	275	251	267	132
20	299	261	248	263	129
21	315	270	252	262	131
22	340	263	250	261	129
23	352	266	253	258	129
24	368	269	252	261	130
25	379	253	239	240	122
26	394	259	246	254	127
27	402	267	249	259	129
28	422	260	247	252	127
29	439	271	253	263	131
30	450	268	255	263	131
31	476	282	250	264	133
32	489	278	257	270	134
33	500	308	293	299	150

Here:

t, h – time from the start of settling into the mode – temperature of 650⁰C (after the emergency shut-downs, the total time at this temperature is taken into account),

R1,2 (K1+K2), R2,3 (K2+K3), R3,4 (K3+K4), mΩ– resistances of 2 contacts + resistance of the porous electrode, resistance of a single cell being measured excluding the resistances of current-leading wires;

r1, r2, r3, r4, mΩ - resistances of current leads;

r12, r23, r34, r14, r13, r24, mΩ – resistances between the cell contacts measured directly with the help of an AC bridge:

Computation of contact resistances is shown in different examples (data 1,2,15,32 from Table 2.131,28) is shown in Table.2.15. We have also represented the auxiliary computation values, varying which one may trace the correctness of measurements and course of computations.

Table 2.15

Directly measured (in italics) and calculated resistance values for the points:				
Value and its relation with the others	№ i/i			
	1	2	15	32
<i>r12=r1+r2+R1</i>	629	666	548	556
<i>r23=r2+r3+R2</i>	630	654	533	532
<i>r34=r3+r4+R3</i>	617	649	540	542
<i>r14=r1+r4+R1+R2+R3</i>	1368	1462	1077	1080
<i>r13=r1+r3+R1+R2</i>	1004	1065	807	808
<i>r24=r2+r4+R2+R3</i>	993	1049	801	799
<i>a1=r13-r12=r3-r2+R2</i>	375	399	259	252
<i>a2=r13-r23=r1-r2+R1</i>	374	412	274	276
<i>a3=r24-r23=r4-r3+R3</i>	363	396	268	267
<i>a4=r24-r34=r2-r3+R2</i>	376	400	261	257
<i>a5=r14-r13=r4-r3+R3</i>	365	396	270	272
<i>a6=r14-r24=r1-r2+R1</i>	376	412	276	281
<i>a7=r14-r12=r4-r2+R2+R3</i>	739	796	529	524
<i>a8=r14-r23=r1+r4-r2-r3+R1+R3</i>	739	808	544	548
<i>a9=r14-r34=r1-r3+R1+R2</i>	752	812	537	538
<i>a10=r12-r23=r1-r3+R1-R2</i>	0	12	15	24
<i>a11=r23-r34=r2-r4+R2-R3</i>	13	4	-7	-10
<i>a9-a10=2R2</i>	752	800	523	514
<i>a1-a4=2r3-2r2</i>	-2	-1	-2	-5
<i>a12=2r23+(a1-a4)=4r3+2R2</i>	1258	1306	1065	1059
<i>4r3=a12-(a9-a10)</i>	506	506	542	545
R1= r12-r1-r2	375	412	275	278
R2=r23-r2-r3	376	400	261	257
R3=r34-r3-r4	363	396	269	270
K=(R1+R2+R3)/6	186	201	134	134
r1=	127	127	136	138
r2=	127	127	137	140
r3=	126	127	135	135
r4=	127	127	136	138

2.3.4. Research on corrosion stability of thin sheet samples in the melt of lithium and potassium carbonates at 650°C during 500 h.

For corrosion testing, the specimens in the form of thin plates with the size of about 20x10x0.8 mm were used. Before testing, the specimens were polished, cleaned and weighed on scales of VLR-200 model, class 2 (error – 0.5 mg). The surface area varied within the limits of 3.5 – 4.5 cm².

After testing, the specimens were extracted from the congealed salt, washed from carbonates by the diluted hydrochloric acid (1:4), dried and weighed. The rate of adhesion (g/m²h) of a specimen was calculated by formula:

$$K = (m - m')/St,$$

where: m – initial mass of the specimen, g.; m' – mass of the specimen after removal of corrosion products, g.; S – surface area of the specimen before testing, m²; t – time, h.

At the increase of the specimen mass, the abatement was calculated with the account of formation of the compounds of LiFeO₂ – type (by the data of X-ray phase analysis).

We have carried out gravimetric testing of alloys X30H45IOT and 20X23H18 (310S) in the melt of Li and Ka carbonates of eutectic composition (62:38 mol. %) in the atmosphere of gas mixtures: anode (0.20 H₂ + 0.80 CO₂) + 0.20 H₂O (60°C in equilibrium, with water) and cathode (0.05 O₂ + 0.05 CO₂ + 0.20 H₂O + N₂ (balance)).

Chemical composition of alloys is shown in Table 2.16.

Table 2.16

Main elements' content in alloys, % mass.

Alloy	Cr	Ni	Fe	Ti	Al	Y	Si	Mn	C
X30H45IOT	29,5	44,5	Oct.	0,25	0,68	0,035	0,74	0,59	0,014
20X23H18	23	18	58	0,2	-	-	1	2	0,20

The results of corrosion testing in the melt of Li and Ka carbonates at temperature of 650°C during 500 h. are represented in Table 2.17. Since in most cases we observed the increase of the mass of specimens due to the oxide film formation, the decrease was calculated taking account of the oxide compounds formation of LiFeO₂ type (according to the data of X-ray phase analysis).

Table 2.17

Average corrosion rate by gravitometric data

Alloy	Decrease of mass (-Δm), r	Surface area, cm ²	Corrosion losses, g/m ²	Corrosion rate, g/m ² h
Atmosphere: anode				
X30H45IOT	0,00058	4,70	1,2	0,0024
20X23H18	0,0013	3,52	3,6	0,0073
Atmosphere: cathode				
X30H45IOT	0,0033	4,6	7,2	0,015
20X23H18	0.017	3,53	48	0,095

X-ray phase analysis was done on a software-hardware complex comprising of a general-

purpose diffractometer DRON-3 and a PC "Pentium-II". X-ray diagrams were taken from the surface of specimens on the reflection in $\text{Cu}_{\text{K}\alpha}$ radiation. Voltage on a tube – 40 kV, current – 20 mA, irradiated area – 10 mm^2 .

The following phases were detected on the surface of specimens:

Atmosphere: anode

X30H45IOT: (Ni, Fe), LiFeO_2 , LiCrO_2 , NiCr_2O_4 ;
20X23H18: LiFeO_2 , LiCrO_2 , epsilon- Fe_2O_3 , NiCr_2O_4 ;

Atmosphere: cathode

X30H45IOT: LiFeO_2 , LiCrO_2 , (Ni, Fe), LiNiO_2 ;
20X23H18: LiFeO_2 , LiCrO_2 , NiCr_2O_4 , Fe_2O_3 ;

The sections for **metallographic examination** were prepared in the following way: the specimen was placed in a form in vertical position and poured with the Wood alloy. Then it was hand-polished by the abrasive paper. Finish polishing was made applying a diamond paste ACM 1/0 HOM. The ready polished microsections were examined using an optical microscope NEOPHOT-32 (Karl Zeiss Jena).

The results of metallographic studies are as follows.

Anode atmosphere:

X30H45IOT: On the surface of the specimens one may see a solid oxide film being black and dull. On the cross-microsection, using a microscope one may observe a solid gray porous oxide film with the thickness of 5-10 μm .

20X23H18: On the surface one may see a solid oxide black and dull film. Using a microscope one may observe 2 layers: the external layer - gray porous oxide film with the thickness of 20-25 μm . The internal layer is dark-gray and porous with the thickness of 5-10 μm .

Cathode atmosphere:

X30H45IOT: Using a microscope one may observe a gray porous oxide layer with the thickness of 5-10 μm , sometimes up to 15 μm . Under the oxide layer, there exists an internal oxidation zone with the depth of 10-12 μm . The total depth of oxidation amounts to 20-25 μm .

20X23H18: There is a solid dark-gray dull porous oxide film on the surface of the specimens. Using a microscope one may observe 2 layers: the external layer - gray porous oxide film with the thickness of 10-15 μm , sometimes - 10-30 μm . The internal layer is dark-gray, porous with the thickness of 5-10 μm , sometimes - 25-35 μm .

Table 2.18

Thickness of oxide layers on micro-cross-sections of the specimens (metallography).

Alloy	External oxide layer, μm	Internal oxide layer, μm	Total length, μm
Atmosphere: (anode)			
X30H45IOT	5-10	-	5-10
20X23H18	20-25	5-10	25-35
Atmosphere: (cathode)			
X30H45IOT	5-15	10-12	15-25
20X23H18	10-30	5-35	15-65

To carry out micro-X-ray spectral analysis, the cross-sections of the specimens from the low-melting-point Wood alloy were used. They were analyzed applying a "Comebax" instrument. The results are shown in Fig. 2.5.-2.8.

Anode atmosphere:

X30H45IOT: On a micro-cross-section along the scanning line, one may observe an oxide layer with the thickness of 15 μm . At the inner bound, the oxide layer is doped with Al, closer to the surface-with Ni, Fe and Cr.

Along the scanning line, one may observe a changed zone (18 μm), with approximately double decrease of Cr content.

20X23H18: On a micro-cross-section along the scanning line, one may observe an oxide layer with the thickness of 20 μm . The internal oxide layer (8 μm) is doped with Si and Cr, the external one-with Fe.

Along the scanning line, one may observe a changed zone (8 μm), with approximately double decrease of Cr content, while Ni and Fe content increases.

Cathode atmosphere:

X30H45IOT: On a micro-cross-section along the oxygen scanning line, one may observe an oxide layer with the thickness of 11 μm . At the inner bound, the oxide layer is doped with Cr, closer to the surface-with Ni and Fe.

Along the Cr scanning line, one may detect a changed zone (18 μm) with approximately double decrease of Cr content.

20X23H18: On a micro-cross-section along the oxygen scanning line, one may observe an oxide layer with the thickness of 70 μm . At the inner bound, the oxide layer (42 μm) is doped with Si and Cr, the outer layer (28 μm) -with Ni and Fe. Along the Cr scanning line, one may detect a changed zone (6 μm) with approximately double decrease of Cr content.

Fig. 2.5. Steel X30H45iOT. Atmosphere: (anode)

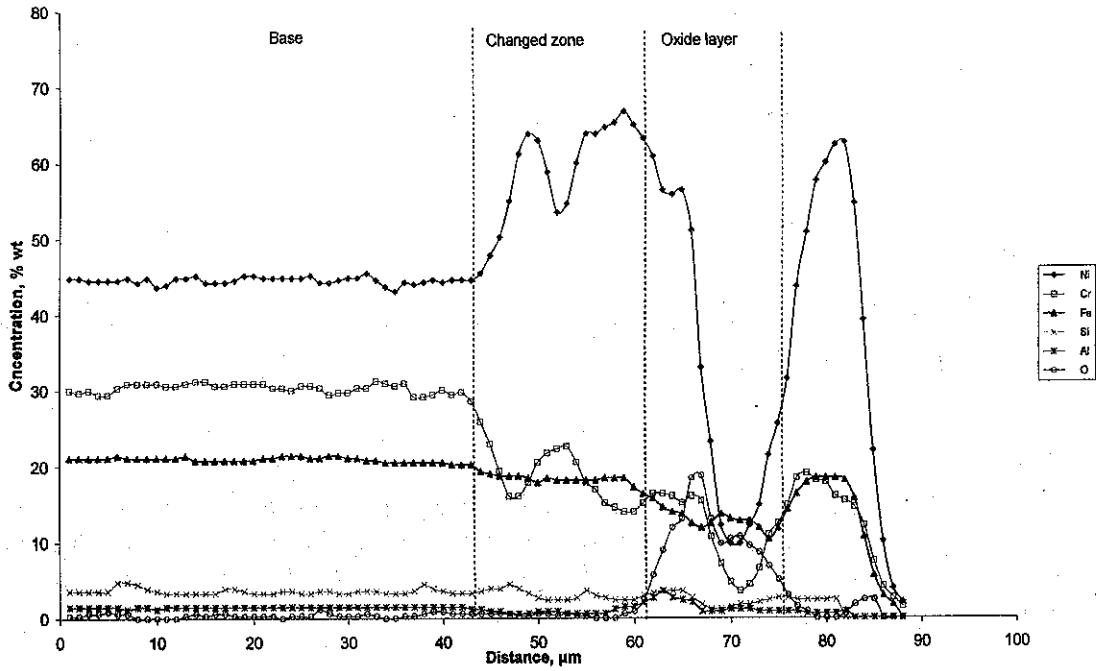


Fig. 2.6. Steel 20X23H18. Atmosphere: (anode)

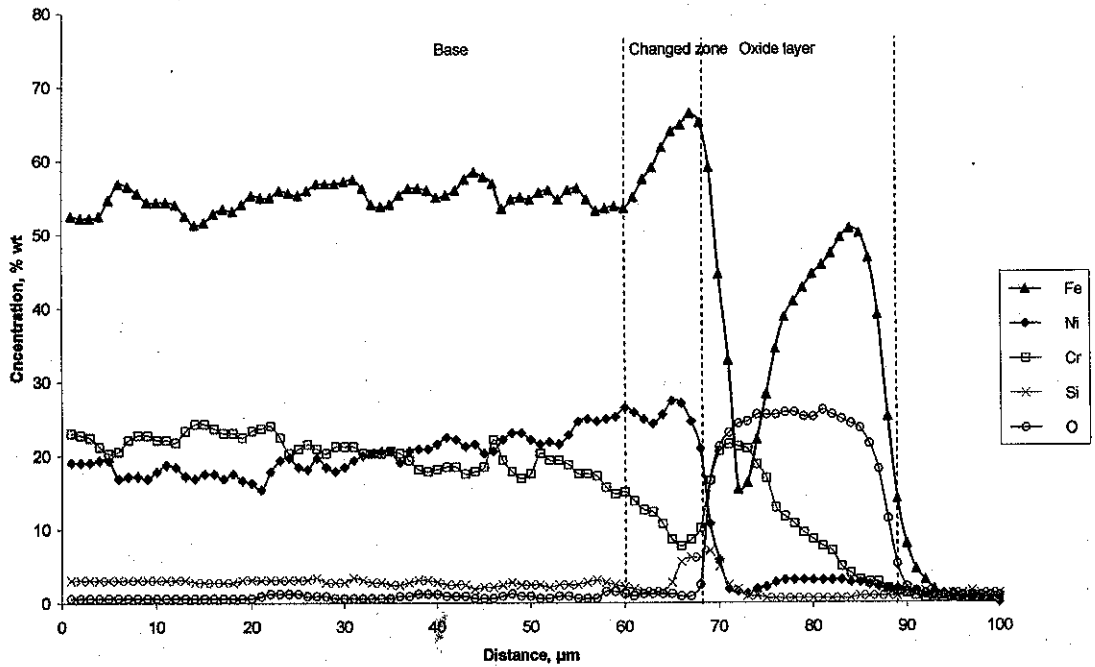


Fig. 2.7. Alloy X30H45IOT. Atmosphere: (cathode)

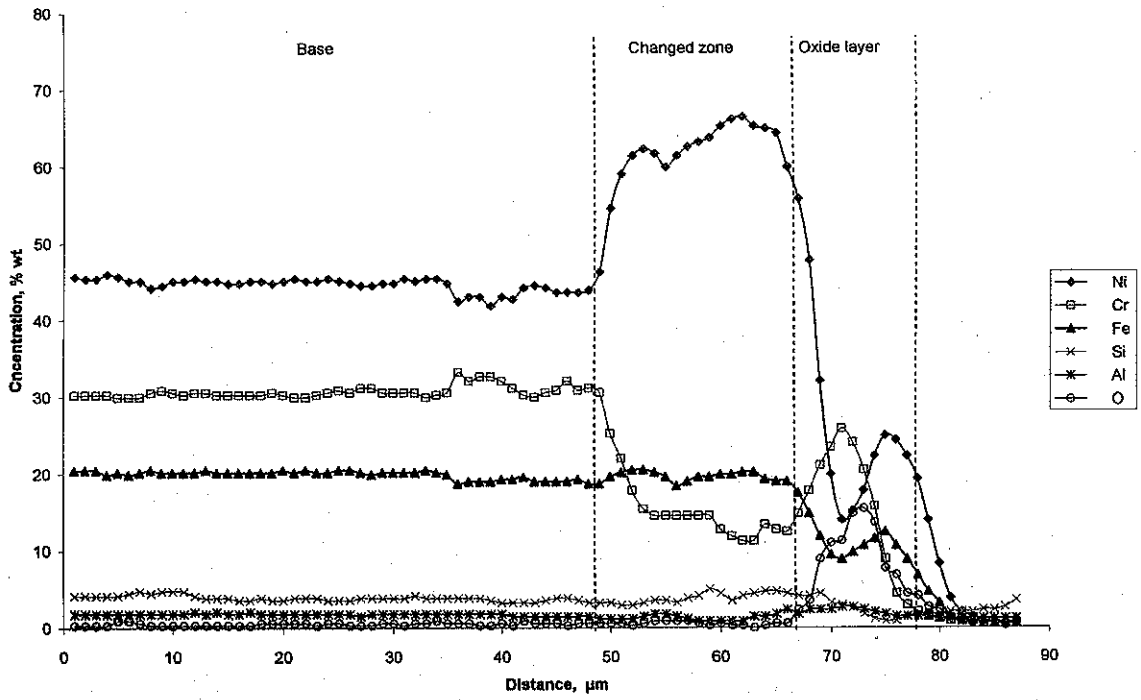


Fig. 2.8. Steel 20X23H18. Atmosphere (cathode)

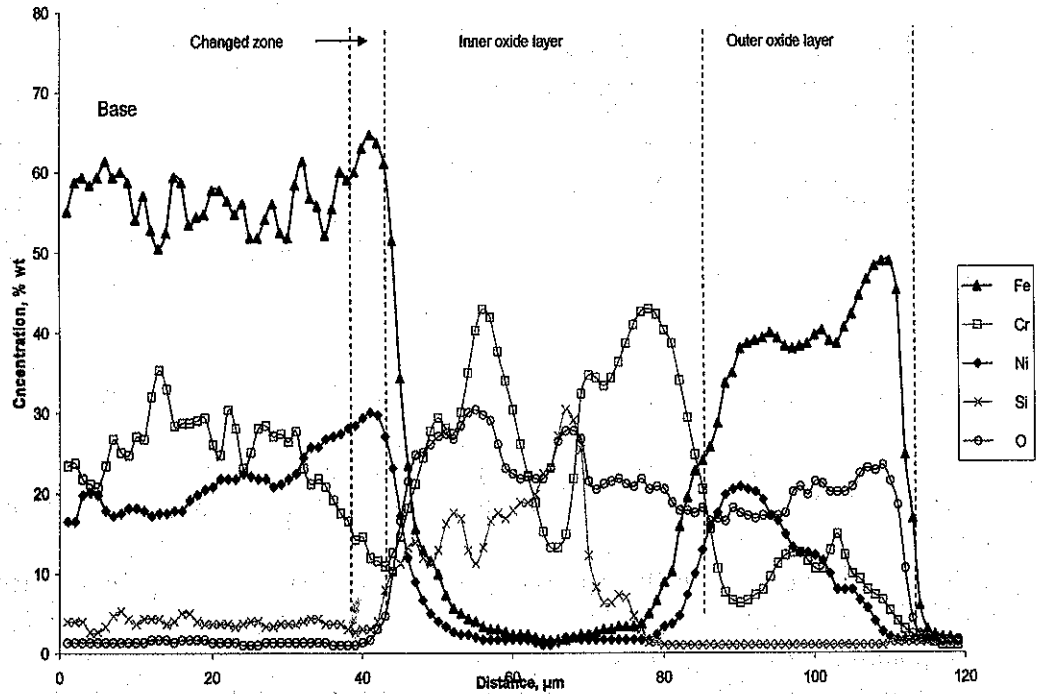


Table 2.19

Layers' thickness on micro-cross-sections of specimens according to micro-X-ray spectrum analysis data.

Alloy	Outer oxide layer, μm	Inner oxide layer, μm	Changed zone, μm
Atmosphere: (anode)			
X30H45IOT(Y)	15	-	18
20X23H18	12	8	8
Atmosphere: (cathode)			
X30H45IOT(Y)	11	-	18
20X23H18	28	42	6

To have a more exact comparison in terms of corrosion rate, the data obtained by gravimetric method are transferred from $\text{g/m}^2\text{ч}$ into mm/year by formula:

$$K = V * 8,76 / d,$$

where K – depth of corrosion, mm/year ; V – corrosion rate, $\text{g/m}^2\text{ч}$; d – alloy density, g/cm^3 ; 8,76 – coefficient derived from the number of hours contained in a year (8760) divided by 1000.

Table 2.20

Depth of corrosion of alloys (500 h) by gravitometric data

Alloy	Corrosion rate, $\text{g/m}^2\text{h}$	Alloy density, g/cm^3	Depth of corrosion, mm/year
Atmosphere: (anode)			
X30H45IOT(Y)	0,0024	8,1	0,0026
20X23H18	0,0073	7,88	0,0081
Atmosphere: (cathode)			
X30H45IOT(Y)	0,015	8,1	0,016
20X23H18	0,095	7,88	0,105

2.4. Test smelting in industrial furnaces. Fabrication of forgings for rolled sheet stock.

The technology of the pilot industrial batch of the metal sheets with the dimensions 0,8x820x1420 mm from the alloy of the X30H45IOT type has been developed. It included the following kinds of works.

- Fabrication of forged billets in Public Corporation "Metallurgical Plant «Electrostal»».
- Fabrication of the batch of thin rolled metal with the dimensions of 0,8 x 712 x 1296 mm in Public Corporation «Ashinsky Metallurgical Plant».
- Smelting of the alloy in an open induction furnace with the capacity of 1,0 ton using commercial charge materials: ferro-"armko" or electrotechnical steel 10895, metal chromium or ferrochromium FCH 006, nickel of H1 or H1Y grade, aluminum A-97, metal titanium BT-1-0, metal manganese MM-95, ferrosilicium $\Phi\text{C}-65$, yttrium.

Metal chromium or ferrochromium is added into liquid metal during fusing of the charge material. After melting the slag is taken away, after which a new one is formed. Deoxidation of the slag is effected by boron-calcium. After brightening of the slag, the specified quantities of manganese and aluminum are added.

3-5 minutes before the metal is ready, metal titanium is added in the quantity of 0,25% taking into account the already available in the charge materials. 2-3 minutes before the discharge, itrium is added into the metal.

- Before discharging from the furnace, a sample is taken from the furnace for being tested for forgeability.
- Pouring of the metal is effected from "above" in the argon protective atmosphere into the moulds for round ingots with the mass of 500-600 kg. The funnel diameter is 35-40 mm. Backfilling of the added part is effected by non-ferriferous thermit. The curing time of the ingots in the moulds is not less than 2 hours. The cooled ingots undergo mechanical treatment for the depth of 10-15 mm from each side with an eye to remove the surface defects.
- Heating of the ingots for forging is done as follows:
 - Temperature of the furnace at filling – not higher than 850⁰C;
 - Duration of heating - 10 hours;
 - Heating temperature of the ingots before forging - 1180⁰C;

The ingots are forged at hammers into the flat bars with the cross-section of 45x185 mm with intermediate heating cycles.

• After the control of the metal quality and its conformity with the specifications the billets are transported for the further rolling into the sheets.

• Rolling includes two phases:

The first stage – hot-rolled sheet - MILL "1500":

BILLET	HEATING BEFORE ROLLING	MILL	THERMAL TREATMENT	ETCHING OF THE SHEETS	STRAIGHTENING	CUTTING
→ 26,5- 65,0x185- 225x x830-1030 mm	→ IN A CIRCULAR FURNACE	→ "1500"	→ IN A ROLL-TYPE FURNACE	→ (SODA-AND-ACID)	→ (11-ROLLS STRAIGHTENING MACHINE)	

After the first stage we have the product (thermally treated, etched).

Second Phase – cold-rolled sheet – MILL "1400"

• The ingots are heated in the furnace up to the temperature of 1150⁰C. Hot rolling is effected at the rolling mill "1500" with the intermediate heating cycles into the sheets with the thickness of 2,5-3,0 mm.

• Further the sheets are thermally treated in a straightway furnace by the mode: 1100⁰C-1150⁰C, water shower cooling. After soda-and-acid etching and fettling the sheets are transported to the mill "1400", where they undergo cold rolling up to the required thickness (during several alterations including thermal treatment and etching).

The sheets with the sizes 0.8x820x1420 mm undergo thermal treatment by the above mode and etching. After finishing operations the quality of the product is controlled.

In Public Corporation «Metallurgical Plant «Electrostal»» in compliance with the elaborated technological scheme the alloy of the X30H45IOT-type was smelted.

Actual chemical composition (%% mass): C - 0,014; Si - 0,74; Mn - 0,59; S - 0,007; P - 0,013; Cr - 29,5; Ni - 44,5; Al - 0,68; Ti - 0,25; Y - 0,035.

The ingot was forged into 5 billets with the sizes of 45x185x830-840 mm and 280 kg mass each.

After smelting in Public Corporation «Metallurgical Plant «Electrostal»» and forging into ingots, we have studied the properties of alloy X30H45IOT (composition: C-0,014; Si-0,74; Mn-0,59; S - 0,007; P-0,013; Cr-29,5; Ni-44,5; Al-0,68; Ti-0,25; Y -0,035; Fe-the remainder) from an industrial melt in order to determine the technological modes for the production of a pilot-industrial batch of sheet metal in Public Corporation «Ashinsky Metallurgical Plant».

The results of testing ingots from X30H45IOT alloy are represented in Tables 2.21 – 2.25.

Table 2.21

Contamination of the X30H45IOT alloy (all-Russian State Standard 1778-III4) by metal-free impurities

N ^o N ^o of the sheet-bar	SO	PO	BS	PS	NDS	S	SN	PN
1	0,5	0,5	0,5	0,5	0,5	0,5	3	3
2	0,5	0,5	0,5	0,5	0,5	0,5	1	2,5
3	0,5	0,5	0,5	0,5	0,5	0,5	2	3
4	0,5	0,5	0,5	0,5	0,5	0,5	2	2,5
5	0,5	0,5	0,5	0,5	0,5	0,5	3	2
6	0,5	0,5	0,5	0,5	0,5	0,5	2	2,5

SO – stitch oxides;
PO – point oxides;
BS – brittle silicates;
PS – plastic silicates;

NDS – non-deformable silicates;
S - sulphides;
SN – stitch nitrides;
PN – point nitrides.

Table 2.22

Contamination of the X30H45IOT alloy (ASTM B45 method A) by metal-free impurities

N ^o N ^o of the sheet-bar	A		B		C		D	
	M	Б	M	Б	M	Б	M	Б
1								
2	0	0	0	0	0	0	0	0
3	0	0	0	0	0	0	0	0
4	0	0	0	0	0	0	0	0
5	0	0	0	0	0	0	0	0
6	0	0	0	0	0	0	0	0

Table 2.23

Mechanical properties of X30H45IOT alloy (state as delivered)

Testing temperature, °C	σ_{BH} N/mm ²	$\sigma_{0,2}$ N/mm ²	δ , %	ψ , %
20	720	450	36,0	74,9
600	460	290	20,0	26,6
700	340	270	24,8	31,1
800	245	210	40,0	32,4
900	145	135	52,8	75,0

Table 2.24

Mechanical properties of X30H45IOT alloy after thermal treatment under conditions: 1050 °C, cooling in the air

Testing temperature, °C	σ_{Bp} N/mm ²	$\sigma_{0,2}$ N/mm ²	δ , %	ψ , %
20	685	330	43,2	78,8
600	475	165	40,0	50,7
700	360	160	38,0	45,3

Table 2.25

Impact viscosity of X30H45IOT alloy

Thermal treatment mode	Testing temperature, °C	KCU, J/cm ²
State as delivered (without thermal treatment)	20	185,0
	600	140,0
	700	166,3
	800	168,8
Thermal treatment by regime: 1050 °C, cooling in the air	20	275,0
	600	217,5
	700	193,8
	800	225,0

The ingots were sent to Public Corporation "Ashinsky Metallurgical Works" ", where the required normative-technical documentation was worked out and a pilot batch of 25 sheet metal pieces with the size of 0,8x820x1420mm was fabricated (see picture 2.1).

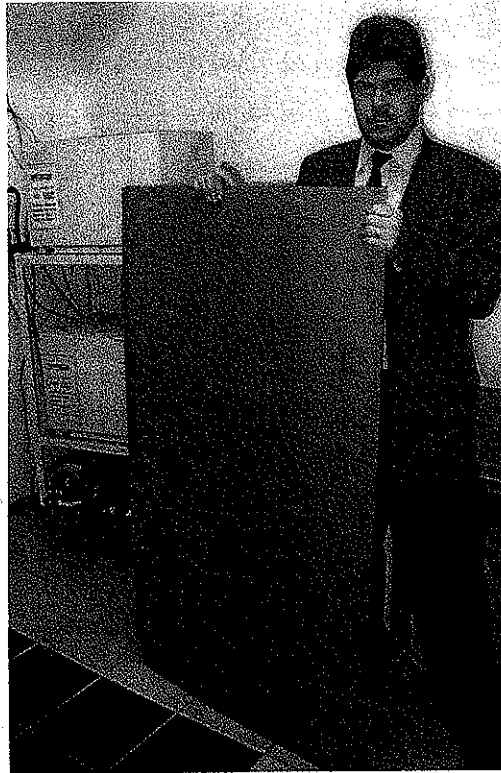


Photo 2.1.

2.5. Delivery of a batch of sheets to the Partner for the research

Getting ready to deliver a batch of sheets to the Partner in FGUP TSNIICHERMET named after I.P. Bardin, an independent customs examination was carried out and a decision was issued №002/161/ЦКП dated 6 April 2004, authorizing the delivery to the USA without licensing of:

1. Batch of sheets from X30H45IOT alloy with the size of 1420x820x0,8 (mm), quantity - 12 pcs.;
2. Batch of nickel-coated sheets from 20X23H18 steel with the size of 1420x712x0.4(mm), quantity - 3 pcs.;
3. Batch of sheets from X30H45IOT alloy with the size of 180x180x0,8 (mm), quantity - 4 pcs.;
4. Batch of sheets from 20X23H18 steel with the size of 180x180x0.4 (mm), quantity - 4 pcs.,
Due to the change in the terms of project, just the two last items have been sent to the firm FCE (in more detail see p.1.1.9.).

The new terms are reflected in the supplement to the Project ADDENDUM #3, signed by the ISTC (Moscow), RFNC-VNIIEF (Sarov) and US DOE (Washington) representatives.

2.6. Cost evaluation for manufacturing of a batch of sheets

We have analyzed the cost data on the technology to produce a test-industrial batch of sheets for bipolar plates with the size of 712 x 1296 x 0.55 mm with the annual order amount up to 400000 plates from X30H45IOT alloy in Russia basing on:

- fabrication of a batch of forged ingots in Public Corporation "Metallurgical Works Elektrostal".
- fabrication of a batch of sheet rolled metal with the size of 0,8 x 712 x 1296 mm in Public Corporation "Ashinsky Metallurgical Works" or in Public Corporation «Metchel».

Public Corporation "Metallurgical Works Elektrostal", Public Corporation "Ashinsky Metallurgical Works" and Public Corporation «Metchel» are some of the largest producers of corrosion-resistant steels and alloys produced in the form of thin sheet rolled metal, including the steel of 310S type.

The price structure for a 1000 kg batch of sheets with the output of ready rolled products with the size of 0,55x1296x712 mm (3,9 kg.) at their cold rolling depending on the order amount is represented in Table 2.26.

Table 2.26

Price structure for a 1000 kg batch of sheets depending on the order amount

№	Expense item	Order amount						Economy of scale, % (2-200 tn)
		2 tn		20 tn		200 tn		
		Expenses, \$	% of the price including value added tax (VAT)	Expenses, \$	% of the price including value added tax (VAT)	Expenses, \$	% of the price including value added tax (VAT)	
1	Basic materials: charge materials, modifiers, ligature, de-oxidizers	8466	38,32	8212	39,11	6858	38,87	-19
2	Auxiliary materials: etching solutions, lubricants, diluents	262	1,19	249	1,19	236	1,34	-10
3	Wages of the personnel of foundry- forging manufacturing department	2311	10,46	2267	10,80	2201	12,48	-4,76
4	Wages of the personnel of rolling-etching manufacturing department	2439	11,04	2392	11,39	2323	13,17	-4,76
5	Overheads of foundry- forging manufacturing department, including technological adjustment, certification	3996	18,09	3548	16,90	2607	14,77	-34,77
6	Overheads of rolling-etching manufacturing department	420	1,90	338	1,61	230	1,30	-45,23
7	Transport charges	828	3,75	786	3,74	497	2,81	-40
8	Total	18722	84,75	17793	84,75	14951	84,75	
9	VAT	3370		3203		2691		
10	Price, including VAT	22092		20996		17642		
11	Price of a sheet (0,55x1296x712mm, (3,9 kg.)), \$	86		82		69		-20,14

2.7. Conclusions

2.7.1. We have carried out a comprehensive analysis of corrosion resistance of the group of promising alloys and selected the most promising alloy 30Cr-45Ni-1Al, doped with Ti and Y for being used as the material for separators.

2.7.2. We have adjusted the technology of industrial smelting of the base alloy 30Cr-45Ni-1Al and of Y, Ti-doped alloys.

2.7.3. On a laboratory rolling mill, we have elaborated the technology to produce thin sheet rolled products from the base alloy 30Cr-45Ni-1Al and Y, Ti-doped alloys. The technology includes both hot and cold rolling stages.

2.7.4. A technology for the production of an industrial pilot batch of the sheets from the Y, Ti-doped alloy X30H45IOT with the size of 0,8x820x1420 mm was elaborated, including:

- fabrication of forged sheet rods in Public Corporation «Metallurgical Works «Elektrostal»».
- fabrication of the batch of sheet rolled metal with the size of 0,8x820x1420 mm in Public Corporation «Ashinsky Metallurgical Works».

2.7.5. We have smelted the Y, Ti – doped alloy 30Cr-45Ni-1Al (identification grade X30H45IOT) prepared in an industrial induction furnace (1tn capacity) using commercial charge materials, ligature and oxidizers. The ingots were forged into a flat bar with intermediate heating up. The final composition of the alloy (C-0,014; Si-0,74; Mn-0,59; S - 0,007; P-0,013; Cr-29,5; Ni-44,5; Al-0,68; Ti-0,25; Y -0,035; Fe- remainder) was determined based upon the requirements on manufacturability and stability of the structure. The X30H45IOT alloy has good mechanical characteristics, in particular, σ_{bp} 475 N/mm² at temperature of 600 °C, while the Russian analog of 310S (20X23H18) steel has σ_{bp} 430 N/mm² at these temperatures. At temperatures of 20 °C the alloy X30H45IOT has high viscosity δ , 43,2 %, while the steel 20X23H18 – just 33%. This permits to conduct cold rolling up to the less thickness. We have studied their mechanical properties on thin sheet specimens in the temperature range of 20-700°C. The alloy was tested for weldability; it may be welded using all welding techniques (argon-arc, laser, electron-beam welding) without restrictions.

2.7.6. We have worked out normative-technical documentation and fabricated a pilot batch of sheet products (25 pieces) with the size of 0,8x820x1420mm.

2.7.7. We have carried out parallel testing of corrosion resistance of thin sheet specimens of the Russian analog of steel 310S and the new alloy X30H45IOT from the pilot batch of sheets in the melt of lithium and potassium carbonates at temperature of 650°C during 500 h in gas mixtures atmosphere: anode (0.20 H₂ + 0.80 CO₂) + 0.20 H₂O (60°C in equilibrium with water)) and cathode one (0.05 O₂ + 0.05 CO₂ + 0.20 H₂O + N₂ (balance)). Corrosion rate made 0,095 g/m²h for the steel of 310S type and 0,015 g/m²h for the new alloy under cathode conditions. Under anode conditions, the corrosion rate made 0,0073 g/m²h and 0,0024 g/m²h, accordingly. Thus the new alloy X30H45IOT under cathode conditions has the corrosion resistance ≈6 times higher and under anode conditions ≈3 times higher than that with the steel of 310S type.

2.7.8. We have developed a system of investigation into electric conduction of the contacts of metal materials with porous electrodes under FC conditions. We have carried out parallel testing of conduction of the contacts of metal materials composed of a trilaminar cell with porous electrodes of thin sheet specimens of the Russian analog of steel 310S and the new alloy X30H45IOT from a pilot batch of sheets at temperature of 650°C during 500 h in gas mixtures

atmospheres: the anode ($0.20 \text{ H}_2 + 0.80 \text{ CO}_2$) + $0.20 \text{ H}_2\text{O}$ (60°C in equilibrium with water)) and cathode ones ($0.05 \text{ O}_2 + 0.05 \text{ CO}_2 + 0.20 \text{ H}_2\text{O} + \text{N}_2$ (balance)). The electric resistance amounted to $192 \text{ m}\Omega/\text{cm}^2$ for steel of 310S type and $247 \text{ m}\Omega/\text{cm}^2$ for the new alloy in cathode conditions. In anode conditions, the electric resistance was $134 \text{ m}\Omega/\text{cm}^2$ and $158 \text{ m}\Omega/\text{cm}^2$, accordingly. In such a way, the new alloy X30H45IOT has the electric specific resistance $\approx 30\%$ higher in cathode conditions and $\approx 20\%$ higher in anode conditions than the Russian analog of steel 310S.

2.7.9. An independent customs examination was carried out and a decision was issued authorizing the delivery to the USA without licensing of a pilot batch of sheets from X30H45IOT alloy with the size of $1420 \times 820 \times 0,8 \text{ mm}$ and of specimens from the pilot batch with the size of $0,8 \times 180 \times 180 \text{ mm}$. They are designed for experimental testing at the first stage.

2.7.10. Price analysis was made for the domestic fabrication of experimental-industrial batch of sheets for the bipolar plate with the size of $712 \times 1296 \times 0,55 \text{ mm}$ with the annual order amount up to 400000 plates from the alloy X30H45IOT. The price per a sheet with the size of $0,55 \times 1296 \times 712 \text{ mm}$ (3,9 kg.) produced by rolling method from X30H45IOT alloy amounts to $\approx 69\text{\$}$ provided the order amount exceeds 50000 sheets. At transition from a 500 sheets to a 50000 sheets order amount, the economy of scale amounts to $\approx 20\%$. The price includes all expenses incurred before shipment from a seaport excluding customs taxes.

2.7.11. In a process of works execution, a new alloy was developed and an application for the patent of the Russian Federation was made entitled «Fe-Ni-based corrosion-resistant alloy», the authors- Mishanin S.V., et al.

3. New ceramic materials for an MCFC bipolar plate and an anode (Task 3)

3.1. Development of pore-free cermet compositions on the basis of LiAlO_2 and Ni

3.1.1. Study of a microstructure and electric conductivity of cermets

Selection of $\gamma\text{-LiAlO}_2$ and Ni components to make compositions was caused by the properties of the components. $\gamma\text{-LiAlO}_2$ has high corrosion stability in melts of aggressive chemical compounds /1, 2/. Ni is an electrically conductive material and is also stable to the influence of aggressive environment /3/. Samples of the following cermet compositions were made for tests by a hot-pressing method 80% $\gamma\text{-LiAlO}_2$ +20%Ni, 60%TiN+40%Ni and 40%TiN+60% Ni. Results of research on microstructure and on electric conductivity of cermets are described in detail in /6, 7/. Micro images of a fracture of the cermet of 60% $\gamma\text{-LiAlO}_2$ + 40% Ni composition that has the best complex of properties is given in Fig.3.1.

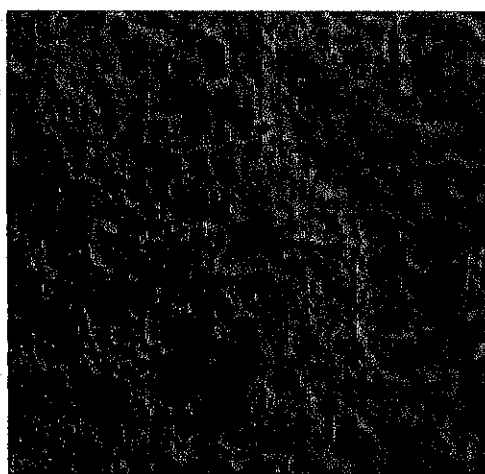
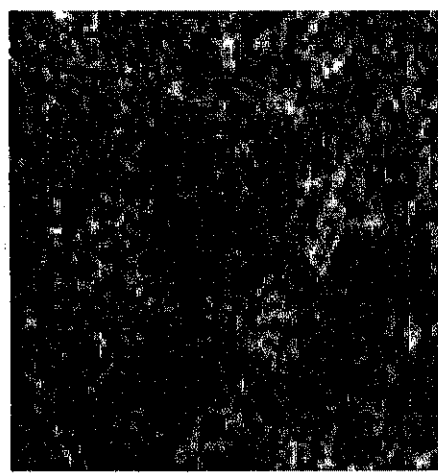
SEI - 10 μm BEI - 10 μm

Fig.3.1. Microimages of the fracture of the best cermet 60% $\gamma\text{-LiAlO}_2$ + 40% Ni

Table 3.1 shows results of measurements of electric conductivity of cermets.

Table 3.1

Material	Resistance, Ohm	Specific resistance, Ohm \cdot mm ² / m	Specific conductance, MCm / m
80% $\gamma\text{-LiAlO}_2$ + 20% Ni	$2,9 \times 10^6$	10^9	10^{-9}
60% $\gamma\text{-LiAlO}_2$ + 40% Ni	0,0071	5,9	0,169
40% $\gamma\text{-LiAlO}_2$ + 60% Ni	0,0011	1,03	0,951

3.1.2. Research on corrosion stability of cermets in the melt of electrolyte during 100 hours

60% γ - LiAlO_2 + 40%Ni cermet composition was chosen for corrosion tests as it had the best parameters in specific resistance (5.9 ohm \cdot mm²/m) and corrosion stability in the electrolyte melt during 40 hours /6, 7/. 12 samples were exposed to the anode conditions of an MCFC (see Appendix 1) during 100 hours. Corrosion stability was evaluated using a gravimetric analysis. Changes in the mass (weight) of the samples being tested were determined. Each 25 hours 3 samples were taken out of the cell. They were rinsed, dried and weighed. The other samples stayed within the cell. The results of the tests are given in Table3.2.

Table 3.2

Composition of the sample	$\Delta m / S, g/cm^2$			
	25 hours	50 hours	75 hours	100 hours
60% γ -LiAlO ₂ +40%Ni	0,0017	0,0025	0,0026	0,0035
Steel 20X23H18T*				0,0014

*Values are given for comparison

3.2. Development of pore-free cermets on the basis of BaCeO₃ conductive ceramics with metal binders of Ni, Ni-Mo.

3.2.1. Properties of the powder and sintered BaCeO₃ ceramics.

In order to improve heat resistance of the nickel matrix under elevated temperatures, there was performed a study of possible introduction of a fine-dispersed powder of BaCeO₃ composition. BaCeO₃ lattice is cubic, a structural type is K18 (type of CaTiO₃), O_h1-Pm3m, a = 4,386 Å [4]. Powder of barium -cerium oxide was used here, produced by JSC «Krain», Yekaterinburg. Images of particles and a bar chart of particle distribution in sizes are given in Fig. 3.2. The minimum size of particles is 1.3 microns; the maximum one is 35 microns. The average value is 8.9 microns; however, most particles have a size of 3 – 6 microns. Large particles are conglomerations formed of separated not large particles. Particles of the powder are mostly of a round shape.

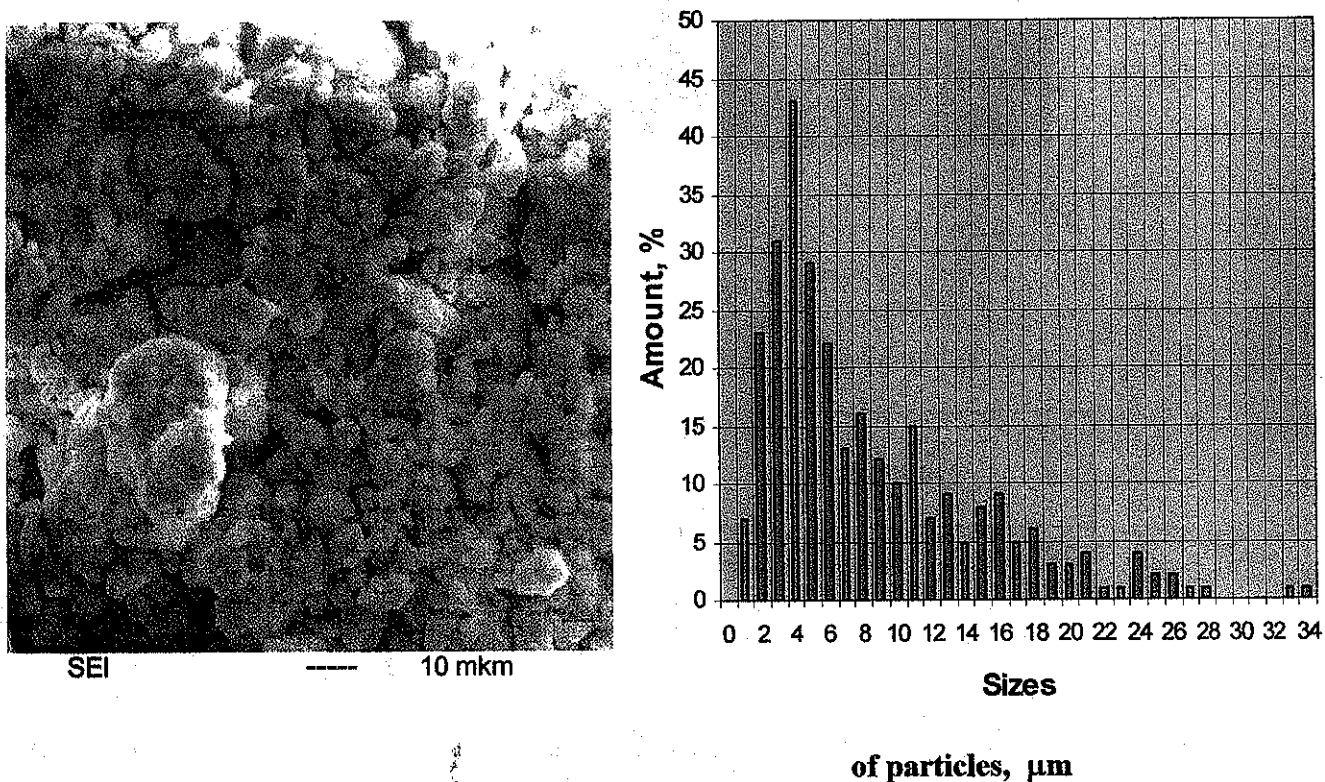


Fig. 3.2. Powder of BaCeO₃. Electron images of particles and granulometric composition.

Experiments to produce compact ceramics using a hot-pressing method and a method of free sintering of previously compacted samples were performed to find basic parameters of BaCeO_3 material.

In hot-pressing experiments the ceramics was protected from interaction with a graphite mold with a 1.5-2-mm layer of boron nitride. It was found out that at 1500°C in the graphite mold a full decomposition of the material takes place.

At the temperature of hot pressing of 1300°C a solid sample (its density was 6.25 g/cm^3) was produced, but however it cracked. It was evidently caused by a high level of internal stresses in the material. An attempt to reduce the stresses by 1-hour annealing at 1000°C , after hot pressing at 1300°C , did not result into considerable reduction of internal stresses.

In experiments on free sintering, the BaCeO_3 powder was previously compacted in a steel mold to form tablets 15 mm in diameter. Compacting pressure was 170Mpa. Then the tablets were put into an electric resistance furnace on a substrate made of alumina ceramics and were covered with Al_2O_3 powder. Sintering was done in the air; the temperature of isothermal exposure was 1300°C ; the time of exposure was 2 hours.

After sintering the tablets kept the shape, cracks were not observed on them. The density of tablets was 4.30 g/cm^3 .

Study of their microstructure was done with Neophot 32 microscope at magnification of x400. Microstructure of the sintered BaCeO_3 ceramics is shown in Fig. 3.3.



Fig. 3.3. Microstructure of free sintered BaCeO_3 ceramics.

The sample has a porous two-phase structure: a gray matrix and light gray splinter-like incorporations distributed along the specimen. In the process of a specimen production a powder-like fine-dispersed thin coating was formed at the surface as a result of interaction with the moisture and it considerably impeded its analysis and photographing (formation of a thin coating can be caused by the presence of not-reacted components in the powder, most probably cerium compounds). Because of the relief of the surface and formation of a thin coating at the surface we could not measure microhardness of the sample.

3.2.2 Electro conductivity of BaCeO_3 at a high temperature.

When electric conductivity of compact ceramics was evaluated, it was found out that at the room temperature BaCeO_3 is an insulator. An evaluation experiment was done to study the influence of the temperature on the electric conductivity of ceramics. A ceramic tablet was put between two electrodes made of stainless steel; the electrodes were fixed at the top and at the bottom with ceramic disks, and the assembly was put into a muffle furnace. Conductors from the

electrodes were led outside and connected to the device to determine the electric resistance (see Fig. 3.4.)

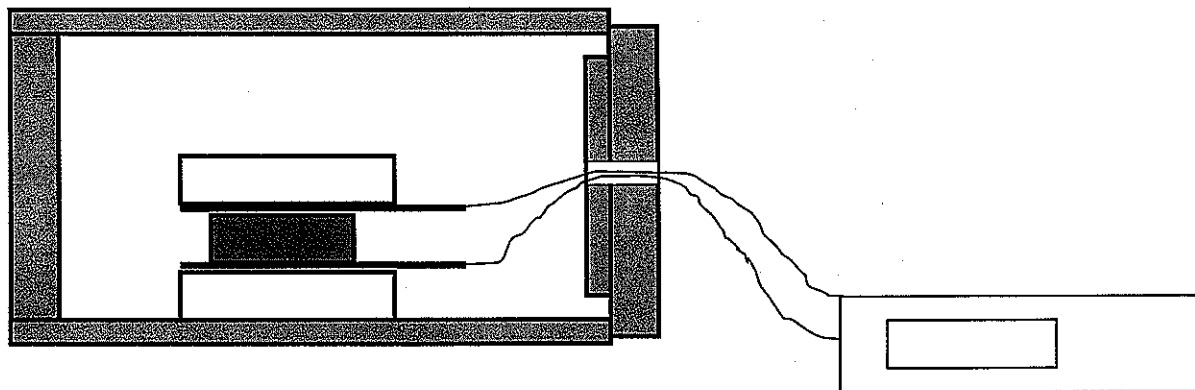


Fig. 3.4. A sketch of an experiment to evaluate electric conductivity of BaCeO₃ ceramics as a function of temperature.

The temperature in the furnace was determined by a thermocouple. In the process of heating it appeared that when the temperature increased up to 300°C the electric conductivity of the sample started to go down drastically from the value of 20 MOhm at 20°C to the value of 500 Ohm at 750°C. The resistance of the sample as a function of temperature is given in Fig. 3.5.

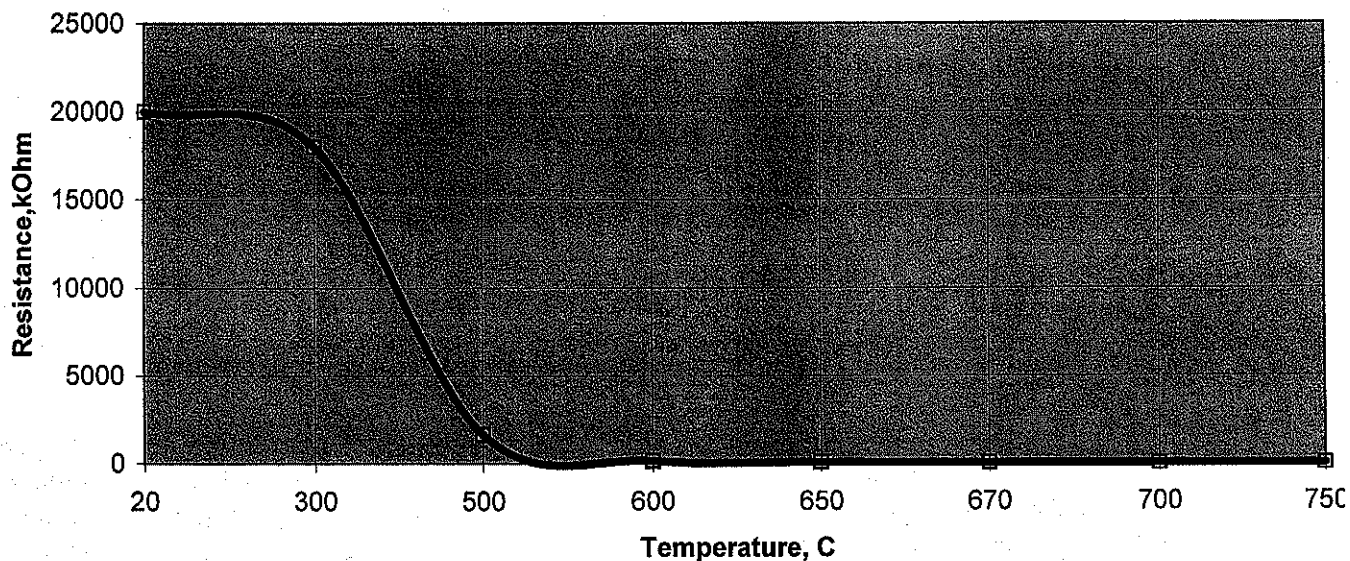


Fig. 3.5 Electric resistance of a sample made of BaCeO₃ as a function of temperature.

3.2.3 Manufacturing and microstructure of cermets on the basis of BaCeO_3 with metal binders of Ni, Ni-Mo.

Previous experiments revealed that an optimum "metal/ceramics" ratio is 3 / 2. Nickel powder (ПНЭ-1 (PNE-1) according to the state standard GOST 9722-79) was used as a metal substrate. Molybdenum was introduced into nickel to reduce limiting wetting angle at the «metal – ceramics» interface /3/.

Mixtures of the following composition - BaCeO_3 40 wt. % + Ni 60 wt. % and BaCeO_3 40 wt. % + Ni 42 wt. % + Mo 18 wt. % - were prepared by mixing in the biconical mixer with metal balls during 8 hours. Then a composition of "a powder-a binder" was prepared, where a binder was polyisobutylene P-20 in the quantity of 10 % of the total weight of the composition. The quantity of the binder was established in experiments basing on condition of forming a solid plate without any breaks by rolling. The obtained composition was dried and rolled on a bending (a mill). Using multiple roll in mutually perpendicular directions, a solid plate not less than 70 mm wide was formed. Briquettes of 15 or 50 mm were cut out of the plate; the size depended on a function of the samples.

Thickness of the samples ready for the corrosion tests after hot pressing made up 2.3 – 2.5 mm; the diameter of the samples was 15 mm. The samples for electric conductivity tests were made of billets 50 mm in diameter and 1.5 mm thick. Each briquette was covered with a composition on the basis of boron nitride to prevent interaction of BaCeO_3 oxide ceramics with the graphite of the mold.

Briquettes prepared in such a way were put into a graphite mold (Fig. 3.6.) and they underwent hot pressing in vacuum. Maximum temperature of hot pressing was 1200°C ; the pressure of compacting was 15 MPa.

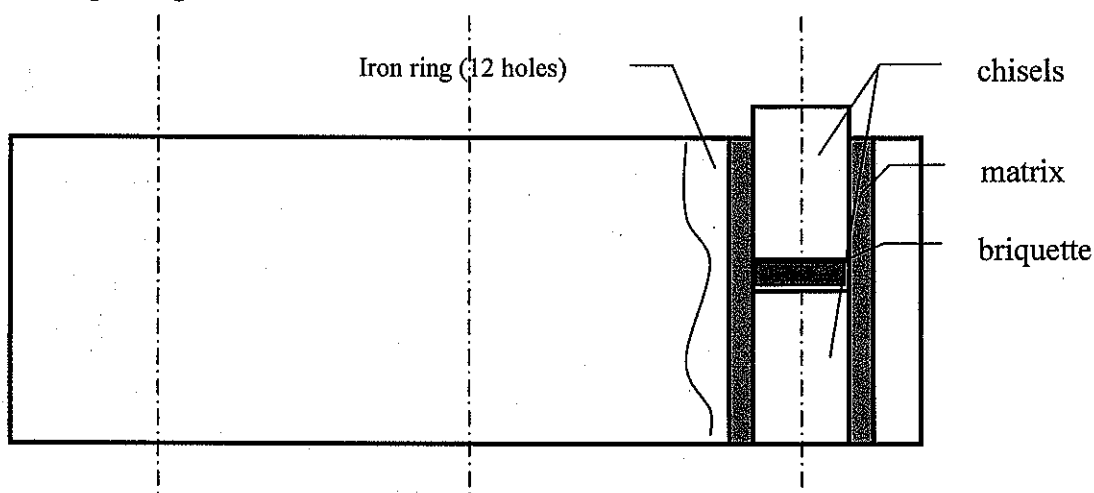


Fig. 3.6. A scheme of loading a mold for hot pressing of samples.

After the mold was cooled down the samples were taken out, the remaining protective coating of boron nitride was removed and the upper layer of the material was polished away.

The surface of all samples is hard enough and has metal shining. Average density determined by hydrostatic weighing in the water made up 7.46 g/cm^3 for BaCeO_3 40 wt. % + Ni 60 wt. % and 7.92 g/cm^3 for BaCeO_3 40 wt. % + Ni 42 wt. % + Mo 18 wt. % composition.

When making billets for the samples to determine electric conductivity (disks 50 mm in diameter and 1 mm thick), briquettes were also protected from interaction with the graphite of the mold.

Microstructure of the samples at magnification of $\times 400$ is given in Fig. 3.7 and 3.8. The microstructure was studied without etching (because of active destruction of the ceramic component during etching of a nickel matrix). Despite some differences in compositions, both materials have the same construction (structure) and consist of two phases – a metal phase of a white color and a porous phase of a dark gray color, which is distributed along the field of the specimen in a

quite uniform way. Microhardness of a metal phase in the material of BaCeO_3 40 wt. % + Ni 60 wt. % is 190 kilogram-force/ mm^2 , microhardness in the metal phase of BaCeO_3 40 wt. % + Ni 42 wt. % + Mo 18 wt. % is 230 kilogram-force/ mm^2 . Microhardness of the ceramic phase is 490 and 320 kilogram-force / mm^2 , respectively.



Fig. 3.7. Microstructure of BaCeO_3 40 wt. % + Ni 60 wt. % composite material. Magnification is x 400.

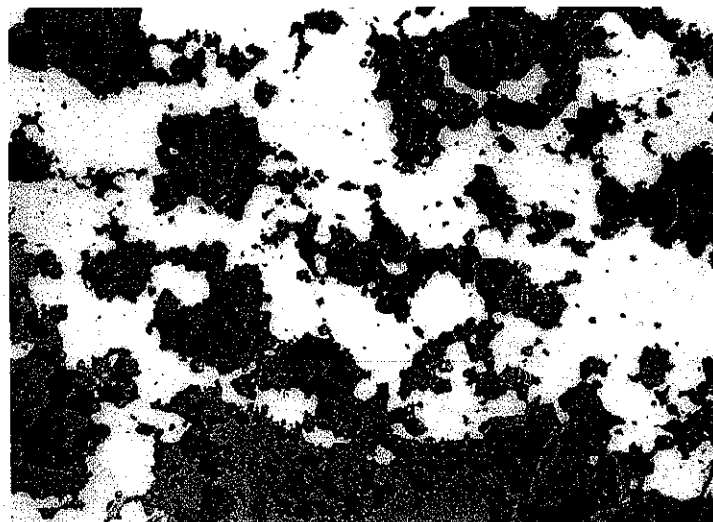


Fig. 3.8. Microstructure of BaCeO_3 40 wt. % + Ni 42 wt. % + Mo 18 wt. % composite material. Magnification x 400.

3.2.4 Electric conductivity of cermets on the basis of BaCeO_3 with metal binders of Ni, Ni-Mo.

Electric conductivity was calculated by specific resistance of materials that was determined by MO-62 bridge with an error of not more than 5 % at 20°C. Results of electric conductivity measurements of the materials 60 % Ni + 40 % BaCeO_3 and 42 % Ni + 18 % Mo + 40 % BaCeO_3 are given in Table 3.3.

Table 3.3

No	Material	Sizes of the sample, mm	Specific resistance, Ohm mm ² /m	Specific electric conductivity, MCm/mm
1	60%Ni+40% BaCeO ₃	48 x 9 x 1,5	0,260	3,84
2	60%Ni+40% BaCeO ₃	38 x 9 x 1,5	0,258	3,88
3	42%Ni+18%Mo+40% BaCeO ₃	47 x 9 x 1,5	2,34	0.43
4	42%Ni+18%Mo+40% BaCeO ₃	38 x 9 x 1,5	2,35	0.42

Basing on the results of electric conductivity we can make a conclusion that introduction of molybdenum as an additive drastically reduces electric conductivity (9 times!) of the composite material (when "metal/ceramics" ratio is kept).

3.2.5 Corrosion stability tests of cermets on the basis of BaCeO₃ with metal binders of Ni, Ni-Mo.

Conditions of corrosion stability tests are given in Appendix 3. Results of the tests for the samples of 60%Ni+40% BaCeO₃ and 42%Ni+18%Mo+40% BaCeO₃ compositions are given in Table 3.4.

Table 3.4

Material	Corrosion losses after 100 hour tests Δm/S, g/cm ²
60%Ni+40% BaCeO ₃	-0,2640
42%Ni+18%Mo+40% BaCeO ₃	-0,4350
Steel 20X23H18*	0,0014

*Values are given for comparison

As it comes from the results of the tests, cermets with BaCeO₃ under conditions of MCFC operation have unsatisfactory corrosion stability. Rather quick dissolution of the material takes place; traces of destruction are visually observed at the edges of the samples. Corrosion losses of the samples are 180 times higher (for the composition of 60%Ni+40% BaCeO₃) and 310 times higher (for the composition of 42%Ni+18%Mo+40% BaCeO₃), than those for the corrosion stable 20X23H18T steel.

3.3. Development of pore-free cermets on the basis of ceramics reinforced with metal fiber.

3.3.1 Manufacturing of cermets on the basis of ceramics reinforced with metal fiber.

Samples of 40 % γ-LiAlO₂ + 60 % Ni and 40 % TiN + 60 % Ni cermets reinforced with metal wire meshes of six compositions were prepared for hot pressing tests:

1) 40 % γ-LiAlO₂ + 60 % Ni reinforced with a wire mesh made of 12X18H10T stainless steel (diameter of the wire is 0.1 mm, total thickness of the wire mesh is 0.25 mm);

2) 40 % TiN + 60 % Ni reinforced with a wire mesh made of 12X18H10T stainless steel (diameter of the wire is 0.1 mm, total thickness of the wire mesh is 0.25 mm);

3) 40 % γ-LiAlO₂ + 60 % Ni reinforced with nickel wire mesh 045H (diameter of the wire is 0.1 mm, total thickness of the wire mesh is 0.25 mm);

4) 40 % TiN + 60 % Ni reinforced with nickel wire mesh 045H (diameter of the wire is 0.1 mm, total thickness of the wire mesh is 0.25 mm);

5) 40 % γ-LiAlO₂ + 60 % Ni reinforced with concertina wire material made of nichrome wire X20H80 (diameter of the wire is 0.1 mm, total thickness of the mat is 1 mm);

6) 40 % TiN + 60 % Ni reinforced with concertina wire material made of nichrome wire X20H80 (diameter of the wire is 0.1 mm, total thickness of the mat is 1 mm).

γ -LiAlO₂ has high corrosion stability when particularly operates in melts of chemical compounds /1,2/. TiN has high values of corrosion stability, scale resistance and electric conductivity /5/. Introduction of these nickel and metal meshes promotes upgrading of the above-mentioned properties.

Samples for tests were made by hot pressing

Solution of P20C polyisobutylene in nephras (gasoline) was introduced into powders before hot pressing. Weight of polyisobutylene was 14% of the total weight of the powder with a binder. After evaporation of nephras (gasoline) the powder with the binder was rolled to produce a homogeneous mass. Then disks of certain sizes were cut out of this mass. A mesh in a shape of a disk or a concertina wire material was put between two of these disks. Billets prepared in such a way were put into graphite molds and then into the induction-vacuum plant.

Hot pressing was done in an induction-vacuum plant following the mode: temperature of exposure – 1200°C, time of exposure – 15 minutes, pressure - 150 kg/cm².

3.3.2 Micro structural research on cermets on the basis of ceramics reinforced with metal fiber.

Microstructural research was done on the samples of the six cermet compositions specified above. Besides the microstructural research there was performed a phase analysis of all cermet compositions under the study; their microhardness was also measured using micro hardness measurement device ПИМТ-3 (PMT-3) following state standard GOST 9450-76.

Microstructure of the 40 % γ -LiAlO₂ + 60 % Ni cermet composition reinforced with a mesh of 12X18H10T stainless steel is given in Fig. 3.9 and it consists of a dark phase of γ -LiAlO₂ and a light phase of the nickel binder. γ -LiAlO₂ phase (dark sections) is porous, its microhardness is $H_{20} = 16.1 - 23.3$ kgf/mm². Light nickel binder is distributed in a fairly uniform way and occupies about 50 % of the area of the specimen. Nickel phase has an elongated winding shape and the sizes of 2.5 – 25 microns; microhardness is $H_{20} = 234$ kgf/mm². As it is shown by the phase analysis, there are no any intermediate phases in the area close to the reinforcing steel mesh. Microhardness of the steel mesh is $H_{100} = 177 - 194$ kgf/mm².

Steel mesh →

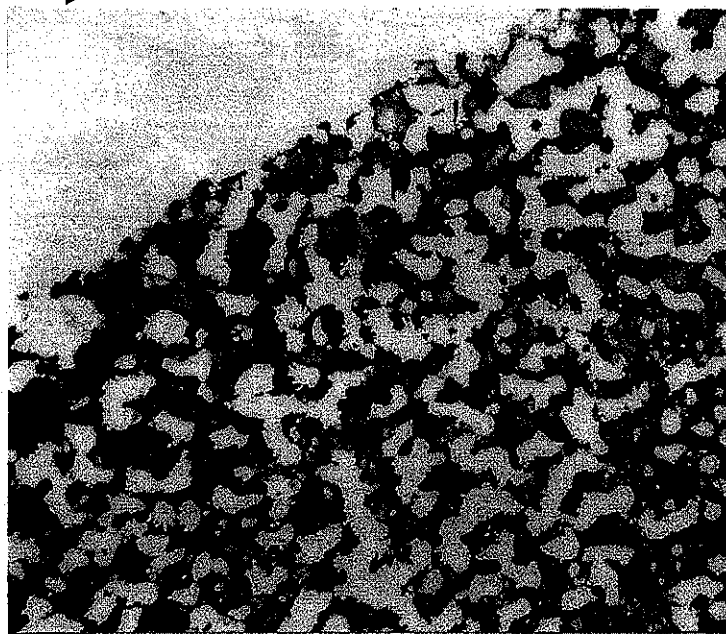


Fig.3.9. - Microstructure of 40 % γ -LiAlO₂ + 60 % Ni cermet composition reinforced with a mesh of 12X18H10T stainless steel, x 500.

Microstructure 40 % TiN + 60 % cermet composition reinforced with a mesh of 12X18H10T stainless steel is given in Fig. 3.10. Incorporations of TiN phase of a yellow color are distributed in a uniform way in the nickel binder of a light gray color and occupy about 50 % of the area of the specimen. Size of TiN particles makes up 1 – 10 microns, microhardness $H_{50} = 1006 - 1072 \text{ kgf/mm}^2$. Microhardness of the nickel binder makes up $H_{20} = 186 \text{ kgf/mm}^2$.

As it was shown by the phase analysis of the area adjacent to the steel mesh, there were no intermediate compounds detected. Microhardness of steel wire was $H_{20} = 179 - 186 \text{ kgf/mm}^2$.

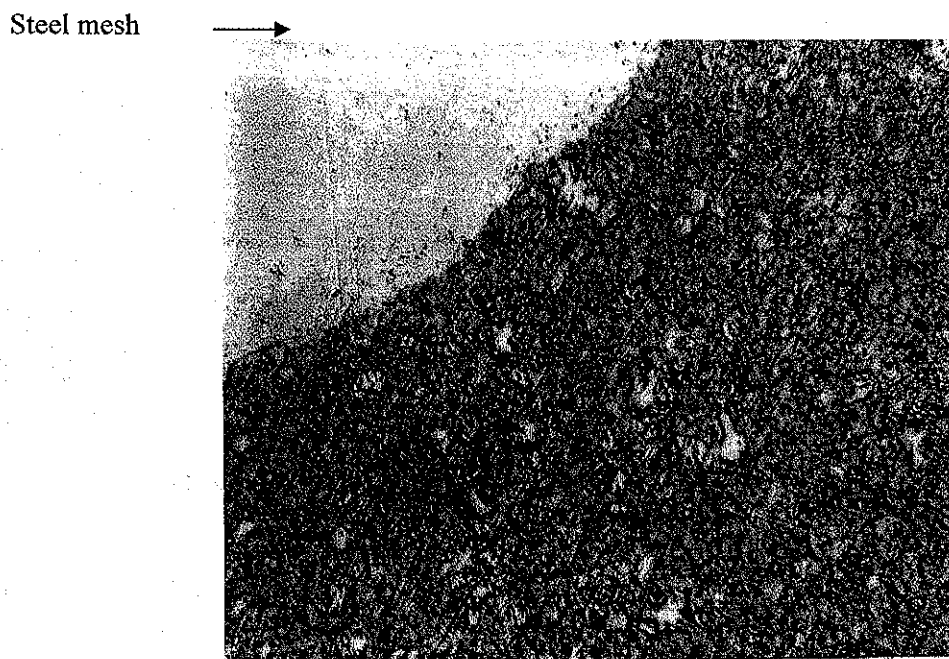


Fig.3.10. – Microstructure of 40 % TiN + 60 % Ni cermet composition reinforced with a mesh of 12X18H10T stainless steel, x 500.

Microstructure of 40 % $\gamma\text{-LiAlO}_2$ + 60 % Ni cermet composition reinforced with nickel mesh 045H is shown in Fig.3.11. Microstructure of the studied cermet composition is a mixture of two phases: a dark one of $\gamma\text{-LiAlO}_2$ and a light gray one of the nickel binder. Phases are distributed in a quite uniform way as related to each other in the ratio 1:1. A dark phase of $\gamma\text{-LiAlO}_2$ is porous, its microhardness is $H_{20} = 37.4 - 42.3 \text{ kgf/mm}^2$. The nickel binder has a winding elongated shape and a size of up to 50 microns, microhardness is $H_{20} = 186 - 195 \text{ kgf/mm}^2$.

Nickel mesh has dispersed incorporations of a dark color of a “needle-like” shape. On the side of the nickel mesh along its interface with the mixture of phases of $\gamma\text{-LiAlO}_2$ and nickel a darker gray phase of probably LiNiO_2 can be detected. It can be also confirmed by the performed phase analysis. Values of microhardness of this gray phase have a broad spread: $H_{20} = 429 - 526 \text{ kgf/mm}^2$, and microhardness of the nickel wire – $H_{20} = 165 - 186 \text{ kgf/mm}^2$.

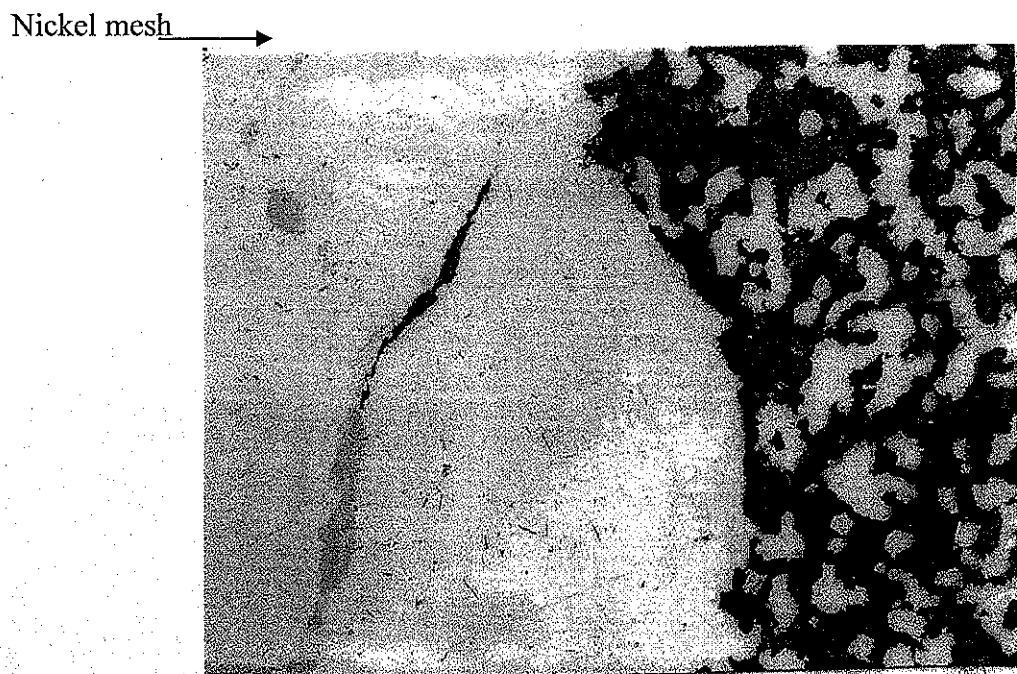


Fig.3.11. – Microstructure of 40 % γ -LiAlO₂ + 60 % Ni cermet composition reinforced with a nickel mesh 045H, x 500.

Microstructure 40 % TiN + 60 % Ni cermet composition reinforced with a nickel mesh 045H is analogous to the microstructure of 40 % TiN + 60 % Ni cermet composition reinforced with a 12X18H10T stainless steel mesh. Dispersed particles of TiN phase (a yellow color) are distributed in a quite uniform way in the nickel binder (a light gray color), and the ratio of two phases is 1:1 (Fig.3.12.). Sizes of TiN particles are 0.5 – 25 microns, microhardness is $H_{20} = 1426 - 1610 \text{ kgf/mm}^2$. Microhardness of the nickel binder makes up $H_{20} = 234 \text{ kgf/mm}^2$. According to the data of the phase analysis no intermediate phases were detected. Microhardness of the nickel mesh makes up $H_{50} = 210 \text{ kgf/mm}^2$.

← Nickel mesh

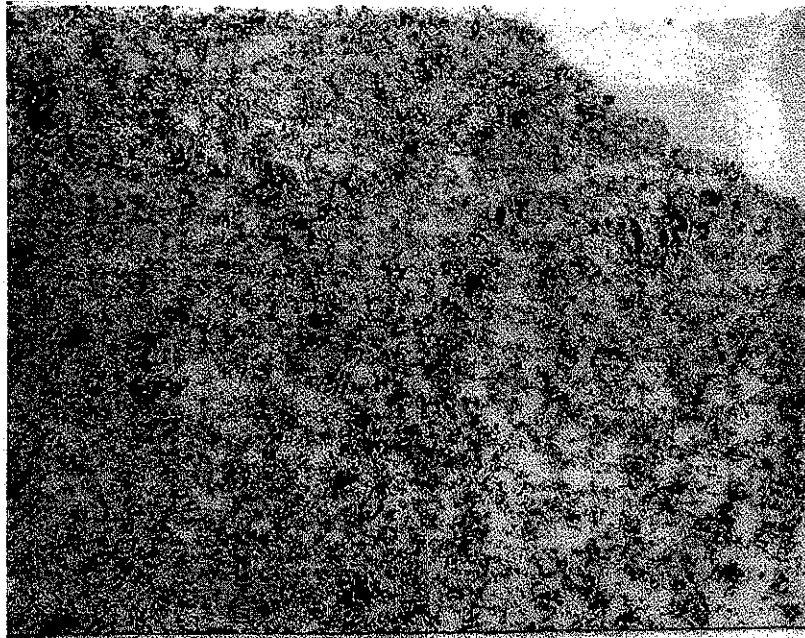


Fig.3.12. – Microstructure of 40 % TiN + 60 % Ni cermet composition reinforced with a nickel mesh 045H, x 500.

Microstructure of 40 % γ -LiAlO₂ + 60 % Ni cermet composition reinforced with a concertina wire material made of X20H80 nichrome wire comprises a mixture of a light phase of γ -LiAlO₂ and a dark phase of Ni among which nichrome wire is located (Fig.3.13.). Sections of a light phase, the size of which is 50 – 100 microns, are distributed in a uniform way along the area of the specimen under the study. Sections of the gray phase are present in the form of small incorporations of 20 – 50 microns and in the form of larger sections of globular shape of 150 – 250 microns. The light phase occupies the largest part of the specimen (Fig.3.14.). No additional phases are revealed close to the nichrome wire. Microhardness of the studied sample makes up $H_{100} = 170 - 235 \text{ kgf/mm}^2$.



Fig.3.13. – Microstructure of 40 % γ -LiAlO₂ + 60 % Ni cermet composition reinforced with a concertina wire material made of X20H80 nichrome wire, x 25.

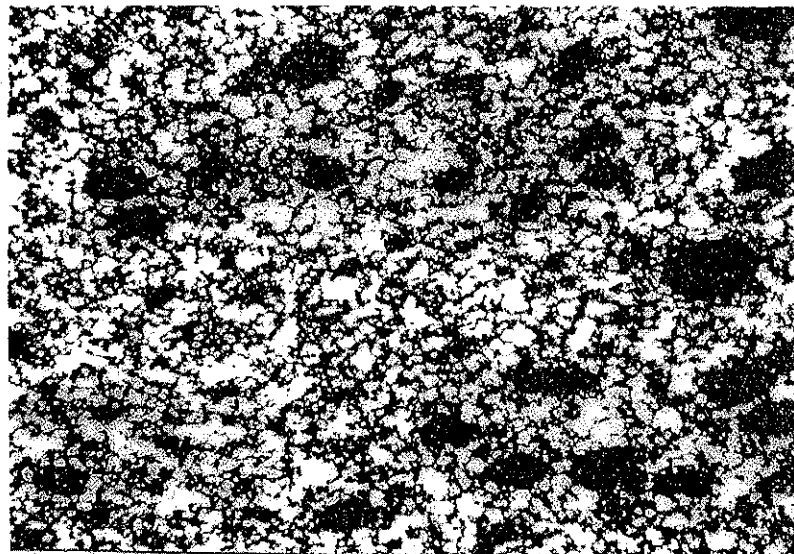


Fig.3.14. – Microstructure of 40 % γ -LiAlO₂ + 60 % Ni cermet composition reinforced with a concertina wire material made of X20H80 nichrome wire, x 50.

Microstructure 40 % TiN + 60 % Ni cermet composition reinforced with a concertina wire material made of X20H80 nichrome wire consists of a mixture of a gray phase with a yellow shade of TiN and a light phase of Ni among which nichrome wire is located (Fig.3.15). Sections of the nickel phase 100 – 200 microns in size occupy the largest part of the area of the specimen. Sections of Ni phase have the sizes of 50 – 100 microns (Fig.3.16.). No additional phases were revealed close to the nichrome wire. Microhardness of the studied sample makes up $H_{100} = 212 - 272 \text{ kgf/mm}^2$.

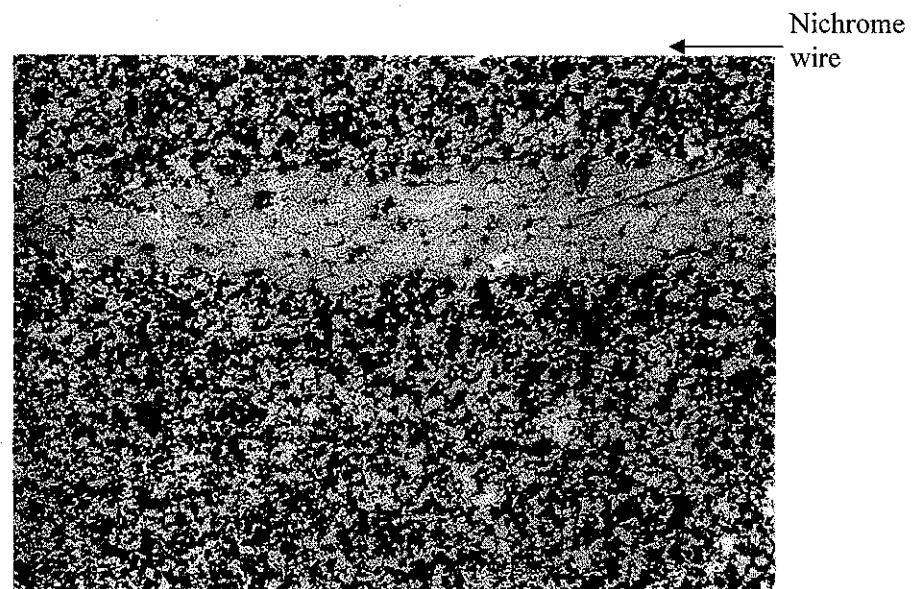


Fig.3.15. – Microstructure 40 % TiN + 60 % Ni cermet composition reinforced with a concertina wire material made of X20H80 nichrome wire, x 25.

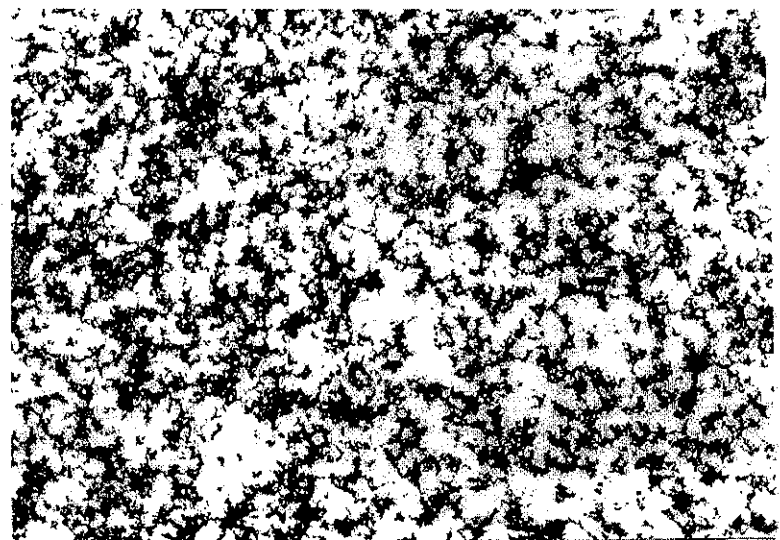


Fig.3.16. – Microstructure 40 % TiN + 60 % Ni cermet composition reinforced with a concertina wire material made of X20H80 nichrome wire x 50

3.3.3 Electric conductivity of cermets on the basis of ceramics reinforced with metal fiber.

Measurements of electric conductivity of the samples were done using a direct-current bridge of MO-62 type with an error of not more than 5 % at 20⁰C.

Results of electric conductivity measurements are given in Table 3.5.

Table 3.5

Electric Conductivity

№	Material	Sizes of the sample, mm	Resistance, Ohm	Specific resistance, Ohm•mm ² /m	Specific electric conductivity, M•Cm/m
1	40 % γ -LiAlO ₂ + 60 % Ni + mesh of 12X18H10T stainless steel	11,6 x 2,7 x 0,35	0.00914	0.74	1,35
2	40 % γ -LiAlO ₂ + 60 % Ni + mesh of 12X18H10T stainless steel	12,9 x 2,7 x 0,35	0.01005	0.74	1,35
3	40 % TiN + 60 % Ni + mesh of 12X18H10T stainless steel	19 x 3,6 x 0,37	0.00392	0.27	3,64
4	40 % TiN + 60 % Ni + mesh of 12X18H10T stainless steel	18 x 3,7 x 0,38	0.00517	0.35	2,85
5	40 % TiN + 60 % Ni + mesh of 12X18H10T stainless steel	18,5 x 3,7 x 0,38	0.0047	0.35	2,85
6	40 % γ -LiAlO ₂ + 60 % Ni + 045H nickel mesh	23 x 3,7 x 0,38	0.01495	0.88	1,13
7	40 % γ -LiAlO ₂ + 60 % Ni + 045H nickel mesh	22,7 x 3,5 x 0,41	0.01564	0.99	1,01
8	40 % γ -LiAlO ₂ + 60 % Ni + 045H nickel mesh	22,5 x 3,2 x 0,35	0.01262	0.63	1,59
9	40 % TiN + 60 % Ni + 045H nickel mesh	23 x 3,7 x 0,38	0.00389	0.23	4,28
10	40 % TiN + 60 % Ni + 045H nickel mesh	23,8 x 3,7 x 0,38	0.00415	0.25	4,08
11	40 % TiN + 60 % Ni + 045H nickel mesh	23,5 x 3,7 x 0,38	0.00445	0.27	3,76
12	40 % γ -LiAlO ₂ + 60 % Ni + X20H80 nichrome material	14 x 4,5 x 0,53	0.0102	1,74	0,57
13	40 % γ -LiAlO ₂ + 60 % Ni + X20H80 nichrome material	13 x 3,3 x 0,55	0.0120	1,68	0,60
14	40 % γ -LiAlO ₂ + 60 % Ni + X20H80 nichrome material	12,3 x 4,2 x 0,53	0.0099	1,79	0,56
15	40 % TiN + 60 % Ni + X20H80 nichrome material	13 x 3,5 x 0,43	0.0068	0.79	1,27
16	40 % TiN + 60 % Ni + X20H80 nichrome material	13 x 3,8 x 0,42	0.00413	0.82	1,22
17	40 % TiN + 60 % Ni + X20H80 nichrome material	14 x 3,5 x 0,43	0.0054	0.81	1,23

3.3.4 Research on corrosion stability of cermets on the basis of ceramics reinforced with metal fiber.

Tests of cermet compositions on corrosion stability were done under the anode operating conditions of a molten carbonate fuel cell (see Appendix 3). The tests were held during 100 hours. Evaluation of corrosion stability was done using gravimetric method and lay in finding the changes in the mass of the samples under the study.

Dependencies of changes of the reduced mass of the samples of cermet compositions under the study are given in Table 3.6. Analogous data on 20X23H18T steel are given there too for comparison.

Table 3.6

No	Material	$\Delta m/s$ after 100-hour tests, g/cm^2
1	40 % γ -LiAlO ₂ + 60 % Ni + mesh of 12X18H10T stainless steel	0.0012
2	40 % TiN + 60 % Ni + mesh of 12X18H10T stainless steel	0.0042
3	40 % γ -LiAlO ₂ + 60 % Ni + 045H nickel mesh	-0.0014
4	40 % TiN + 60 % Ni + 045H nickel mesh	0.0095
5	40 % γ -LiAlO ₂ + 60 % Ni + X20H80 nichrome wire material	0.0014
6	40 % TiN + 60 % Ni + X20H80 nichrome wire material	0.0047
7	20X23H18 steel	0.0014

3.4. Tests of bipolar plates within a MCFC cell

Research on possible development of pore-free cermet materials for bipolar plates was practically completed during the first year of the Project. The best compositions were identified. They are the following compositions: 60% LiAlO₂ + 40% Ni and 40% TiN + 60% Ni, reinforced with 045H nickel mesh. Ring parts were made of the specified compositions (see Fig.3.17) to imitate circumferential part, and disks were made (see Fig.3.18) to imitate the central part of a bipolar plate within a fuel cell. Thickness of the ring and of the disks was 2 mm.

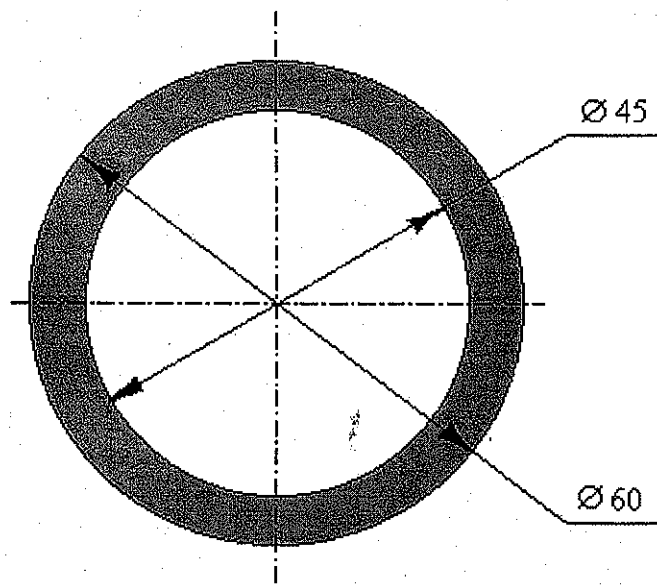


Fig. 3.17

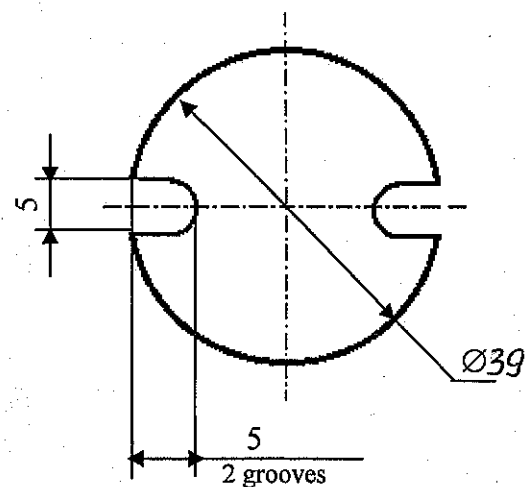


Fig. 3.18

The specified parts of a dense cermet material were tested during 100 hours within a MCFC. There were no visual changes in the material; deeper analysis was not done as the Task was changed.

Three 100x100 mm plates of each of the materials (60% LiAlO_2 + 40% Ni and 40% TiN + 60% Ni reinforced with nickel 045H mesh) were made to be sent to the Customer. Maximum thickness of the plates was 2mm. After the modes had been polished using the defective samples, it was planned to adjust the thickness of the plates to the minimum possible value. A package of document was prepared to send the plates to the customer. However, pore-free cermet plates were not sent to the Customer as the Customer replaced them with the porous metal ceramic plates to be sent to him according to the new additional task (see i.3.7).

3.5. Manufacturing and research on porous metal-ceramic plates as anodes for MCFC

3.5.1. Formulation of the task

The task to develop a porous anode of the metal-ceramic on the basis of nickel with an additive of LiAlO_2 was set by the collaborator at the meeting with them and the representative of FCE in November, 2003 (see more details in i.1.1.9.), and according to «ADDENDUM #3» it was introduced as: «**Research on possible creation of porous cermet composition on the basis of LiAlO_2 and Ni for an MCFC anode with good electric conductivity and porosity of 50 – 60%. Creep tests to evaluate the shrinkage of the material at 650°C and pressure of 2 atmospheres in a standard anode environment with humidification at 60°C.**» To evaluate the possibility to develop a porous metal-ceramic anode basing on the experience in the work with porous metal ceramic it is enough to study a composition on the basis of nickel with the additive of 5% and 15% of LiAlO_2 by weight.

3.5.2. Free sintering in vacuum.

A powder mixture was prepared by mixing nickel powder of PRV-N-1 (IPB-H1) brand with LiAlO_2 in a biconical mixer during 8 hours. Steel balls were added in the container for better mixing.

The powder mixture with 5% wt of LiAlO_2 was pressed in the steel mold \varnothing 15 mm. The pressure was selected in such a way that it would ensure the minimum strength of the compressing. There were selected two values of pressure: 40 and 50 MPa, as when the pressure was 30 MPa we could not form the material.

The tablets produced under the pressure of 40 - 50 MPa had a very low mechanical strength; the relative strength of the material was 49 – 52 %.

Free sintering of tablets was done in the induction furnace in the vacuum with the residual pressure of 10^{-1} Pa. For these purposes the tablets were put into the graphite crucible and were covered with the powder of electrocorundum (see Fig. 3.19.).

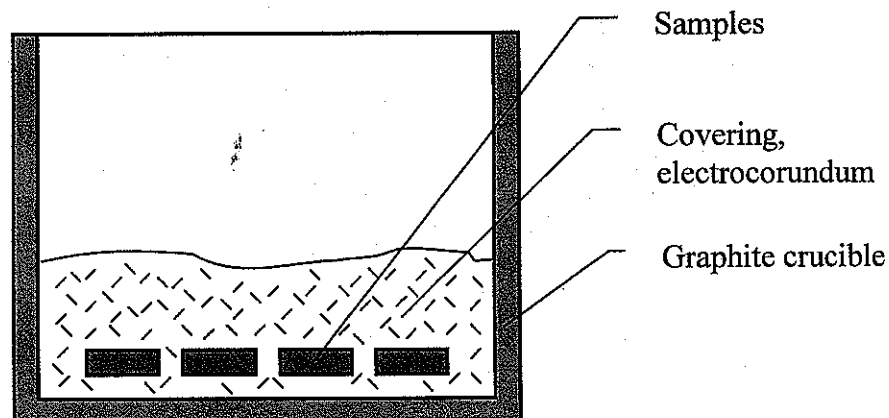


Fig. 3.19. A layout of free sintering of porous samples.

The samples in the crucible were sintered in the following mode:

- Heating up to the temperature of 980°C;
- 1-hour exposure at 980 – 1020°C;
- Cooling-down "with the furnace".

After the furnace was cooled-down to the room temperature the samples were put out of the work chamber of the furnace. The average density of the samples was calculated (see Table 3.7).

Table 3.7.

Density of the samples sintered at 1000°C; 1 hour exposure.

№ i/i	Compacting pressure, MPa	Density, g/cm ³	Relative density, %	Porosity, %
1	40	4,24	53	47
2		4,45	56	44
3		4,36	55	45
1	50	4,45	56	44
2		4,25	53	47
3		4,51	56	44

3.5.3. Making samples of porous metal-ceramic plates using pore forming agent

To make samples of 5%LiAlO₂ + 95%Ni and 15%LiAlO₂ + 85%Ni ceramic materials with porosity more than 50% using a pore-forming agent NiCO₃ · n Ni(OH)₂ · m H₂O in an optimum quantity was introduced as a pore-forming agent into the specified powder compositions.

Preliminary compacting was used to ensure uniform distribution of the material along the area of the plate. It was done by rolling of a plastic composition prepared with an organic binder (a solution of П-20 poly-isobutylene in gasoline). An optimum quantity of the binder was defined for compositions with 5 % and 15 % of LiAlO₂.

The plastic composition was rolled many times on mills in cross-perpendicular directions to improve uniformity of the material. Thickness of the rolled stock was 3 mm.

Disks 35 mm in diameter and 3 mm thick were made from the produced mass (2 disks for each composition). The disks were annealed in hydrogen in the following mode: heating up to 850°C during 8 hours, two-hour exposure at 850°C.

Porosity of the produced disks was 58 %, but the surface of the disks was covered by alligating, some of cracks were through.

The mode of annealing was changed to get rid of these drawbacks: the time of heating up to 850°C was increased from 8 to 70 hours. However, the slow heating up resulted in the situation when poly-isobutylene within the rolled stock, not having burnt out, came to its liquid state, leaked and spoiled the blanks.

Considering the limited time for the work we did not look for other compositions and manufacturing modes of porous plates using a pore forming agent.

3.5.4. Hot pressing in a mold

Methods of free sintering and manufacturing of plates using a pore-forming agent appeared not to be suitable for manufacturing of thin (1 – 1.5 mm) porous plates 100 x 100 mm in size. Hot pressing in a mold could be one of the methods to make thin flat porous metal ceramic plates. It ensures the necessary clearance between the punches.

A mold was made to provide high porosity and necessary sizes; it ensured the clearance of 1.5 mm between the punches in the extreme low position. The clearance was provided by a pusher that rested against butt-end of the matrix preventing the influence of the pressure on the part (see Fig. 3.20).

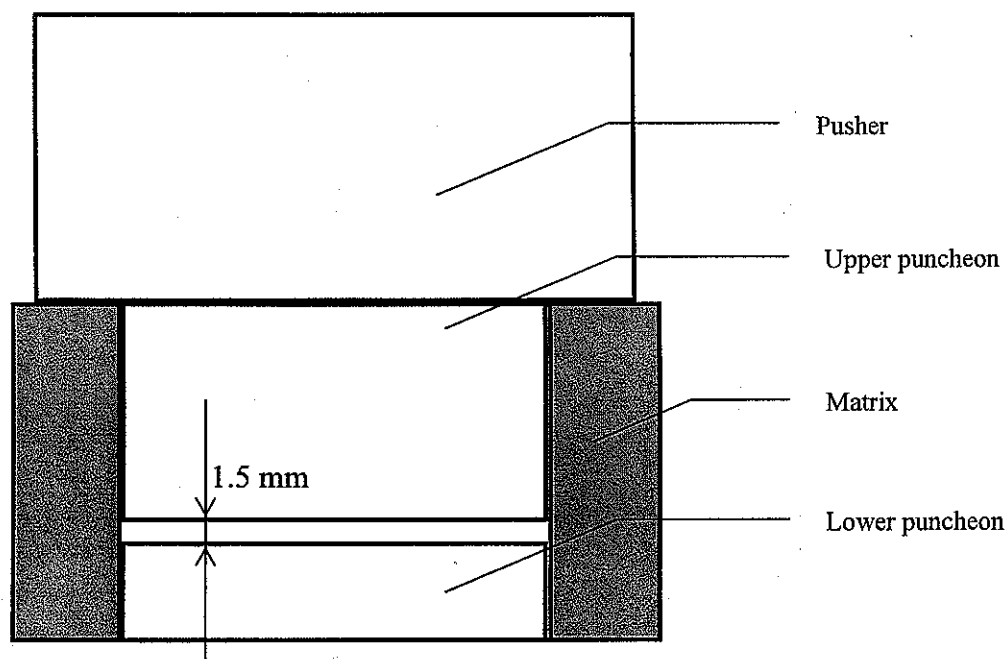


Fig. 3.20. Layout of hot pressing of 100 x 100 mm porous plates.

Preliminary compacting was used to ensure uniform distribution of the material along the area of the plate. It was done by rolling of the plastic composition prepared with an organic binder (a solution of Π -20 poly-isobutylene in gasoline). There was determined an optimum quantity of the binder for compositions with 5 % and 15 % LiAlO_2 .

The plastic composition was rolled many times on mills in cross-perpendicular directions to improve uniformity of the material. Thickness of the rolled stock was selected in such a way that the mass of the briquette 105 x 105 mm in size would correspond to the calculated one (considering full burning out of the binder and the residual porosity at the level of 45 – 50 %).

The produced briquette was covered with a layer of aluminum oxide on all sides to protect the material of the plate from interaction with the graphite of the mold during hot pressing (nickel easily forms strong carbides at a high temperature). A 0.5-mm plastic composition of the powder of aluminum oxide (Al_2O_3) with poly-isobutylene was prepared for these purposes. The briquette was covered on all sides by this rolling.

Then the briquette with the protective layer was put into the graphite matrix and it underwent hot pressing in vacuum (residual pressure of 10^{-1} Pa) in the following mode:

1. Heating (5 – 7°C / min.) up to the temperature of 500°C;
2. Exposure to 500 – 550°C during 30 min. (to burn out the binder);
3. Heating to 1000°C at the rate of 20°C / min, pressing in the range of temperatures of 550 – 800°C (pressure of compacting is 10 MPa), take off the pressure after shrinkage is completed;
4. 1 hour exposure at 980 – 1020°C;
5. Cooling down “with the furnace”.

After cooling down of the work chamber of the furnace the graphite mold was disassembled and the plate was taken out. The protective powder-like layer was removed from the surface of the plate.

The average density of plates produced by hot pressing was determined by calculations on the formula:

$$\gamma = m / abh \text{ (g/cm}^3\text{)},$$

where:

m is a weight of the plate, g;

a , b , h are linear sizes of the plate, cm.

The values of the density and porosity of the produced anodes are given in Table 3.8.

Table 3.8

Composition	Average density, g/cm ³	Average density, %	Porosity, %
Ni + 5% LiAlO ₂	3,73	47	53
Ni + 15% LiAlO ₂	4,05	60	40

Electric conductivity of the material was determined using samples in the form of ingots taking measurements by E7-14 device. Resistance was calculated by:

$$\rho = RS / L \text{ (Ohm mm}^2\text{/m),}$$

where:

R is resistance of the sample, Ohm;

S is a cross-section of the sample, mm²;

L is the length of the sample, m.

Specific electric conductivity was calculated by the formula:

$$\sigma = 1/\rho \text{ (MCm/m)}$$

The determined results on electric resistance and electric conductivity are shown in Table 3.9.

Table 3.9.

No i/i	Composition	Sizes of the sample, mm	Resistance, Ohm	Specific Resistance, Ohm mm ² /m	Specific elec- tric conductiv- ity, MCm/m
1	Ni + 5% LiAlO ₂	49x10x1,72	0,0018	0,65	1,58
2	Ni + 5% LiAlO ₂	46x7,1x1,6	0,0023	0,57	1,75
3	Ni + 5% LiAlO ₂	34x8x1,56	0,0022	0,80	1,25
Average value				0,67	1,53
1	Ni + 15% LiAlO ₂	85x6,2x1,65	0,0098	1,17	0,84
2	Ni + 15% LiAlO ₂	55x6,1x1,65	0,0061	1,12	0,89
3	Ni + 15% LiAlO ₂	55x6,1x1,62	0,0065	1,16	0,86
Average value				1,15	0,86

Increase of the ceramic in the material from 5% to 15% results into increase of the resistance of the material by one and a half or two times.

3.5.5. Results of the tests on creep stability

Samples of 5% and 15% LiAlO₂ porous metal ceramic plates were tested for their resistance to creep. The tests were made with samples produced by hot pressing and with implementation of a pore-forming agent. The tests were held in the anode environment (80% H₂, 20% CO₂, humidification at 60°C) at 650°C during 100 hours and pressure of ~ 3 atm. The heating was done without pressure at the raise of temperature up to 650°C, the samples were saturated with the electrolyte.

Fig. 3.21 shows an experimental cell where the tests were held. The samples with the matrix electrolyte were put into a pan of stainless steel and then they were put inside the thermal unit.

Results of the tests are given in Table 3.10.

Table 3.10

Results of the creep tests of porous plates.

№ of the sample	Content of LiAlO_2	Sizes of the sample, mm				Weight, g	Porosity before the test	Porosity after the test
		Before the tests		After the test				
		Thickness	Diameter	Thickness	Diameter			
1.	5% (free sintering)	3,13	15,1	2,90	15,4	2,472710	48,6	46,7
2.	5% (free sintering)	3,10	15,1	2,82	15,45	2,398236	49,7	47,2
3.	5% (hot pressing)	4,95	14,0	3,15	15,1	2,510158	61,7	48,2
4.	15%(hot pressing)	5,29	14,0	3,39	14,6	2,442984	62,3	45,9
5	5% (with pore-forming agent)	3,32	31,65	1,63	33,65	7,244294	67,7	41,8
6	15%(with pore-forming agent)	2,42	33,20	1,93	31,90	6,620421	60,3	46,1

The results show that the content increase for LiAlO_2 in a porous plate reduces creep inconsiderably. Shrinkage of the plates mainly depends on the way they were produced. The least shrinkage of 4-5% is in samples produced by free sintering and 22-26% shrinkage is in the samples produced by hot pressing.

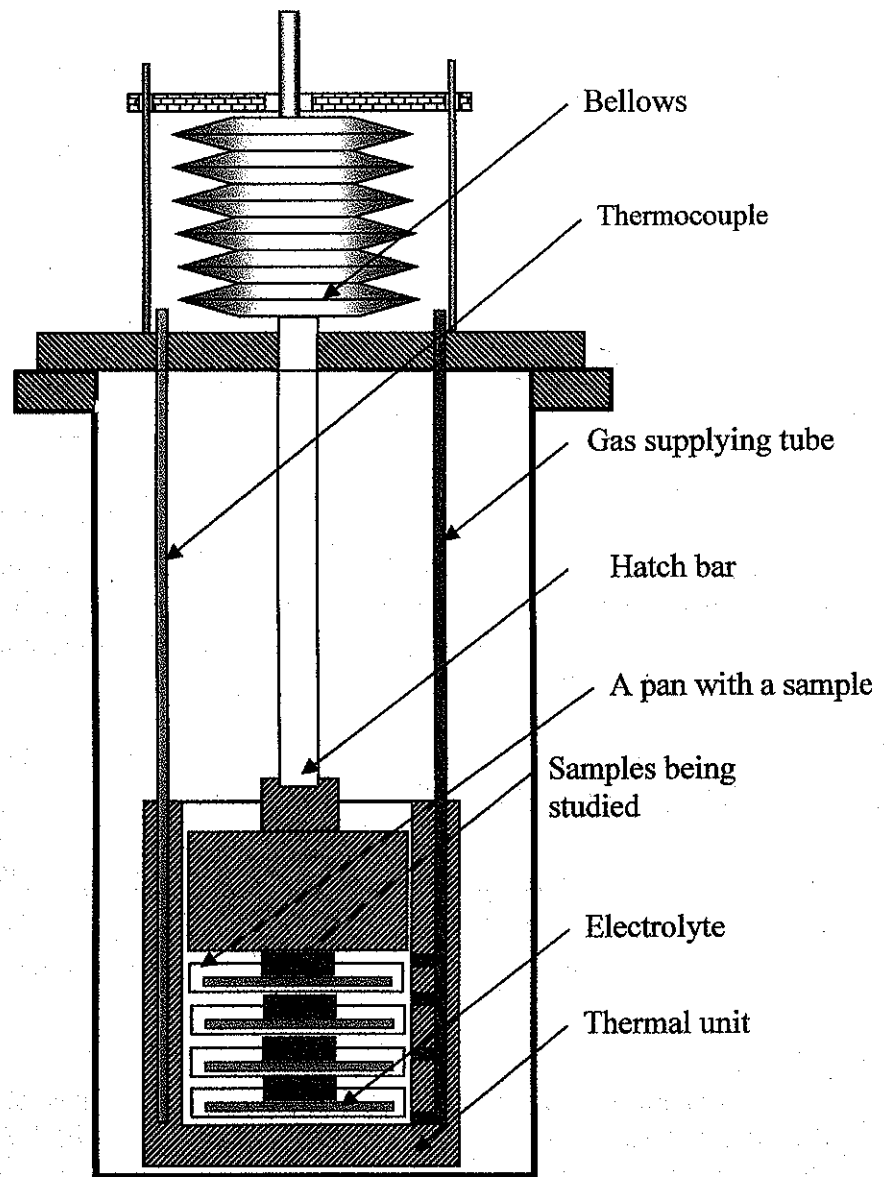


Fig.3.21. A layout of a cell to be tested for creep

3.6. Research on intermetallide compounds.

Within Task 3, a wide class of metal ceramic materials was studied. However, **intermetallide compounds** can be of particular interest as MCFC materials. Intermetallides have high electrical conductivity (in fact they are metals, see Table 3.11). Besides, many of them have a high mechanical strength, and they are refractory and temperature-resistant.

Table 3.11

Material	Sizes of the sample, mm	Specific resistance, Ohm mm ² /mm	Specific electric conductivity, MS/m
IIB-H70IO30 (NiAl)	18,3 x 9 x 1,5	0,202	4,95
IIB-H70IO30 (NiAl)	29 x 9 x 1,5	0,204	4,90
IIB-H85IO15 (Ni ₃ Al)	45 x 9 x 1,5	0,55	1,81
IIB-H85IO15 (Ni ₃ Al)	15,7 x 9 x 1,5	0,54	1,85

Such compounds are available in Ni – Al system, for example (NiAl and Ni₃Al). These compounds in powders are industrially produced in Russia. Preliminary tests under operating conditions of an MCFC anode have shown that NiAl-based material has resistance comparable with corrosion resistant steel (see Table 3.12).

Table 3.12

A gravimetric method. The temperature is 650°C, the melt of Li₂/K₂CO₃ eutectics, H₂+CO₂+H₂O environment, after 100 hours.

Material	Corrosion losses after 100 hour tests, Δm/S, g/cm ²
IIB-H70IO30 (NiAl)	-0,0002
IIB-H85IO15 (Ni ₃ Al)	Destruction in 25 hours
Steel 20X23H18*	0,0014

*Values are given for comparison

Results of intermetallide tests (NiAl and Ni₃Al) have shown that they are very different despite similarity of physical-mechanical properties. If a IIB-H70IO30-based material (NiAl) has shown excellent stability, IIB-H85IO15 (Ni₃Al) in 25 hours of tests dissolved so that it was not possible to section it for weighing.

Tests have proved that implementation of the material on the basis of NiAl intermetallide within an MCFC can be promising. NiAl powder (IIB-H70IO30) has been produced by the Russian industry for a long time, and that could also be counted in favor of further research on implementation of these materials in MCFC.

3.7. Delivery of porous metal ceramic plates to FCE

According to «ADDENDUM #3», the delivery of pore-free plates was replaced with the delivery of porous metal ceramic plates: «Task 3.9. Manufacturing of a pilot batch of porous samples (2-3 samples 10 x 10 cm. Sending (export) of the samples to FCE ».

Two 10x10 cm samples were made by hot pressing and prepared for the delivery. A new set of documents was prepared. Properly packed samples and documents were passed to ISTC in compliance with the “Acceptance report and conveyance deed (dated May 17, 2004)” to be sent to FCE.

3.8. Conclusions

3.8.1. As it is shown by the results of the research, the best complex of properties for bipolar plates was demonstrated by the following cermet compositions: 60% γ -LiAlO₂+40%Ni and 40 % TiN + 60 % Ni reinforced with 045H nickel mesh. Samples 100*100 mm in size of the best cermet compositions were made to be tested in ANL or FCE as bipolar plates. However, the customer replaced delivery of the pore-free plates with the delivery of porous metal ceramic plates on a new additional task.

3.8.2. As it is shown by the research on cermets with BaCeO₃, it is not reasonable to use BaCeO₃ in materials for MCFC plates neither as a ceramic basis nor for strengthening of a metal matrix as it has low corrosion stability in the electrolyte environment.

3.8.3. Samples of the best compositions on i.3.8.1 were made and tested in a single MCFC cell during 100 hours. No visual changes in the material were revealed. There was no deeper analysis as Task 3 was changed.

3.8.4. On the basis of experimental results there was chosen the way to produce porous metal ceramic plates for MCFC anodes - it is a method of hot pressing.

3.8.5. There were made and studied plates of the following compositions: 5%LiAlO₂ + 95%Ni and 15%LiAlO₂ + 85%Ni. They have the following properties:

- Porosity is of about 50%;
- Increase of ceramics in the material from 5% to 15% results in the increase of the resistance of the material by 1.5 – 2 times;
- Increase of LiAlO₂ content in a porous plate decreases creep inconsiderably. Shrinkage of the plate mainly depends on the way it was made. The least shrinkage of 4-5% is in samples produced by free sintering and 22-26% shrinkage is in the samples produced by hot pressing.

3.8.6. Test results have shown that implementation of the materials on the basis of NiAl intermetallide within MCFC can be promising. The material on the basis of NiAl has stability comparable with corrosion resistant steel. The powder of NiAl (IIB-H70IO30) has been produced by Russian industry for a long time.

3.8.7. Two samples 10x10 cm in size were made by hot pressing method and were passed to ISTC in compliance with the "Acceptance report and conveyance deed (dated May 17, 2004)" to be sent to FCE.

List of References

1. C.E. Johnson, K.R. Kummerer, E.Roth. Ceramic breeder material. Journal of Nuclear Materials 155-157 (1988) 188-201.
2. J. Charpin and others. Investigations of γ lithium aluminate as tritium breeding material for a fusion reactor blanket. Fusion Engineering and Design 8 (1989) 407-413.
3. G.A. Libenson. Manufacturing of powder products. Moscow. «Metallurgy», 1990, p.178-180.
4. L.I. Mirkin. Reference book on X-ray structural analysis of materials. Moscow «State Publishing House of Literature of Physics and Mathematics », 1961.
5. P.S. Kisly, N. I. Bondarchuk, M. S. Borovikova et al. Cermets. Kiev. Naukova dumka. 1985. 272 p.
6. ICTC Project #2281p. Development of New Materials for Fuel Cells. Technical Report for the 2nd quarter (September 01, 2002 – November 30, 2002).
7. ICTC Project #2281p. Development of New Materials for Fuel Cells. Technical Report for the 3rd quarter (December 01, 2002 – February 28, 2003).

4. DEVELOPMENT OF A NEW ALLOY AND ALLOYS WITH CERAMIC COATING FOR SOFC.

4.1. Development of Ti – V, Ti – Nb alloys.

As a result of preliminary theoretical analysis based upon the assumption that the required properties may be achieved by creating the certain phase composition and controllable combination of submicroregions with definite atomic-crystal, electron and magnetic configurations, we have determined new alloys' compositions being promising from the viewpoint of the required TEC value. These are Ti-(35-45 mass.%) Nb and Ti-(20-35 mass.%)V alloys.

4.1.1 Development of the technology to make Ti – V, Ti – Nb alloys.

A technology was elaborated to produce Ti-V and Ti- Nb alloys with the following composition (% mass): Ti-V (22, 25, 28, 32%V); Ti-Nb (36,38, 40,44 %Nb). Smelting of the ingots of alloys was effected by means of 4-fold remelting with the intermediate ingot processing into scobs.

Smelting in the form of 100-500 g ingots was effected in an electrovacuum furnace. The alloys' components were dried in a furnace in the air medium at temperature of 200 °C during 1 hour to remove adsorption moisture. Then they were compacted into Ø50 mm briquettes on a 50tn press. The obtained briquettes were placed on a copper water-cooled pan, after which the melting space of the furnace was vacuumized up to the residual pressure of 5×10^{-3} mm mercury column. After that, argon was fed into the furnace up to the pressure of 0,5 - 0,6 atm.

Smelting was conducted with the use of an electric arc on a tungsten electrode.

After the arc ignition they first smelted a so-called "heter" (a piece of titanium cellular, or sponge) in order to remove oxygen from the furnace that may get into the furnace together with argon. "Heter" was held in molten condition during 20-30 s, and then started the ingot smelting.

After complete smelting the melting process was interrupted, the ingot was placed upside-down and smelted once again. To obtain a homogeneous composition, this procedure was consistently executed 3-5 times.

4.1.2. Research on the properties of Ti – V, Ti – Nb alloys

The alloys' characteristics were studied in both hardened and deformed (by rolling) states using the X-ray and electron microscopy, dilatometry. The studied temperature interval was between -196 °C (minus 196) and 800 °C.

The phase analysis, texture and the phase lattice parameters at various temperatures were determined applying an X-ray diffractometer with the radiation monochromatized by Cu K_{α} and Cr K_{α} . The error in measuring the lattice parameter amounted to 0.0004 nm. It was fixed that at Nb content less than 34% the alloys have the orthorhombic martensite (α'' -phase) structure. If the Nb concentration exceeded 38%, the alloys' structure represented the body-centered cubic β -phase. Detection of abnormal temperature dependence of the α'' -phase appeared a fundamental result. The b parameter increases as the temperature decreases from 200 up to minus 196 °C, while the a and c parameters are characterized by normal temperature dependence, i.e. they decrease with the decrease of temperature. At thermocycling in the stated temperature range, all these three parameters change irreversibly. The abnormal change of the parameter of the α'' -martensite lattice results in the abnormal thermal expansion of the Ti-Nb alloys. Besides the abnormal behavior of the parameter of the α'' -phase lattice, the reversible change of the phase composition ($\alpha'' \leftrightarrow \beta$) was detected at thermocycling, which in its features is similar to thermoelastic martensite transformation.

Quantitative analysis of deformations into thermal expansion of the reversible change of the orthorhombic martensite ($\alpha'' \leftrightarrow \beta$) quantity and of the abnormal temperature behavior of the α'' -phase parameter was made. It was shown that the abnormal behavior of the b parameter is a determining factor in the decreased or even negative TEC values. In this connection, combining the α'' - and β -phases content, one may realize the values of thermal expansion in the interval $(-10 \div +10) \times 10^{-6} \text{ K}^{-1}$ in the alloys titan-niobium and titan-vanadium. TEC-temperature dependencies of the Ti-V and Ti-Nb systems are represented in Tables 4.1.1 and 4.1.2.

4.1.3. Research on TEC of the 8% YSZ electrolyte.

We have carried out dilatometric research into TEC of electrolyte 8% YSZ in the range of temperatures of $(100 \div 900) \text{ }^\circ\text{C}$ in the air and in vacuum. TEC value is independent of gas medium and varies in the range of $(7,8 \div 9,8) 10^{-6} \text{ C}^{-1}$ (see Fig. 4.1.1, 4.1.2).

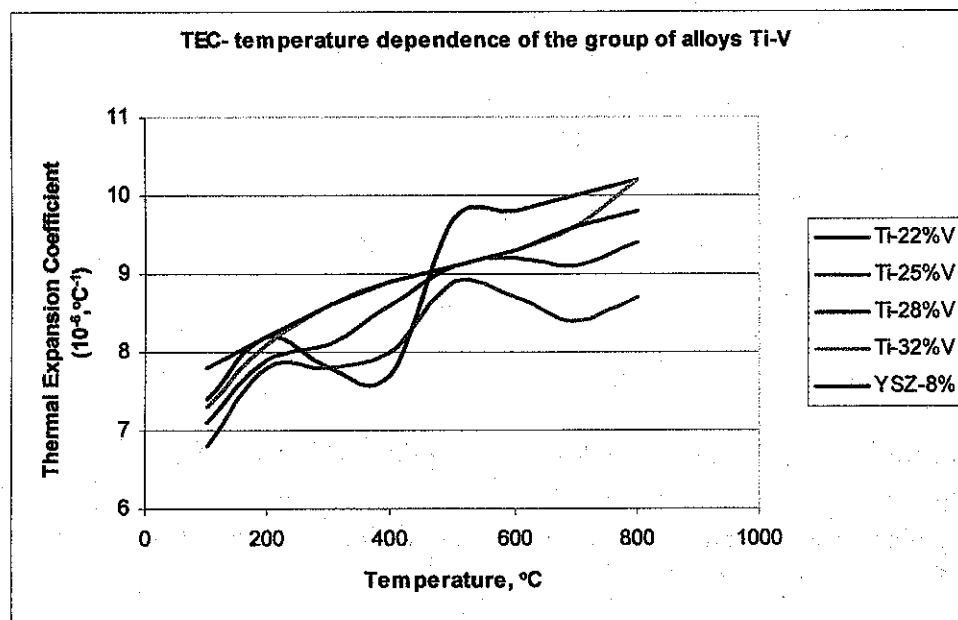


Fig. 4.1.1

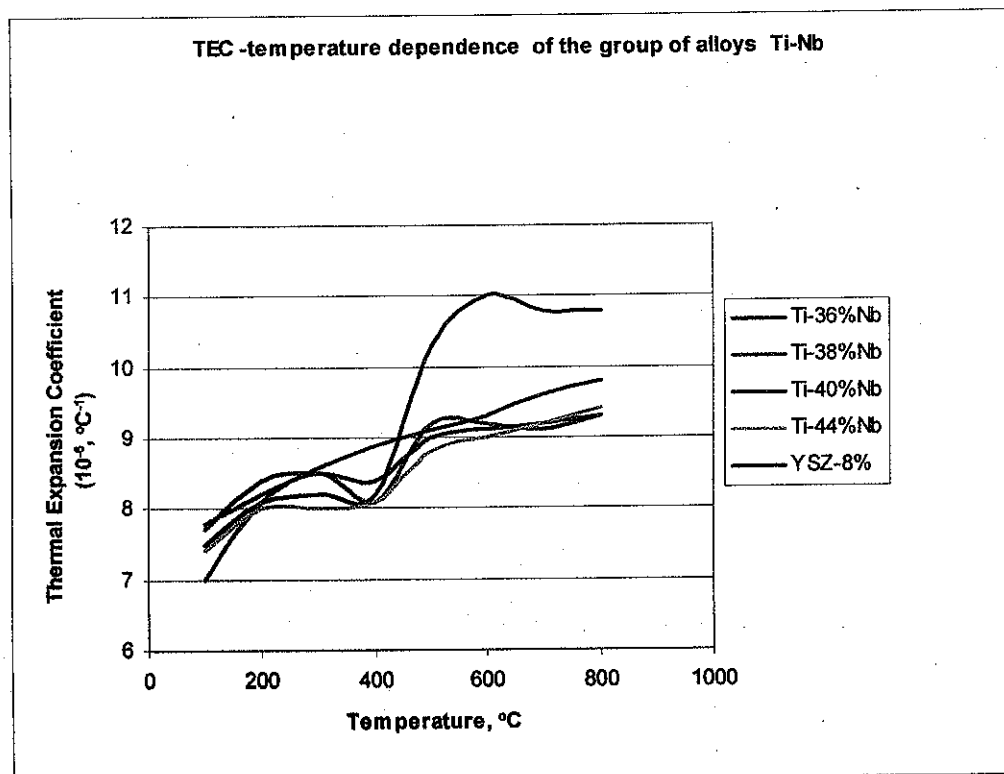


Fig 4.1.2

4.1.4. Research on alloys of the Ti-Nb system.

Corrosion rate of 56Ti-44Nb- alloy in gas medium ($H_2 + 0.2CO_2 + H_2O$) at temperature of 900 °C during 800 hours amounted to 0,5% mass. The surface structure is a coarse-grained one with the size of grains up to 1,5 mm, which consist of small elongated particles of 5-9 μm . The oxide film is mainly formed by Ti- oxide (see Fig. 4.1.3, 4.1.4).

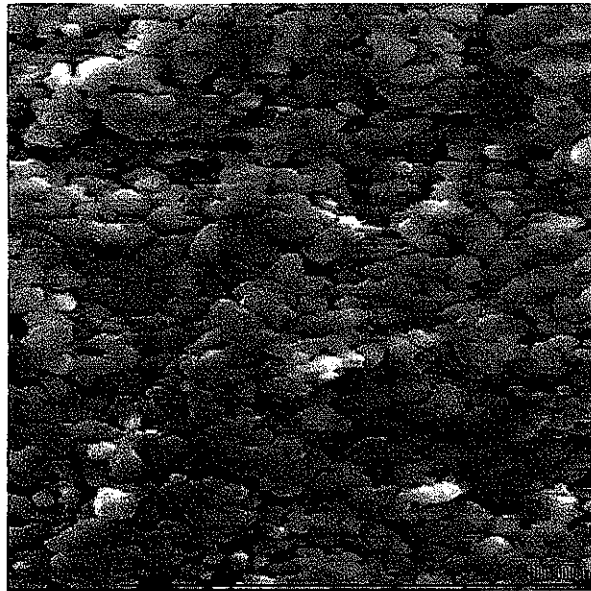


Fig. 4.1.3.

The surface of 56Ti-44Nb alloy after its operation in gas medium
($H_2 + 0.2CO_2 + H_2O$) during 800 h. at 900 °C

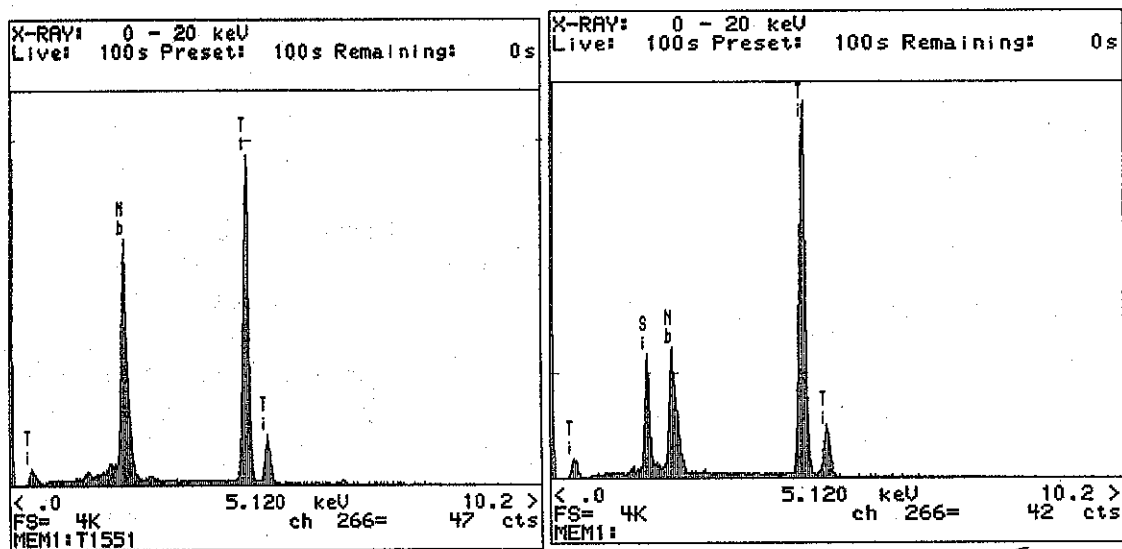


Fig. 4.1.4. X-ray spectra from the surface of 56Ti-44Nb alloy (before and after testing)

Corrosion rate of Ti-based alloys at high temperatures is higher than that of ferrite steels.

To improve the corrosion rate of Ti-based alloys, a technology was elaborated and intermetallics-based coatings mainly containing Ni, Al and rare-earth metals were coated on the specimens of alloys. In this case we used the technology of diffusion ion-plasma deposition from the gas phase when the support (substrate) after getting the intermetallide layer was exposed to annealing. At annealing, a diffusion zone between the intermetallide and support is formed, thus providing good adhesion to the support.

4.1.5. Conclusions.

4.1.5.1. We have elaborated the technology and smelted the ingots of Ti-Nb-based alloys with the following composition (% mass): Ti-V (22, 25, 28, 32%V); Ti-Nb (36,38, 40,44 %Nb).

4.1.5.2. We have studied the characteristics of Ti-Nb-based alloys being in the deformed (by rolling) states applying X-ray and electron microscopy and dilatometry. Theoretical assumptions on the relations about the dependence between the phase composition and physical properties have been confirmed. Combining the composition of α'' and β -phases in alloys one may achieve the TEC values in the range of $(7 \div 11) \times 10^{-6} \text{ C}^{-1}$.

4.1.5.3. The corrosion rate of Ti-based alloys at temperatures of 900°C exceeds that of the ferrite steels. To improve the heat resistance of Ti-based alloys, the technology was elaborated and the intermetallides-based coatings, mainly containing Ni, Al and rare-earth metals were deposited onto the surface of specimens.

4.1.5.4. An independent customs examination was carried out and a decision was issued №002/236/LICHP dated 11.07.04, authorizing the delivery to the USA without licensing of a test-industrial batch of specimens from 68Ti-32V and 60Ti-40Nb alloys with the sizes of 0,6x25x25mm 4 pcs of each type to be experimentally studied in ANL.

4.1.5.5. We have analyzed the cost data on the technology and production of a test-industrial batch of metal ribbon from 60Ti-40Nb alloy with the thickness of 0.6mm for bipolar plate in Public Corporation "Metallurgical Works Elektrostal". The estimated cost of 1 kg of such ribbon is about \$44.

4.2. Development alloys with low Cr content.

4.2.1. Smelting of specimens and selection of deoxidizers.

Smelting was conducted in a Balzers vacuum induction furnace. The mass of a melt made 1 kg. The adjustment of smelting modes and selection of deoxidizers were effected while melting several alloy compositions, which are most inclined to swelling. For deoxidation, Ni-Mg (15%) ligature counting 0,05% upon 1 kg melt, silicon, purified manganese and aluminium in different combinations were used. The optimal results were obtained using Al as deoxidizer counting 0,07% upon 1 kg melt. The metal was poured into 40mm cylindrical casting molds with an extension for drawing out a contraction cavity.

The ingots appropriate for each adjusted melting mode were obtained for the further metallurgical recasting. All the melts were checked for chemical composition.

4.2.2. Adjustment of the ingots deformation technology.

Deformation of the obtained ingots was executed in two ways:

- applying a free forging method with a hammer strength of 100kg per square inch with further application of forgings in swages in order to get round rods with a 25mm profile. The rods were fabricated with the regular structure without any surface and inner cracks;
- applying a screw rolling method of the ingot from $\varnothing 35$ mm into $\varnothing 15$ mm. The rods obtained in such a way have the insufficiently regular structure in the central zone. To eliminate the above defect, one should provide higher degree of stretching in a process of rolling. This requires that the initial diameter of blank material should be increased, which in the task being solved is technologically

inexpedient. The small length of the blanks (about 70mm) also creates additional problems at screw rolling.

From the rods obtained, specimens for dilatometric studies were fabricated.

4.2.3. Adjustment of the technique to measure linear expansion temperature coefficient (LETC) and dilatometer tests.

Thermal expansion was measured at heating rate of 2-5 °C/min applying a quartz dilatometer Linsais (Germany). For the calibration, a high-accuracy micrometer and special metrological etalons from molybdenum ($TEC=5 \times 10^{-6}, K^{-1}$) and from 32HK alloy (superinvar, $TEC=0.5 \times 10^{-6}, K^{-1}$) were used. The dilatometer sensitivity made $\sim 0.5 \mu m/mm$, while the accuracy of TEC determination made $\sim \pm 0.2 \times 10^{-6}, K^{-1}$.

Among the curves detected by a dilatometer $\Delta l/l=f(T)$ we determined the differential $\alpha = dl/dT$ and average $\alpha_{20-T} = \Delta l / \Delta T$ TEC values.

The first ones are associated with the peculiarities of magnetic structure and thermal expansion. In practice one usually deals with the average TEC values, since just these values are used in computing the structures, including multiplayer ones. Therefore in the present Report we shall cite only the average TEC values in the specified temperature range.

It was ascertained that the stretching $\Delta l/l$ of the specimens of all studied alloys increases with the growth of temperature, where the character of temperature dependence $\Delta l/l$ is to a great extent determined by the composition. For the alloys with comparatively low Curie temperature ($T_C < 100^\circ C$) of Fe-Ni composition (<30%)-Cr(>10-%) and high enough Curie temperature ($T_C > 600^\circ C$) of Fe-Ni composition (>30%)-Co(>34%)-Cr(<10-%), the $\Delta l/l$ value changes practically linearly with temperature (see. Fig.4.2.1). If the value T_C is in the range of 100-500 °C, one may distinguish two sections with different inclinations on the curves $\Delta l/l=f(T)$ and the bend (inflection) temperature T_{bend} distinctly appears (see Fig.4.2.2). At temperatures below T_{bend} one may observe lower TEC values, while at $T > T_{bend}$, TEC values are higher. According to the data available, T_{bend} is determined by peculiarities of magnetic structure near the Curie point. As a rule, T_{bend} is about 50-100°C lower than T_C . Bend temperature T_{bend} increases as Ni and Co concentration grows and decreases with Cr concentration.

Table 4.2.1 represents the data on chemical composition of the selected group of alloys with TEC that is close to that of the ferrite steels in the temperature range of 20-800 °C.

Table 4.2.1

Designation	Composition of alloys with TEC values in the range of $(12,2 \div 13,6) \cdot 10^{-6} \text{ } ^\circ\text{C}^{-1}$ (by the result of chemical analysis), mass%			
	Fe	Ni	Co	Cr
32Ni20Co6Cr	Bal.	32,0 (32,2)	20,0 (20,2)	6,0 (5,9)
36Ni20Co6Cr	Bal.	36,0 (35,8)	20,0 (19,8)	6,0 (6,1)
40Ni20Co6Cr	Bal.	40,0 (39,6)	20,0 (20,1)	6,0 (5,9)
32Ni30Co6Cr	Bal.	32,0 (32,0)	30,0 (30,2)	6,0 (5,8)
34Ni30Co6Cr	Bal.	34,0 (34,3)	30,0 (29,9)	6,0 (5,7)
38Ni30Co6Cr	Bal.	38,0 (37,7)	30,0 (30,1)	6,0 (5,8)
42Ni30Co6Cr	Bal.	42,0 (42,2)	30,0 (30,0)	6,0 (6,1)
2Ni60Co10Cr	Bal.	2,0(2,0)	60,0(60,0)	10,0 (10,1)
2Ni62Co10Cr	Bal.	2,0(2,0)	62,0(62,0)	10,0(10,0)
2Ni66Co10Cr	Bal.	2,0(2,0)	66,0(66,0)	10,0(10,1)

TEC –temperature dependencies of the alloys and ceramics YSZ-8% are represented in Fig. 4.2.1 and 4.2.2.

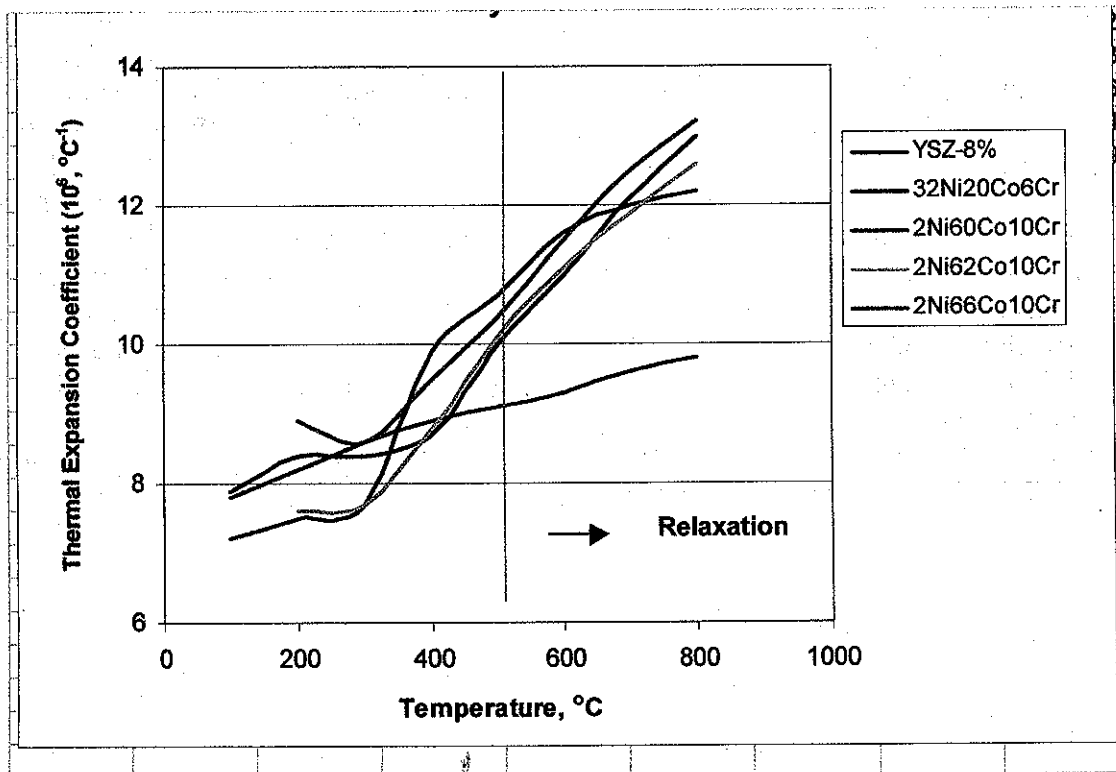


Fig 4.2.1

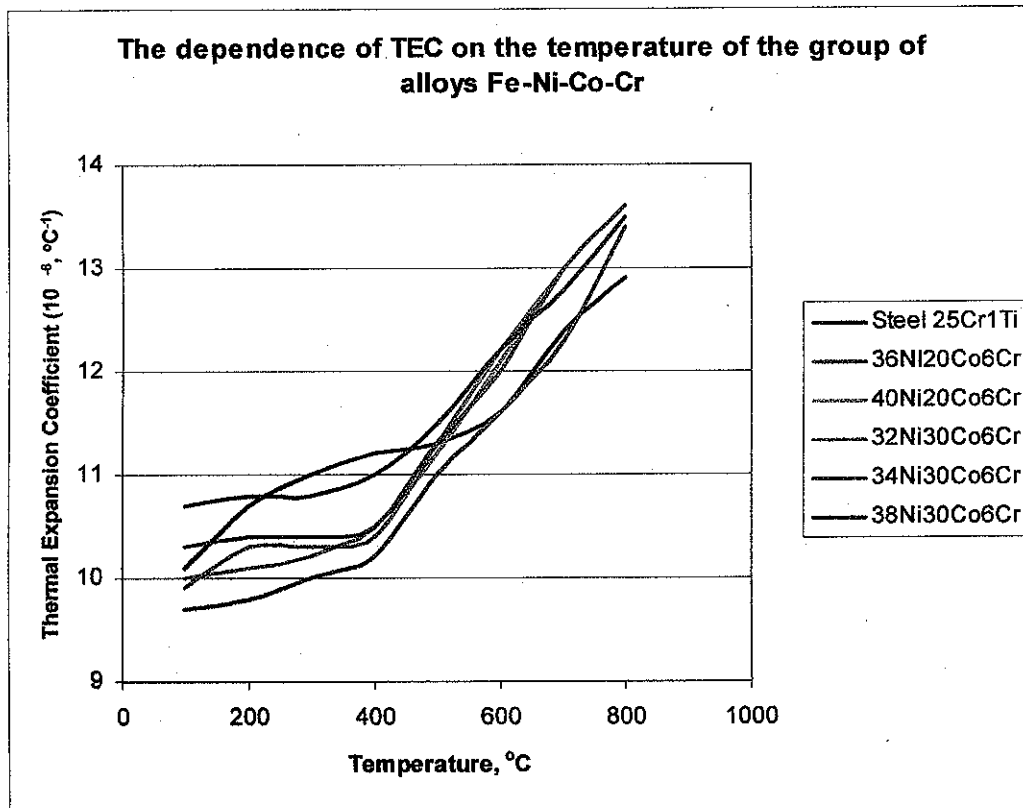


Fig. 4.2.2

4.2.4. Evaluation of mechanical stress in metal-ceramic compounds

At the exploitation of the junctions in fuel cells, heating and cooling (thermocycling) occurs in the temperature range of $20 \leftrightarrow (800-850)^\circ\text{C}$. The difference in thermal expansion between metal and ceramics results in the appearance of stresses at variations of temperature.

Such stresses values may be estimated by means of the expression

$$\sigma = (\text{TEC}_{\text{met.}} - \text{TEC}_{\text{cer.}}) \cdot \Delta T \cdot E_{\text{met.}} \cdot E_{\text{cer.}} / (E_{\text{met.}} + E_{\text{cer.}}),$$

where $\text{TEC}_{\text{met.}}$ and $\text{TEC}_{\text{cer.}}$ – average values of metal and ceramic TEC in the temperature range of ΔT , $E_{\text{met.}}$ и $E_{\text{cer.}}$ – elastic modulus of metal and ceramics. Since the data on $E=f(T)$ for the alloys of Fe-Ni-Co-Cr –system under development are presently not available, the E-values for the alloys with similar composition were used for computations: X20H80 and X16H45IO3. The data on Zr ceramics' modulus of elasticity were represented by the Institute of Physical Chemistry of RAS, while the data on TEC of the ceramics $\text{ZrO}_2-(10-12)\% \text{Y}_2\text{O}_3$ – by RFNC-VNIITF (see Fig. 4.2.6.)

Calculations of stresses arising at heating of the junctions metal-ceramics in the temperature range of $100-800^\circ\text{C}$, made within the frameworks of the above assumptions, have resulted in as follows.

New alloys.

Aloy H32K20X6 (Fig.4.2.3). Due to the closeness of metal and ceramics TEC in the temperature range of $20-400^\circ\text{C}$, the internal stresses' level is close to zero. In the range of $500-800^\circ\text{C}$, σ^s monotonically increases with temperature, achieving the value of 100 N/mm^2 , which makes ap-

proximately $0.8 \sigma_{0.2}$ of the alloy at temperature of 800°C . Thus in all the studied range of temperatures, the stress value in the junction metal-ceramics is less than the yield point of the alloy.

Alloy H40K20X10 (Fig.4.2.4). In all the studied range of temperatures, the stress level in the junction increases with temperature, achieving the value of $\sim 125 \text{ N/mm}^2$ at 800°C . The value of the relation $\sigma^s/\sigma_{0.2}$ also monotonically increases with the growth of temperature. At 500°C it makes ~ 0.4 , while at $800^{\circ}\text{C} \sim 1.05$, which is somewhat higher than the yield point of the alloy.

Alloy H2K62X10 (Fig.4.2.5). The change of internal stresses in the junction has a non-monotonous character. At low temperatures ($100 - 400^{\circ}\text{C}$), tension stresses arise, while at higher ones – pressure tensions. The absolute stresses' values in a critical for relaxation interval (below 500°C) do not exceed 25 N/mm^2 . In this case the relation $\sigma^s/\sigma_{0.2}$ does not exceed 0.1 , which is not just below the yield point, but below the proportional limit as well. In the range of temperatures of $500-800^{\circ}\text{C}$, the stress level increases up to 110 N/mm^2 , however even at 800°C it does not exceed the yield point ($\sigma^s/\sigma_{0.2} < 1$).

The obtained results permit to make the following conclusions:

- In the temperature range where the relaxation processes are hampered the stress level in the joints of the alloys with Zr ceramics does not exceed 25 N/mm^2 , which makes $\sim 10\%$ of the yield point.
- In the temperature range where the relaxation processes are facilitated ($500-800^{\circ}\text{C}$), σ^s of the materials under development does not exceed 110 N/mm^2 , which is close to the yield point, $\sigma^s/\sigma_{0.2} \leq 1$.

4.2.5. Residual postrelaxation stresses (rough estimation).

Relaxation processes running at temperatures above 500°C , decrease the stresses arising in the alloy as a result of cooling.

According to the existent concepts, the mechanism stress relaxation processes is determined by the composition and structure of alloy, by the impurities content, processes of ageing and dispersion hardening. At low temperatures ($T \leq (0.1-0.3)T_{in}$), stress relaxation takes place due to a lattice resistance, sliding of dislocations, phonon deceleration, redistribution of interstitial impurities in the field of twinning stresses. At higher temperatures, ($T \geq (0.1-0.3)T_{in}$), relaxation processes are controlled by sliding of dislocations, shift of dislocations due to bulk diffusion, dynamical recrystallization, transfer from sliding to (over)crawling, processes of phases' separation (by means of dispersion hardening), grain-boundary diffusion. Each mechanism is described by its own expression with time- and temperature- depending constants. The detailed consideration of relaxation is now under development. The following data and assumptions have been used for the rough estimation. It was supposed that the relaxation occurs by the exponential law:

$$\sigma_{rel.} = \sigma_0 \exp(-bT)^k$$

where b и k are the constants.

The results of corresponding computations, for example, for the H2K62X10 alloy are represented in Fig. 4.2.56. One may notice that below 400°C , $\sigma_{rel.}$ is close to σ^s . Relaxation effects reveal themselves at temperatures above $400-500^{\circ}\text{C}$. With the increase of temperature, the level of residual (after relaxation) stresses decreases and at $700-800^{\circ}\text{C}$ such decrease achieves a 5-7-fold level.

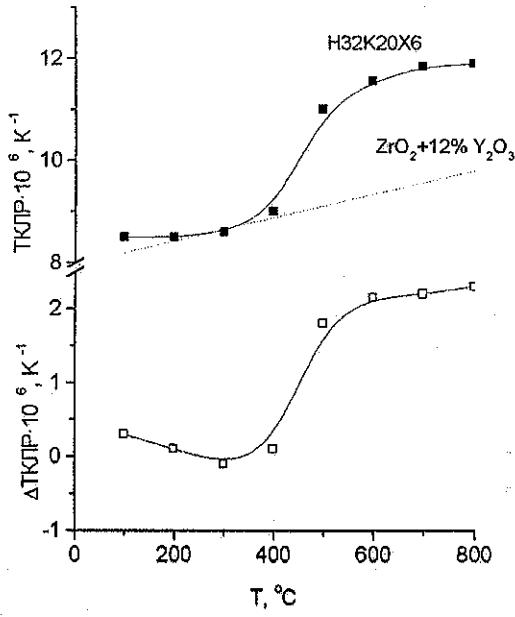


Fig. 4.2.3a

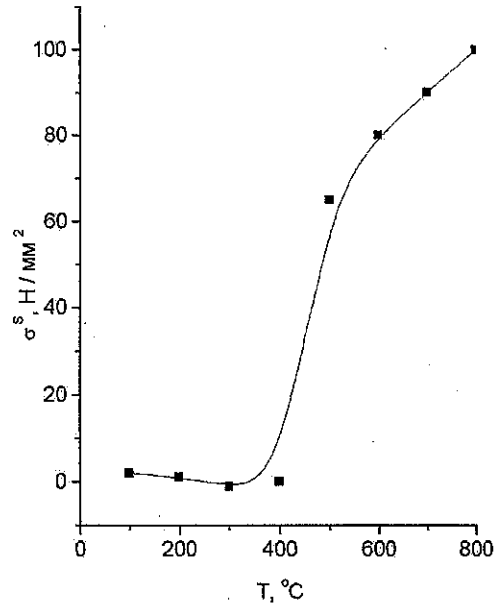


Fig. 4.2.3b

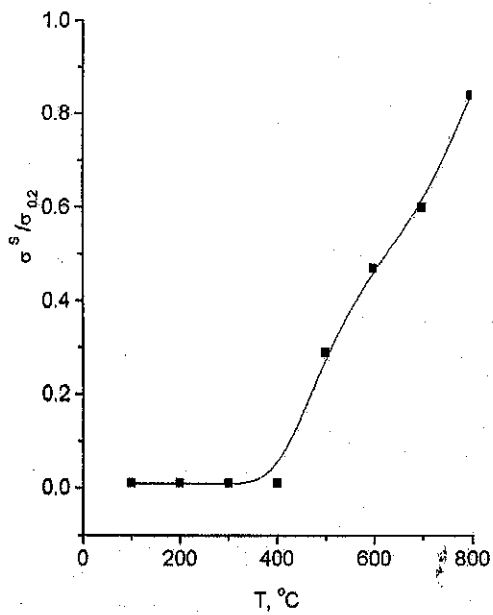


Fig. 4.2.3c

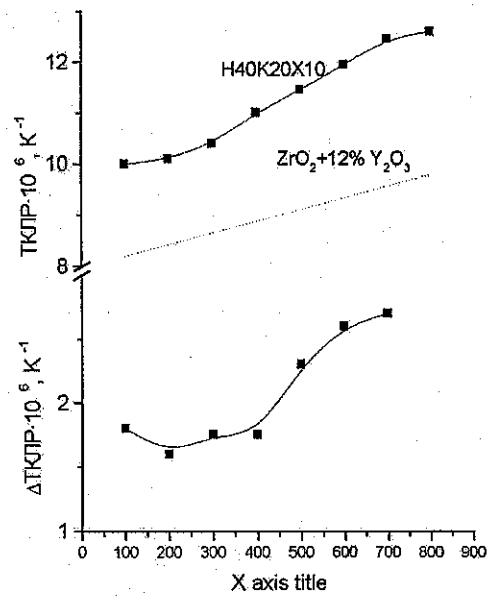


Fig. 4.2.4a

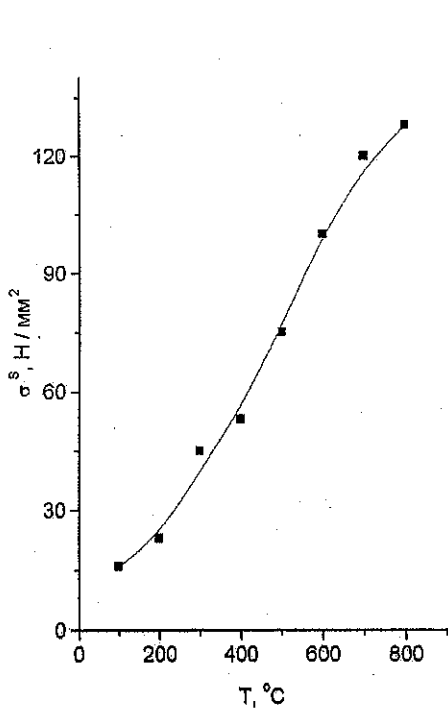


Fig. 4.2.4b

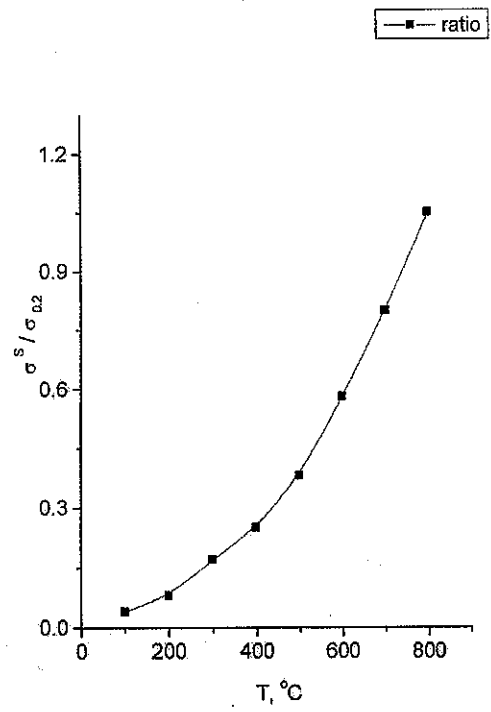


Fig. 4.2.4c

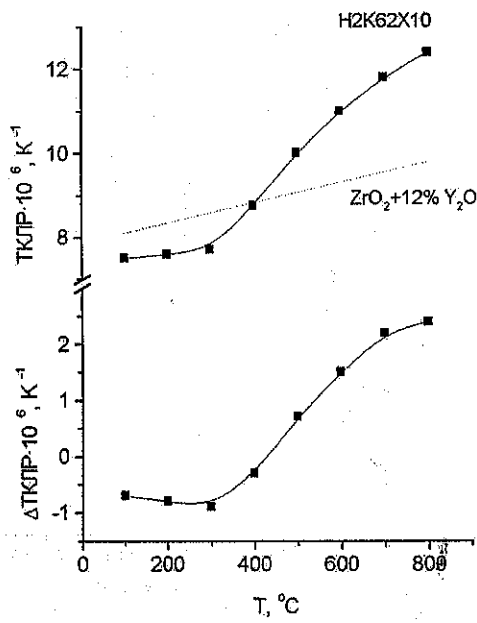


Fig. 4.2.5a

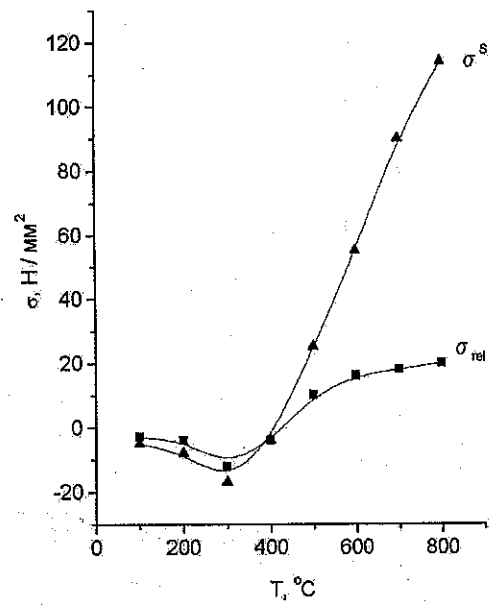


Fig. 4.2.5b

Alloy 44Ni-20Co-6Cr .

The X-ray spectra analysis demonstrates that after testing in cathode conditions, in corrosion products' spectra, the most intensive lines belong to Fe, oxygen and Co. Hence, the compound Fe, Co and Cr oxides dominate in the structure of this coating.

After testing in anode conditions, the most distinct lines the in X-ray spectrum of the specimens' surface belong to Cr, oxygen, Fe and Ni. Consequently, these elements form the compound oxide layer.

Diffraction patterns from the specimens' surface demonstrate that the oxides formed in cathode medium contain Fe_3O_4 , Cr_2O_3 and compound Fe and Co oxides.

In anode medium, the Cr-based oxides were formed: Cr_2O_3 and a small amount of $\text{CrO/Cr}_3\text{O}_4$. Based upon the fact that all the lines relating to Cr oxides are of low intensity, the formed oxide layer is evidently very thin.

4.2.8. Conclusions

4.2.8.1. The appropriate technology was elaborated and a group of specimens were fabricated from Fe-Ni-Co-Cr alloys. Dilatometric studies were carried out and the group of specimens was selected with TEC being in the range of $(12,2 \div 13,6) \cdot 10^{-6} \text{ } ^\circ\text{C}^{-1}$ at temperatures up to $800 \text{ } ^\circ\text{C}^{-1}$, that is the one being close to ferrite steels and YSZ ceramics.

4.2.8.2. We have estimated internal thermoelastic stresses σ^s , arising in the junctions metal/ceramics at their heating taking account of relaxation effects. The calculation results demonstrate that:

- In the temperature range where relaxation processes are hampered (500°C), the σ^s level in the junctions of the new alloys with Zr ceramics does not exceed 25 MPa, which makes ~10% from the yield point;
- In the temperature range where relaxation processes are facilitated ($500\text{-}800 \text{ } ^\circ\text{C}$), the σ^s level of the new alloys does not exceed 110 MPa, which is close to the yield point, $\sigma^s/\sigma_{0,2} \leq 1$.

4.2.8.3. We have carried out parallel testing of Cr diffusion into a cathode ($\text{La}_{0,6}\text{Sr}_{0,4}\text{MnO}_4$ (MLS)) from the alloys Fe-Ni-Co-Cr with various content of Cr and steel 25Cr1Ti in air medium at 900°C depending on time. Cr diffusion from the steel 25Cr1Ti into MLS after 800 curing hours amounts to 4%. Cr diffusion from Fe-Ni-Co-Cr alloys may be observed at contact times of 800 hours and more, at that the diffusion is practically not observed with the alloys containing Cr 6%.

4.2.8.4. We have carried out parallel testing of the corrosion resistance of the ferrite steel 25Cr1Ti and a group of alloys Fe-Ni-Co-Cr in anode ($5\%\text{H}_2 + 50\%\text{H}_2\text{O} + 20\%\text{CO}_2 + 25\%\text{N}_2$) and cathode ($5\%\text{H}_2\text{O} + \text{air}$) atmosphere. In cathode medium, all the studied materials are subjected to intensive corrosion with the formation of a loose layer of corrosion products. In anode medium, the corrosion of materials is substantially lower, the layer of corrosion products has mainly dense form. The oxide layer on the ferrite commercial steel has a more expressed grain effect. In anode and cathode medium, the oxide films arise on the steel surface that are formed by Cr_2O_3 and $\text{Cr}_{1,3}\text{Fe}_{0,7}\text{O}_3$, compounds, though in anode medium they are thicker.

In cathode medium, the oxide films formed by the compounds Cr_2O_3 , Fe_3O_4 and compound Fe and Co oxides arise on the surface of alloys of Ni-Co-Cr-Fe system. In anode medium, the oxide films are formed by Cr_2O_3 and a small amount of $\text{CrO/Cr}_3\text{O}_4$.

The corrosion rate of alloys in cathode medium is several times higher than that in anode medium. As compared with the ferrite commercial steel, the corrosion rate of the best alloy of Fe-Ni-Co-Cr system in cathode atmosphere is 6,5 times lower, than that of 25Cr-1Ti steel.

4.2.8.5. An independent customs expertise was carried out and a decision was issued authorizing the delivery to the USA without licensing of the pilot models of the alloy of Ni-Co-Cr-Fe system for experimental studying at the first stage.

4.2.8.6. We have analyzed the cost data for the technology of a pilot batch of 0,5 mm sheet metal from the alloy of Ni-Co-Cr-Fe system to be used as SOFC interconnectors. They were fabricated in Public Corporation "Metallurgical Works "Electrostal"". The approximate cost of 1 kg of such sheets is about \$36.

4.2.8.7. At carrying out the works on Task 4, a patentable technical solution was obtained and an application for a patent of the Russian Federation " High-Temperature FC with Solid Electrolyte" was made, the authors - Mishanin S.V., et.al. .

4.3. Development of ferrite stainless steel (brand 400) with an oxide coating

4.3.1. Materials for coatings

Implementation of a protective coating on the surface of a separator plate can be one of methods to reduce FC degradation. Such coating should be stable in FC operation conditions, have rather high electric conductivity (not worse than conductivity of the cathode) and impede chromium diffusion into the surface of the electrode.

Complex oxides with a structure of a perovskite with a high electronic conductivity are of the most interest as a coating material. Some publications /1,2/ describe the results of research on high temperature corrosion of chromium steel with a coating of cathode materials ($\text{La}_{0.6}\text{Sr}_{0.4}\text{CoO}_3$ and $\text{La}_{0.9}\text{Sr}_{0.1}\text{CoO}_3$). It is shown that reduction of rate of chromium transport in the coated steel can reach 99% as compared to the not coated steel. The following oxides were selected in the mentioned works: strontium lanthanum manganite $\text{La}_{0.6}\text{MnSr}_{0.4}\text{O}_3$ and nickel oxide that is used as a material for an oxygen electrode /3/. Thermal expansion coefficient of NiO is 12.6×10^{-6} ($100 - 800^\circ\text{C}$), specific electric conductivity is $-6.7\text{Ohm}\cdot\text{m}$. at 863°K and $1.4\text{Ohm}\cdot\text{m}$. at 1273°K . To improve conductivity of the coating it is possible to dope nickel oxide with lithium and to use $\text{Li}_x\text{Ni}_y\text{O}$ as a coating material, where $x=0.1-0.2$, $y=0.8-0.9$.

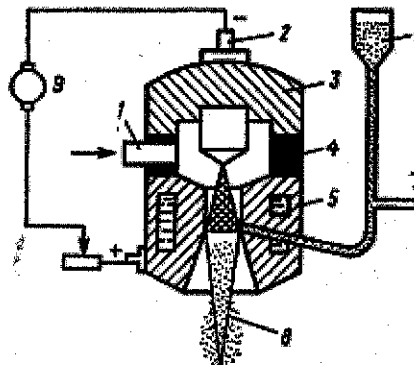
4.3.2 Polishing of the coating application process

Plasma sputtering method is suggested for coating application. The idea of the plasma method is in the following: in special devices – plasmatrones - an electric arc is formed between a tungsten cathode and a copper anode (which is a water cooled nozzle). The arc heats up the working gas (argon, helium, nitrogen) up to a high temperature; it is supplied to the chamber of the plasmatrone with swirls. The heated gas comes from the nozzle as a plasma jet, the average temperature of which at the outlet of the nozzle is several thousands of degrees. Such temperature is sufficient for melting any substances that exist in a solid state. These substances are supplied into the plasma jet as a powder, wire or rods. A scheme of plasmatron is given in Fig.4.3.1.

Choosing operating modes of the plasmatron, it is possible to do sputtering of different materials (metals, oxides, carbides, silicides, organic materials). Sputtering can be performed both in ordinary environment and in the inert environment. The coatings produced by plasma sputtering method have a good density and good adhesion with the substrate.

Plasma sputtering method is used in many areas of engineering, including SOFC production as it was shown by information study /4,5/.

When working at the task of the Project, a coating application process was worked through and polished in the open environment using UPU-8M plasma unit in chamber 6-3170, and in the argon using UPU-3D unit.



- 1 – an inlet of plasma forming gas, 2 – current supply, 3 – a cathode, 4 – an insulator,
 5 – an anode, 6 – a powder batcher, 7 – an inlet of transporting gas,
 8 – a plasma jet, 9 – a power supply source.

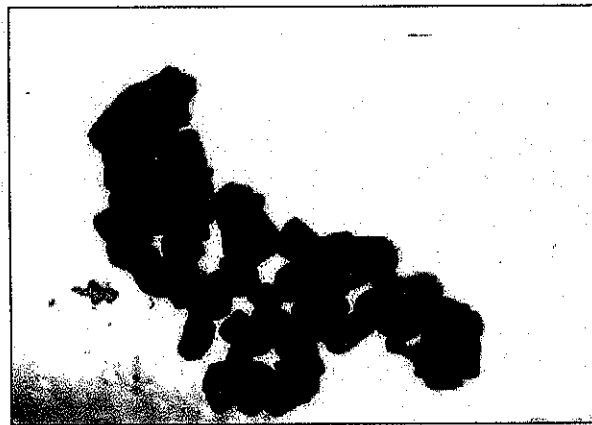
Fig.4.3.1. Scheme of a plasmatron for sputtering

Coatings to be studied were applied onto flat samples – disks 25mm in diameter, made of 12X17, 08X17T, 20X13 steel. Thickness of the samples varied from 0.4mm to 0.8mm. In the process of sputtering the samples were installed in a mandrel and were fixed there with the help of a vacuum pencil.

The strength of the coating adhesion was determined following the glue method, when the disk coated on two sides was glued to the claws. Density and porosity of the coatings was determined by method of hydrostatic weighing in distilled water.

Before the coating was applied the surface of the samples, they underwent abrasive-jet treatment with silicon carbide with grain №№12, 16.

Sputtering of coatings on the basis of NiO was done with a powder less than 40microns; coatings of strontium lanthanum manganite was done with a powder as it was supplied. Average size of particles of $\text{La}_{0.6}\text{MnSr}_{0.4}\text{O}_3$ powder that was defined with an electronic microscope is 0.3microns. Particles have mostly the shape of cut crystals (see Fig.4.3.2).



x18000

Fig. 4.3.2. Particles of $\text{La}_{0.6}\text{Sr}_{0.4}\text{MnO}_3$

When defining sputtering modes, approximate calculations of the minimum power of the plasma jet was made by the following formula /6/:

$$P_{\ominus} = 2,99 \cdot \frac{V^{1,5} \cdot d_p \cdot D^{0,5}}{R_0^{1,25} \cdot L_p^{0,6} \cdot \eta},$$

where:

P_{\ominus} - minimum electric power of the plasma arc, kBA;

V – flow rate of plasma forming gas;

d_p – diameter of particles;

$D = T^2 C_e^2 \rho_p$ - melting difficulty,

T - melting temperature;

C_e - equivalent heat capacity of the material;

ρ_p - density of the materials of the particle;

R_0 - radius of the nozzle;

L_p - path of particle in the isothermal part of the jet;

η - efficiency of the plasmatrone.

Calculated value of the minimum electrical power for NiO powder made up ≈ 12.6 kVA. Then, using simplex planning method, parameters of sputtering mode were optimized. Coefficient of material deposition was chosen as a criterion of optimization. As a result, the selected power of the plasma arc was determine as $\approx 14-16$ kVA for both powders.

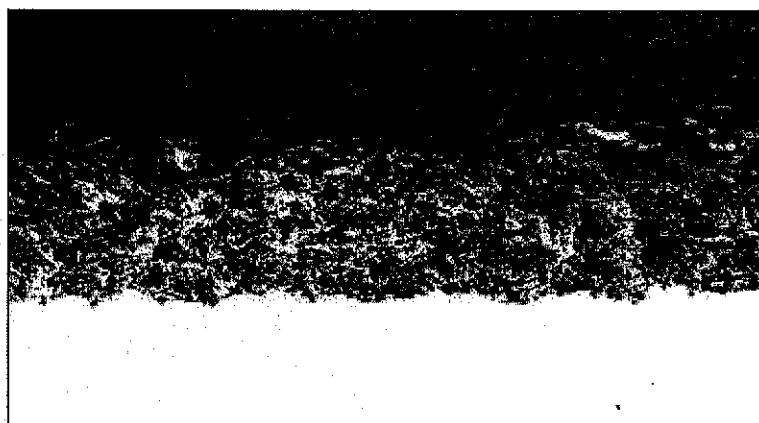
4.3.3 Results of research on the properties of the coatings

As it was shown by the research on sputtering modes optimization, it is possible to produce plasma coatings from $\text{La}_{0.6}\text{MnSr}_{0.4}\text{O}_3$ and lithium doped NiO with thickness of 0.03 – 0.10mm. Sputtering can be done both in the air and in the argon. When doing sputtering of $\text{La}_{0.6}\text{MnSr}_{0.4}\text{O}_3$ powder, there are some difficulties caused by a very small size of particles. The table 4.3.1 below shows the basic properties of the produced coatings.

Table 4.3.1

Material of the coating	Environment of sputtering	Strength of adhesion, MPa		Density, g/cm^3	Open porosity, %
		initial	After 50hour tests		
Lithium doped NiO ($\text{Li}_{0.2}\text{Ni}_{0.8}\text{O}$)	air	22,7-29,9	8,3-14,0	4,90-4,81	8,5-10,5
	argon	26,7-30,1	9.8-14,6	5,03-4,94	7.5-8,3
$\text{La}_{0.6}\text{MnSr}_{0.4}\text{O}_3$	air	13,5-18,9		5,01-4,87	15,3-17,1
	argon	11,0-15,7		4,97-4,83	15,9-18,4

Table 4.3.2 shows the data obtained using the samples made of 12X17 steel. As it was shown by the research on a group of steel (12X17, 08X17T, 20X13), the material of the sample does not influence the strength of adhesion and the density of the coating. Microstructure of the coatings is shown in Fig.4.3.3.



a)



b)

Figure 4.3.3. Microstructure of the coatings, x250

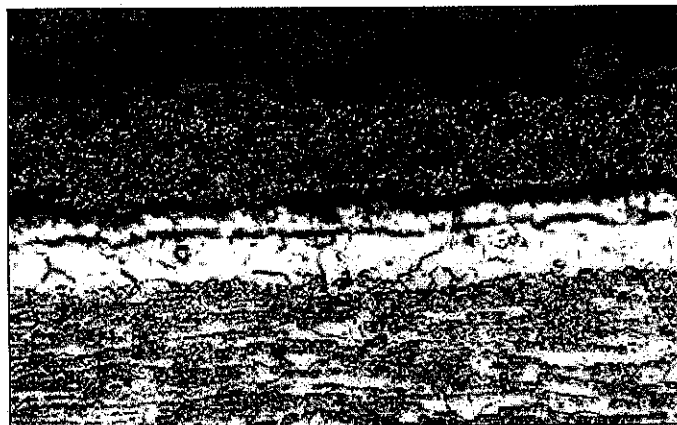
a) $\text{La}_{0.6}\text{MnSr}_{0.4}\text{O}_3$,

b) NiO doped with lithium.

X-ray phase analysis of $\text{La}_{0.6}\text{MnSr}_{0.4}\text{O}_3$ powder and of plasma coatings from it has shown the following. Initial powder is monophase and has a structure of $\text{La}_{0.6}\text{MnSr}_{0.4}\text{O}_3$ with cubic lattice. Coatings, despite sputtering conditions (argon or air), mostly consist of $\text{La}_{0.6}\text{MnSr}_{0.4}\text{O}_3$. Other substance, supposedly $\text{La}_{0.7}\text{MnSr}_{1.3}\text{O}_4$, is present there in a little quantity (less than 10%), and it is more in the coatings sputtered in the argon than in the ones sputtered in the air. Parameters of the $\text{La}_{0.6}\text{MnSr}_{0.4}\text{O}_3$ lattice before and after sputtering has not practically changed, but $\text{La}_{0.6}\text{MnSr}_{0.4}\text{O}_3$ after sputtering has a completely different structure – microstresses increased, smaller crystals were formed etc.; increase of semi-width testifies to that.

In order to improve adhesion properties of the coatings their thermal was done in vacuum at $850\text{-}900\text{C}^0$; it was from 40 min to 7 hours long. However, improvement of adhesion strength was observed neither in case of $\text{La}_{0.6}\text{MnSr}_{0.4}\text{O}_3$ coating nor in case of coating of NiO doped with lithium. Lithium doped NiO coating changed its color from the black one (before thermal treatment) to the light gray one (after thermal treatment). After thermal treatment cracks were revealed on the coatings sputtered in argon. It is evidently caused by structural changes in the coating. In the process of plasma sputtering nickel oxide is partly reduced. This is confirmed by the fact that electric conductivity of NiO layer drastically goes down. Thermal treatment in vacuum intensifies the degree of its reduction; evaporation of lithium from the coating is possible.

Corrosion tests of NiO and lithium-doped NiO were performed in the air at 850C^0 during 50 hours in order to evaluate the influence of external factors on the strength of adhesion. It was found out that adhesion strength went down from $\sim 21.0\text{MPa}$ to $\sim 11.7\text{MPa}$, evidently because of oxidization of the substrate under the coating, as plasma coatings do not protect the steel from oxidation. A black oxide film was formed on a not coated surface of the samples, which left the traces after being rubbed. Fig.4.3.4 shows a specimen of a sample of 12X17 steel after corrosion tests.



x250

Fig.4.3.4. Microstructure of a coating of lithium doped NiO after tests (50 hours).

4.3.4. Results of tests in contact assemblies

Flat samples 28.6 mm in diameter of 15X25T and 15X28 steel were prepared for tests in contact assemblies; they were coated with protective plasma coatings of strontium lanthanum manganate and lithiated nickel oxide. Thickness of the samples was 0.85 mm, thickness of the coating was $\sim 0.05\text{mm}$.

After the tests there was performed analysis of Cr diffusion from the ferrite steel into the cathode material (MLS). The analysis was done after the samples were exposed in the air in contact assemblies during 800 hours at 900C^0 . The following kinds of steel were studied:

- Fe-25Cr-1Ti without a coating and with the coatings of $\text{Li}_{0.1}\text{Ni}_{0.9}\text{O}_4$, $\text{La}_{0.6}\text{Sr}_{0.4}\text{MnO}_3$;
- Fe-28Cr without a coating and with the coatings of $\text{Li}_{0.1}\text{Ni}_{0.9}\text{O}_4$, $\text{La}_{0.6}\text{Sr}_{0.4}\text{MnO}_3$;
- Fe-25Cr-0,1Y without a coating.

Results of the analyses showed:

- The coating of $\text{Li}_{0,1}\text{Ni}_{0,9}\text{O}_4$ blocks diffusion of Cr on steel of Fe-25Cr-1Ti and Fe-28Cr types;
- The coating of $\text{La}_{0,6}\text{Sr}_{0,4}\text{MnO}_3$ blocks diffusion of Cr on Fe-28Cr steel.

There was detected Cr diffusion into MLS samples as deep as 20 microns in the contact with the following materials:

- Fe-28Cr steel without a coating as much as (6-9) % wt.;
- Fe-25Cr-1Ti steel without a coating as much as 3.7 % wt.;
- Fe-25Cr-1Ti steel with a coating of $\text{La}_{0,6}\text{Sr}_{0,4}\text{MnO}_3$ as much as (0,2-0,3) % wt.;
- Fe-25Cr-0,1Y steel without a coating as much as (10-12) % wt.

4.3.5 Conclusions

4.3.5.1. Modes of plasma coating application of $\text{La}_{0,6}\text{MnSr}_{0,4}\text{O}_3$, and lithium doped NiO ($\text{Li}_{0,2}\text{Ni}_{0,8}\text{O}$) were worked through. Basic properties of the coating were determined: adhesion strength, density, open porosity, phase composition, microstructure. It was found out that thermal treatment of the coatings in vacuum does not lead to upgrading of their adhesion with the substrate.

4.3.5.2. After corrosion tests of NiO and lithium doped NiO in the air at 850C^0 during 50 hours deterioration of adhesion strength was observed. It was evidently caused by oxidization of the substrate under the coating.

4.3.5.3. Flat samples of 15X25T and 15X28 steel with protective plasma coatings of strontium lanthanum manganate and lithiated nickel oxide were prepared and tested in contact assemblies in the air during 800 hours at $900\text{ }^\circ\text{C}$. The specified coatings block Cr diffusion from the ferrite steel into the cathode material (MLS).

4.4.5.4. Basing on the gained experience and on the analysis of perspectives of implementation of coatings in SOFC production, it seems not very cost-effective to apply plasma coatings in argon. Plasma sputtering is not a low-cost method of coating application. Judging by estimations, the cost of $\text{La}_{0,6}\text{MnSr}_{0,4}\text{O}_3$ coating application onto the area of 1dm^2 makes up about 15\$. When the process of sputtering is done in argon the cost goes up minimum 3 times, without any considerable upgrading in the quality of the coating.

4.4. Delivery of batch of sheets to the Partner for the research

In the process of preparation of a batch of sheets for the Partner in FGUPTSNIICHRMET named after I.P.Bardin, an independent customs expertise was carried out and a decision was issued under the number of №002/236/ИЦИР dated 11 June 2004 authorizing the delivery to the USA without licensing of:

1. Specimens of alloy 68Ti-32V with the size of 25x25x0,6 (mm), 4 pcs.;
2. Specimens of alloy 60Ti-40Nb with the size of 25x25x0,6 (mm), 4 pcs.;
3. Specimens of alloy 32Ni-20Co-6Cr-42Fe with the size of 100x100x0.5 (mm), 2 pcs.;
4. Specimens of alloy 34Ni-30Co-6Cr-30Fe with the size of 100x100x0.5 (mm), 2 pcs.;
5. Specimens of alloy 44Ni-20Co-6Cr-30Fe with the size of 25x120x0.35 (mm), 2 pcs.

The new terms are reflected in the supplement to the Project ADDENDUM #3, signed by ISTC (Moscow), RFNC-VNIIEF (Sarov) and US DOE (Washington) representatives.

4.5. Evaluation of the manufacturing cost of alloys on the basis of Fe-Ni-Co-Cr and Ti – Nb systems.

We have analyzed the cost data for the technology of a pilot batch of 0.5 mm metal tape from the alloy of Ni-Co-Cr-Fe system to be used as SOFC interconnectors. They were fabricated in Public Corporation "Metallurgical Works "Electrostal"". The price structure (ruble/kg) of 1 kg of 0.5-0.6 mm metal tape fabricated by rolling method applying the production run equipment is represented in Table 4.5.1.

Table 4.5.1.

Expense items	Ni34-Co30-Cr6	Ti + 40%Nb
Charge materials, deoxidizers, ligature	500	660
Power inputs	50	50
Salary including taxes and allocation	40	50
Amortization of equipment (smelting and rolling)	90	100
Other expenses (certification)	50	40
Total	730	900
Planned profit	140	180
Total	870	1080
Value added tax (VAT)	160	190
Price	1030	1270

List of References

- 1 C.Gindorf, L.Singheiser, K.Hilpert "Vaporization studies of pure chromia and chromium containing alloys in humid air". High Temperature Materials Chemistry. Proceedings of the 10th International IUPAC Conference, 10-14 April 2000, Germany, part 2.
2. K.Przybylski, T.Brylewski and J.Prazuch " High temperature oxidation of Fe-Cr steels with regard to their application as interconnectors for solid oxide fuel cells". High Temperature Materials, Chemistry. Proceedings of the 10th International IUPAC Conference, 10-14 April 2000, Germany, part 2.
3. K.Khauffe «Reactions in solids and on its surfaces» part1, Moscow, 1962, page 14.
4. A.G.Gavrilov, A.D.Neiman, L.D.Yushina. Bi₂O₃ module of a fuel pump with an electrolyte on the basis of Bi₂O₃». Abstracts of reports at the XI conference in physical chemistry and electrochemistry of molten and solid electrolytes, part 2. Yekaterinburg, 1998.
5. K.Barthel, S.Rambert, St.Siegmann "Microstructure and Polarization Resistance of Thermally Sprayed Composite Cathodes for Solid Oxide Fuel Cell Use". Journal of Thermal Spray Technology, Vol.:9, Nr.3, 2000.
6. V. I. Yushkov, Y. S. Borisov, S.M. Gershenson «On relation of a necessary thermal power of a plasma jet and thermal physical parameters of the material being sputtered». "Physics and Chemistry of Material Processing», №4,1975.

5. STATUS OF WORKS

The works on the Project are completed in full compliance with the Work Plan on the Project and respective changes reflected in «ADDENDUM #2» and «ADDENDUM #3».

6. A LIST OF PUBLISHED ARTICLES AND REPORTS

- 6.1. ISTC Project #2281p. Development of New Materials for Fuel Cells. Report for the 1st quarter (June 01 2002 – August 31, 2002).
- 6.2. ISTC Project #2281p. Development of New Materials for Fuel Cells. Report for the 2nd quarter (September 01, 2002 – November 30, 2002).
- 6.3. ISTC Project #2281p. Development of New Materials for Fuel Cells. Report for the 3rd quarter (December 01, 2002 – February 28, 2003).
- 6.4. ISTC Project #2281p. Development of New Materials for Fuel Cells. Report for the 4th quarter (March 01, 2003 – May 31, 2003).
- 6.5. ISTC Project #2281p. Development of New Materials for Fuel Cells. Report for the 5th quarter (June 01, 2003 – August 31, 2003).
- 6.6. ISTC Project #2281p. Development of New Materials for Fuel Cells. Report for the 6th quarter (September 01, 2003 – November 30, 2003).
- 6.7. ISTC Project #2281p. Development of New Materials for Fuel Cells. Report for the 7th quarter (December 01, 2003 – February 28, 2004).

7. A LIST OF REPORTS AT THE CONFERENCES AND MEETINGS

7.1. There was a meeting with collaborators from ANL (D. Ehst, M. Krumpelt, D. Carter) on Project #2281p and a Chief Supervisor on the Projects from the ISTC – V.K. Emelianov on September 23-24, 2002 in Sarov.

The goal of the visit: discussion of the tasks of ISTC Project № 2281p and the results of the works performed in the first quarter.

Participants of the Project (RFNC-VNIIEF) described the methodology they use to solve the tasks of the Project and reported the results obtained in the first quarter.

Collaborators were acquainted with design documentation for the technological equipment and attachments (Tasks 1.1 and 3.1), results of corrosion tests (Task 2.1) and results of information study (Task 4).

Project participants (RFNC-VNIIEF) described the methodology of solution of the Tasks of the Project and reported on results of the work for the 1st quarter.

I.D. Goncharov

“Task 1. Cost-effective galvanic nickel coating of 20X23H18 steel for bipolar separator plates of MCFC“.

“Technology of galvanic nickel-plating was improved. The samples for long corrosion tests in the anode conditions of MCFC were made.

Development of design documentation for the line of galvanic baths is being completed. Anode-cathode treatment and nickel-plating of the plates (1500 x 978 x 0.4 mm) will be done in 600-liter sinks. After preliminary calculations, there was prepared an order for chemicals for preparatory treatment operations (anode-cathode treatment) and nickel plating.

There was prepared a SOW for mounting of the line of plating baths in room #302, bld.30B.

Separator plates 1500 x 978 x 0.4 mm in size will be made of a stainless tape (20X23H18 steel) 420mm wide **by welding**. Improvement of a welding procedure using methods of argon-arch welding (AAW) and contact sutural (seam) welding (CSW) is on its way.”

V.I. Rybakov. "Task 1. Development of new materials for fuel cells. Explosion cladding"

"There were chosen two layouts to apply nickel coating by **explosion cladding**. The choice of layouts was stipulated by the conditions of the task being solved, that is application of the coating from 100-micron foil onto the substrate of 20X23H18 steel.

In a "flat" layout, there is a soft plate and a hard plate besides the usual components, which are the plate being sprayed and the fixed plate, a charge of explosives. The soft plate prevents possible welding of the foil and the hard plate prevents the foil from destruction from the hard plate. Besides the "flat" layout, it is possible to implement cladding along a cylindrical surface. For the "cylindrical" layout of plating, the substrate (the part being plated) and a nickel foil are folded to form a tube, which is unfolded after the cladding to give the coated substrate the shape of a plate (a sheet). The choice of the layout was carried out along with the identification of the most preferable composition of the explosive. Besides, design documentation for technological attachments was worked out for practical implementation of the cladding using the selected layouts."

V.G. Kuropatkin «Task 1. 3. Magnetron Sputtering».

"One of the methods to reduce diffusion of elements of steel into the protective nickel layer is to create a barrier layer between the substrate and the nickel layer. There was done analysis of scientific and technological literature, and it was found out that the value of the factor of self-diffusion of the material in the temperature range, where the system of "the substrate - the sprayed-on layer" operates, could be taken as the basic parameter when selecting the proper material for the barrier layer. To perform **magnetron sputtering of the barrier layer** between 20X23H18 steel and nickel, the tools and equipment underwent an expert evaluation. The trial spraying of nickel on 20X23H18 steel was done."

S. V. Mishanin. "Task 2. Development of the material with upgraded corrosion stability for the bipolar plate of molten carbonate fuel cells, development of the technology to produce cold rolled sheets of this material 0.8X819X1500 mm in size."

"There were made groups of monolithic samples from the 30Cr-45Ni-1Al alloys doped with Y, Ti and Cu. The alloys were tested in molten carbonates under the atmosphere of the air – carbon dioxide (20%) gas mixture and the hydrogen – carbon dioxide (20%) gas mixture saturated with water at 55° C. Development of the technique for studying conductivity of contacts of metal materials with porous electrodes under the fuel cell operation conditions was conducted. 20X23H18 steel without coating was used as a constructional metallic alloy to be studied."

V.V. Zoria. "Tasks 1, 2. Feasibility study on giving the background of selection of the bipolar plate material"

"For us to be able to get the selling value of the nickel-plated bipolar plate basing on FOB conditions, Saint-Petersburg, Russia (in compliance with INKOTERMS rules), three variants to establish production of the mentioned-above plates were considered in this Project. They are characterized by the following basic features:

- Automated manufacture of plates with a large portion of manual labor in the specially established enterprise that would be a legal entity. The equipment necessary for galvanic coating application is made in RFNC-VNIIEF;
- a large-lot production on the basis of automatic galvanic lines within a detached legal entity. The equipment necessary for the automatic manufacturing is bought at the most acceptable free market prices;
- business-lot automatic manufacture of plates where the mechanism of leasing is used to purchase necessary equipment."

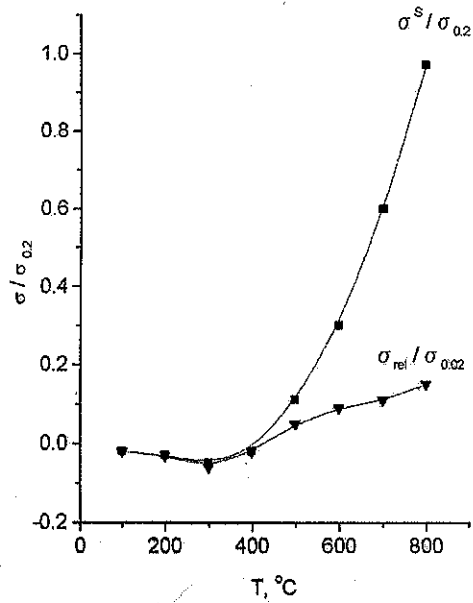


Fig.4.2.5c

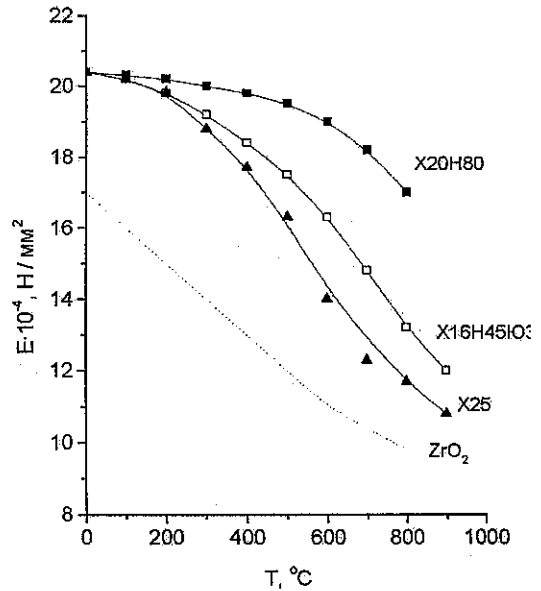


Fig. 4.2.6

We have calculated the internal thermoelastic stresses at heating the junctions metal/ceramics in the temperature range of 20 – 900°C taking account of relaxation processes for the 32Ni20Co6Cr alloy.

Mechanical characteristics of the 32Ni20Co6Cr alloy are represented in Table 4.2.2.

Table 4.2.2.

E (20 °C), GPa	E (700 °C), GPa	$\sigma_{0.2}$ (20 °C), MPa	$\sigma_{0.2}$ (700 °C), MPa
200-220	150-175	170-190	110-130

With the account of characteristics of the 32Ni20Co6Cr alloy, the relaxation dependence for the junction with ceramics YSZ-8% is represented in Fig. 4.2.7.

Relaxation dependence: the function of internal stresses level (σ^s) on temperature through the time t_i , c. Alloy 32Ni20Co6Cr ($T_k^* = 580 - 600$ °C).

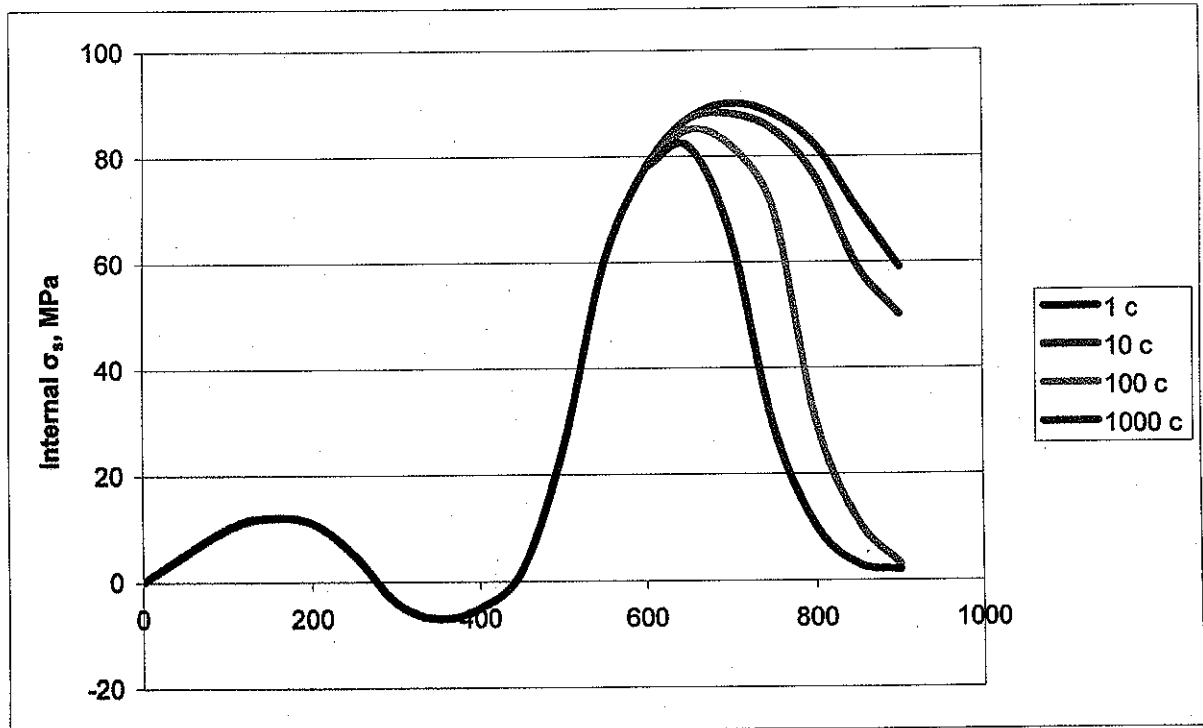


Fig. 4.2.7

The level of internal stresses σ^s , achieving the yield point ($\sigma_{0.2}$) occurs at temperatures close to or exceeding 600°C. At these temperatures, relaxation processes run at a high rate due to the mechanism of sliding and shift of dislocations.

4.2.6. Research on corrosion stability of alloys of Ni-Co-Cr-Fe system and ferrite steel.

We have analyzed Cr diffusion from commercial ferrite steel and Ni-Co-Cr-Fe alloys with different Cr content into a cathode material (MLS ($\text{La}_{0.6}\text{Sr}_{0.4}\text{MnO}_4$ (MLS))). Investigations were carried out after air-curing of the specimens in contact assemblies during 800 hours at temperature of 900 °C. Diffusion-time relation is represented in Fig. 4.2.8.

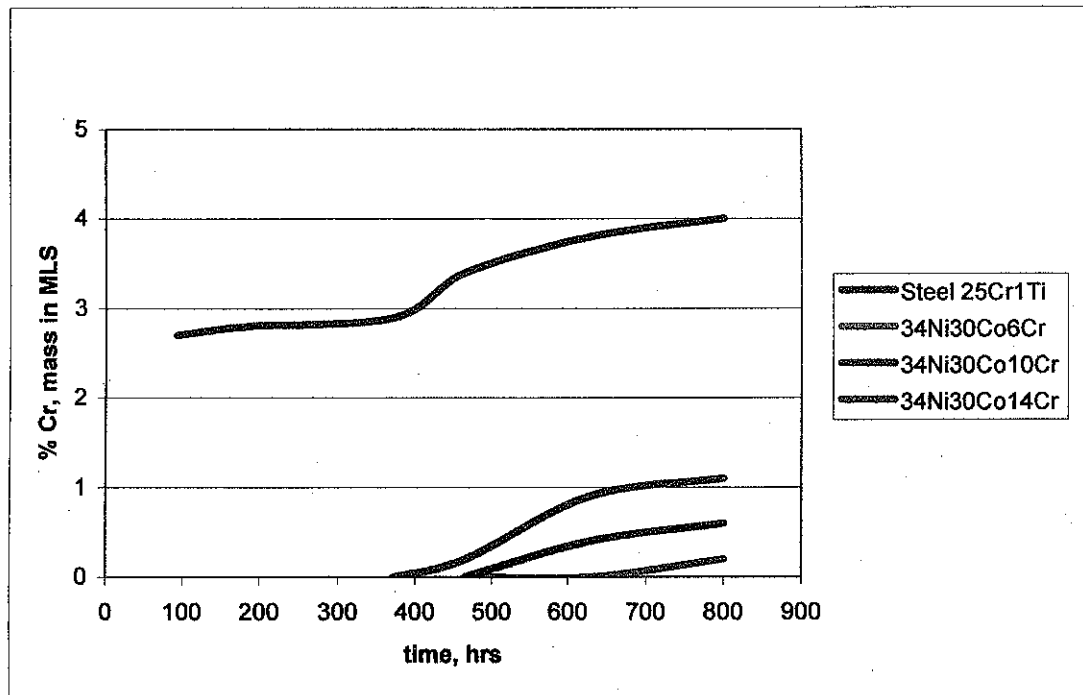


Fig 4.2.8

Cr diffusion from Fe-Ni-Co-Cr alloys may be observed at contact time of 800 hours and more, at that the diffusion is not observed with the alloys containing 6% Cr. The estimation of Cr diffusion on the ruptures of MLS specimens demonstrates that deeper than 20 μm from the surface Cr is Not detected at contacts with the steel 25Cr1Ti.

4.2.7. Research on corrosion stability of alloys of Ni-Co-Cr-Fe system and of 15X25T ferrite steel in the anode and cathode conditions

We have studied the corrosion resistance of metal materials used as SOFC commutating materials in anode (5 % vol. H_2 + 50 % vol. H_2O + 20 % vol. CO_2 + 25 % vol. N_2) and cathode (5 % vol. H_2O + air) gas media at temperature of 800 °C during up to 500 hours.

4.2.7.1 Research methods on corrosion stability

Specimens of materials represented 6 mm metal cylinders 10 mm long.

Before thermal treatment, the specimens were weighed using analytical scales with the error of $\pm 0,2\text{mg}$. To heat the specimens, electric furnaces were used that provided the heating temperature up to (1000 ± 5) C. The specimens were placed in the sealed quartz ampules, 2 specimens in each ampule. Two ampules were prepared for both anode and cathode media, so that in the course of experiment one could withdraw half of the specimens for intermediate checkout. In such a way, 4 ampules (8 specimens) were prepared for each type of material.

The specimens of material were placed in a quartz ampule being open from one end and representing a tube with the olive for a vacuum hose. The wide end of the ampule was soldered. A vacuum hose was pulled on the olive and vacuumed. Piercing the hose with a medical syringe, they introduced the specified quantity of gaseous components, while the specified quantity of water was injected using a microsyringe. The total gas amount in 100 cm^3 made 0,0017 moles, which corre-

sponds to the gas volume of 0,0380 liters under normal conditions. At 800 C, the pressure in the ampule was ~ 1.4 atm.

To create the cathode medium, the ampule was vacuumized up to the residual pressure of 300 mm. mercury column, after that they introduced 1,5 µl H₂O. To create the anode medium, the ampule was vacuumized up to the residual pressure of 0,1 mm. mercury column, after that they introduced 2ml (0,00085moles) H₂, 8,1ml (0,0034moles) CO₂, 10,1ml (0,0042moles) N₂, 15 µl (0,0085 moles) H₂O.

The total curing time made 500 hours (90 – 95 hours a week of continuous curing) at 800°C.

4.2.7.2. Tests results for samples at 800°C

Corrosion rate numerical values are represented in Fig. 4.2.9 and 4.2.10

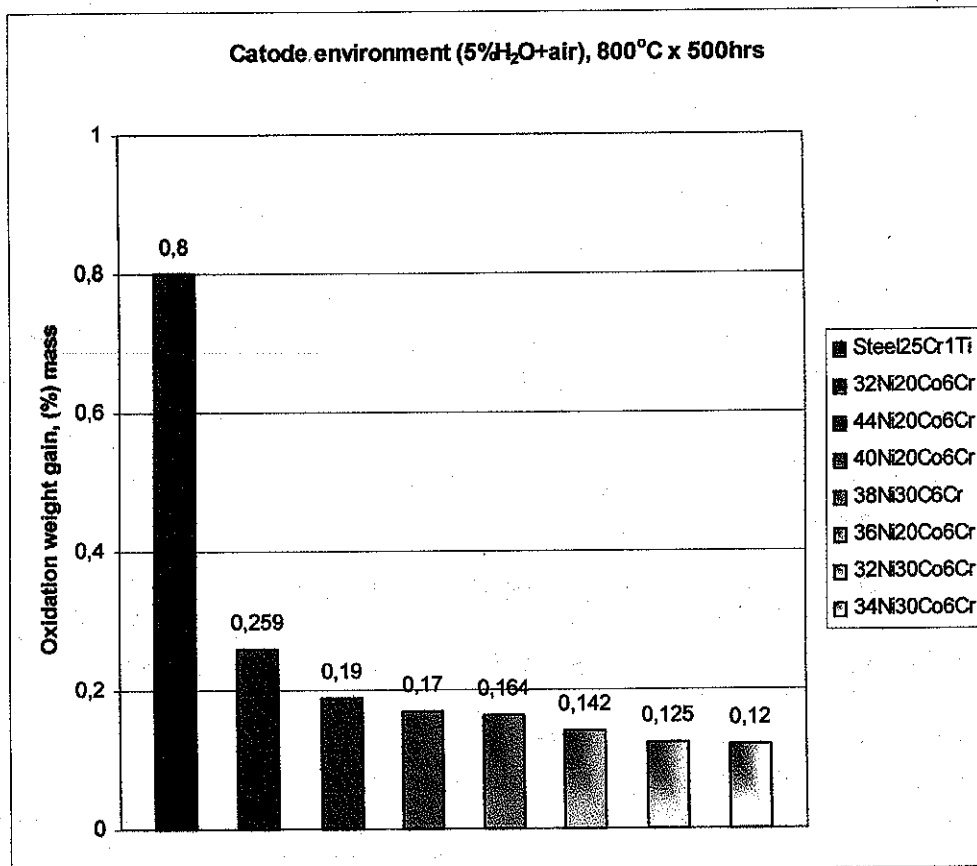


Fig. 4.2.9

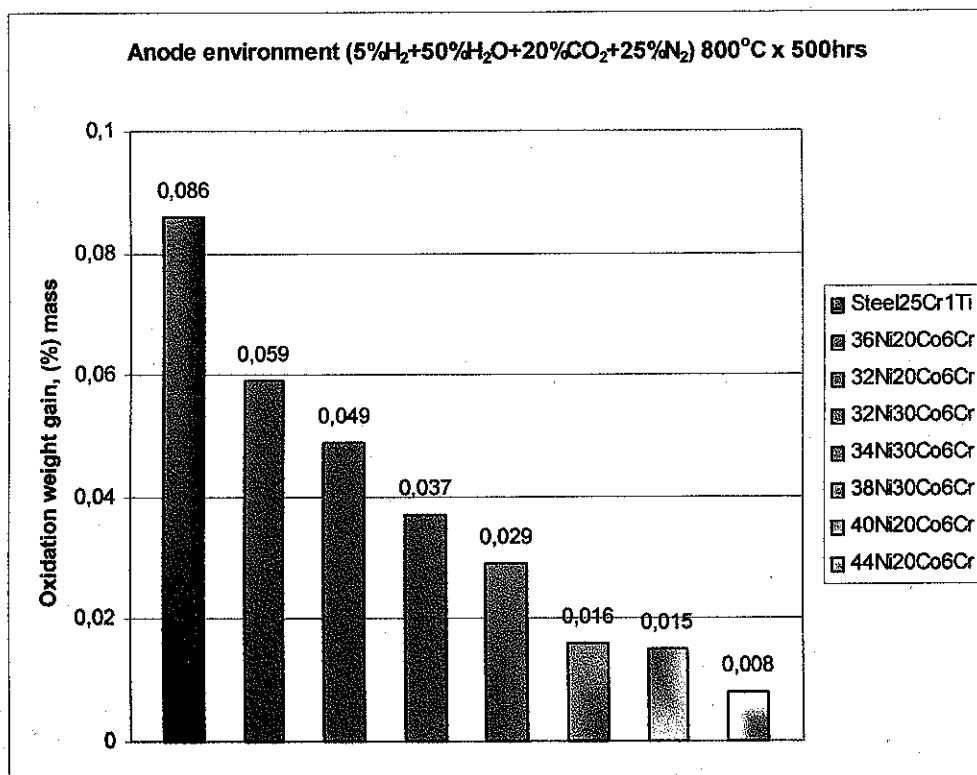


Fig. 4.2.10

The oxidation rate of alloys in cathode medium is several times higher than that in anode one. For example, the oxidation rate of alloy 34Ni-30Co-6Cr in cathode medium is 4 times higher than that in anode one.

As compared with ferrite commercial steel, the oxidation rate of e.g. 34Ni-30Co-6Cr alloy in cathode medium is 6,5 times lower than that of 25Cr-1Ti steel and 3 times lower than that in anode one.

4.2.7.3 Methods and results of micro X-ray spectrum analysis (MXSA) and X-ray phase analysis (XPhA) of the samples

The structure and chemical elemental composition of the specimens' surface were investigated by means of micro-X-ray spectral analysis applying a microprobe JAMP-30 ($U=20$ kV, $I=1 \cdot 10^{-8}$ A) with the X-ray analyzing system AN10000. The X-ray phase analysis was made on an automated X-ray diffractometer Dron-3M ($U=39$ kV, $I=20$ mA).

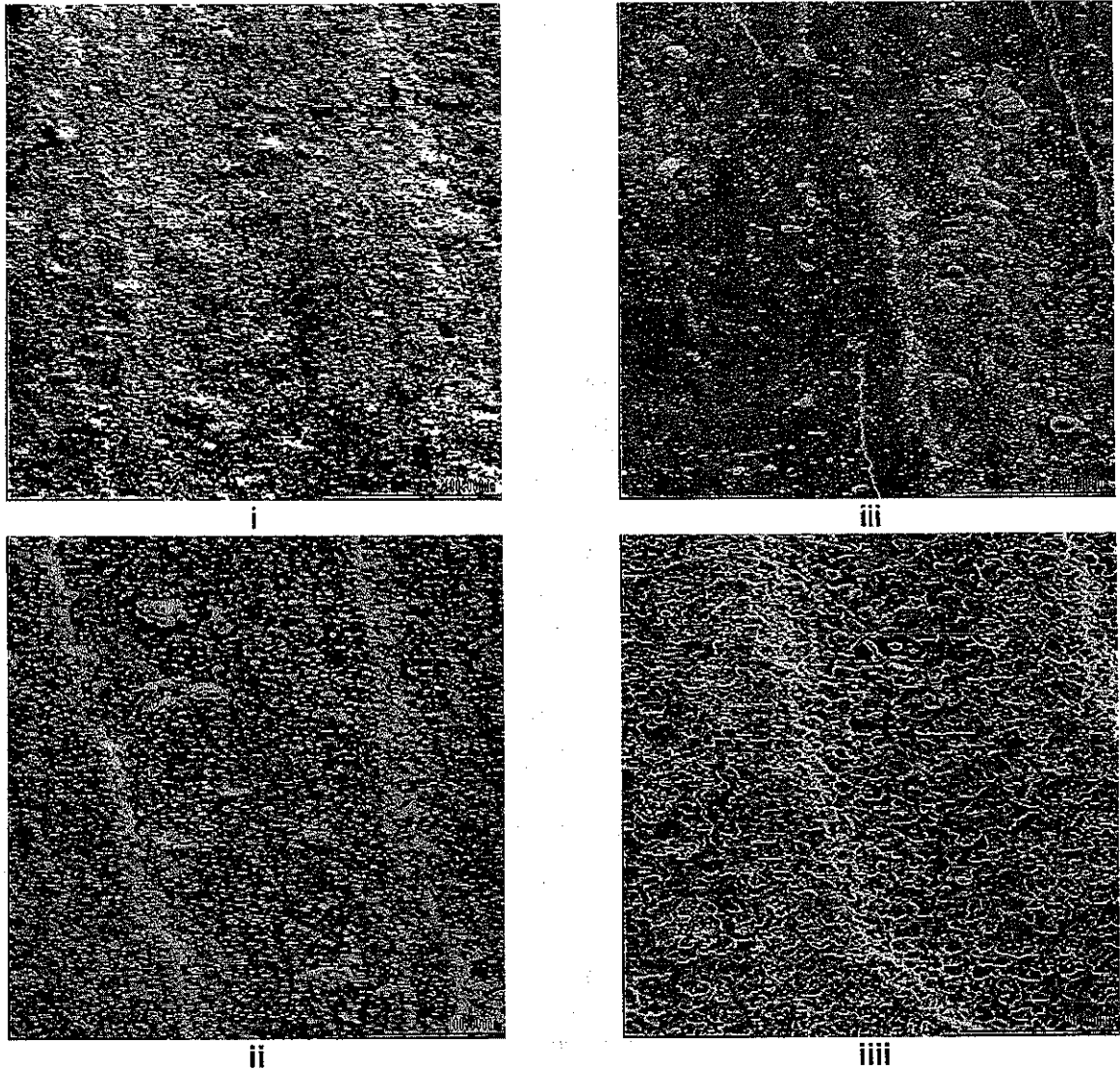
The surface structure of steel 25Cr1Ti (i-ii) и сплава 44Ni20Co6Cr (iii-iiii) after oxidation in anode (5 % vol. H_2 + 50 % vol. H_2O + 20 % vol. CO_2 + 25 % vol. N_2) (i, iii) and cathode (5 % vol. H_2O + air) (ii, iiiii) media at temperature of 800 °C during 500 hours is shown in Fig. 4.2.11.

Commercial steel 25Cr-1Ti.

On the X-ray spectra that reflect the chemical elemental composition of the specimens' surface, the main X-ray lines in both spectra relate just to oxygen and chromium, i.e. these are chiefly Cr oxides that have been formed on the specimens' surface.

Diffractograms from the specimens' surface as well as from the surface cleaned from the oxides are represented by an X-ray line with the interplanar distance $d=0.203$ nm. That corresponds to α -Fe, which is actually the base of ferrite-grade steel, representing a solid Fe-Cr solution based on a

lattice α -Fe (body-centered cubic lattice). The other lines relate to the compounds Cr_2O_3 and $\text{Cr}_{1.3}\text{Fe}_{0.7}\text{O}_3$, since in Fe-Cr steels at temperature of 700-1000°C, a simultaneous transition of two metals into the oxidized state occurs. In this case first of all the embryos of Cr_2O_3 crystals arise on



the surface, in the course of time they grow up and finally form a solid but uneven surface film. On the diffractogram of the cleaned specimen's surface, there exists a line pertinent just to α -Fe.

Thus in anode and cathode media, the Cr-based oxide films are formed on the steel specimens' surface. The ratio of α -Fe lines' intensities in the diffractograms of the specimens justifies the conclusion of micro- X-ray spectral analysis that the oxide coating on the specimen after testing in cathode conditions has a larger thickness.

Fig. 4.2.11.

I. E. Vichkanski. "Task 3. Development of new materials for fuel cells. New anode materials for MCFC".

"Possible implementation of cermet compositions on the basis of LiAlO_2 , TiN , B_4C etc. ceramics with Ni or Ni-Mo binders as an anode is studied; the composition and the technical parameters of their production are studied as they influence the operation properties.

We plan to do the research on cermet materials on the basis of conductive ceramics of BaCeO_3 etc. with metallic binders of Ni, Ni-Cr etc. in order to upgrade the strength and electrical conductivity of the anode."

S.V. Mishanin. "Task 4. Development of a new alloy or alloys with a ceramic coating that would have a better corrosion stability in operation within solid oxide fuel cells".

"Analytical study of the available information was carried out on the following:

1. Physical basis for the invar effect, classification of the alloys according to the temperature coefficient of thermal expansion.
 - 1.1. The effect of alloying elements on the temperature coefficient of linear expansion (TCLE).
 - 1.2. Classification of invar alloys by the TCLE.
2. Invar alloys on the Fe-Ni basis.
 - 2.1 Structure
 - 2.2 Temperature coefficient of linear expansion (TCLE).
3. Alloys with TCLE close to that of the $\text{ZrO}_2+\text{Y}_2\text{O}_3$ ceramics. Their structure, properties and basic technological characteristics.
 - 3.1 Fe-Ni and Fe-Ni-Co-based alloys;
 - 3.2 Fe-Cr-based alloys;
 - 3.3 Fe-Ni-Co-Cr-based alloys;
 - 3.4 Titanium and zirconium alloys;
 - 3.5 Chromium-based alloys;
 - 3.6 Niobium-based alloys;
 - 3.7 Fe-V-based alloys;
 - 3.8 Fe-W-based alloys.

V.P. Vshivkov. "Development of ferrite stainless steel (brand 400) with an oxide coating».

"Research on two materials is performed within the task of the oxide coating application. They seem suitable to be implemented as a ceramic coating of SOFC components as for their physical, technical, technological, and cost parameters. They are strontium lanthanum manganate ($\text{La}_{0.6}\text{Sr}_{0.4}\text{MnO}_3$) and nickel oxide (NiO). Thermal expansion coefficient of NiO is 12.6×10^{-6} ($100 - 800^\circ\text{C}$), its specific electric conductivity is $6.7 \text{ Ohm}\cdot\text{m}$ at 863°K and $1.4 \text{ Ohm}\cdot\text{m}$ at 1273°K . Nickel oxide was doped with lithium to increase the conductivity of the coating. $\text{Li}_x\text{Ni}_y\text{O}$ can be used as the coating material, where $x=0.1-0.2$, $y=0.8-0.9$. Optimization of parameters of the coating spraying mode using nickel oxide is underway."

7.2. Participation and presentations at the 2nd All-Russia Workshop: Fuel Cells and Power Plants on their Basis. («ТЭЭУ-2003») (Novosibirsk, June 29– July 2, 2003). There were the following poster presentations:

DEVELOPMENT OF A TECHNIQUE TO MEASURE RESISTANCES OF CONTACT SEPARATORS WITH CARBONATE FUEL CELL ELECTRODES.

Mishanin S.V.¹, Kozhukhar N.G.¹, Shein I.G.¹, Aaleksandrov K.A.², Batalov N.N.², Kudryakov V.Ya.², Perin S.M.²

¹-RFNC-VNIIEF, Sarov, Russia, e-mail: <mish@aven.vniief.ru>, phone./fax: 83130-43977

²-Institute of High-Temperature Electro-Chemistry UrO RAS, Ekaterinburg, Russia,
e-mail: <Batalov@ihim.uran.ru>

Presently, the main efforts of the developers of molten carbonate electrolyte fuel cells (MCFC) are aimed at the rise of their lifetime. One of the important factor of their working life is a metal separator being a structural component operating not just as a gas-proofing and gas-commutating element, but as a conductor of line current passing through a FC stack. Under MCFC severe operating conditions (650⁰C, carbonate melt), the separator is subjected to corrosion, which results in both the loss of main material and loss of contact between the basic FC units in a FC stack and, accordingly, in the degradation of its operation characteristics. In this connection, we are searching for the optimal materials with respect to their corrosion resistance and the cost, which would have not tended to the formation of the layers with substantial electric resistance on their surface under long-term conditions of MCFC operation. Determination of contact resistances between the adjoint surfaces of FC modules is a problem that is topical enough.

Measurements by the techniques, which are described in literature, have revealed a number of drawbacks of the proposed structures: complexity of adjusting the electrodes from the both sides to a studied plate and some vagueness of the value of real contact resistance between the conductors. The technique to determine contact resistances between the surfaces of separators - current collectors and working porous gas-diffusion electrodes - has an essential drawback: the measured resistance, besides the studied contact resistance includes a portion of current leads' resistance. In their works, the researchers from ANL (USA) neglected that, using the golden contact plates and current leads, regarding them as the ones that are electroconductive enough. Nevertheless, it should be not quite correct to call the resistance values measured in such cells as the contact resistances between the studied separator material and the electrode. We have proposed a technique to measure and compute contact resistances (resistances between the adjoining materials), which permits to estimate the real contact resistance between them.

The resistance $r_{1,2}$ being measured is the sum of resistances of the wires of the measuring instrument and current leads r_1 and r_2 , of two transition layer resistances K_1 and K_2 (the contact ones between the studied plates and the electrode) and the resistance of the electrode R_{electr} itself, which represents a porous, filled with Li-Ka carbonate eutectics plate from Ni oxide (Li-doped) for oxidative medium or metallic nickel for reductive medium under MCFC operating conditions. I.e. $r_{1,2} = r_1 + K_1 + R_{\text{electr}} + K_2 + r_2 = r_1 + r_2 + R_{1,2}$. The structure of a single-element cell is such that it seems impossible to separately measure contact resistances K_1 and K_2 , (in case the plates are similar in composition and shape of metal material they will be the same). In the first approximation, R_{electr} may be neglected, though it may be estimated by a separate measurement with golden contacts and current leads or computed by specific conductivity of the Li-doped Ni oxide or other electrode material, by the thickness and porosity of a plate. Thus, when determining contact resistances, a task arises to single out the resistances of the measuring wires and current leads from the value being measured. Application of the proposed multi-layer cell, where three single cells are series-connected permits to exclude in turn separate current leads and also to include in the circuit the contact resistances of not just two, but of four and six ones. By analogy with a single cell, the actually measured resistances between the electrodes may be divided into constituents (here $R_{n,m} = K_n + K_m + R_{\text{electr}}$):

$$\begin{aligned} r_{1,2} &= r_1 + r_2 + R_{1,2} & r_{2,3} &= r_2 + r_3 + R_{2,3} & r_{3,4} &= r_3 + r_4 + R_{3,4} \\ r_{1,4} &= r_1 + r_4 + R_{1,2} + R_{2,3} + R_{3,4} & r_{1,3} &= r_1 + r_3 + R_{1,2} + R_{2,3} & r_{2,4} &= r_2 + r_4 + R_{2,3} + R_{3,4} \end{aligned} \quad (1)$$

Deducting the values of the measured resistances between different pairs of electrodes one may separate their constituents and directly determine the resistances, both the contact ones and those of the current leads. These constituents are simply excluded from the circuits when measuring different pairs of electrodes. The computations may be made, for example, by such a scheme:

$$r_{1,4} - r_{3,4} - r_{1,2} + r_{2,3} = r_1 - r_3 + R_{1,2} + R_{2,3} - r_1 + r_3 - R_{1,2} + R_{2,3} = 2R_{2,3}$$

$$2r_{2,3} - r_{1,3} + r_{1,2} + r_{2,4} - r_{3,4} - 2R_{2,3} = 4r_2; \quad r_{2,3} - r_3 - R_{2,3} = r_3 \quad (2)$$

The test results have demonstrated the likeness of the values of contact resistances of steel 20X23H18 specimens in cathode and anode atmospheres.

CORROSION OF SOME ALLOYS AND STEELS IN THE MELTS OF Li AND Ka CARBONATES

Mishanin S.V.¹, Kozhukhar N.G.¹, Shein I.G.¹, Aaleksandrov K.A.², Batalov N.N.², Kudryakov V.Ya.², Perin S.M.²

¹-RFNC-VNIIEF, Sarov, Russia, e-mail: <mish@aven.vniief.ru>, phone./fax: 83130-43977

²-Institute of High-Temperature Electro-Chemistry UrO RAS, Ekaterinburg, Russia, e-mail: v.kudryakov@ihte.uran.ru

Molten carbonates of alkali metals are of practical interest because of their application as an electrolyte for high-temperature fuel cells.

The goal of the given work is to study the corrosion behavior of steels and alloys of 17 grades in the melt of Li and Ka carbonates (68/32 mol.%) at temperature of 650 °C in the atmosphere of air – 20% carbon dioxide mixture.

To prepare salt mixtures, the “хч” - qualified chemical agents with were used. The experiments were carried out in leak-proof containers from stainless steel 12X18H10T; the melt was placed into the alundum melting pots.

Cylinders with 8mm diameter and the height of 10mm (surface area is about 3,5 cm²) were used as the specimens. Before testing, they were polished, degreased and weighed on analytical scales БПЖ-200g. 7-8 specimens located in separate alundum melting pot were studied in parallel.

By gravimetric data, the following sequence (in decreasing order of corrosion resistance) was obtained: ХН45Ю, ХН60Ю, 36ХНЮФ, ХН35БТЮ, ХН32Т, 06ХН28МДТ, 10Х23Н18, 20Х23Н18, 15Х25Т, 20Х25Н20С2, 12Х18Н10Т, ХН78Т, ХН55МБЮ, ХН73МБТЮ, ХН75МБТЮ, ХН77ТЮР, ХН60БТ.

The average corrosion rate in this sequence increases from 0,028 g/(m²h) up to 14,3 g/(m²h).

It was demonstrated that the first 5 alloys have the corrosion resistance exceeding that of the steels 10Х23Н18, 20Х23Н18 (domestic analogs of steel SS310) and that they may be recommended for the application in molten-carbonate fuel cells. To analyze corrosion products, metallography, radiography, X-ray electron spectroscopy and chemical analysis were used as well.

7.3. Participation at the VIII International Conference «Hydrogen Materials Science & Chemistry of Carbon Nanomaterials» Sudak, Crimea, UKRAINE, September 14-20, 2003.

HIGH-TEMPERATURE INVAR ALLOYS DESTINED TO MATCH WITH CERAMICS OF HIGH-TEMPERATURE FUEL CELLS.

Yu.L.Rodionov, I.A.Korms, S.V.Mishanin¹ and B.M.Mogutnov.

Central Science and Research Institute of Ferrous Metallurgy after I.P.Bardin, 9/23, 2nd Baumanskaya str., Moscow 105005, Russia

1) Russian Federal Nuclear Center – All-Russian Scientific-Research Institute of Experimental Physics, Sarov, Nizhni Novgorod region, 607190, Russia.

The work is devoted to the development of alloys for coordination in heat expansion with Zirconium ceramics $ZrO_2+(10-12)\% Y_2O_3$ of the fuel cells operating at the temperature of 800-900° C. Metal materials applied for the fabrication of the components of such elements should have the following complex of properties.

1. Heat resistance up to 900 °C combined with high corrosion resistance.
2. Invariability – the value of heat expansion in the range of temperatures 100 - 850 °C should be in the interval $(6,9-10)\times 10^{-6} K^{-1}$.
3. Stability of properties at thermocycling in the interval between 200-850 °C.
4. Increased yield point ($\sigma_{0,2}$)
5. Ability to relax strains in the range of thermocycling.
6. Decreased coefficient of elasticity.

Literature data on the materials of the observed type have been analyzed, that enabled to single out the following groups of alloys:

1. Invar Fe-(38-47%)Ni and Fe-Ni-Co alloys;
2. Heat resistant alloys of Fe-Ni-Cr and Ni-Cr system with the composition Fe-(30-50%)Ni-(12-30%)Cr and Ni-20% Cr;
3. Double alloys Fe-(20-40%)Cr, Fe-(10-35%)V, Fe-(10-20%)W, Fe-(15-30%)Mo;
4. Titanium alloys Ti-V, Ti-Cr, Ti-Mo, Ti-Nb;
5. Alloys of Fe-Ni-Co-Cr system with the composition Fe-(30-45%)Ni-(10-40%)Co-(6-25%)Cr.

The majority of the above alloys did not meet all the listed requirements. In particular, up to the last moment the heat – resistant materials with the heat expansion close to that of Zr ceramics were not available.

To create multifunctional by a large number of parameters alloys based on the Fe-Ni system including heat – resistant invar alloys with the high level of mechanical properties, we have developed a new scientific approach. Its essence is in that by means of creating in the alloy the adjustable combination of nano (submicro) – regions with the specified atomic-crystal, magnet and electron configurations, one may provide the required thermophysical, mechanical and heat-resistant properties in the predetermined combinations. Formation of the required local atomic-crystal and magnet structure is effected by the selection of composition, controlled phase transformations, dozed deformation and heating. Based on the results of thermodynamic analysis and on the determined regularities between the fine atomic-crystal and magnet structures and phase transformations, we have determined the challenging range of concentrations of the Fe-Ni-Co-Cr system, which may realize the alloys' requirements for the coupling with the Zr ceramics of the FC. The Ni and Co content is close to that of the heat-resistant alloys, while the Cr concentration amounts to 5-15%.

The ingots with the mass of ~1 kg were melted in an induction-vacuum furnace and forged in the air atmosphere at 1100-900 °C. The samples designed for dilatometric measurements had the form of a cylinder with the dimensions $\varnothing 4 \times 25$ mm. Heat expansion measurements were conducted applying a quartz dilatometer Linsais (Germany) in the temperature range of 20-100- °C.

It was determined that the lengthening $\Delta l/l$ of the samples of all the examined alloys increases as the temperature grows, where the character of the temperature dependence $\Delta l/l$ is substantially determined by the composition. For the alloys with a comparatively low Curie temperature ($T_C < 100$ °C) of the composition Fe-Ni(<30%)-Cr(>10-%)) and high enough Curie temperature ($T_C > 600$ °C) of the composition Fe-Ni(>30%)-Co(>34%)-Cr(<10-%)) the $\Delta l/l$ value changes practically linearly with the temperature. If T_C is in the range of 100-500 °C, then two regions with different tilts are revealed at the curves $\Delta l/l = f(T)$ and the inflexion (bend) temperature T_{nep} is distinctly revealed. At temperatures below T_{nep} one may observe lower values of the

linear expansion temperature coefficient, while at $T > T_{nep}$, these values are higher. According to the available data T_{nep} is determined by the peculiarities of the magnet structure in the region of the Curie point. Generally, T_{nep} is approximately 50-100 °C lower than T_C . Temperature T_{nep} increases as the Ni and Co content rises and decreases with the increase of Cr content.

For the studied Fe-Ni-Co-Cr and Fe-Cr alloys, the least difference in linear expansion temperature coefficient with the ceramics $ZrO_2+12\%Y_2O_3$ is observed for the H32K20X6, H40K20X10, H2K62X10 and X20 alloys. They have been investigated more thoroughly. Besides measuring linear expansion temperature coefficient, the calculations have been made of:

- the difference between metal and ceramics linear expansion temperature coefficient (LETC), $\Delta LETC$;
- internal strains in the juncture metal/ceramics, σ^s , depending on the temperature;
- the relation between the internal strains in the juncture and the metal yield point, $\sigma^s/\sigma_{0.2}$.

Moreover, a rough estimation of the relaxed strains in the juncture metal/ceramics was made.

The common characteristics of the temperature functions of the promising materials under development are as follows. At comparatively low temperatures, the $\Delta LETC$ temperature progress is insignificant. The essential changes begin at more than 400-500 °C and at 800 °C, $\Delta LETC$ achieves the value of $(2-2.5) \times 10^{-6} K^{-1}$, which is independent of the structure of the composition.

For the known heat-resistant X20H80 and X16H45IO3 alloys, $\Delta LETC$ changes with the temperature in a similar way, however the $\Delta LETC$ value 3-10 times exceeds the corresponding value for the alloys investigated. Especially tangible is the difference between the two studied types of materials below 500 °C, i.e. in the region of temperatures where the strain relaxation in the juncture metal/ceramics is difficult. In particular, for X20H80, $\Delta LETC$ equals to $\sim 5.5 \times 10^{-6} K^{-1}$, and for X16H45IO3 - $\sim 7 \times 10^{-6} K^{-1}$. That essentially differs from the values $(0.2-1.5) \times 10^{-6} K^{-1}$, being characteristic of the alloys under development. The results of investigation into the strains in the juncture metal/ceramics permit to make the following conclusions.

- In the region of temperatures where the relaxation processes are hampered, the strain level in the junctures of the studied alloys with Zr ceramics does not exceed 25 H/mm², that comprises $\sim 10\%$ of the yield point. For the known heat-resistant alloys, the yield point in this range of temperatures $\sigma^s \approx 200 N/mm^2$, that is close to the yield point and even exceeds it.
- In the range of temperatures where the relaxation processes are facilitated (500-800 °C), σ^s of the materials under development does not exceed 110 N/mm², that is close to the yield point, $\sigma^s/\sigma_{0.2} \leq 1$. For the known heat-resistant alloys, in this region of temperatures σ^s achieves 240-400 N/mm², which 2-3 times exceeds the yield point.

The residual strains in the material being a result of relaxation at heating were estimated. It was supposed that the relaxation occurs by the exponential law

$$\sigma_{rel.} = \sigma_0 \exp(-bT)^k,$$

where b and k are the constants. The time and temperature dependence of $\sigma_{rel.}/\sigma_0$ relation is close to that for the alloys H42X5T1 and ЭИ142. The results of corresponding computations for the alloys under development demonstrate that the $\sigma_{rel.}$ value is close to the strain value in the juncture. The relaxation effects are revealed under the temperatures above 400-500 °C. With the temperature increase the level of the residual strains after relaxation decreases and at 700-800 °C this decrease achieves a 5-7-fold level. For the commercial alloys of the X20H80 type, the level of the residual strains 2-3 times exceeds the one for the materials under development for the whole range of operating temperatures.

7.4. A meeting to discuss the results of the Partner's ISTC Project #2281p took place in the Argonne National Laboratory (USA, Chicago, November 17 – 23, 2003).

The following people took part in it: from ANL they were Michael Krumpelt, a coordinator of the Partner, David Ehst, Tomas Kaun and Terry Cruse.

From FCE they were: Chao-Yi-Yuh – a collaborator on the Project, and from the Russian party they were Project participants: A.M. Gorelov, V.V. Zoria, E.P. Piskunov, S.V. Goncharova.

The meeting had several goals:

- 1) To discuss with US collaborators and industrial partners basic results of the work performed in the 2-5 quarters of ISTC Partner Project №2281p «Development of New Materials for Fuel Cells».
- 2) To discuss and coordinate trends and methods of further tests and research with collaborators from the Argonne National Laboratory and specialists from Fuel Cell Energy (Danbury, Connecticut, USA).
- 3) To clarify and coordinate technical parameters and geometry of samples and the number samples and quantity of the deliverables.

Main Results of the Discussions.

The parties came to the conclusion that the Project tasks were being solved completely and on terms.

Summarizing the results of the discussion, the employees of ANL and FCE proposed to perform the additional investigations under the ISTC Project. These investigations concern a possibility for the development of porous metal-ceramic anode for MCFC and new materials for SOFC without any change of the financing amount at the expense of the fund redistribution for the Tasks 1,2 (manufacture and nickel-plating of large plates with dimensions of 712 × 1296 mm and their delivery to the USA are not required).

7.5. Participation in the «First International Conference on Fuel Cell Development and Deployment» (07 March 2004 - 10 March 2004, Storrs, CT, USA.). Sponsors CT Global Fuel Cell Center, Univ. of Connecticut.

TECHNOLOGY DEVELOPMENT AND COST EVALUATION OF MANUFACTURING OF ONE-SIDE COATED STAINLESS STEEL PLATES FOR MCFC

I Goncharov¹⁾, A. Gorelov¹⁾, V. Malinov¹⁾, V. Zorya²⁾

¹⁾ Russian Federal Nuclear Center – VNIIEF, Bld. 37, Mira Av., Sarov, N. Novgorod Region, Russia, 607189; Tel/Fax: (7)-(83130)-45798; E-mail: gorelov@astra.vniief.ru

²⁾ Sarov State Institute of Physics and Technology, Bld. 6, Dukhova Str., Sarov, N. Novgorod Region, Russia, 607189; Tel/Fax: (7)-(831-30)-34809; E-mail: zv@sarfti.sarov.ru

A task of upgrading corrosion stability of 20X23H18 stainless steel (of S 310 type) for MCFC bipolar plates through the application of one-side nickel coatings 50-80 microns thick is being considered. The galvanic nickel plating is simple in implementation and cost-effective. Tests of protective properties of the coatings on 20X23H18 steel plates were performed at 650°C in H₂, CO₂ (20%, 80%) environment humidified at 65°C in the usual presence of carbonate melts.

Tests of the samples revealed that the galvanic nickel coating performs its protective function under MCFC conditions during 1500 hours; microstructure of the substrate of 20X23H18 steel kept its small austenite grains without any traces of inter-crystalline corrosion. However, the inter-crystalline corrosion with the electrolyte filled pore formation starts in the coating; Fe diffuses through the pores.

A combined coating was worked out to improve the stability. After 1500-hour tests the coating remained pore-free; there were no traces of the above mentioned characteristics. The combined coating can appear to be a promising technology because it fits the general way of galvanic deposition used.

There was established a galvanic line to polish the technological process of manufacturing and the integrated production of the plates 800 x 1400 mm in size. A feasibility analysis of the cost to manufacture the plates under conditions of a large-scale production was performed. It is projected that the plate cost under full-scale production can be decreased to the level of US\$45 per piece.

7.6. Participation in «Lucerne FUEL CELL FORUM 2004» (Lucerne, Switzerland, June 27 – July 03 2004) with poster presentations.

HIGH-TEMPERATURE INVAR ALLOYS DESTINED TO MATCH WITH CERAMICS F HIGH-TEMPERATURE FUEL CELLS.

Sergey Mishanin¹⁾, Aleksandr Gorelov¹⁾ Irina Korms²⁾, Boris Mogutnov²⁾ and Yuriy Rodionov²⁾.

¹⁾ Russian Federal Nuclear Center-VNIIEF, Bld 37, Mira Av., Sarov, Nizhniy Novgorod Region, Russia, 607189; Tel/Fax: -(7)-(831-30)-43977

²⁾ Bardin Central Science and Research Institute of Ferrous Metallurgy, Moscow, Russia

The work is devoted to the development of alloys for coordination in heat expansion with Zirconium ceramics $ZrO_2+(8-12)\%Y_2O_3$ of the fuel cells operating at the temperature of 800-900° C. Metal materials applied for the fabrication of the components of such elements should have the well-known complex of properties.

The majority of the existing alloys did not meet all requirements of the high temperature fuel cells. In particular, up to the last moment the heat – resistant materials with the heat expansion close to that of Zr ceramics were not available.

To create multifunctional by a large number of parameters alloys based on the Fe-Ni system including heat – resistant invar alloys with the high level of mechanical properties, we have developed a new scientific approach. Its essence is in that by means of creating in the alloy the adjustable combination of nano (submicro) – regions with the specified atomic-crystal, magnet and electron configurations, one may provide the required thermo physical, mechanical and heat-resistant properties in the predetermined combinations. Formation of the required local atomic-crystal and magnet structure is effected by the selection of composition, controlled phase transformations, dozed deformation and heating. Based on the results of thermodynamic analysis and on the determined regularities between the fine atomic-crystal and magnet structures and phase transformations, we have determined the challenging range of concentrations of the Fe-Ni-Co-Cr system, which may realize the alloys' requirements for the coupling with the Zr ceramics of the FC. The Ni and Co content is close to that of the heat-resistant alloys, while the Cr concentration amounts to 5-15%.

The results on the various composite materials and alloys behavior under the high-temperature fuel cell conditions are obtained.

DEVELOPMENT OF THE TI – V AND TI – NB ALLOYS FOR CURRENT COLLECTOR OF PLANAR SOFC.

Sergey Mishanin¹⁾, Vladimir Malinov¹⁾, Irina Korms²⁾, Boris Mogutnov²⁾ and Yuriy Rodionov²⁾.

¹⁾ Russian Federal Nuclear Center-VNIIEF, Bld 37, Mira Av., Sarov, Nizhniy Novgorod Region, Russia, 607189; Tel/Fax: -(7)-(831-30)-43977

²⁾ Bardin Central Science and Research Institute of Ferrous Metallurgy, Moscow, Russia

As a result of preliminary theoretical analysis the promising alloy compositions were determined to obtain the required temperature linear expansion coefficient (TEC). These are the Ti-(36-44 mass.%) Nb and Ti-(22-32, mass.%)V alloys.

Based on the technology elaborated, the Ti- and Nb/ V -based ingots were smelted with the following compositions (% mass): Ti-V (22, 25, 28, 32%V); Ti-Nb (36,38,40,44 %Nb) by means of remelting with the intermediate processing of the ingot into scobs.

The alloys' characteristics were studied in both hardened and deformed (by rolling) states using the X-ray and electron microscopy, dilatometry. The temperature interval of studies was between 20 and 800 °C.

Besides the abnormal behavior of the parameter of the lattice of the α'' -phase, the reversible change of the phase composition ($\alpha'' \leftrightarrow \beta$) was detected at thermocycling, which in its features is similar to thermoelastic martensite transformation.

Quantitative analysis of the depositions into thermal expansion of the reversible change of the orthorhombic martensite ($\alpha'' \leftrightarrow \beta$) quantity and of the abnormal temperature behavior of the parameter of the α'' -phase was made. It was shown that the abnormal behavior of the α'' -parameter is a determining factor in the decreased TEC value.

In this connection, combining the α'' - and β -phases content, one may realize the values of thermal expansion in the interval $(+5 \div +11) \times 10^{-6} \text{ K}^{-1}$ in the alloys titan-niobium and titan-vanadium. The results on the various composite materials and alloys behavior under the high-temperature fuel cell conditions are obtained.

8. INFORMATION ON PATENTS AND RIGHTS

8.1. In the process of work on Task 2, a new alloy was developed. The materials were prepared and delivered to the Industrial Property Federal Inspection (registration №2004119088, dated 24.07.04) for carrying out the inspection in essence for the patent «Corrosion-Resistant Fe-Ni-based Alloy» (International Classification of Inventions (MKI)⁷ C22C 19/03).

Subject of invention.

Corrosion-resistant Fe-Ni-based alloy containing chromium, nickel, aluminum, yttrium and iron differing in that it additionally contains carbon, titanium, silicon and manganese with the following ratio of components (mass.%):

carbon	not exceeding 0,2
silicon	0,1 – 0,8
manganese	0,1 – 0,8
chromium	28,0-32,0
nickel	43,0-47,0
aluminium	0,4-1,0
titanium	0,1-0,5
yttrium	0,03 – 0,05
iron	remainder,

At that, the sums of Al and Si and of Al and Ti must be equal to:

$$\begin{aligned} & \bullet \quad [\%Al] + [\%Si] = 0,5 \div 1,8 \% \\ & \quad [\%Al] + [\%Ti] \leq 1,5\%. \end{aligned}$$

8.2. When doing the works on Task 4, a patentable decision was obtained. The materials were prepared and delivered to the Industrial Property Federal Inspection (registration №2004119087, dated 24.07.04) for carrying out the inspection in essence for the patent «High-Temperature Solid Electrolyte Fuel Cell» (International Classification of Inventions (MKI)⁷ H01M8/10; H01M8/12).

Subject of invention.

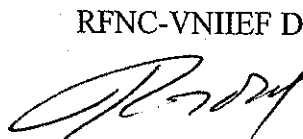
1. High-temperature solid electrolyte fuel cell, in which the metal intercell junctions are made from iron and chromium - containing alloy, differing in that the alloy additionally contains Co and Ni with the following ratio of components (mass.%):

Cr - 5 ÷ 15
Ni - 20 ÷ 35
Co - 30 ÷ 45
Fe - remainder,

where the ratio between Ni and Co total content and Cr content are in the interval of 4 ÷ 13.

2. High-temperature solid electrolyte fuel cell by p.1, differing in that the alloy contains concomitant admixtures, such as carbon and/or nitrogen, and/or silicon, and/or sulphur, and/or phosphorus, and/or manganese, and/or copper, at that their total content not exceeding 1%.

RFNC-VNIIEF Director Deputy

 V. G. Rogachev

Manager of #2281p Project

 A.M. Gorelov

Content of Section 4 of the Work Plan after the First Correction**Scope of Activities.**

Pursuant to the Tasks of the project its implementation is based on fulfillment of the activities at the following stages in accordance with the technical schedule:

TASK 1

Task 1.1. Purchases of indispensable materials and equipment. Designing and manufacturing of technological appliances necessary for the research and manufacturing of plates 0.4 x 712 x 1296 mm in size using 20X23H18 stainless steel. Preparation of the necessary equipment.

Duration - 3 months.

Task 1.2. Application of the nickel coatings onto the surface of 20X23H18 stainless steel (on one side) using **galvanic and explosion cladding techniques**. Thermal treatment of the galvanic coatings at 800°C during one hour. The plates are coated on one side. Nickel foil 100 micron thick is used here. Different options of explosion cladding are studied. Corrosion resistant tests of the nickel coated plates during 100 hours in the anode environment (20% of H₂; 80% of CO₂; humidification at 60 °C) are to be done. The quality of the obtained coatings is checked by different means of optical and electronic microscopy, as well as with the means of spectral radiography.

Duration - 3 months.

Task 1.3. Corrosion tests of nickel-coated samples (coated using the galvanic method and the explosion cladding) in the anode environment of an MCFC at 650°C during 1500 hours. Development and manufacturing of a line of galvanic plating baths (4 units) to ensure application of nickel coating onto the plates 0.4 x 712 x 1296 mm in size.

Duration - 6 months.

Task 1.4. Mounting and launching into operation of a galvanic line (4 baths) to provide coating of plates 0.4 x 712 x 1296 mm in size. Improvement of the welding technology for the plates 712 x 1296 mm in size using tapes 0.4 m wide of the samples of 20X23H18 stainless steel.

Duration - 6 months.

Task 1.5. Adjustment of the galvanic method and of a method of explosion cladding when nickel coating is applied onto stainless steel plates 0.4 x 712 x 1296 mm in size. The plates are nickel coated on one side. Possible implementation of barrier layers of different metals on 20X23H18 steel to prevent the diffusion of the steel components into the nickel coating are studied. The quality of the obtained coatings is checked by different means of optical and electronic microscopy, and also by means of spectral radiography.

Duration - 9 months.

Task 1.6. Manufacturing and sending of two nickel coated plates to FCE for further investigation. A feasibility study to assess the cost of the nickel coated bipolar plate in case of the galvanic method implementation for the plates 0.4 x 712 x 1296 mm in size under conditions of a large scale manufacture.

Duration - 6 months.

TASK 2

Task 2.1. Manufacturing of a group of monolithic samples of alloys that have 30Cr-45Ni-1Al content doped with Y or Ti. Research on them in the melt of lithium and potassium carbonates in the environment of (air+20%CO₂) and (H₂+20%CO₂+H₂O) at 650⁰C during 200 hours.

Gravimetric research of the samples after the tests; research on their phase structure and surface texture, distribution of concentrations of chemical members in surface layers before tests and after them. Choosing the best alloy.

Duration – 3 months.

Task 2.2. Manufacturing of thin sheet cold-rolled samples of the most corrosion resistant alloy to research on conductivity of the oxide films. The samples will be in the form of a tape 0,8x100 mm in size made using the laboratory equipment.

Study of the straining-plastic characteristics.

Development of a technology to produce thin sheet cold-rolled stock in the form of sheets 0.8 x 712 x 1296 mm in size, including the modes of intermediate and final thermal treatment and etching, the number of attempts.

Duration – 9 months.

Task 2.3. Research on conductivity of the oxide films in the melt of lithium and potassium carbonates in the environment of (5%O₂+5%CO₂+20% H₂O+70% N₂) and (20%H₂+80CO₂, humidification at 60⁰C) at 650⁰C during 500 hours using thin sheet samples of 1 sq. Inch made of the best serially produced alloy and of the new alloy. Study of their phase structure and surface texture, distribution of concentrations of chemical members in surface layers before tests and after them.

Duration – 12 months.

Task 2.4. Definition of technological spread of an elemental composition for the basic forming components of a new alloy in case of commercial production

Experimental melts in industrial furnaces. Manufacturing of forgings for roll stock.

Manufacturing of a pilot batch of cold sheet roll stock in the form of sheets 0.8 x 712 x 1296 mm in size, using an intermediate hot roll. Control of accuracy of roll stock and surface quality in accordance with the actual norms and standards in an iron and steel industry of Russia.

Duration – 9 months.

Task 2.5. Supply of 10 sheets of the best alloy 0.8 x 712 x 1296 mm in size to the Partner.

Duration – 6 months.

Task 2.6. A feasibility study to assess the cost of the bipolar plate 0.8 x 712 x 1296 mm in size and 0.55 mm thick made of a new alloy in case it is produced by method of a coiled stock and the volume of annual order makes up ~ 40000 plates.

Duration – 9 months.

TASK 3

Task 3.1. Purchase of the necessary equipment and materials. Designing and manufacturing of equipment, tools and appliances. Preparation of the necessary equipment.

Duration - 3 months.

Task 3.2. Development of cermet compositions based on LiAlO_2 and Ni. Research on the influence of the composition of cermets and of the technological factors on the properties of materials. Study of the microstructure of the samples and their electrical conductivity. Corrosion tests of the cermet samples in the anode environment of an MCFC during 100 hours.

Duration - 6 months.

Task 3.3. Development of cermets on the basis of conducting ceramics (BaCeO_3) with metal binders of Ni, Ni-Mo. Research on the composition of the cermets on the basis of conducting ceramics and technological factors as they influence the properties of materials. Study of the microstructure of the samples and their electrical conductivity. Study of corrosion stability of the samples made of the cermets on the basis of conducting ceramics in the anode environment of an MCFC during 100 hours.

Duration - 9 months.

Task 3.4. Development of composites on the basis of ceramics (LiAlO_2 , TiN, B_4C etc.), reinforced with metal fiber (filaments) (Ni, Ni-Cr etc.). Research on the composition of the reinforced composites and technological factors as they influence the properties of materials. Study of the microstructure of the samples and their electrical conductivity. Study of corrosion stability of the samples made of reinforced composites in the anode environment of an MCFC during 100 hours.

Duration - 3 months.

Task 3.5. Analysis of the microstructure and of the chemical composition of the samples of the worked out materials before and after the corrosion tests.

Duration - 3 months.

Task 3.6. Analysis of corrosion stability of two or three best worked-out materials in the anode and cathode environment of an MCFC during 100 hours, study of the microstructure and chemical composition of the samples before and after the corrosion tests.

Duration - 6 months.

Task 3.7. Test of the best material in an MCFC assembly.

Duration - 6 months.

Task 3.8. Manufacturing of the pilot batch of samples (2-3 samples 10 x 10 cm). Sending them to ANL.

Duration - 6 months.

TASK 4

Task 4.1. Development of Ti-V; Ti-Nb alloys.

Analysis of phase composition alloys on the basis of Ti-V and Ti-Nb. Experimental research on TLEC and identifying of parameters of thermal treatment. Selection of coating composition to upgrade corrosion stability. Manufacture of pilot thin sheet samples.

Duration - 18 months.

Task 4.2. Development of alloys with the low content of Cr.

A detail estimation of serially produced deformed alloys, especially as far as their corrosion stability is concerned. Testing of the samples of alloys of Fe-Ni-Co-Cr system at 850°C in different gas environment. Study of corrosion products formed at the surface of the

samples using X-ray, metallographic and other methods of analysis. Manufacturing of experimental thin sheet samples.

Duration – 21 months.

Task 4.3. Development of ferrite stainless steel (brand 400) with the oxide coating.

Experimental research on adjustment of oxide coating application mode using plasma technique. Analysis of a capability to spray composite oxide coatings on thin sheet samples. Testing of the coating under operational conditions of a SOFC cathode.

Duration – 21 months.

Appendix 2

THE SECOND CORRECTION OF THE WORK PLAN

Old duration of the Project– 21 months (June 01, 2002 - February 28, 2004).

New duration of the Project – 24 months (June 01, 2002 – May 31, 2004).

Item to be revised	Work Plan text	Revised text
REVISIONS IN THE TEXT OF THE WORKPLAN		
Task 1.6	Manufacturing and sending (export) of two nickel coated plates to ANL for further examination. Technical and economical analysis and evaluation of the cost of the bipolar plate with galvanic nickel coating 0.4 x 712x 1296 mm under conditions of mass production. Two plates 0.4 x 712x 1296 mm with nickel coating on one side – 7 quarter Report – 7 quarter Sending (export) of two plates with nickel coating to ANL – 7 quarter	Preparation and sending (export) of four plates of steel 20X23H18 to FCE (USA) 0.4*180*180 mm in size for further examination. Technical and economical analysis and evaluation of the cost of the bipolar plate with galvanic nickel coating 0.4 x 712x 1296 mm under conditions of mass production. Sending to FCE of evaluations of the cost of the plates. Report.
Task 2.3.	Research on conductivity of oxide films in the melt of lithium and potassium carbonates in the environment (5%O ₂ +5%CO ₂ +20%H ₂ O +70% N ₂) and (20%H ₂ +80%CO ₂ , humidification at 60 ⁰ C) at 650 ⁰ C during 500 hours using thin sheet samples with the area of 1 square inch of the best serially produced alloy and a new alloy. Analysis of: phase composition and structure of the surface; concentration distribution for chemical elements in the surface layers of the samples before and after the tests. Duration – 12 months.	Completion of the research on of oxide films in the melt of lithium and potassium carbonates in the anode and cathode environment at 650 ⁰ C using thin sheet samples with the area of 1 square inch. Research is to be conducted in comparison of the Russian steel analogous to 310S and a new alloy. Evaluations of the conductivity, Analysis of testing results.
Task 2.5.	Sending to the Partner of 10 plates of the best alloy 0.8x 712x 1296 mm. Duration – 6 months.	Sending to the Partner of 4 plates of a new alloy 0. 8 x 180x 180 mm.

Task 2.6.	Technical and economical analysis and evaluation of the cost of the bipolar plate 712x 1296 mm and 0.55 mm thick made of a new alloy, when it is made using method of coiled stock when the annual order makes up ~ 400000 plates. Duration – 9 months.	Technical and economical analysis and evaluation of the cost of the bipolar plate 712x 1296 mm and 0.55 mm thick made of a new alloy, when it is made using method of coiled stock with the growth of the annual order up to 400000 plates. Sending to FCE of cost evaluation for the plates. Report.
Task 3.8	Manufacturing of a pilot batch of samples (2-3 samples 10 x 10 cm). Sending (export) of the samples to ANL. Pilot batch of samples - 6 quarter Sending (export) of cermet samples to ANL - 7 quarter	Research on possible creation of porous cermet composition on the basis of Li-AIO₂ and Ni for an MCFC anode with the good electric conductivity and porosity of 50 – 60%. Creep tests to evaluate the shrinkage of the material at 650°C and pressure of 2 atmospheres in a standard anode environment with humidification at 60°C.
Task 3.9		Manufacturing of a pilot batch of porous samples (2-3 samples 10 x 10 cm Sending (export) of the samples to FCE. Report.
Task 4.1.	Development of a new material for a bipolar plate of SOFC using new alloys on the basis of Ti-V and Ti-Nb systems. Records of corrosion stability tests of the alloys – 4 quarter Manufacturing of pilot samples and sending them to ANL -7 quarter	Development of a new material for a bipolar plate of SOFC using new alloys on the basis of Ti-V and Ti-Nb systems. Corrosion stability tests of the alloys, analysis of the results of the tests. Cost evaluation for the alloys. Manufacturing of the pilot samples- one from each of Ti-V and Ti-Nb systems,- and sending them to ANL. Report.
Task 4.2.	Development of the material for a SOFC bipolar plate with a low content of Cr basing on systems of Fe-Ni-Co-Cr. Tests and comparison of monolithic samples of the alloys at 850°C during 1000 hours in the air. Research on operation of the improved selected alloys and identification of parameters of Cr diffusion into the cathode of a fuel cell from the alloys with a low content of Cr under conditions of immediate contact of the alloy with the cathode material (La _{0.6} Sr _{0.4} MnO ₃); Sending (export) of 2-3 samples of the material 100×100mm (10 units) of alloys to ANL - 7 quarter.	Development of the material for a SOFC bipolar plate with a low content of Cr basing on systems of Fe-Ni-Co-Cr. Tests of the alloys with the minimum content of Cr and Co in the anode and cathode environment (5% H₂ + 50%H₂O + 20%CO₂ + 25%N₂// 2-5%H₂O + air) during 500 hours; study of the oxide films after the tests. Sending (export) of thin sheet samples of three of the best alloys (2 of each with the area of 100 sq. cm) to ANL.

Task 4.3.	Development of the material for a SOFC bipolar plate of ferrite stainless steel из ферритной нержавеющей стали (brand 400) with an oxide coating and of technological processes of oxide coating application. Sending (export) of samples of the steel with an oxide coating to ANL - 7quarter	Development of the material for a SOFC bipolar plate of ferrite stainless steel (brand 400) with an oxide coating and of technological processes of oxide coating application. Report.
----------------------	---	---

Appendix 3

TESTING METHODS FOR CORROSION STABILITY

Experiments to determine protective properties of coatings on 20X23H18 steel were done in accordance with FCE and ANL recommendations, at the temperature of 650°C in the environment of H₂, CO₂ (20%, 80%) humidified with water at 65°C; at the surface of the samples there was a film of eutectic melt of lithium and potassium carbonates (62 mole% Li₂CO₃, 38 mole% K₂CO₃).

Research was done using a cell A0712/3-JI53, which is given in Figure 1. The samples under the research (3) were located in nickel dishes (7). They were located between two porous nickel plates to ensure free supply of the gas to the surface of the samples (2). Electrolyte in the form of an electrolyte plate was on the top of the porous plate; when melted, the electrolyte partly filled the pores of the porous plates (2) and wetted the surface of the samples forming a thin film of the electrolyte at the surface. Dishes assembled in such a way were located inside a steel block (unit) (8) in order to level the temperature field. Gas supply holes were made in the internal walls of the block (unit) and that provided immediate supply of the gas mixture (H₂, CO₂, H₂O) to the dishes. The assembly was pressed with a load (6) to ensure a uniform contact of the samples with porous nickel plates impregnated with the electrolyte. The block with dishes was located inside a hermetic container (9), where a constant temperature (650°C) and gas environment were kept. The temperature was controlled with the help of a thermocouple (5). A "Proterm 100" temperature regulator was used to keep the temperature constant. Gas environment was monitored with the help of «GIAM 14» analyzer. Every 250 hours one dish with samples was taken out, which were then washed from carbonates in the distilled water; then their metallographic analysis was done. The samples were washed in a separate glass during 10 days; every day the distilled water there was changed.

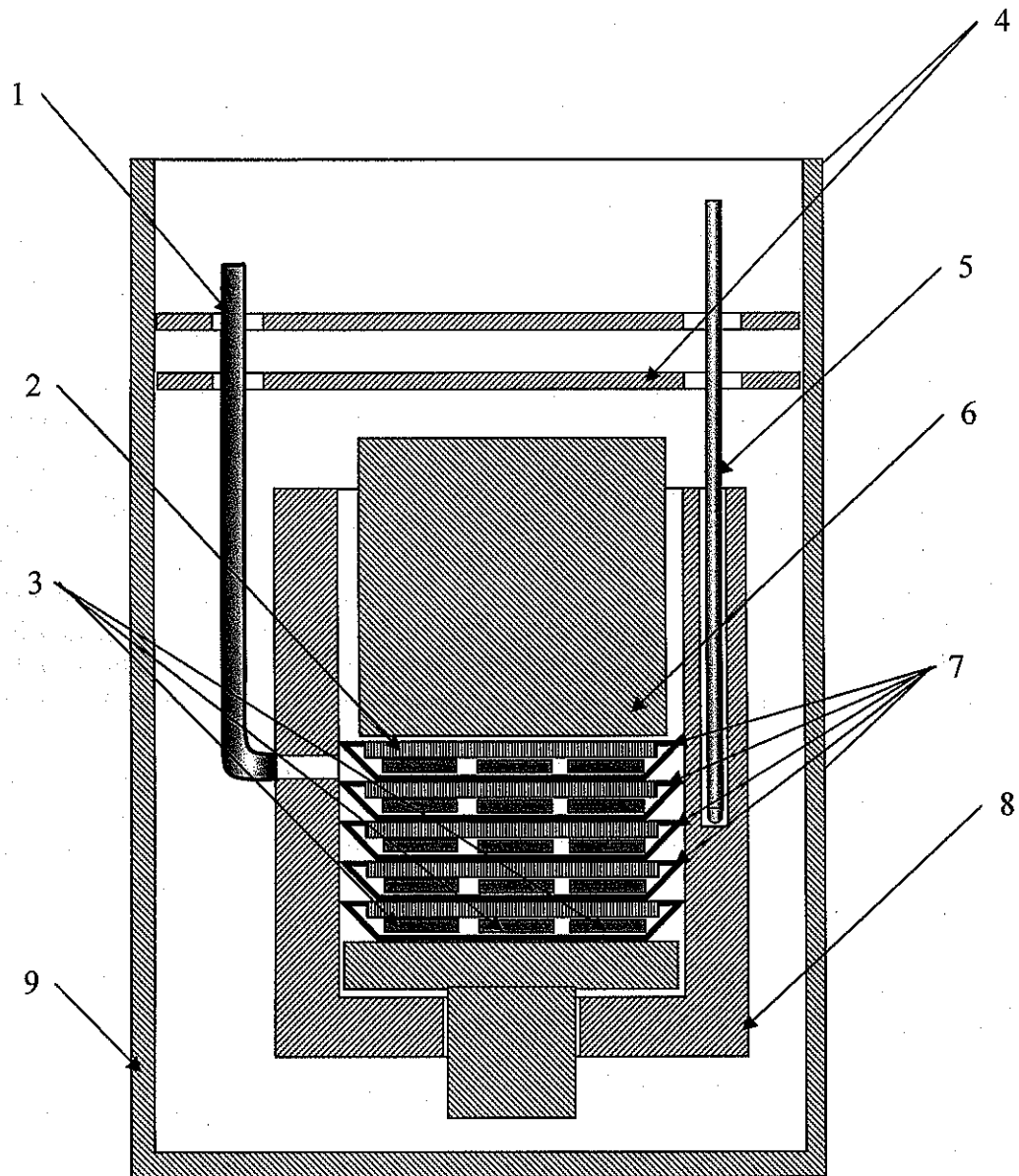


Fig. A-1.

- 1 – a gas supply tube
- 2 – a porous nickel plate
- 3 – samples
- 4 – heat shields
- 5 – a thermocouple
- 6 – a hold-down (pressing) load
- 7 – nickel dishes
- 8 – a thermal block (unit)
- 9 – a hermetic container

Appendix 4

TECHNICAL AND ECONOMICAL ANALYSIS OF ESTABLISHMENT OF AN ENTERPRISE TO MAKE BIPOLAR SEPARATOR PLATES**1. Target setting**

Within Task 1 of the Work Plan of ISTC Project №2281p there was planned to perform a feasibility study of the cost parameters of bipolar plates made of 20X23H18 stainless steel coated with galvanic nickel.

According to the initial information from Fuel Cell Energy, the final goal of the production should be the level of production of 400 thousand of full-size plates a year. For us to be able to get the selling value of the nickel-plated bipolar plate basing on FOB conditions, Saint-Petersburg, Russia (in compliance with INKOTERMS rules), three variants to establish production of the mentioned-above plates were considered in this Project. They are characterized by the following basic properties features:

- automatized manufacture of plates with a large portion of manual labor in the specially established enterprise that would be a legal entity. The equipment necessary for galvanic coating application is made in RFNC-VNIIEF;
- a large-scale production on the basis of automatic galvanic lines within the detached legal entity. The equipment necessary for automatic manufacture is bought at the most acceptable free market prices;
- a large-scale automatic manufacture of plates where the mechanism of leasing is used to purchase necessary equipment.

Allocation of manufacturing facilities is supposed within the limits of an industrial zone of the Sarov Closed Administrative Area (CAA), Nizhniy Novgorod Region. Potentially such allocation of manufacturing facilities may have some positive features:

1. The Russian Government stimulates creation of defense conversion highly technological workplaces in CAA. In particular, the regional and local acts for support of innovational activity accepted in Nizhniy Novgorod Region and in Sarov allow us to reduce or avoid taxation in at least two positions - in the tax to profit and the tax to property.
2. In CAA Sarov there are enough of highly skilled personnel (designers, technologists, workers that serve automatic transfer lines, workers that work with the advanced systems of diagnostics etc.).
3. Within the carried out the defense conversion in RFNC-VNIIEF in Sarov, necessary floor spaces and rooms become free.

However, when making calculations of the technical and economic analysis of the cost of manufacture of nickel plating of bipolar plates the above-stated opportunities to low down the price of plates were not considered. The above-stated reserves can be used for indemnification to risk of the project.

Cost characteristics of manufacture of nickel-plated bipolar plates are submitted below.

2. Approach #1. Automized production of the nickel-plated bipolar plates based at RFNC-VNIIEF.

2.1. A scheme of the galvanic site

A key point in this approach is manufacturing of the equipment (Galvanic baths and baths for preliminary processing of plates) for nickel-plating of separator plates at RFNC-VNIIEF (manufacturing is automatized, but the portion of manual labor is quite sufficient).

When establishing the enterprise there is no need to install all production equipment. A galvanic workshop will gradually expand at the expense of step-by-step introduction into operation of new galvanic sites.

A scheme of a galvanic site is given in Figure 2.1.

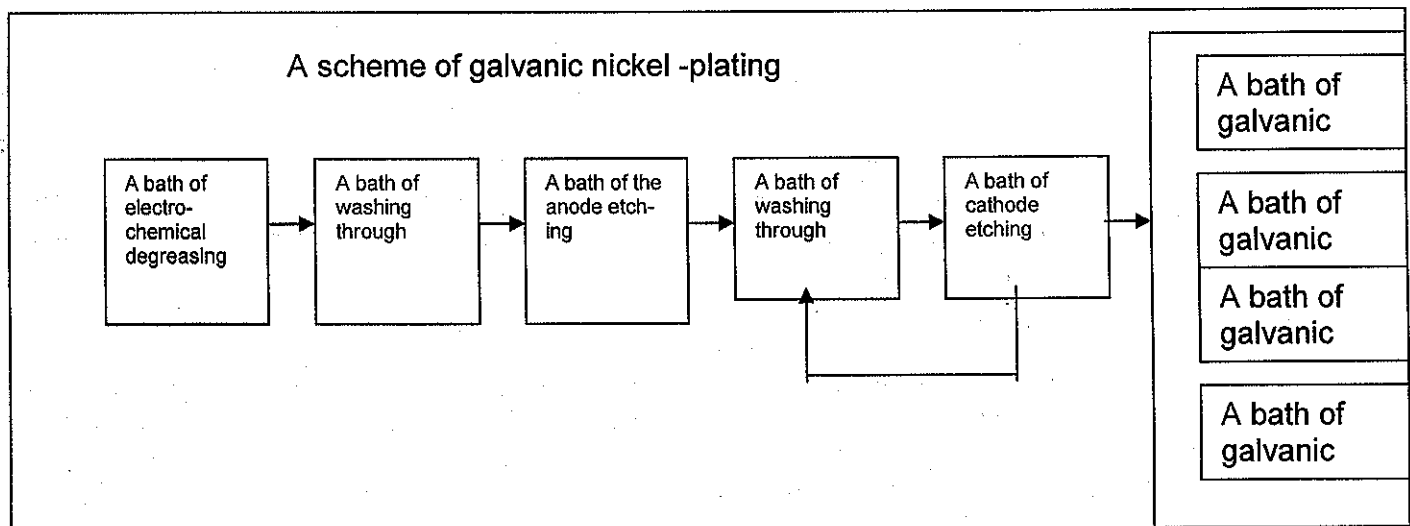


Fig. 2.1. A scheme of galvanic site

One galvanic site comprises:

- A bath of electrochemical degreasing (ECD). Run time (t) of 1 plate is $1,5 \pm 2$ min.;
- 2 ablation baths ($t=1 \pm 2$ min): for ablation after ECD and after the anode etching;
- Anode etching bath ($t=15$ min);
- Cathode etching bath ($t=1 \pm 1,5$ min)
- Baths of galvanic nickel plating. Time to apply a nickel coating 80 microns thick is 6 hours.

From the maximum time of preliminary treatment of the plates (15 min) we calculate the number of galvanic baths that can be served by a line of baths of preliminary treatment - 9 baths. 1 bath accommodates 2 plates.

It is taken that:

- The number of charging per day for one bath is 3;
- Mode of operation – three shifts, continuous process;
- A number of working days per month is 30.

2.2. Variable Costs.

The content of variable costs is given in Table 2.1.

Table 2.1.

Materials to make separator plates

Materials	Units	Q-ty	Price in rubles	Total in rubles
Nickel anodes 10 mm appr. 1.2x1.0 m in size	units	1,00	6 000,00	6 000,00
20X23H18 steel 40 microns	kg	3,08	130,00	400,25
Total				6 400,25

Nickel anodes are supplied by a manufacturer; they are 10 mm thick. Such anode is enough to coat 16 steel plates 1296*712 mm in size.

2.3. Constant (fixed) non-production costs.

When an enterprise is established administrative and management costs are inevitable; they come from the salary of the management personnel and constant non-production costs (see Tables 2.2, 2.3):

Table 2.2.

Salary of the management personnel

Position	Number of people	Salary, Rubles per month	Salary, Rubles per year
Director	1	30 000	360 000
Accountant	1	20 000	240 000
Storekeeper	1	6 000	72 000
Electrician	1	9 000	108 000
Cleaner	1	3 500	42 000
Total	5	68 500	822 000

Table 2.3.

Administrative and management costs of an enterprise

Expenditure	Total, rubles per month
Electricity for administrative rooms	2 395
Hot water	4 043
Cold water	1 427
Sewage	2 833
Heating	1 088
Communication	7 800
Total	19 586

2.4. Total Production Costs.

Fixed production costs in the case under consideration are of discreet fixed character as they depend on the number of production sites that vary in leaps and bounds.

Table 2.4.

Production costs per 1 galvanic site.

Expenditures	Total, rubles per year
Electricity for manufacturing rooms	68 429
Cold water	2 736
Sewage	2 678
Heating	5 712
Total	79 555

Table 2.5.

Production costs per 1 galvanic site.

Position	Number of people	Total per month, rubles	Total per year, rubles
Section manager	1	15 000	180 000
Galvanizer	3	10 000	360 000
Carver (scissors)	1	9 000	108 000
Analyst	1	9 000	108 000
Total	6	43 000	756 000

Symbolically fixed costs comprise the costs of chemicals to fill galvanic baths. These costs are at the start of the production, with the development of the production it is necessary to add $\approx 2\%$ of chemicals a year to sustain the acid environment.

Table 2.6.

Chemical materials to fill the baths of the galvanic site

Materials	Units	Q-ty	Price, rubles	Total, rubles
Chemicals per 1 bath of galvanic nickel-plating (bath volume is 650 l)				
Na ₂ SO ₄	kg	71,25	85,00	6 056,25
MgSO ₄ *10H ₂ O	kg	47,50	42,00	1 995,00
H ₃ BO ₃	kg	14,25	60,00	855,00
NaCl	kg	7,13	25,00	178,13
NiSO ₄ *10H ₂ O	kg	35,63	60,00	2 137,50
Total				11 221,88
Transport and quota purchase costs, 13%				458,84
Total per 1 bath for Galvanic nickel-plating				12 680,72
Chemicals per 1 bath of degreasing *(volume of a bath is 236 l)				
NaOH	kg	8,50	40,00	340,00
Na ₂ CO ₃	kg	17,00	70,00	1 190,00
H ₂ SO ₄ 20%	kg	38,59	22,00	848,98
Total				2 378,98
Transport and quota purchase costs, 13%				309,27

2.5. Initial (capital) investments.

When doing calculation of the cost there were used common in the Russian Federation (RF) items:

- in the RF there is separate accounting of the basic and additional salary. Additional salary in the Project was calculated as 10,2% of the basic one. Additional salary is used to cover regular and educational leaves;
- the next position of the calculation used is additional sum to the salary. In the Project it was taken as 35,6% of the basic and additional salary. In Russia such extra charges for the salary are compulsory fees for the enterprises to pay to the social, retirement, medical etc. funds.
- profit tax in the Project was taken as 8%. It is necessary to note that Clause 25 of the Tax Code of the RF the profit is defined as a value of incomes surpassing the operation costs of the enterprise in the reported period. So, when calculating the price of different things you need to take profit into account;
- From January 1, 2004 the rate on the value added tax (VAT) in the RF is 18%. VAT is calculated from the value of aggregate costs of a thing, profit including.

Capital investments in manufacturing of the equipment on the basis of RFNC-VNIIEF for 1 site are given in Table 2.7.

Table 2.7

Capital investments to make equipment

position #	Calculation	Total, rubles
1	Initial and raw materials	66 352,30
2	Basic salary	232 616,42
3	Additional salary, 10,2%	23 726,88
4	Additional sum to the salary, 35,9% from i.2+i.3	92 027,24
5	Overheads, 144,5% of i.2+i.3	370 416,07
6	Production prime cost	785 138,91
7	Profit, 8%	62 811,11
8	Work price	847 950,02
9	VAT, 18%	152 631,00
10	Selling price	1 000 581,03

Calculations of the costs by positions 1 and 2 of Table 2.7 are given in Tables 2.8 and 2.9, respectively.

Table 2.8.

Initial and raw materials

№ ii	Materials	Unit s	Q-ty	Price, rubles	Total, ru- bles
Equipment: 4 baths for galvanic nickel plating and 5 baths of preliminary treatment of plates					
1	Stainless steel (sheet) 20X25H20C2	kg	1 507,97	35	52 778,85
	Transport and quota purchase costs, 13%				6 861,25
	Total				59 640,10

Riggings (attachments)					
1	Copper	kg	2	130	260,00
2	Stainless steel	kg	2	35	70,00
Total					330,00
Transport and quota purchase costs, 13%					42,90
Total per 1 unit of attachments					372,90
Total per attachments for 1 site (18 units)					6 712,20
Total: Materials for baths of 1 site of galvanic nickel plating					66 352,30

Table 2.9.

Basic Salary				
№ ii	Type of work	Labor-intensiveness, standard hour	Rate, rubles	Basic Salary, rubles
Equipment				
1	Mechanical operations according to the 6 th grade, by the job.	1600	14,987	23 979,20
2	Metal work according to the 6 th grade, by the job.	4600	14,987	68 940,20
3	Wiring according to the 5 th grade, by the job.	1400	13,725	19 215,00
4	Electric welding to the 5 th grade, by the job.	300	13,725	4 117,50
Total				116 251,90
Addition (fringe payment) (20%-CAA)				23 250,38
Premium for the workers, 50%				58 125,95
Total				197 628,23
Attachments				
1	Mechanical operations according to the 6 th grade, by the job.	45	13,263	596,84
2	Metal work according to the 5 th grade, by the job.	45	12,146	546,57
Total				1 143,41
Addition (20%-CAA)				228,68
Premium for the workers 50%				571,70
Total per 1 set of the attachments				1 943,79
Total cost of labor – intensiveness to make equipment and attachments (for 18 sets)				232 616,42

In addition to capital investments there were referred the following costs:

- 1) According to the technological process, after application of the nickel coating it is necessary to cut the edges of the plates. So, we need alligator shears. Including the cost of their launching into operation their cost will make 1 200 thousands of rubles;
- 2) An industrial carrier is necessary for transportation of the plates from the finished-products storage area to the site and back. Its cost is 600 thousand rubles;
- 3) Working area is necessary to accommodate the production; its sizes should be 55m² for each galvanic site. The working area is to be increased for each new site respectively;
- 4) Office rooms are necessary to accommodate managerial personnel; their area should be 40 m².

2.6. Price pattern

Considering the integrity of 1 galvanic site we may account for its full productivity: 4 cycles per day, 2 plates in 1 bath during 350 working days a year. When all 9 baths of 1 site are used it is possible to make 25200 plates a year.

Basing on the specified productivity, production cost of 1 plate was calculated in case of different volumes of production (a pitch of 25.2 thousand units).

Table 2.10.

Price pattern for the production of separator plates.

A batch, number of plates	25 200	50 400	75 600	100 800	378 000	403 200
A number of galvanic sites	1	2	3	4	15	16
Variable costs of a batch	19 536 390	39 072 780	58 609 170	78 145 560	293 045 849	312 582 239
Fixed production costs	1 180 612	2 361 224	3 541 836	4 722 447	17 709 178	18 889 790
Fixes non-production costs	1 137 506	1 137 506	1 137 506	1 137 506	1 137 506	1 137 506
Initial investments including the capital ones	965 558	1 065 616	1 165 674	1 265 732	2 366 372	2 466 430
Packing	14 175	28 350	42 525	56 700	212 625	226 800
Transport costs, 15%	3 425 136	6 549 821	9 674 507	12 799 192	47 170 729	50 295 415
Profit, 10%	2 625 938	5 021 530	7 417 122	9 812 714	36 164 226	38 559 818
VAT, 18%	5 199 357	9 942 629	14 685 901	19 429 173	71 605 167	76 348 439
Customs fees	209 487	418 973	628 460	837 946	3 142 298	3 351 785
Cost of a batch	34 294 158	65 598 428	96 902 699	128 206 970	472 553 949	503 858 220
Cost of 1 plate, rubles	1 361	1 302	1 282	1 272	1 250	1 250
Cost 1 plate, \$	45,36	43,39	42,73	42,40	41,67	41,65

Table 2.10 take account for the customs fees of \$100 per 1ton of exported products.

Expenses for transportation of products within the RF are taken in percentage from the prime cost and are shown in the line «Transport costs». The percentage is approximate and taken according to the statistics in RFNC-VNIEF.

Packing is made of planed boards to separate the goods. The cost of 1 cubic mete of the boards is 1500 rubles.

Remuneration of labor, that are a part of fixed production and non-production costs, comprise payments to the block social tax of 36% of the fund of remuneration of labor.

The structure of costs is visually represented in Fig.2.2 and 2.3.

Tendencies in variation of the price of 1 one plate calculated in approach №1 are shown in Fig.2.4.

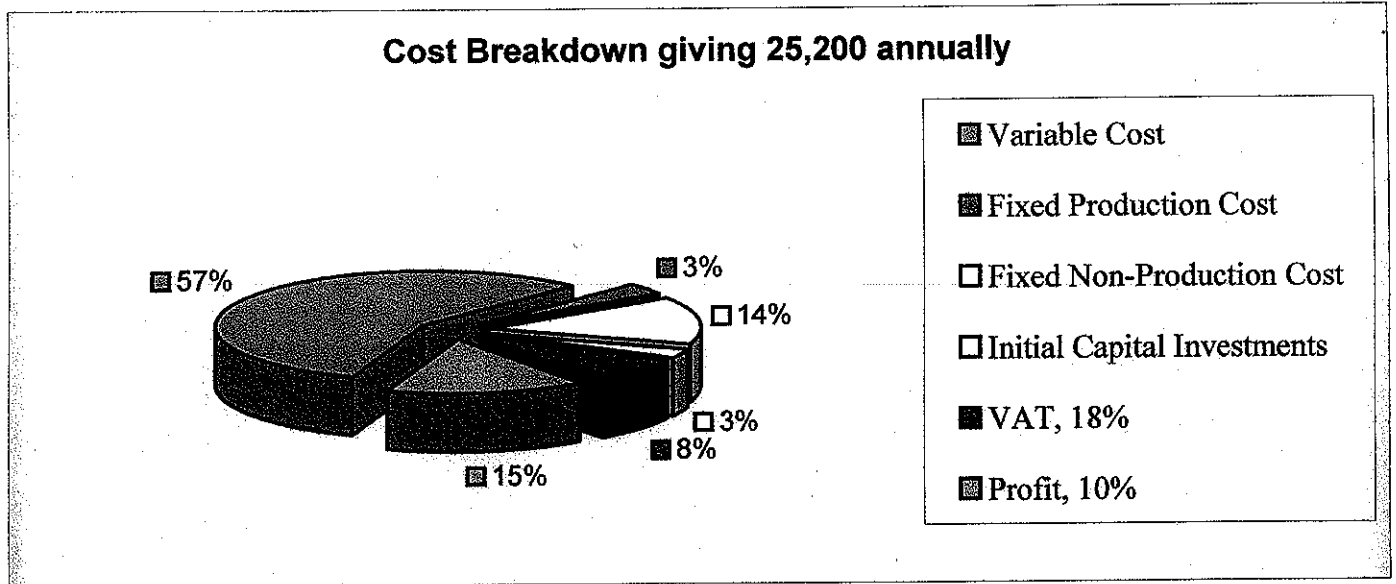


Fig.2.2.

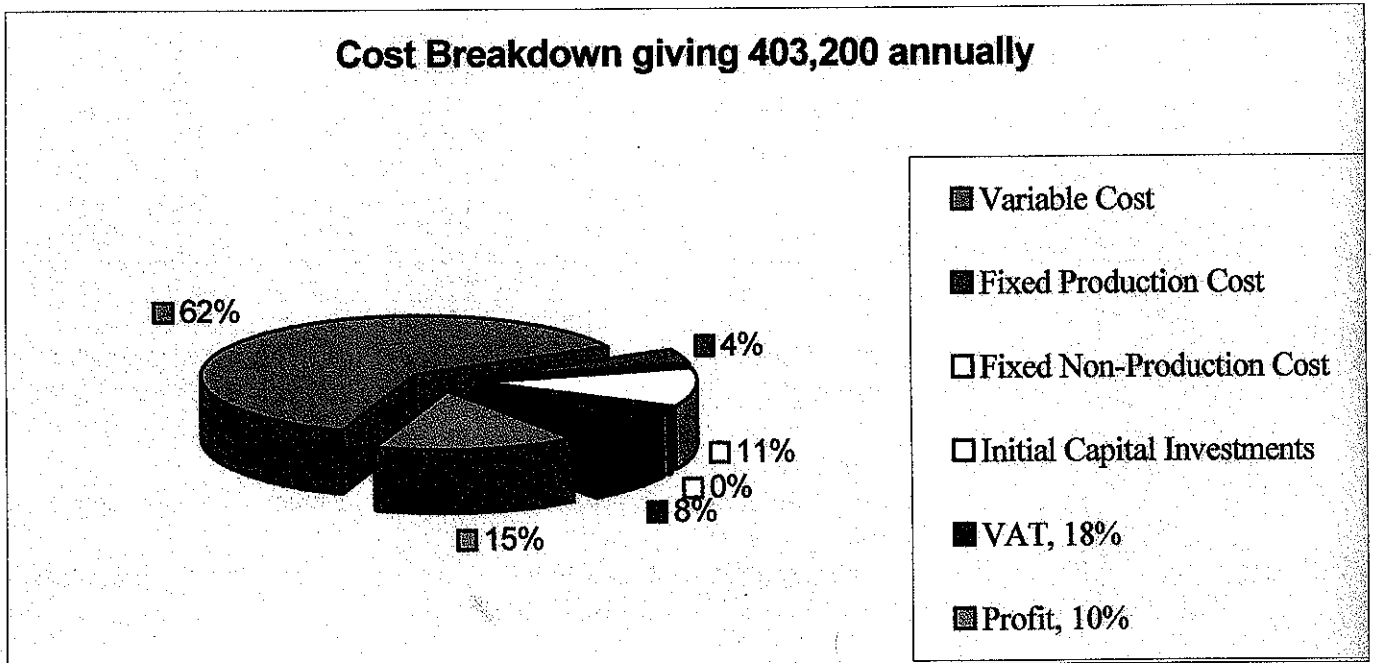


Fig.2.3.

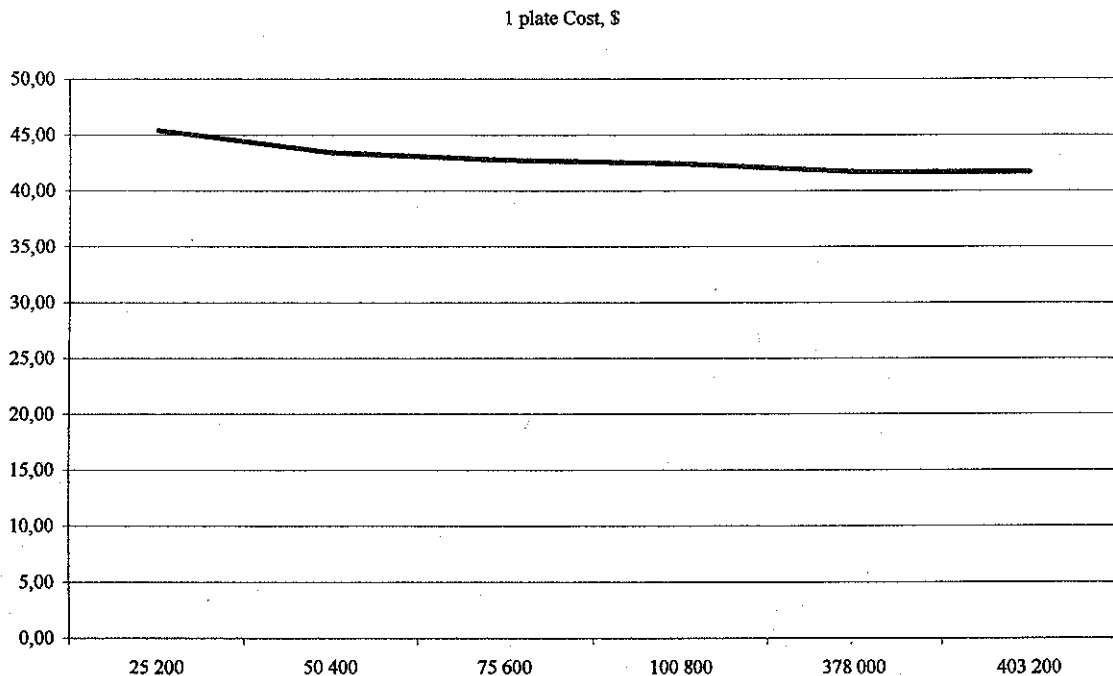


Fig. 2.4. The cost of 1 plate as a function of the volume of production for the variant of automated production.

3. Approach №2. Automated production of the nickel-plated bipolar plates with a robot-controlled production line.

In the second approach there was considered creation of fully automated production with robot-controlled production lines.

After analysis of the price proposals from different companies that produce automated galvanic lines the project participants decided to focus on the possibilities of Nizhny Novgorod Science and Production Enterprise "ROBOTEK". ROBOTEK Company was founded in 1992 and it is a leading developer and producer in Russia of low-waste automated galvanic lines by special projects. Robot-controlled galvanic lines produced by ROBOTEK are reliable in operation and are used in many enterprises of different industry – from the aviation one to the watch one all over European part of Russia - from Izhevsk to Saint Petersburg, from Uglich to Volgograd. The company makes a design to the Statement of Work and specifications of the customer. It provides manufacturing, turn-key delivery, 12-month after-sales service.

Performance characteristics of a galvanic line.

I. Production capacity:

1. Sizes of a sheet:
 - length, mm – 1296;
 - height, mm – 712;
 - thickness, mm – 0.4.
2. Coating – Ni, on one side.

3. Thickness of the coating, microns – 80.
4. Production, units/year – 400000.

II. Accepted standards:

1. Rate of nickel deposition, microns/min. – 0,38.
2. Sheets per a bath at a time, units – 4.
3. Mode of operation – three shifts (21 hours a day).
4. Number of working days a month – 23.
5. Usage of equipment – 0,85.
6. Distance between the anode and the cathode in the bath, mm – 200.
7. A number of cathodes in the bath, units – 2.

III. Performance calculation:

1. Necessary amount of lines – 6.
2. A number of baths for nickel-plating in a line – 12.
3. A number of technological positions in a line - 30.

IV. Some performance attributes of a nickel-plating line:

1. Sizes:
 - length, mm – 6500;
 - width, mm – 4200;
 - height, mm – 3800.
2. Installed capacity:
 - electrochemical treatment, kW – 300;
 - electric heating and drying, kW – 436;
 - electric drive, kW – 11,5;
 - total, kW – 747,5.
3. Productivity, hangings per hour- 3,4;
4. Productivity, sheets per hour – 13,6.

V. Maintenance staff:

1. Operator – 1 per line.
2. Hanger bracket builder – 1 per line.
3. Adjuster – 1 per 2 lines.
4. Production engineer – 1 for 6 lines.

VI. Cost of one line:

1. Cost of a set of equipment of one line, rubles – 7164700.
2. Cost of start-and-adjustment works, rubles – 716470.
3. Cost of all lines, «turn key», rubles - 7881170.

Environmental friendliness of the robot-controlled galvanic lines is provided by the following:

- fail-safety – implementation of current-free (blind) baths that are emptied by the immersed pump (it comes into a set of a line);
- low waste – considerable return of the solution carried away by the components being processed back to the process baths; it is provided by the drippage time programmed for each bath, implementation of sprayer ablation etc.

Calculations based on the initial data above have shown that for the order of 400 000 units a year to be fulfilled 6 galvanic lines, with 12 baths for nickel plating are to be installed. The entire site will comprise 30 of such technological positions.

The following standards were accepted for calculations:

- Nickel deposition rate, microns/min – 0,38;
- Loading of sheets into a bath at a time, units – 4;
- Mode of operation – three shifts (21 hours a day);
- A number of working days a month – 23;

- Usage of equipment – 0,85;
- A number of cathodes in a bath, units – 2.

It is important to note that reaching full productive capacity in the first years will not be necessary. Growth of production volumes will be provided by launching into operation of new sites. The volume of production in the first year will make 10 000 plates a year. During this period the adjustment of equipment will be performed, production schedule will be specified and quality control system will be worked through.

Common for the second and the first approaches will be variable costs (Table2.1), constant non-productive costs (Table2.2, 2.3), symbolically constant expenses (Table2.6), carrier to take the material from the storage place (the cost is 600 000 rubles), mechanical shears (cost 1200 thousand rubles).

Approach #2 is different from approach #1 in the cost of equipment, in the cost of industrial premises, in constant production costs.

Table 3.1.

Field cost	
	Total, rubles a year
Electricity for industrial premises	25 592 371
Fees to public utilities	2 860 816
Total	28 453 187

Table 3.2.

Production salary			
	Number of workers at 6 sites	Salary, ru- bles per month	Salary, ru- bles per year
Section manager	2	15 000	360000
Operator	6	10 000	720 000
Assembler (builder)	6	9 000	648 000
Production engineer	1	9 000	108 000
Adjuster	3	9 000	324 000
Total	18		2 160 000

Acquisition, setting up and launching of the galvanic equipment of 6 sites will make 47 287 020 rubles

Construction of the premises to accommodate the production will make about 26 850 thousand rubles

Calculations of the cost of 1 plate are given in Table3.3.

Table 3.3.

Price of production of separator plates.

Item of expenses / batch, q-ty	50 000	100 000	150 000	200 000	250 000	300 000	350 000	400 000
Variable costs of a batch	38 762 678	77 525 357	116 288 035	155 050 714	193 813 392	232 576 070	271 338 749	310 101 427
Fixed production costs a year	31 734 169							
Fixed non-production costs a year	1 506 452	1 506 452	1 506 452	1 506 452				
Initial investments including the capital ones	5 530 785	5 530 785	5 530 785	5 530 785				
Packing	28 125	56 250	84 375	112 500	140 625	168 750	196 875	225 000
Transport costs, 15%	11 634 331	17 452 952	23 271 572	29 090 193	34 908 813	40 727 434	46 546 054	52 364 675
Vat, 18%	16 055 377	24 085 074	32 114 770	40 144 466	48 174 163	56 203 859	64 233 555	72 263 251
Profit, 10%	7 756 221	11 635 301	15 514 382	19 393 462	23 272 542	27 151 623	31 030 703	34 909 783
Customs fees	415 648	831 296	1 246 944	1 662 592	2 078 240	2 493 888	2 909 536	3 325 183
Cost of a batch	113 423 787	170 357 635	227 291 484	284 225 332	341 159 181	398 093 029	455 026 878	511 960 726
Cost of 1 plate, rubles	2 268	1 704	1 515	1 421	1 365	1 327	1 300	1 280
Cost of 1 plate, \$	75,62	56,79	50,51	47,37	45,49	44,23	43,34	42,66

Customs fees and packing are calculated the same as for the first approach.

However, in approach #2 a factor of step-by-step introduction of galvanic sites was not considered. This would allow us to reduce the final cost of the first batches of plates.

Visual presentation of the costs is given in Fig.3.1 and 3.2.

Tendencies in variation of the price of 1 one plate calculated in approach №2 are shown in Fig.3.3.

Cost Breakdown giving 50,000 annually

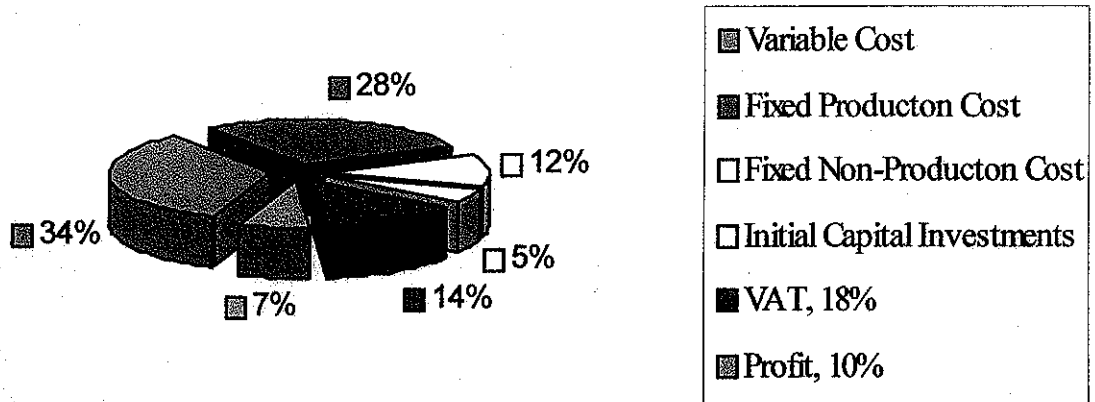


Fig.3.1

Cost Breakdown giving 400,000 annually

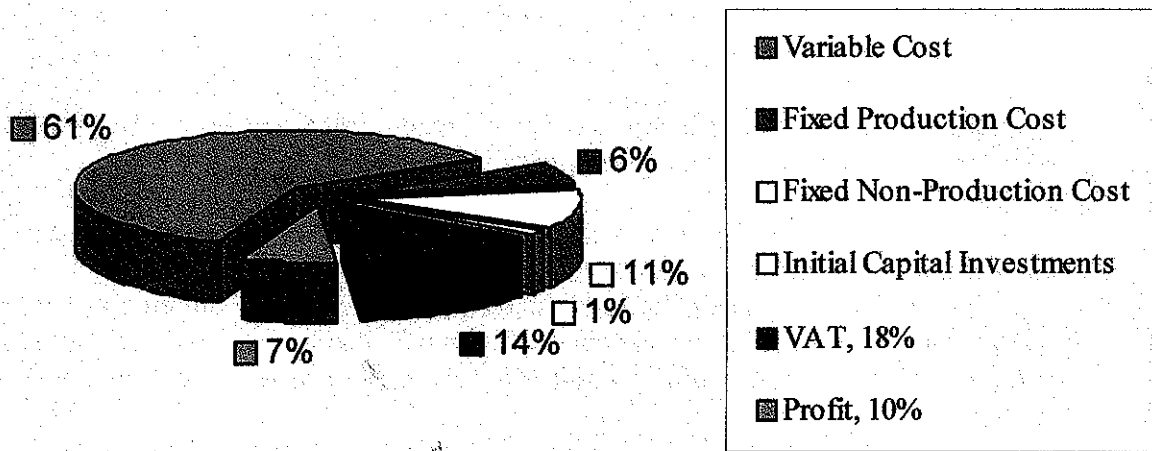


Fig.3.2.

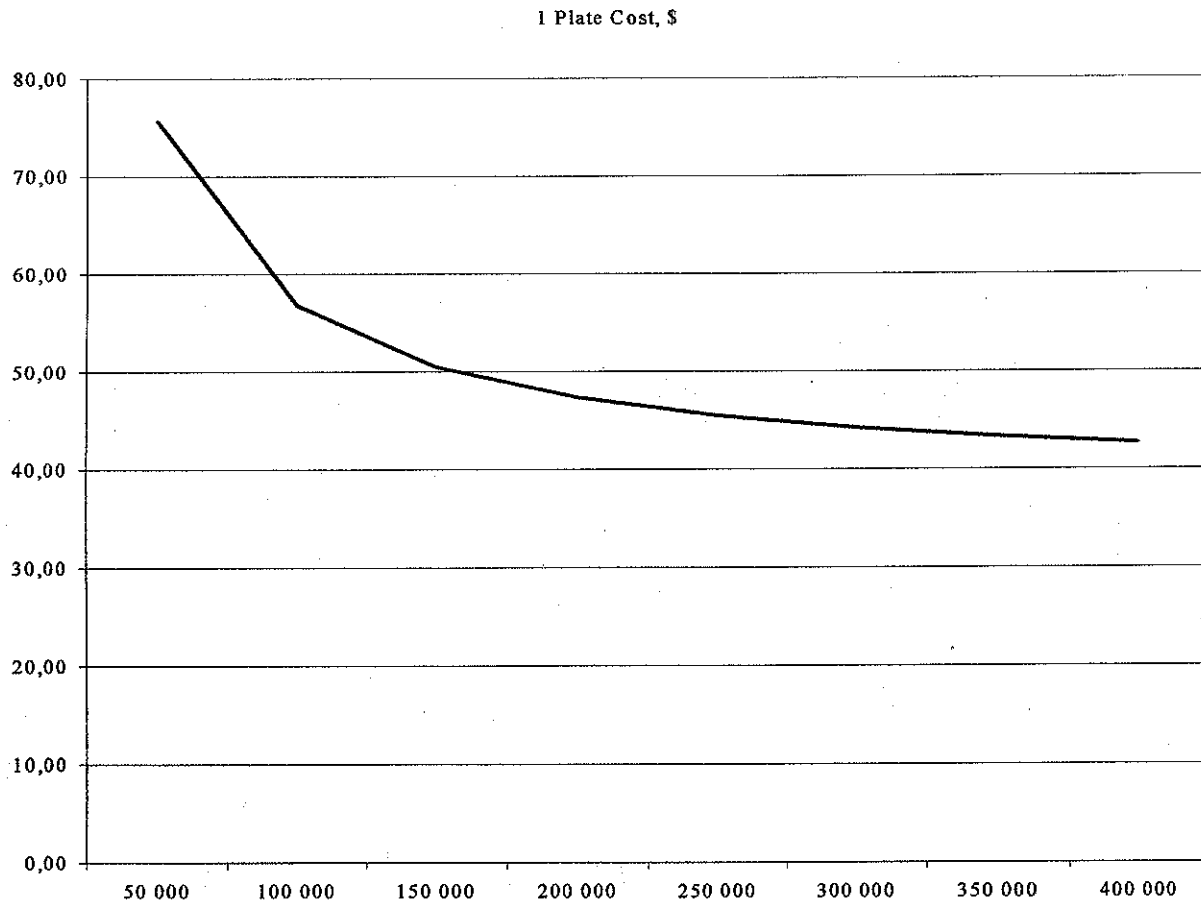


Fig. 3.3. The cost of 1 plate as a function of the volume of production for the variant of automated production

4. Approach №3. Automated production of nickel-plated bipolar plates implementing robot-controlled carrier under leasing conditions.

At present in the RF there is an active work in legislation, norms and standards and infrastructure aimed at encouragement of various leasing forms in industry.

Ministry for Taxes and Duties of the RF put the following requirements for the leasing deals:

1. The term of lease must be not less than 30 years;
2. The lease should give moderate (acceptable) for the renter; a moderate profit is within 8 - 15%;
3. The renter should have a choice of external proposals.

When organizing a joint production of components for power plants on the basis of fuel cells (FC PP) it is important to take into consideration the following aspects characteristic for the leasing agreement:

1. Leasing payments refer to the prime cost of the product (work, service) of the leasing recipient (Federal Law 3164-FZ, clause 28 i. 6, clause 29, i. 3), that reduces the taxable basis (profit tax);

2. Leasing payments comprise the following besides the payment for the basic service:
- Depreciation for the period of the agreement;
 - Investment outlay (expenses);
 - Interest on credits used by the leasing-issuer to acquire the leased property;
 - Payments for additional services of leasing-issuer under the agreement;
 - Value added tax;
 - Insurance contributions for the subject of a leasing agreement, if made by leasing-issuer;
 - Property tax paid by leasing-issuer (#164-FZ, clause 29. i. 2);

3. Accelerated depreciation of the subject of leasing is possible on mutual agreement (№164-FZ, clause 31 i. 1). In case of accelerated depreciation a uniform (linear) method is used for its calculation, when established norm of depreciation charges increases by the acceleration factor, which is to be not more than 3. Enterprises are allowed to set themselves the factors of depreciation acceleration that are not more than 2 for equipment, machines, mechanisms and connection structures, including the devices of electric power supply (governmental) regulation of the RF №967);

4. Decrease needs in capital investments are provided by possible delay in leasing payments for the period of not more than 180 days since the day the object of leasing starts to be used (№164-FZ, clause 28 i. 3);

5. There is a decrease of tax payments for property of the enterprise as the cost of objects of leasing is reflected in the assets lease receiver only in the case when it becomes his property after the term of leasing agreement is over. Before that it is in the balance of leasing-issuer.

In the considered approach we suppose leasing to acquire the equipment and premises.

In the first years of operation there is no need to reach full productive capacity of 400 000 units per year. Growth of production volumes takes place during the first 6 years of work. Plan of production calculated for 10 years of the work of the enterprise is given in Table 4.1.

Table 4.1.

		Planned volume of deliveries									
Product	Units	1 year	2 year	3 year	4 year	5 year	6 year	7 year	8 year	9 year	10 years
Plates	units	20 000	50 000	100 000	200 000	300 000	400 000	400 000	400 000	400 000	400 000

Launching into operation of automatic galvanic lines to reach full productive capacity will go evenly during 6 years. The equipment is supposed to be taken on leasing with payment by installments during 10 years since the time of acquisition.

The list of necessary equipment and of the costs of acquisition of premises, as well as the time of launching into operation and the cost are given in Table 4.2.

Table 4.2.

Leasing		
Name	Date of launching into operation	Cost (rubles)
Galvanic site 1	01.01.2005	7 164 700
Galvanic site 2	01.01.2006	7 164 700
Galvanic site 3	01.01.2007	7 164 700
Galvanic site 4	01.01.2008	7 164 700
Galvanic site 5	01.01.2009	7 164 700
Galvanic site 6	01.01.2010	7 164 700
Working area	01.01.2005	13 200 000
Office rooms	01.01.2005	600 000
Carrier	01.01.2005	600 000
Shears for metal 1	01.01.2005	1 200 000
Shears for metal 2	01.01.2009	1 200 000

When calculating leasing payments we take a rate of 18% interest per annum. Period of pay-back of a credit for leasing for all the equipment is 10 years, for the premises and constructions it is 25 years.

Total direct costs make up 795,67 rubles (see Table 4.3). The largest part of the cost comes to main materials. Auxiliary materials comprise chemical powders used to keep acid-base balance in galvanic baths and degreasing baths.

Table 4.3.

Direct expenses				
Material	Units	Price (ru- bles)	Expense	Total (rubles)
Basic materials				778,40
Nickel anodes 10 mm 1.2x1 m appr. in size	units	6 000,000	0,063	378,00
20X23H18 Steel 40 microns	kg	130,000	3,080	400,40
Auxiliary materials				0,82
H ₂ SO ₄ 20%	r	0,022	0,116	0,00
H ₃ BO ₃	r	0,060	1,026	0,06
MgSO ₂	r	0,042	3,420	0,14
Na ₂ CO ₃	r	0,070	0,051	0,00
Na ₂ SO ₄	r	0,085	5,130	0,44
NaCl	r	0,025	0,513	0,01
NaOH	r	0,040	0,026	0,00
NiSO ₄	r	0,060	2,565	0,15
Other expenses				11,05
Customs fees	kg	3,000	3,500	10,50
Packing	dm ³	15,000	0,037	0,55
Piece rate				5,40
Carver with the shears for metal				5,40
Total				795,67

The number of people at production sites directly depends on the galvanic sites launched into operation.

The number of people comes from the following distribution of the workers at the sites:

- An operator – 1 per a site
- A builder of hanger brackets – 1 per a site
- An adjuster – 0,5 per a site
- A production engineer – 1 per 6 sites

Fund of salaries is calculated from the necessary demand for man power and monthly salary for a full unit:

- An operator – 10 000 rubles/month.
- A builder of hanger brackets – 10 000 rubles/ month.
- An adjuster – 10 000 rubles/ month.
- A production engineer – 18 000 rubles/ month.

When reaching full production capacity the number of main employees will make 16 people and a year fund of salaries will be 2 016 000 rubles

Total expenses for management are shown in Table 4.4.

Table 4.4.

Total expenses		
Position	Total (rubles)	Payment
Management		
Electricity	250	Monthly, all the Project
Expenses for public services	50 500	Monthly, all the Project
Communication	900	Monthly, all the Project

Overhead production charges comprise the cost of electricity and cost of chemicals to launch galvanic lines.

Their distribution during 10 years of work is shown in Table 4.5.

Table 4.5.

Overhead production charges										
	1 year	2 year	3 year	4 year	5 year	6 year	7 year	8 year	9 year	10 year
Electricity	3 268 000	6 535 900	9 803 900	13 071 800	16 339 800	19 607 700				
Chemicals	139 421	139 421	139 421	139 421	139 421	139 421				
Total	3 407 421	6 675 321	9 943 321	13 211 221	16 479 221	19 747 121	19 607 700	19 607 700	19 607 700	19 607 700

Costs of the staff are given in Table 4.6.

Table 4.6.

Planned Staff			
Position	Number	Salary (rubles)	Payment
Management			
Director	1	30 000	Monthly, all the Project
Accountant	1	20 000	Monthly, all the Project
Storekeeper	2	6 000	Monthly, all the Project
Cleaner	3	3 500	Monthly, all the Project
Electrician	2	9 000	Monthly, all the Project

When in operation, the taxes given in Table 4.7 will influence the pricing:

Table 4.7.

Taxes			
Tax	Basis	Period	Rate
Profit tax	Profit	Month	24 %
VAT	Added value.	Month	18 %
Property tax	Property	Month	2 %
Payments to the retirement fund	Salary	Month	28 %
Payments to Medical Ins. Fund	Salary	Month	3.6 %
Payments to Social Sec. Fund	Salary	Month	4 %
Tax for industrial injuries	Salary	Month	0.6 %

Considering all the taxes and costs the selling price of 1 plate will make 1107 rubles.

Refinancing rate of 16% (annual) was used in calculations, which gradually decreases every year by 1%. It is connected with the improvement of the economic situation in the RF and taken according to the statistics data for the last years.

Rate of Inflation during the first 1 year of operation is 12% and every year it goes down by 1%, and it is also connected to statistics.

The integral parameters taken with account for discounting are given in Table 4.8:

Table 4.8.

Parameter	Rubles
Rate of discounting	16.00 %
Payback period	44 Month
Discounting period of payback	50 Month.
Net Present Value	44167689 rubles
Index of profitability	5.94
Internal Rate of Return	90.09%
Modified Internal Rate of Return	53.78 %
Duration	5.92 years

5. Conclusions.

1. The calculations substantiated the possibility of a large-scale production of bipolar plates with a nickel coating when the following economic parameters are reached.
- the cost of 1 bipolar plate – \$44.

- the size of a batch – 400 000 plates a year.

2. Implementation of a leasing mechanism allows us to upgrade considerably the economic efficiency of the project and reach the level of payback of 44 months.

Basic parameters of the project are given in Table 5.

Table 5.

Parameter	
Price of 1 plate	1 107 rubles
Discounting rate	16,00 %
Period of payback	44 months
Discounting period of payback	50 months
Net Present Value	44 167 689 rubles
Profitability index	5,94
Internal Rate of Return	90.09 %
Modified Internal Rate of Return	53.78 %
Duration	5.92 years

